MULTIDISCIPLINARY CENTER FOR EARTHQUAKE ENGINEERING RESEARCH
A National Center of Excellence in Advanced Technology Applications

ISSN 1520-295X

Scissor-Jack-Damper Energy Dissipation System

by

Ani N. Sigaher-Boyle and Michael C. Constantinou
University at Buffalo, State University of New York
Department of Civil, Structural and Environmental Engineering
Ketter Hall
Buffalo, New York 14260

Technical Report MCEER-04-0010

December 1, 2004

This research was conducted at the University at Buffalo, State University of New York and was supported primarily by the Earthquake Engineering Research Centers Program of the National Science Foundation under award number EEC-9701471.

Scissor-Jack-Damper Energy Dissipation System

by

Ani N. Sigaher-Boyle[1] and Michael C. Constantinou[2]

Publication Date: December 1, 2004
Submittal Date: August 16, 2004

Technical Report MCEER-04-0010

Task Number 6.2.2

NSF Master Contract Number EEC-9701471

1 Former Graduate Student, Department of Civil, Structural and Environmental Engineering, University at Buffalo, State University of New York
2 Professor, Department of Civil, Structural and Environmental Engineering, University at Buffalo, State University of New York

MULTIDISCIPLINARY CENTER FOR EARTHQUAKE ENGINEERING RESEARCH
University at Buffalo, State University of New York
Red Jacket Quadrangle, Buffalo, NY 14261

Preface

The Multidisciplinary Center for Earthquake Engineering Research (MCEER) is a national center of excellence in advanced technology applications that is dedicated to the reduction of earthquake losses nationwide. Headquartered at the University at Buffalo, State University of New York, the Center was originally established by the National Science Foundation in 1986, as the National Center for Earthquake Engineering Research (NCEER).

Comprising a consortium of researchers from numerous disciplines and institutions throughout the United States, the Center's mission is to reduce earthquake losses through research and the application of advanced technologies that improve engineering, pre-earthquake planning and post-earthquake recovery strategies. Toward this end, the Center coordinates a nationwide program of multidisciplinary team research, education and outreach activities.

MCEER's research is conducted under the sponsorship of two major federal agencies: the National Science Foundation (NSF) and the Federal Highway Administration (FHWA), and the State of New York. Significant support is derived from the Federal Emergency Management Agency (FEMA), other state governments, academic institutions, foreign governments and private industry.

MCEER's NSF-sponsored research objectives are twofold: to increase resilience by developing seismic evaluation and rehabilitation strategies for the post-disaster facilities and systems (hospitals, electrical and water lifelines, and bridges and highways) that society expects to be operational following an earthquake; and to further enhance resilience by developing improved emergency management capabilities to ensure an effective response and recovery following the earthquake (see the figure below).

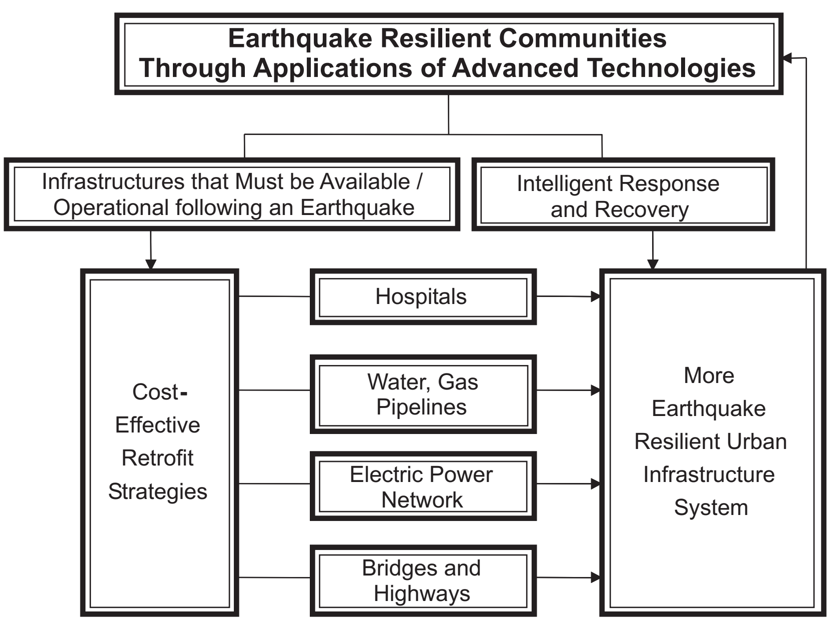

A cross-program activity focuses on the establishment of an effective experimental and analytical network to facilitate the exchange of information between researchers located in various institutions across the country. These are complemented by, and integrated with, other MCEER activities in education, outreach, technology transfer, and industry partnerships.

This report describes an energy dissipation system configuration that extends the utility of fluid viscous damping devices to structural systems that are characterized by small interstory drifts and velocities. The geometry of the brace and damper assembly is such that the system resembles a jacking mechanism, and thus the name "scissor-jack-damper energy dissipation system" is adopted. The system is a variant of the toggle-brace-damper system, and offers the advantage of a more compact configuration. A theoretical treatment of the scissor-jack-damper system is presented and its effectiveness is demonstrated through testing of a large-scale steel framed model structure under imposed harmonic displacement on the strong floor, as well as dynamic excitations on the earthquake simulator. Experiments demonstrate that despite its small size, the scissor-jack system provides a significant amount of damping while also substantially reducing the seismic response of the tested structure. Comparisons of response-history and simplified analyses with the experimental findings produce results that are consistent. Application of the scissor-jack-damper system in a new building structure in Cyprus is described.

ABSTRACT

Installation of damping devices has been limited to diagonal or chevron brace configurations until the recent development of the toggle-brace configurations. These configurations magnify the effect of damping devices, thus facilitating their use in stiff framing systems. Such systems are not good candidates for supplemental damping when conventional diagonal or chevron brace configurations are used, due to the high cost of the damping system. This report introduces the scissor-jack-damper system that was developed as a variant of the toggle-brace-damper systems. An additional advantage of the scissor-jack-damper to the toggle-brace-damper system is in the compactness of the configuration. A theoretical treatment of the scissor-jack-damper system is presented and the effectiveness is demonstrated through testing of a large-scale steel framed model structure under imposed harmonic displacement on the strong floor, as well as dynamic excitations on the earthquake simulator. Experiments demonstrate that despite the small size of the damping device considered, the scissor-jack system provided a considerably significant amount of damping while also substantially reducing the seismic response of the tested structure. Comparisons of response-history and simplified analyses with the experimental findings produce results that are consistent. Application of the scissor-jack-damper system in a new building structure in Cyprus is described.

ACKNOWLEDGMENTS

Financial support for this project was provided by the Multidisciplinary Center for Earthquake Engineering Research (MCEER), tasks on Rehabilitation Strategies for Buildings and Experimental Facilities Network, and by Taylor Devices, Inc., of North Tonawanda, New York. Taylor Devices also manufactured the damping devices.

The authors wish to thank the staff of the Structural Engineering and Earthquake Simulation Laboratory; Mr. Mark Pitman, Mr. Daniel Walch and late Mr. Richard Cizdziel, for their continuous help with the preparation and testing of the model.

TABLE OF CONTENTS

TABLE OF CONTENTS (cont'd)

LIST OF ILLUSTRATIONS

LIST OF ILLUSTRATIONS (cont'd)

LIST OF ILLUSTRATIONS (Cont'd)

LIST OF ILLUSTRATIONS (cont'd)

LIST OF TABLES

SECTION 1

INTRODUCTION

1.1 Passive Energy Dissipation Systems

Conventional methods of seismic design rely on ductile behavior of structural members for energy dissipation. Such design is based on the principle that inelastic or nonlinear behavior will take place in selected components of the framing system, in the form of localized and/or spread plastic hinges. Examples include hinging in beams adjacent to the beam-to-column connections in the widely used moment-resisting frame, buckling of braces in a concentrically braced frame, and yielding of shear links in an eccentrically braced frame. The main disadvantage associated with conventional earthquake-resistant design is that all inelastic action (thus energy dissipation) is provided by elements that form part of the gravity-load-resisting system. Any damage to the gravity-load-resisting system as a result of inelastic action is typically costly, or may be irreparable.

In the past decade, the use of supplemental damping devices in building (and bridge) structures has become an increasingly popular approach to remedy the deficiencies inherent in conventional seismic design. These devices, commonly known as 'dampers', dissipate earthquake-induced energy through either hysteretic action (e.g., yielding of metals, sliding friction) or viscoelastic/viscous action (e.g., fluid viscous dampers, solid and fluid viscoelastic dampers). In comparison with conventional earthquake-resistant design, the underlying objective of implementing energy dissipation devices in structural systems is to limit or eliminate damage to the structural frame by dissipating most of the earthquake-induced energy, which would otherwise be absorbed by the load-bearing-system through inelastic deformations. An additional advantage related to the use of energy dissipation devices is that they can be replaced relatively easily after a major seismic event. Besides earthquake protection, viscoelastic and viscous energy dissipation systems are eminently suitable for reducing wind-induced vibrations. The interested reader is referred to the following for a comprehensive review of this technology: Federal Emergency Management Agency (1997), Soong and Dargush (1997), Constantinou et al. (1998), and Hanson and Soong (2001).

Today, many countries utilize various types of damping devices as protective systems. The advantages offered by supplemental energy dissipation systems and the increasing number of applications utilizing these systems in the design or retrofit of building structures have spurred the need for systematic, robust and validated guidelines for the modeling, analysis, design and testing of various damping devices. Extensive analytical and experimental studies have been conducted that have investigated various kinds of supplemental damping systems, leading to a better understanding of the characteristics of damping devices and their effects on the earthquake response of structures. Analysis and design tools towards implementing these systems in the construction of new earthquake-resistant structures, as well as in the retrofit of existing structures for improved seismic performance have subsequently been proposed. Furthermore, several code-oriented documents, provisions and guidelines, on the design, testing and incorporation of damping devices in building structures have been developed. The most up-to-date of these publications are those of the Federal Emergency Management Agency (*FEMA 273 Guidelines* and *FEMA 274 Commentary* 1997, *FEMA 356 Prestandard and Commentary* 2000, *FEMA 368 Provisions* and *FEMA 369 Commentary* 2000, and the upcoming *FEMA* 2003), which contain the latest analysis and design guidelines for buildings with energy dissipation systems, as well as with seismic isolation systems. An overview of the code-oriented procedures related to the implementation of passive energy dissipation devices in building structures developed since the 1990s can be found in the recent work of Ramirez (Ramirez et al. 2001). This work concentrates on analysis and design procedures for displacement- and velocity-dependent dampers in new buildings and was utilized in writing the section on Structures with Damping Systems of FEMA 368 (2000) and the upcoming FEMA (2003).

The application of seismic energy dissipation systems differs in various countries. In Japan, the majority of the applications utilize yielding steel devices and viscoelastic fluid or solid devices. In the United States, engineers have primarily used fluid viscous dampers. In all of these applications, damping devices have either been installed in-line with diagonal bracing or as horizontal elements atop chevron bracing (Soong and Dargush 1997, Constantinou et al. 1998). The popularity of these configurations is based on the engineers' familiarity with such bracing systems in steel construction and the fact that all experimental research studies have utilized only these two configurations for energy dissipation systems.

Stiff structural systems such as reinforced concrete shear wall or steel-braced dual systems undergo small interstory drifts and velocities when subjected to dynamic excitation. Since significant drifts and velocities are required for effective energy dissipation, it may appear that such systems are not suitable for the addition of damping devices. This observation is valid in the case of conventional damper configurations involving diagonal or chevron installations, in which, the damper displacement is less than or equal to the interstory drift. For example, in a stiff code-compliant building, interstory displacements will likely not exceed 15 mm (0.6 in) in the design earthquake. Conventionally configured damping systems in such a building will require large damper forces for moderate levels of supplemental damping, leading to an increase in the cost of the damping system. In addition, small-stroke damping devices require special detailing, which further increases their size and therefore, their cost.

Given that the major shortcomings associated with conventional configurations of supplemental damping systems in stiff structures are due to small interstory drifts and velocities, one might reasonably ponder the possibility of using non-traditional configurations that can magnify the damper displacement for a given interstory drift. Such magnification allows for the use of dampers with smaller force outputs (smaller damper volume) and larger strokes, resulting in reduced cost. These configurations can be used for stiff and flexible framing systems, as well as for limiting vibrations caused by wind.

A variety of mechanisms that can magnify displacements can be inspired by experiences in other disciplines, especially mechanical engineering. One may find it helpful to review one of the many publications with illustrations of concepts and devices in this field (e.g., Chironis 1991). While magnifying mechanisms are widely utilized in the construction and operation of machinery, their use in applications of earthquake and wind vibration protection of structures, however, is a novel approach.

1.2 Scope and Organization of this Report

This report describes an energy dissipation system configuration that extends the utility of fluid viscous damping devices to structural systems that are characterized by small interstory drifts and velocities. The geometry of the brace and damper assembly is such that the system resembles a jacking mechanism, and thus the name "scissor-jack-damper energy dissipation system" is adopted. The development of this configuration followed that of the toggle-brace-damper system, also developed and tested at the University at Buffalo (Hammel 1997, Constantinou et al. 1997, and Constantinou et al. 2001). Both systems utilize innovative mechanisms to amplify displacements and accordingly lower force demands in the energy dissipation devices. The magnifying mechanism in turn amplifies the damper force through its shallow truss configuration and delivers it to the structural frame. In addition to overcoming the limitations related to small drifts, the scissor-jack-damper system allows for open space due to its compact geometry and is therefore desirable architecturally.

This report consists of eight sections, followed by a list of references and the appendices. The concept underlying the scissor-jack-damper system and discussions on various issues that affect its behavior are presented in Section 2. Section 3 describes the experimental program, which includes strong floor tests with imposed cyclic displacement and earthquake-simulator testing. Sample results from the experimental program are given in Section 4. Section 5 focuses on the analytical modeling of the tested structure and prediction of response using the program SAP2000. Section 6 presents an overview of simplified analysis methods for structures with added damping systems, and illustrates the application of these methods to the tested model to estimate its fundamental period and damping ratio. Prediction of peak dynamic response from displacement and acceleration response spectra of ground motions is also illustrated in this section. Section 7 introduces the first application of the scissor-jack-damper system in the design of a new building structure in Cyprus. Summary and conclusions are outlined in Section 8. References and four appendices (including manufacturing drawings, strong floor and earthquake simulator test results and an input file for response-history analysis) follow. Parts of the work described in this report have previously been presented or briefly described in several conferences and publications (Whittaker and Constantinou 1999a, 1999b and 2000, Constantinou et al. 2000, Constantinou 2000, Constantinou and Sigaher 2000, and Hanson and Soong 2001). The first detailed publication on the scissor-jack-damper system is Sigaher and Constantinou (2003), which essentially represents a summary of this report.

SECTION 2

SCISSOR-JACK-DAMPER ENERGY DISSIPATION SYSTEM

2.1 Energy Dissipation Systems with Magnifying Mechanisms

It is possible to encounter in the field of mechanics and engineering a number of configurations that magnify displacements and hence can be implemented in energy dissipation systems for stiff structures.

The DREAMY damping system, developed by the Taisei Corporation in Japan, utilizes such a magnifying mechanism (Hibino et al. 1989). As illustrated in Figure 2-1, this system makes use of the lever principle to magnify displacements (the deformed configuration in Figure 2-1 is valid provided that the bracing is rigid). Also shown in Figure 2-1 are the relationships between the lateral interstory drift u and the damper deformation u_D, and the damping shear force F and the damper force F_D, in which f denotes the displacement magnification factor. The DREAMY system is simple in concept and is functional. The drawbacks, however, are the sizeable dimensions, large sections (due to the presence of bending forces) and details involved in the pin connections, which make this system cumbersome to construct.

Kani et al. (1992) have designed a similar system comprised of an inverted T-shaped lever and a pair of fluid dampers, which amplify the damping effect.

Another energy dissipation system that makes use of a magnifying technique is the "coupled truss and damping system" that was utilized in the construction of the 57-story Torre Mayor building in Mexico City (Rahimian 2002, Taylor 2003). Developed in the United States by the Cantor Seinuk Group, this system includes a damping mechanism between a pair of vertical trusses, which primarily deflect in cantilever mode under an external load. To illustrate the concept, Figure 2-2 depicts a simplified model of a floor from a multi-story, high-rise building. The springs represent the effect of the axial flexibility of the stacked columns supporting the floor. Upon an external force, both trusses move in cantilever motion (angle θ) so that the truss columns AC and BD are displaced vertically in opposite directions (note the presence of vertical displacement v in addition to lateral drift u). Nodes C and B at each end of the damper element thus move through a longer relative distance, which results in a larger damper stroke in comparison to conventional diagonal configurations (i.e., without the truss systems). The desired

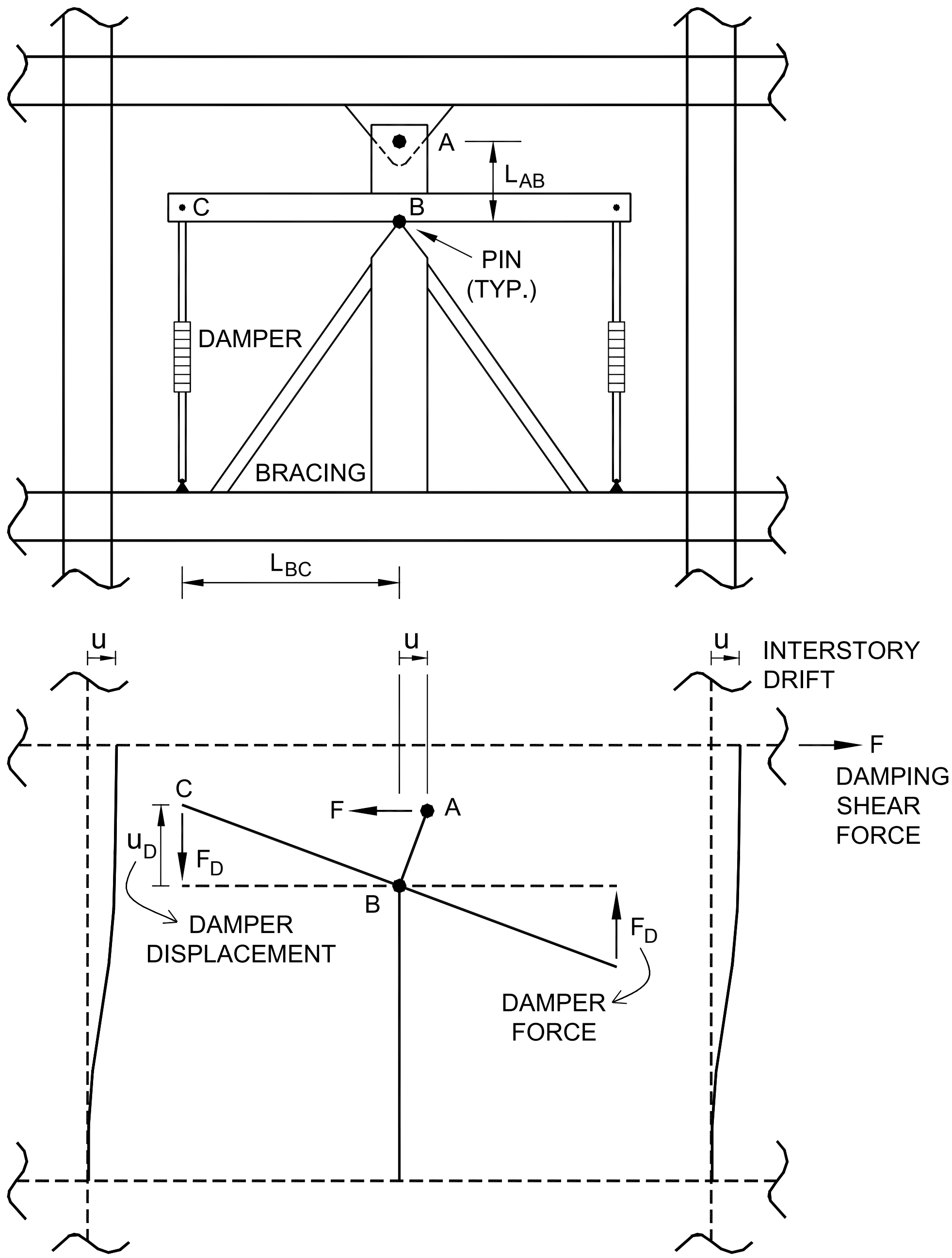

$$u_D = f \cdot u$$

$$f = L_{BC} / L_{AB}$$

$$F = 2 \cdot f \cdot F_D$$

Figure 2-1 Illustration of DREAMY System of Taisei Corporation

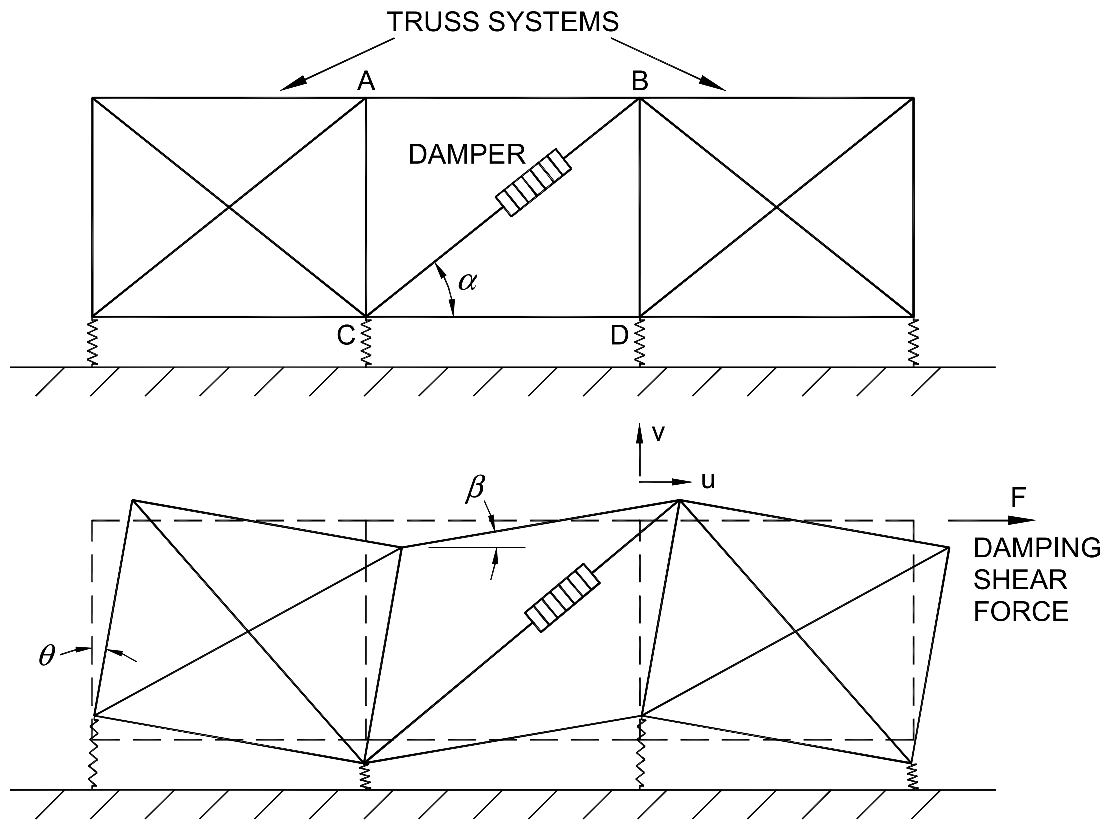

$$u_D = u \cdot cos\,\alpha + v \cdot sin\,\alpha$$

$$F = cos\,\alpha \cdot F_D$$

Figure 2-2 Illustration of Coupled Truss Systems with Damping

cantilever action can also be achieved with the use of solid walls. In the Torre Mayor, a variation of the configuration shown in Figure 2-2 was adapted such that the dampers were placed in-line with diagonal braces, which were configured as diamonds along the height of the building. Since the efficiency of the coupled truss and damping system increases at the upper levels of a building (the effect of the axial flexibility of the supporting columns is more pronounced at upper levels), the system is suitable mostly for high-rise buildings.

In the United States, the recent construction of one 38-story and two 37-story buildings utilizing a "toggle-brace" configuration has been an exception to the custom of using diagonal or chevron brace configurations for damping systems. The toggle-brace-damper system was developed and tested at the University at Buffalo, and is illustrated in Figure 2-3.

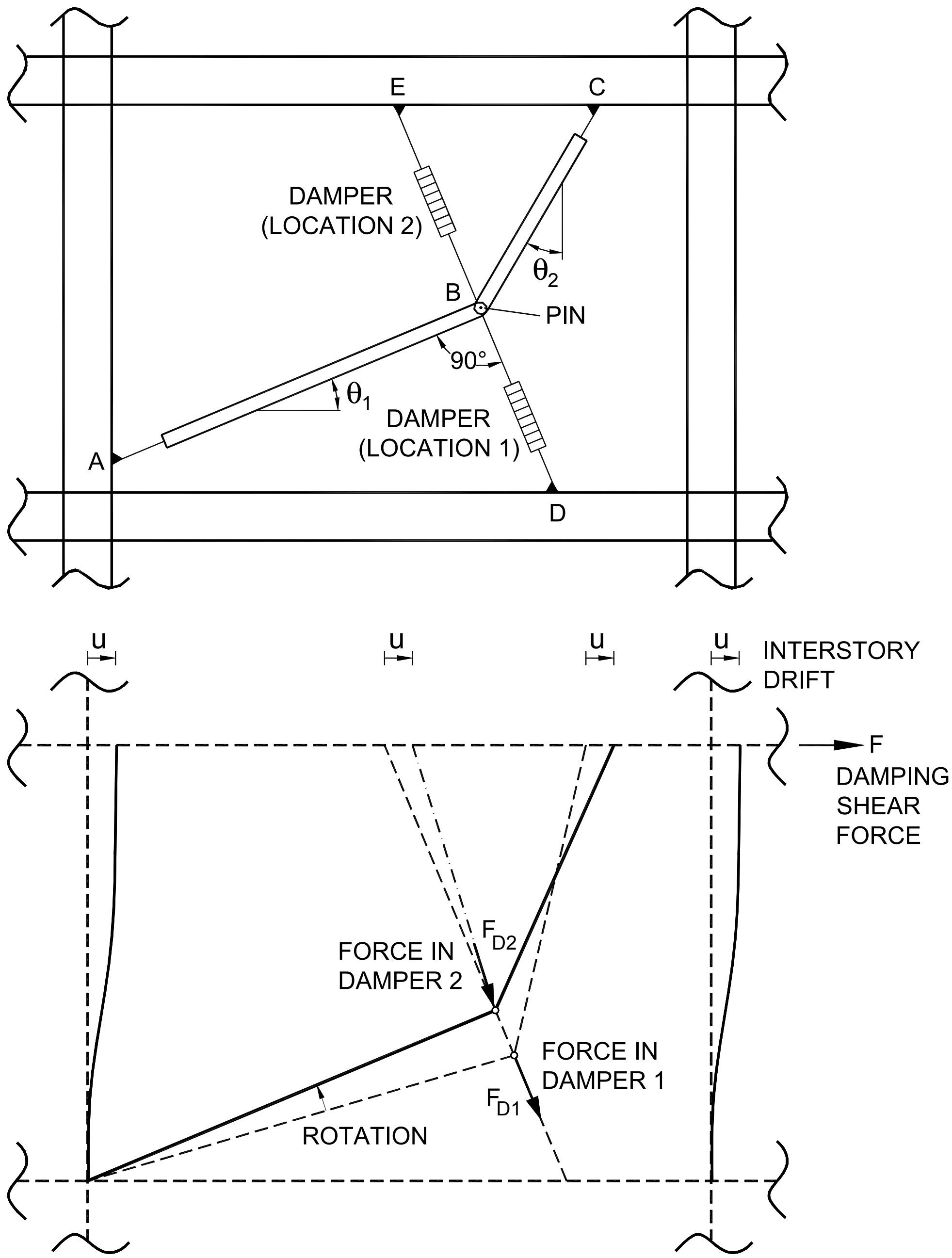

Location 1: $u_{D1} = f_1 \cdot u\,, \quad f_1 = \dfrac{sin\,\theta_2}{cos(\theta_1 + \theta_2\,)}$

Location 2: $u_{D2} = f_2 \cdot u\,, \quad f_2 = \dfrac{sin\,\theta_2}{cos(\theta_1 + \theta_2\,)} + sin\,\theta_1$

$$F = f_1 \cdot F_{D1} + f_2 \cdot F_{D2}$$

Figure 2-3 Illustration of Toggle-Brace-Damper System

As the name implies, this configuration operates based on the toggle mechanism (toggles *ABC* in Figure 2-3), which amplifies the damper displacement for a given interstory drift. This amplification results in reductions in the required damping force and damper size, which may lead to cost savings. The damper force output is magnified through the toggle mechanism and delivered to the framing system by compression or tension in the braces. The toggle-brace configuration is suitable for applications of wind-response reduction and seismic risk mitigation for stiff structures. A theoretical treatment of the system's behavior, along with experimental results confirming the validity of the concept and the developed theory can be found in Hammel (1997), Constantinou et al. (1997), and Constantinou et al. (2001). The last of these references also provides a brief description of the applications in the United States.

An additional consideration related to the application of energy dissipation systems is that in many cases the energy dissipation assemblies occupy entire bays in frames and often violate architectural requirements such as open space and unobstructed view. With the intent of providing an architecturally attractive solution, the scissor-jack-damper system was developed as a variant of the toggle-brace-damper system. The scissor-jack configuration combines the displacement magnification feature with small size, which is achieved through compactness and a near vertical installation.

2.2 Scissor-Jack-Damper Theory

The scissor-jack-damper system is best explained by first reviewing the conventional diagonal and chevron brace configurations, in which the displacement of the energy dissipation devices is either less than (case of diagonal brace) or equal to (case of chevron brace) the drift of the story at which the devices are installed. Consistent with the previous notations of Figures 2-1 to 2-3 if u and u_D denote the interstory drift and the damper relative displacement, respectively, then

$$u_D = f \cdot u \quad (2\text{- }1)$$

where $f =$ magnification factor. For the chevron brace configuration, $f = 1.0$; for the diagonal configuration $f = cos\theta$, where $\theta =$ angle of inclination of the damper with respect to the horizontal axis. The force F_D along the damper axis is similarly related to F, the horizontal component of the damper force exerted on the frame at the degree of freedom u through

$$F = f \cdot F_D \tag{2- 2}$$

Figure 2-4 illustrates a single-story structure with diagonal and chevron brace configurations. Also shown in the figure are the force *F*, and the interstory drift *u*. Consider that this single-story structure has an effective weight *W* and a fundamental period under elastic conditions *T*, and that it is equipped with a linear fluid viscous damper for which

$$F_D = C_o \cdot \dot{u}_D \tag{2- 3}$$

where C_o = damping coefficient and $\dot{u}_D$ = relative velocity between the ends of the damper along its axis. The damping force *F*, exerted on the frame by the damper assembly is given by

$$F = C_o \cdot f^2 \cdot \dot{u} \tag{2- 4}$$

in which $\dot{u}$ = interstory velocity. It follows that the damping ratio of a single-story frame with a linear fluid viscous device can be written as

$$\beta = \frac{C_o \cdot f^2 \cdot g \cdot T}{4 \cdot \pi \cdot W} \tag{2- 5}$$

It is essential to realize the effect of the magnification factor on the damping ratio. As (2-5) suggests, the damping ratio varies proportionally with the square of the magnification factor. In the two conventional configurations in Figure 2-4, a damper designed to provide a damping ratio of 5-percent of critical when installed horizontally (chevron brace), will provide a damping ratio of 3.2-percent of critical in the diagonal configuration.

In contrast to the familiar diagonal and chevron brace configurations, the scissor- jack configuration can achieve magnification factors substantially greater than unity. This is also true for the toggle-brace-damper systems. Figure 2-4 also illustrates the scissor-jack-damper and toggle-brace-damper systems as implemented in a single-story frame. These systems make use of shallow trusses that amplify the effect of the interstory drift on the damper displacement and also amplify the small damper force and deliver it to the structural frame. The expression for the magnification factor *f* under the assumption of small rotations, and its value for a typical geometry are also given in Figure 2-4. A substantial increase in the damping ratio with respect to that provided by conventional damper configurations demonstrates the efficacy of these systems.

Diagonal	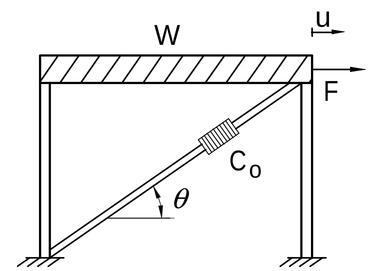	$f = \cos\theta$	$\theta = 37^{o}$ $f = 0.80$ $\beta = 0.03$
Chevron	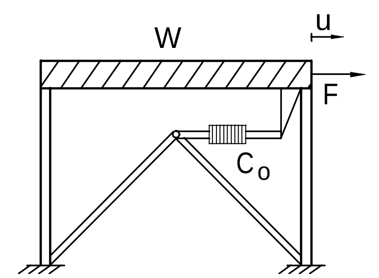	$f = 1.00$	$f = 1.00$ $\beta = 0.05$
Scissor-Jack	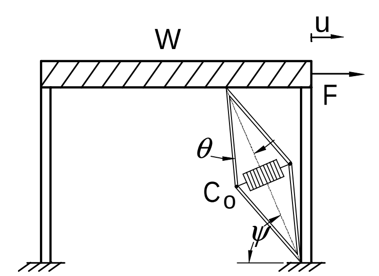	$f = \dfrac{\cos\psi}{\tan\theta}$	$\theta = 9^{o}, \psi = 70^{o}$ $f = 2.16$ $\beta = 0.23$
Upper Toggle	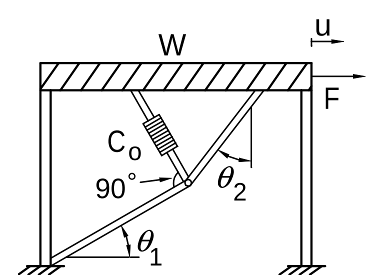	$f = \dfrac{\sin\theta_2}{\cos(\theta_1 + \theta_2)} + \sin\theta_1$	$\theta_1 = 31.9^{o}, \theta_2 = 43.2^{o}$ $f = 3.191$ $\beta = 0.509$
Reverse Toggle	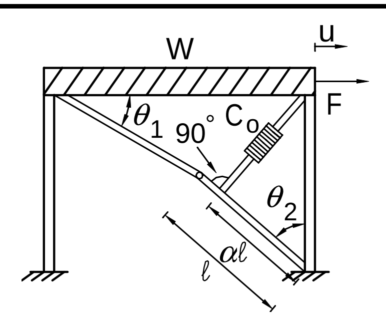	$f = \dfrac{\alpha\cos\theta_1}{\cos(\theta_1 + \theta_2)} - \cos\theta_2$	$\theta_1 = 30^{o}, \theta_2 = 49^{o}$ $\alpha = 0.7$ $f = 2.521$ $\beta = 0.318$

Figure 2-4 Illustration of Diagonal, Chevron Brace, Scissor-Jack-Damper, and Toggle-Brace-Damper Configurations, Magnification Factors, and Damping Ratios of Single-Story Structure with Linear Fluid Viscous Devices

The presence of the magnifying mechanism in the scissor-jack system extends the utility of fluid viscous devices to cases of small interstory drifts and velocities, which are typical of stiff structural systems under seismic excitation and structures subjected to wind load. Also, the absence of bending in the system allows the use of small sections and standard connection details. This damper configuration, therefore, may lead to cost savings, provided that the cost of the scissor-jack support framing is not substantially greater than the cost of the framing that would be required to support the dampers in conventional configurations. In addition to the displacement magnification, the scissor-jack system may be configured to allow for open space, minimal obstruction of view and slender configuration, features that are often desired by architects. Figure 2-5 illustrates various possible installation configurations of a scissor-jack damping system.

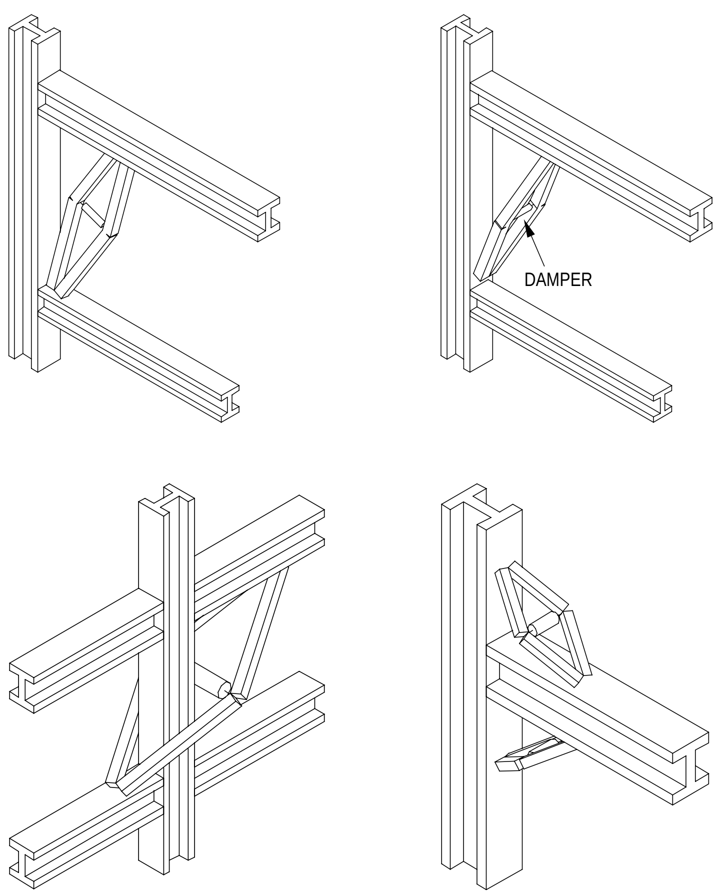

Figure 2-5   Possible Installation Configurations of Scissor-Jack Damping System

2.3 Magnification Factor and Forces in Scissor-Jack System

The effectiveness of the scissor-jack configuration is based on the magnification factor f, defined as the ratio of damper displacement, u_D, to the interstory drift, u. Figure 2-6 presents an analysis of the movement of a single-story frame with a scissor-jack system. The magnification factor is

$$f = \frac{u_D}{u} = \frac{\left|\overline{A'B'} - \overline{AB}\right|}{u} \tag{2- 6}$$

where $\overline{AB}$ and $\overline{A'B'}$ denote the initial and the deformed lengths of the damper, respectively.

It should be noted that the deformed configuration of Figure 2-6 does not take into account any deformations in the frame and any reduction in height due to column extensibility. This is also true for the configurations presented in Figure 2-4 (and eqns. 2-1 to 2-6), in which the damper displacement u_D relates only to the lateral interstory drift u. The column extensibility has negligible effect on the magnification factor for typical values of interstory drift and for low-rise structures. For high-rise structures, column inextensibility cannot be assumed. Deformations due to column extensibility will cause a decrease in the magnification factor for the configurations shown in Figure 2-4. In fact, the coupled truss and damping configuration (see Figure 2-2) was designed to take advantage of the effect of column rotation and axial flexibility of the supporting columns.

Deformations due to frame action may have notable effect on the magnification factor, regardless of the height of the structure. As an example, consider that the beam in Figure 2-6 is simply connected to the column on the left and rigidly connected to the column on the right. Upon an interstory drift towards the right, the beam will deflect upwards, causing a decrease in the damper deformation and thus, in the magnification factor. The opposite will occur when the beam-to-column connections are reversed. This type of amplification/deamplification of the magnification factor will depend on the relative stiffnesses of the beam and the column, and the position of the point of connection of the scissor-jack on the beam. The effect of the frame deformations will be observed in the test results presented in Section 4. It follows that vertical frame deformations will not affect the damper displacement when the damping system extends between the beam-to-column joints, such as the diagonal, chevron and reverse toggle

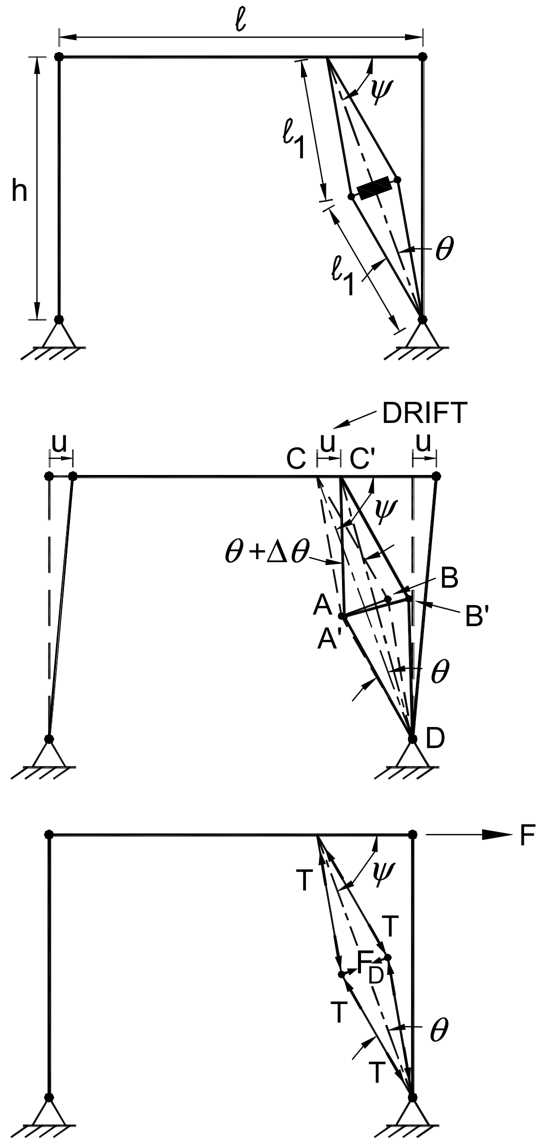

Figure 2-6 Analysis of Scissor-Jack Movement and Analysis of Forces

configurations shown in Figure 2-4.

Whether caused by frame deformations, column rotation and axial flexibility of the supporting columns, vertical deformations may alter the damper displacement and hence the magnification factor of the scissor-jack-damper system. Simple analytical expressions can be written to quantify the effect of vertical deformations on the damper displacement, which will be presented in Section 2.5. The following derivations however, concentrate only on the lateral interstory drift *u*.

In addition to vertical displacements, the displacements due to the forces in the damper and in the scissor-braces (i.e., displacements due to finite stiffness of the scissor-braces) will reduce the magnification factor, regardless of the structural system configuration. This issue will be further explained in the following sections (Sections 2.6 and 6), and its effects will be observed in the test results presented in Section 4.

Based on rigid body kinematics, the damper displacement may be expressed as

$$u_D = \left| \overline{A'B'} - \overline{AB} \right| = \pm 2 \cdot \ell_1 \cdot \left[sin(\theta \pm \Delta\theta) - sin\,\theta \right] \tag{2- 7}$$

where $\Delta\theta$ = angle of rotation of the scissor-braces. Preservation of lengths between points C and D requires that

$$2 \cdot \ell_1 \cdot cos(\theta \pm \Delta\theta) = 2 \cdot \ell_1 \cdot cos\,\theta \mp u \cdot cos\,\psi \tag{2- 8}$$

It must be noted that in writing eq. (2-8), the change in the angle ψ, $\Delta\psi$, is not taken into account. From the deformed configuration of Figure 2-6, one can recognize that $\Delta\psi$ per unit ψ equals the drift ratio, u / h. The drift ratio is typically $u / h \leq 0.01$. For example for $u / h \approx 0.01$, $\Delta\psi \approx 0.01$ rad for $\psi \approx 1$ rad, or $\Delta\psi \approx 0.01 \cdot \psi$. Therefore, $\Delta\psi$ is negligible with respect to $\Delta\theta$ and is not included in the analysis of the scissor-jack movement.

Utilizing eqns. (2-7) and (2-8), the damper displacement and the angle of rotation can be written as

$$u_D = \pm 2 \cdot \ell_1 \cdot \left[sin\left(cos^{-1}\left\{ cos\,\theta \mp \frac{cos\,\psi}{2 \cdot \ell_1} \cdot u \right\} \right) - sin\,\theta \right] \tag{2- 9}$$

$$\pm \Delta\theta = cos^{-1}\left(cos\,\theta \mp \frac{cos\,\psi}{2 \cdot \ell_1} \cdot u \right) - \theta \tag{2- 10}$$

In eqns. (2-7) to (2-10), positive signs hold for drift towards the right (u and $\Delta\theta$ as shown in Figure 2-6) and for damper extension ($u_D > 0$). For drift towards the left, these equations are valid with negative signs.

Equation (2-9) may be used to calculate the damper displacement given a value of drift (provided the latter is small), which is presented in the following subsection. However, the equation cannot be solved for the ratio of two displacements, which is of much practical value. Realizing that for most applications $\Delta\theta$ is very small and u is small in comparison to the dimensions, eqns. (2-7) and (2-8) may be significantly simplified to yield the magnification factor

$$f = \frac{\cos\psi}{\tan\theta} \tag{2- 11}$$

It can be shown that eqns. (2-1) and (2-11) provide a very good approximation to the damper deformation given by (2-9) for $\Delta\theta \leq 0.2 \cdot \theta$. Moreover, (2-11) provides insight into the major factors affecting the performance of the scissor-jack configuration.

The dependence of the magnification factor f on angles θ and ψ is illustrated in Figure 2-7. As the figure suggests, the magnification factor assumes very large values as θ approaches $0°$; but this has no meaning since the scissors tend to act as a single brace inclined at an angle ψ. Rather, when designing such systems, emphasis should be placed on the fact that the magnification factor should have minimal sensitivity to small changes in geometry. A typical geometry is shown in Figures 2-4 and 2-7, which is representative of the tested scissor-jack-damper system (Section 3). Practical values of the magnification factor lie in the range 2 – 5.

In the laboratory, it was possible to configure the scissor-braces within 0.2° of accuracy, and the inclination of the braces was measured frequently. Changes of 0.2° to 0.8° from the original geometry (see Figure 3-1) due to movement in the joints and supports of the model (slippage, distortion), and some inelastic action during repeated testing were observed. It is therefore appropriate to consider changes of ±0.5° in the angles θ and ψ, when designing scissor-brace systems and assessing their sensitivity.

The forces that act on the scissor-jack and on the single-story frame are also shown in Figure 2-6. It should be noted that the frame shown is a mechanism such that force F represents the component of the inertia force that is balanced by forces from the damping system. Considering equilibrium in the original, undeformed configuration reveals the forces that develop in the scissor-braces as

$$T = \frac{1}{2 \cdot \sin\theta} \cdot F_D \tag{2- 12}$$

where T and F_D denote the forces in the brace and damper, respectively. Note that the forces T

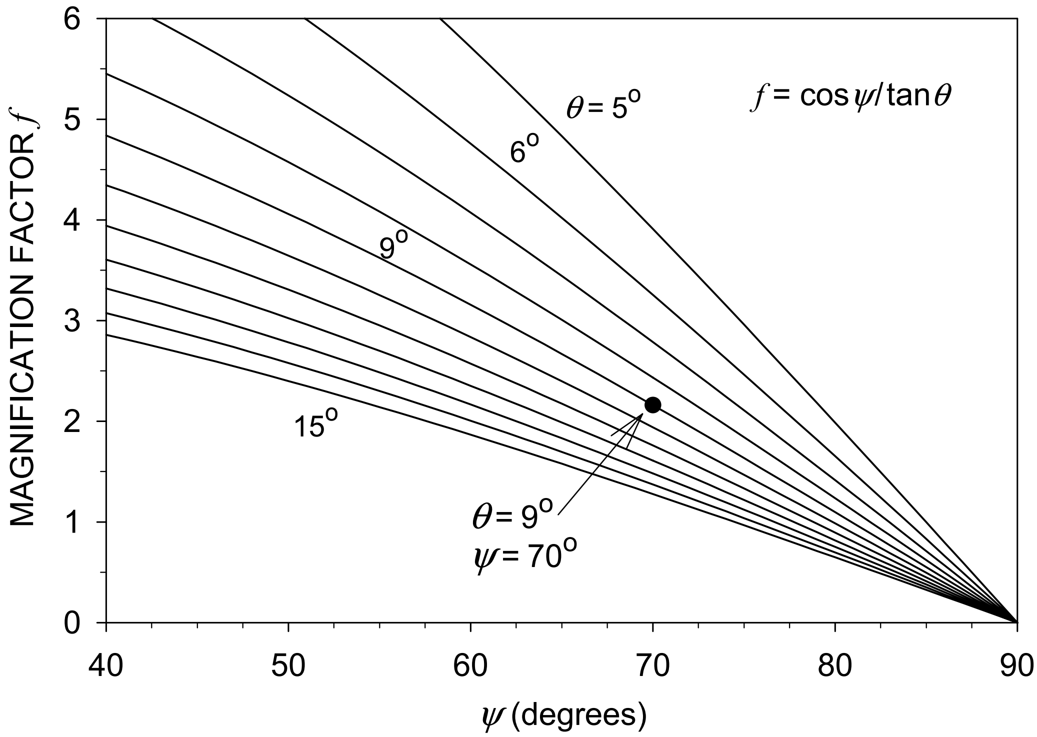

Figure 2-7 Dependency of Magnification Factor on Scissor-Jack Geometry

are greater than the force F_D by a factor of $1/2 \cdot sin\theta$ due to the shallow truss configuration of the scissor-braces. The resultant of the horizontal component of forces T equals force F, that is,

$$F = 2 \cdot T \cdot cos\theta \cdot cos\psi \qquad (2\text{- }13)$$

Equation (2-13) together with (2-12), result in (2-2). That is, the magnification factor can be written as (see eqns. 2-6 and 2-11)

$$f = \frac{u_D}{u} = \frac{F}{F_D} \qquad (2\text{- }14)$$

which proves the accuracy of the analysis presented.

2.4 Analysis of Motion for Large Rotations

The movement of the scissor-jack-damper system for large rotation of the braces can be described using eqns. (2-9) and (2-10). Figure 2-8 presents a comparison of the large rotation (eq. 2-9) and the simplified (eqns. 2-1 and 2-11) relations between the damper displacement and the lateral displacement of the frame, for a geometry that is representative of the tested frame at prototype (full) scale. It must be noted that the large rotation relation requires only the brace length, l_1, to be known. Additional dimensions (l, h) are shown on Figure 2-8 to illustrate what geometry might be used in actual applications.

It is observed that the small rotation theory overpredicts the damper displacement for drift towards the right (positive) and underpredicts the damper displacement for drift towards the left. This phenomenon can be explained by the changes in the geometry of the scissor-jack: for movement towards the right, both angles ψ and θ increase, causing a decrease in the instantaneous magnification factor, which is captured by large rotation analysis. The opposite is true for movement towards the left. The lack of symmetry observed in the damper displacement for positive and negative directions of drift when the large rotation relation is used, is a result of this behavior (see Figures 2-7 and 2-8).

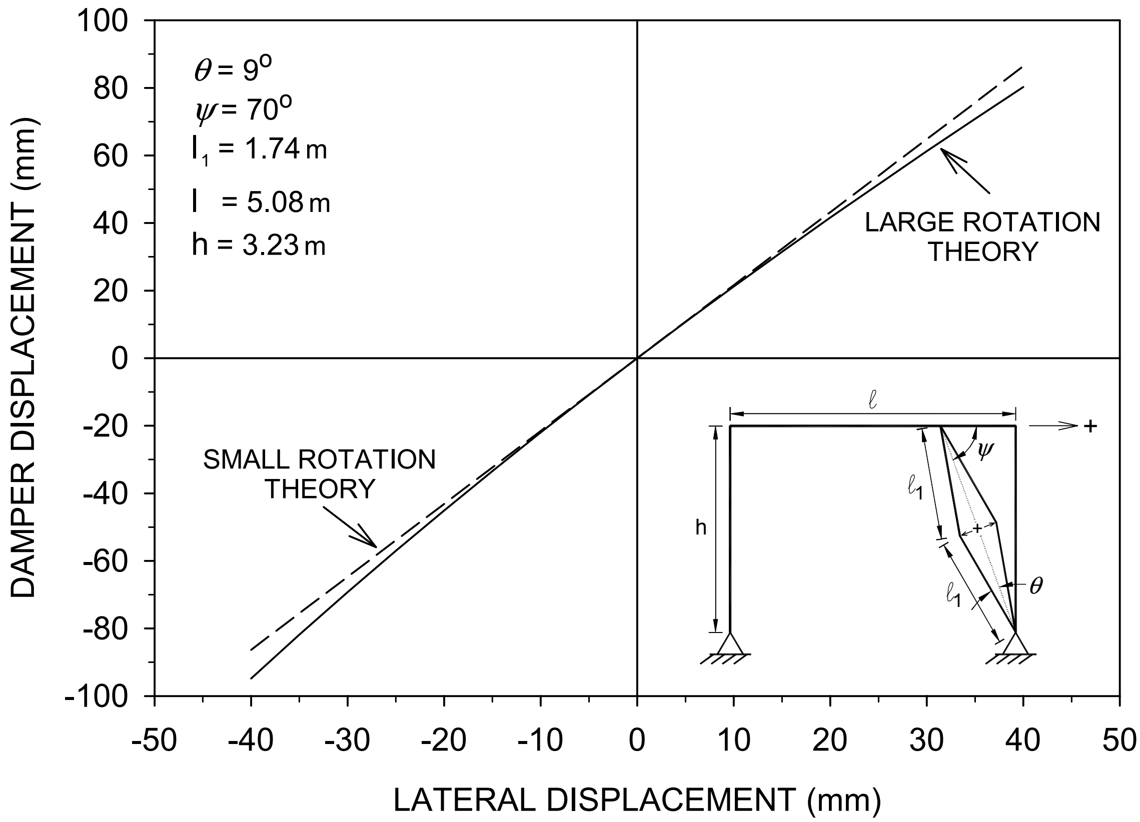

Figure 2-8 Relation between Damper Displacement and Lateral Displacement

2.5 Effect of Vertical Deformations

Previously, the movement of the scissor-jack-damper system was analyzed for lateral interstory drift *u* only. However, the vertical displacements in the frame can also affect the damper deformation in many cases (see Section 2.3). Herein, analysis of the scissor-jack movement (Section 2.3) is revisited, taking into account the effect of vertical deflections of the frame on the damper deformation, and eqns. (2-8) to (2-10) are modified accordingly.

Figure 2-9 presents the deformed configuration of the single-story frame previously depicted in Figure 2-6, inclusive of vertical deformations. Let *v* denote the vertical displacement of point *C* (point of attachment of the scissor-jack to the frame). The lateral interstory drift is denoted by *u*, consistent with the previous notation of Figure 2-6. Assuming all previous sign conventions remain unchanged (i.e., drift towards the right and damper extension are taken positive) and taking downward *v* as positive, the inclusion of *v* can easily be incorporated in (2-8) as

$$2 \cdot \ell_1 \cdot cos(q \pm Dq) = 2 \cdot \ell_1 \cdot cos q \mp ´u \cdot cos y + v \cdot sin y` \qquad (2\text{-}15)$$

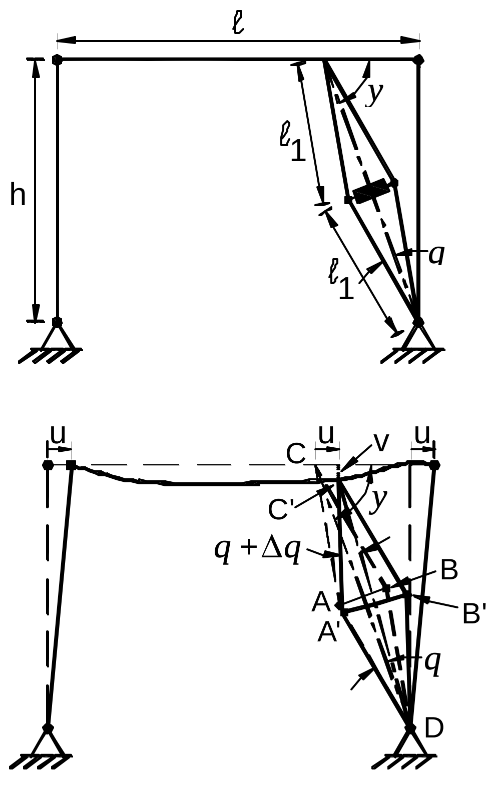

Figure 2-9 Analysis of Scissor-Jack Movement under Horizontal and Vertical Displacements

In light of eqns. (2-7) and (2-15), the damper displacement u_D and the angle of rotation of the scissor-braces Dq can be written as (see eqns. 2-9 and 2-10)

$$u_D = \pm 2 \cdot \ell_1 \cdot \left[sin\left(cos^{-1}\left\{ cosq \mp \frac{(u \cdot cos y + v \cdot sin y)}{2 \cdot \ell_1} \right\} \right) - sinq \right] \qquad (2\text{- }16)$$

$$\pm Dq = cos^{-1}\left(cosq \mp \frac{(u \cdot cos y + v \cdot sin y)}{2 \cdot \ell_1} \right) - q \qquad (2\text{- }17)$$

Since Dq is very small for most applications, eqns. (2-7) and (2-15) may be simplified to give the damper deformation as

$$u_D = u \cdot \frac{cos y}{tanq} + v \cdot \frac{sin y}{tanq} \qquad (2\text{- }18)$$

It must be noted that in the single-story frame of Figure 2-9, the vertical displacement v is shown to be caused by the deformation of the beam only. However, the change of length of the columns may also contribute to the vertical displacement experienced by the damping system.

The vertical displacement v may further be written as a function of the lateral displacement u in the form

$$v = a \cdot u \qquad (2\text{- }19)$$

where a denotes a constant. The magnification factor can then be written as

$$f = \frac{u_D}{u} = \frac{cos y}{tanq} \cdot (1 + a \cdot tan y) \qquad (2\text{- }20)$$

Given the constant a, it is possible to calculate the effect of v on the magnification factor using eq. (2-20). Analysis of the tested frame exclusive of the scissor-jack system resulted in $a \approx \pm 0.1$, where the positive sign corresponds to the rigid-simple beam-to-column configuration (rigid connection on the left and simple connection on the right), which enhances the damper deformation for each direction of drift, and the negative sign represents the simple-rigid beam-to-column configuration. It must be noted that even when the damper force is zero (static conditions), forces develop in the scissor-braces due to friction at the damper-to-brace connections (Section 3), causing $|a|$ to be less than the above quoted value. Figure 2-10 presents the dependency of the magnification factor on angles θ and ψ (calculated using eq. 2-20) for a = ±0.1, superposed upon the results of Figure 2-7 (v = 0).

It is clear from eqns. (2-18) to (2-20), and from Figure (2-10) that calculation of u_D using (2-1), where f is given by (2-11), may overestimate or underestimate u_D (and the related forces and the damping ratio). It will be seen, however, that the use of the theory of the scissor-jack based on lateral drift u only (Sections 2.2 and 2.3) in the application of simplified analysis methods to the tested structure (Section 6) provides results that are in good agreement with the experimental results. This is because in the rigid-simple beam-to-column configuration (for which the analysis was performed), the increase in the magnification factor due to the vertical deformations is offset by the decrease in the magnification factor due to the forces in the damper and in the scissor-braces, so that f given by (2-11) provides satisfactory estimates.

2.6 Effect of Energy Dissipation Assembly Flexibility

The theory and analysis of the scissor-jack-damper system presented in Sections 2.2 and 2.3 are based on the assumption of an infinitely stiff energy dissipation assembly. In general however, the damping system exhibits viscoelastic behavior depending on the geometry, stiffness and damping of the elements comprising the assembly. In the case of a linear viscous damper with a damper coefficient C_o, the energy dissipation assembly can be represented by a spring element in series with the viscous damper. For a multi-story structure, the behavior is then best described by the Maxwell viscoelastic model for which, the horizontal force F_j exerted on the frame at story j by the energy dissipation system is described by

$$F_j + \tau_j \cdot \dot{F}_j = C_{o\,j} \cdot f_j^2 \cdot \dot{u}_j \qquad (2\text{-}21)$$

where $\dot{u}_j$ is the interstory drift velocity at story j, τ_j is the relaxation time which is the ratio of the damping coefficient to the stiffness of the damping assembly at story j, and f_j is the magnification factor at story j. It is of importance to emphasize that the energy dissipation assembly includes, in addition to the damper-bracing assembly, the frame to which all these are connected. Accordingly, the spring component represents the stiffness resulting from a combined action of the braces, damper, and the frame element. For example, significant

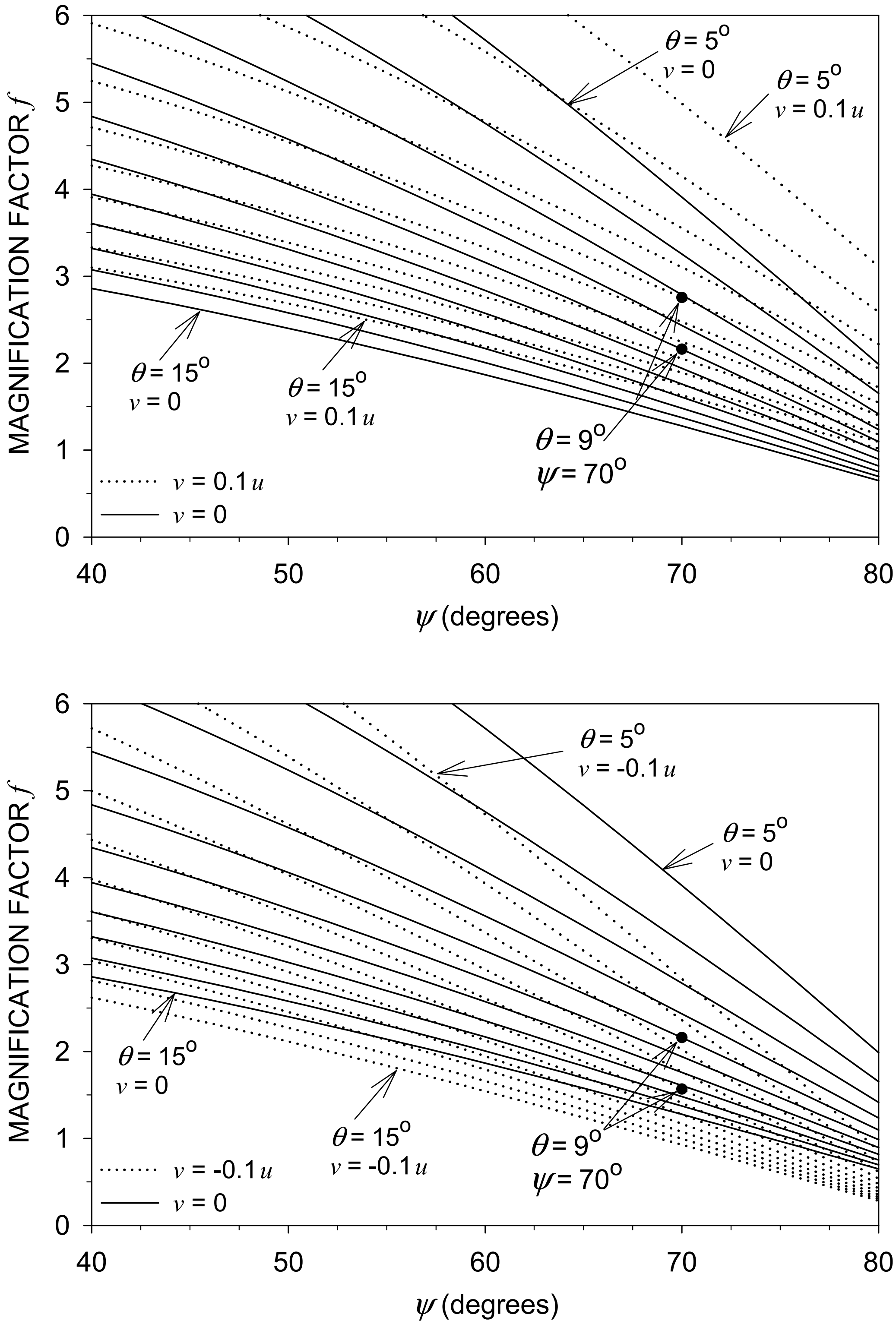

Figure 2-10 Dependency of Magnification Factor on Scissor-Jack Geometry with and without Effect of Vertical Deformations (*a* = 0.1, *top*, and *a* = -0.1, *bottom*)

flexibility will result from frame deformations in structures with scissor-jack-damper systems when installed as shown in Figure 2-4. This is also true for structures with toggle-brace-damper systems as demonstrated by Constantinou et al. (2001). In fact, the development of the reverse toggle-brace-damper system has been motivated by a desire to minimize the flexibility of the energy dissipation assembly.

The force F may be alternatively, in a further simplification, described using the Kelvin viscoelastic model as a function of relative displacement u, and relative velocity $\dot{u}$, as

$$F_j = k'_j(\omega) \cdot f_j^2 \cdot u_j + c'_j(\omega) \cdot f_j^2 \cdot \dot{u}_j \qquad \text{(2- 22)}$$

where k'_j and c'_j are, respectively, the storage stiffness and damping coefficient of the energy dissipation system at story j, which are given by

$$k'_j(\omega) = \frac{C_{oj} \cdot \tau_j \cdot \omega^2}{1 + \tau_j^2 \cdot \omega^2} \quad \text{and} \quad c'_j(\omega) = \frac{C_{oj}}{1 + \tau_j^2 \cdot \omega^2} \qquad \text{(2- 23)}$$

and ω is the frequency of free vibration of the damped structure. The ramifications of the change in the damping force F, from (2-4) to (2-22) are:

a. Introduction of additional lateral stiffness to the frame given by k'
b. Modification (decrease) of the damping coefficient of the frame from C_o to c'
c. Change of the phase angle between the frame damping force, F, and the lateral frame displacement, u, from 90° to Φ, where

$$tan\,\Phi_j = \frac{1}{\tau_j \cdot \omega} \qquad \text{(2- 24)}$$

It should be noted that for infinitely stiff bracing ($\tau_j = 0$), the energy dissipation system behaves as a pure viscous system, and for a single-story structure, eqns. (2-21) to (2-23) reduce to (2-4).

The effect of the flexibility of the energy dissipation assembly on the behavior of the frame will be apparent in the test results presented in Section 4, and will be further studied in the analysis of the tested structure with simplified (approximate) methods (Section 6). The interested reader is also referred to Hanson and Soong (2001) for a comprehensive treatment of this issue.

SECTION 3

EXPERIMENTAL PROGRAM

3.1 Description of Tested Structure

The scissor-jack-damper system was first tested in a frame under an imposed displacement history on the strong floor, and then in a model structure on the earthquake simulator. The model structure was a half-length scale steel frame, which was previously designed and utilized for testing of the toggle-brace-damper system (Hammel 1997, Constantinou et al. 1997, and Constantinou et al. 2001). It consisted of two identical frames that could be tested individually on the strong floor, or together on the earthquake simulator with an added mass on top of the frames. Figure 3-1 illustrates one of the two tested frames with the scissor-jack-damper system. A view of the structure on the earthquake simulator is presented in Figure 3-2. The model features the following characteristics:

1. Beam-to-column connections of the model frames were easily convertible from simple to rigid. This enabled testing with one rigid and one simple connection per frame (referred to as rigid-simple or simple-rigid configurations) and with two rigid configurations per frame (rigid-rigid configuration). The rigid-simple, simple-rigid and rigid-rigid configurations were tested in the strong floor experiments, whereas the earthquake-simulator testing included only rigid-simple and simple-rigid configurations.
2. The scissor-braces were connected to the frame (scissors-to-beam and scissors-to-column connections) utilizing plates, which were designed to undergo mainly rotation. As shown in the detail of Figure 3-1 and in Figure 3-3, these plates were designed with sufficient length to prevent inelastic action. The damper-to-brace connections were designed as true pins to avoid transfer of bending forces to the damper. However, this was not fully accomplished because of the tight pin configuration that exhibited considerable friction. This could be avoided by the use of spherical bushings at both ends of the damper. Figure 3-4 illustrates a close-up of the damper-to-brace connection during installation.
3. The concrete weight used for earthquake-simulator testing comprised of two blocks weighing a total of 142.3 kN, and was secured atop the columns by way of simple

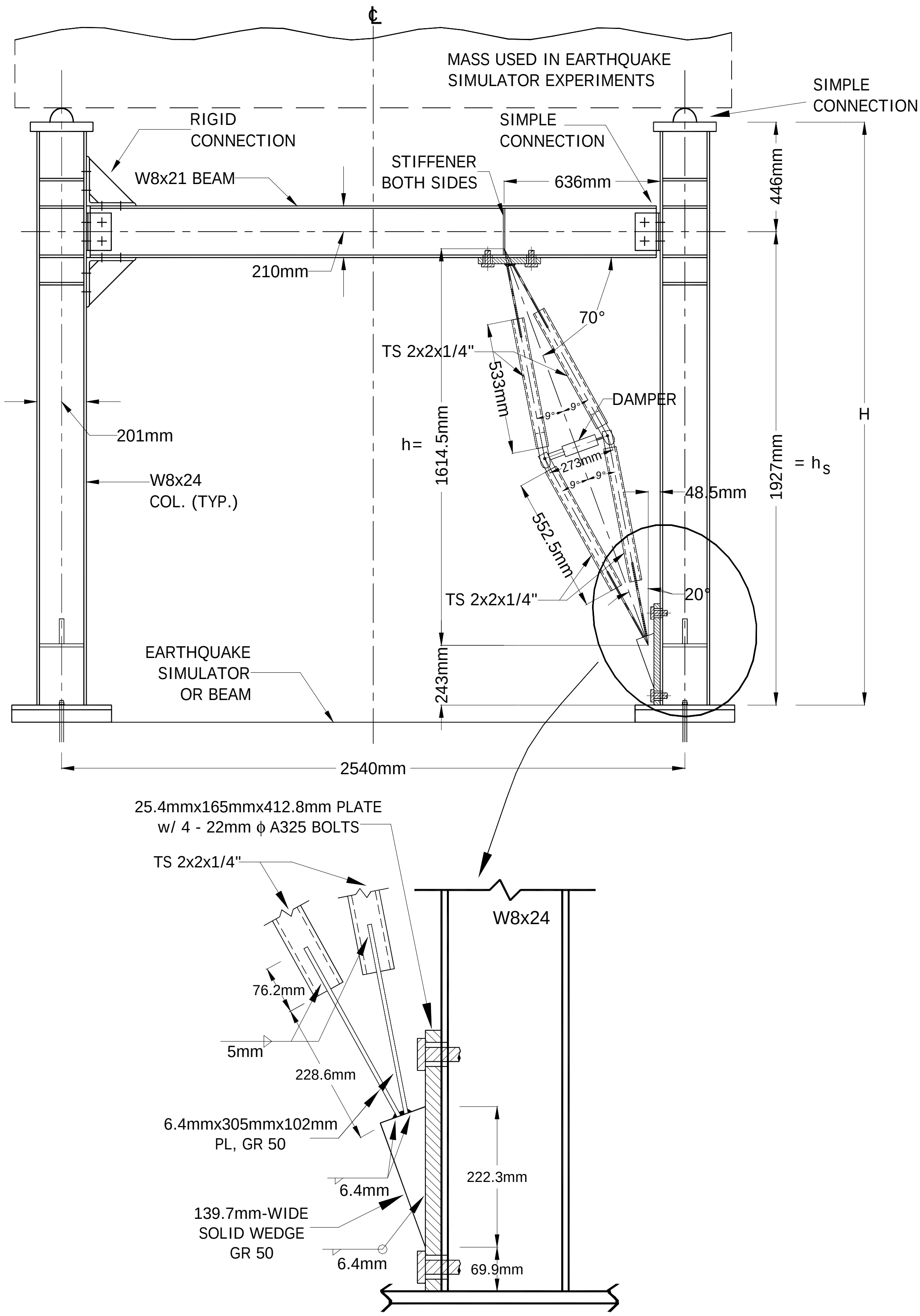

Figure 3-1 Tested Scissor-Jack-Damper Configuration

Figure 3-2 Model with Scissor-Jack Damping System on Buffalo Earthquake Simulator

Figure 3-3 Connection Details of Scissor-Braces to Frame, Scissors-to-Beam (*top*), and Scissors-to-Column (*bottom*) Connection Details

Figure 3-4 Close-up of Damper-to-Brace Connection Detail

connections (see Figures 3-1 and 3-2). The center of mass of these blocks was 1,113 mm above the centerline of the beam.

Further details on the test model, including manufacturing drawings, are presented in Appendix A.

It should be noted that for lateral loading (seismic), the model tested on the earthquake simulator with one rigid and one simple beam-to-column connection (see Figure 3-2) is equivalent to a portal frame with two rigid beam-to-column connections and double bay length. That is, the frame is equivalent to a portal frame of 1,927 mm height and 5,080 mm bay length. It was tested at half-length scale, so the prototype has a height of 3,854 mm a bay length of 10,160 mm. This is illustrated in the sketches of Figure 3-5.

3.2 Fluid Viscous Dampers

A total of three fluid viscous dampers were utilized for the strong floor and for the earthquake-simulator testing. All three dampers were of the run-through piston rod construction (without an accumulator), which prevents changes in the fluid volume upon movement of the piston in either direction, thus the damper operates symmetrically in tension and in compression. In addition, through-rod dampers, unlike dampers with accumulators, are capable of functioning over a very wide frequency range without exhibiting stiffness.

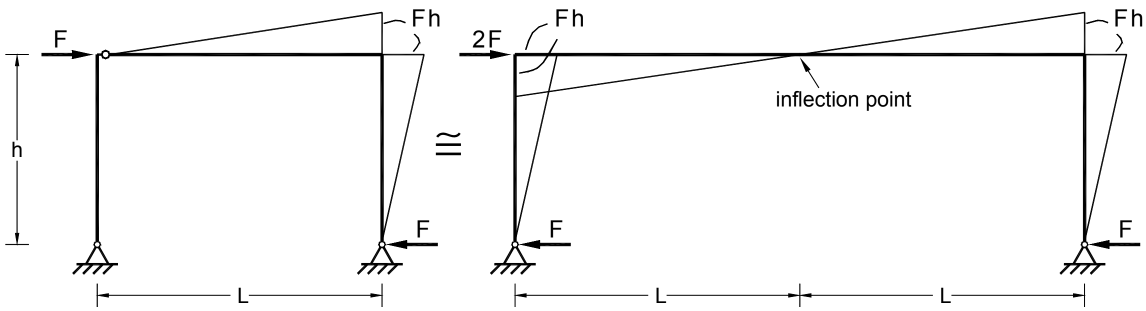

Figure 3-5 Simplified Sketch of Tested Model and Equivalent Portal Frame of Double Bay Length

The geometry of the dampers utilized in the testing of the scissor-jack system is illustrated in Figure 3-6. These dampers were first tested under harmonic motion to extract their characteristics. Figure 3-7 illustrates the testing arrangement in which, sinusoidal motion with specified frequency and amplitude was imposed at the damper piston rod via the actuator, and the resulting reaction force was measured through the load cell. This load cell was also used in the calibration of a strain gage load cell built directly on the body of the damper, for use in the earthquake-simulator testing. Typical recorded force-displacement loops for various frequencies and amplitudes are presented in Figure 3-8. The dampers exhibit purely viscous behavior. From these loops, the peak force - peak velocity characteristics of the dampers were established by extracting the peak force at the instant of zero displacement (peak velocity), as shown in Figure 3-9 (with triangular symbols). It follows that for damper 1 (used in strong floor testing), the behavior is practically linear, which can be described by eq. (2-3) with $C_o = 25.8$ N-sec/mm for velocities up to 500 mm/sec. Dampers 2 and 3 (used in earthquake-simulator testing) could be described as practically having linear behavior for velocities up to 250 mm/sec (with $C_o = 40.0$ N-sec/mm in eq. 2-3). Over a wider range of velocities, these dampers had nonlinear behavior which can be described via $F_D = C_{No} \cdot \dot{u}_D{}^{\alpha}$, where $C_{No} = 137.3$ N-(sec/mm)$^{\alpha}$ and $\alpha = 0.76$.

3.3 Testing of Frame with Scissor-Jack System

One frame with the scissor-jack system (as shown in Figure 3-1) was subjected to sinusoidal displacement of various frequencies and amplitudes at its beam-to-column connection. The

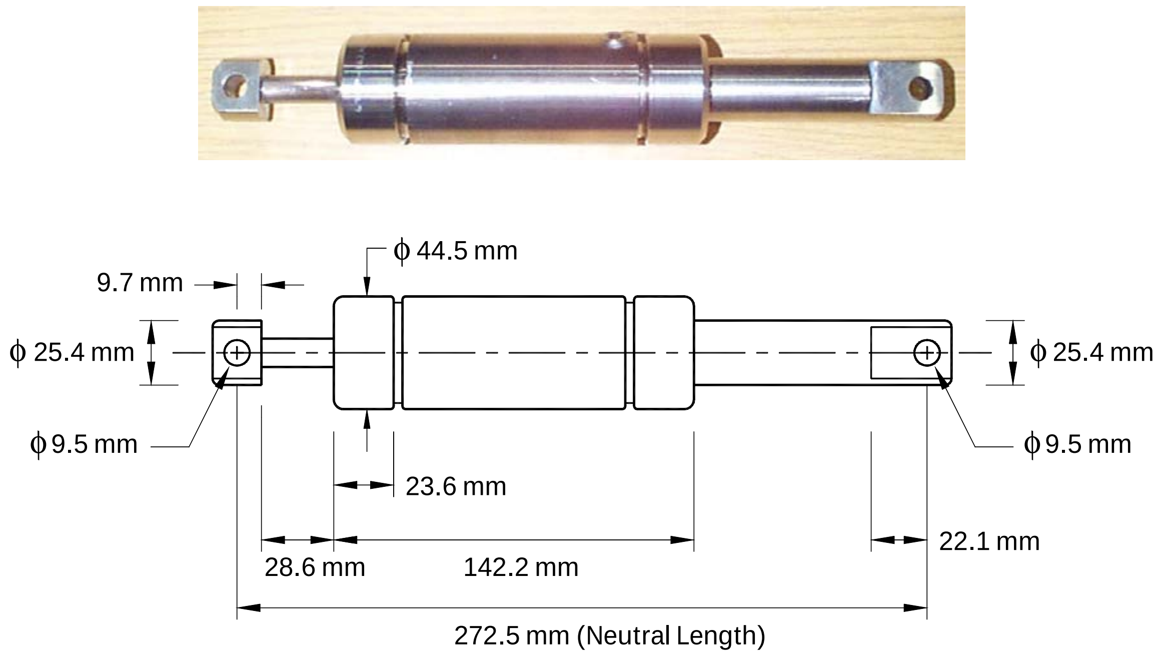

Figure 3-6 View of Fluid Viscous Damper (*top*), and Illustration of Its Geometry (*bottom*)

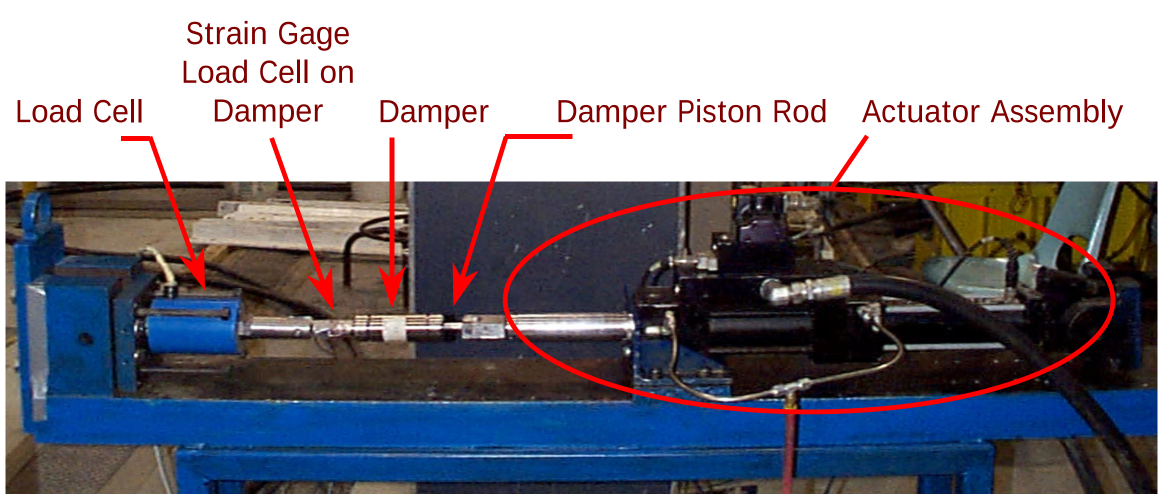

Figure 3-7 View of Damper Test Setup

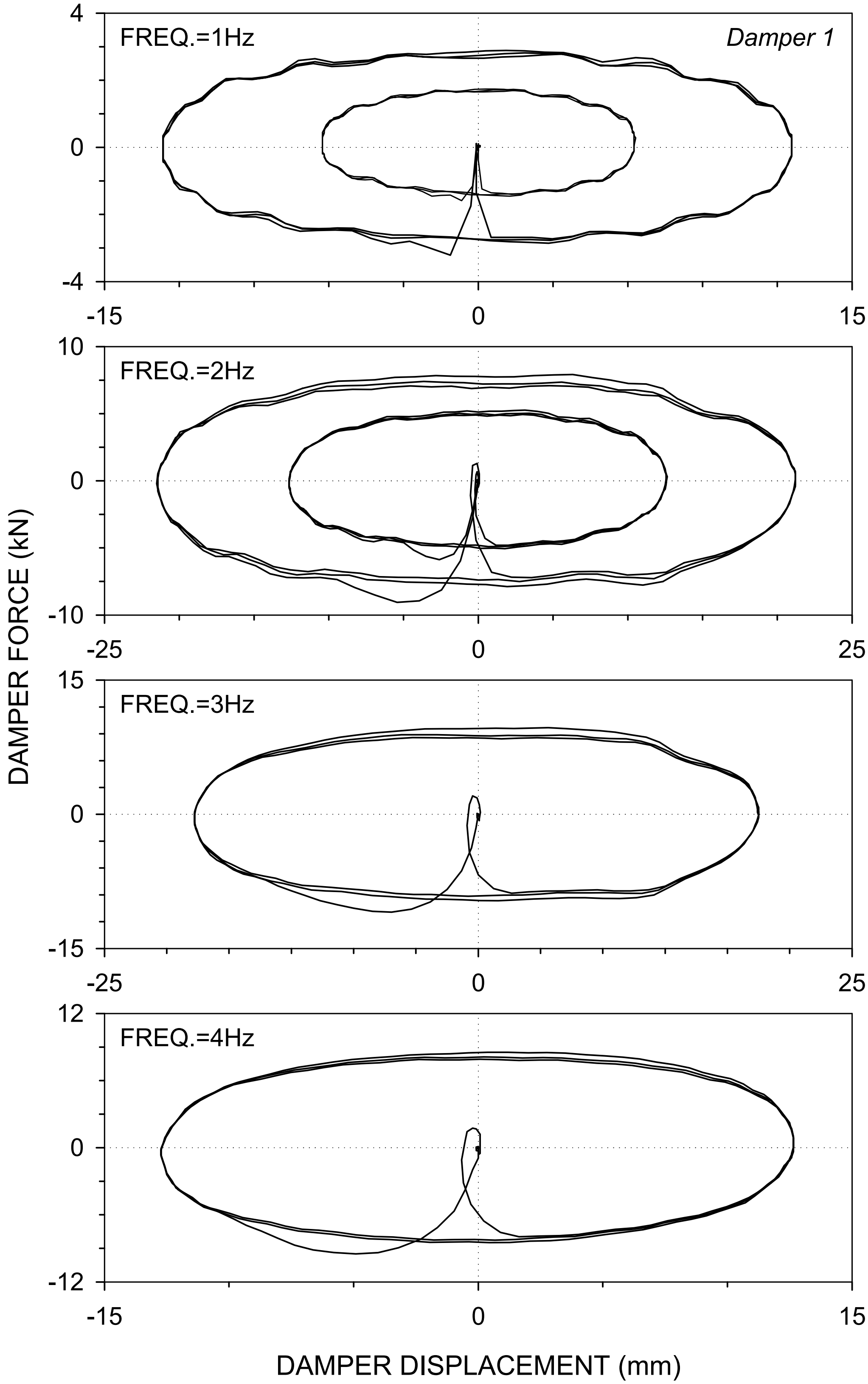

Figure 3-8 Recorded Force-Displacement Loops of Fluid Viscous Damper

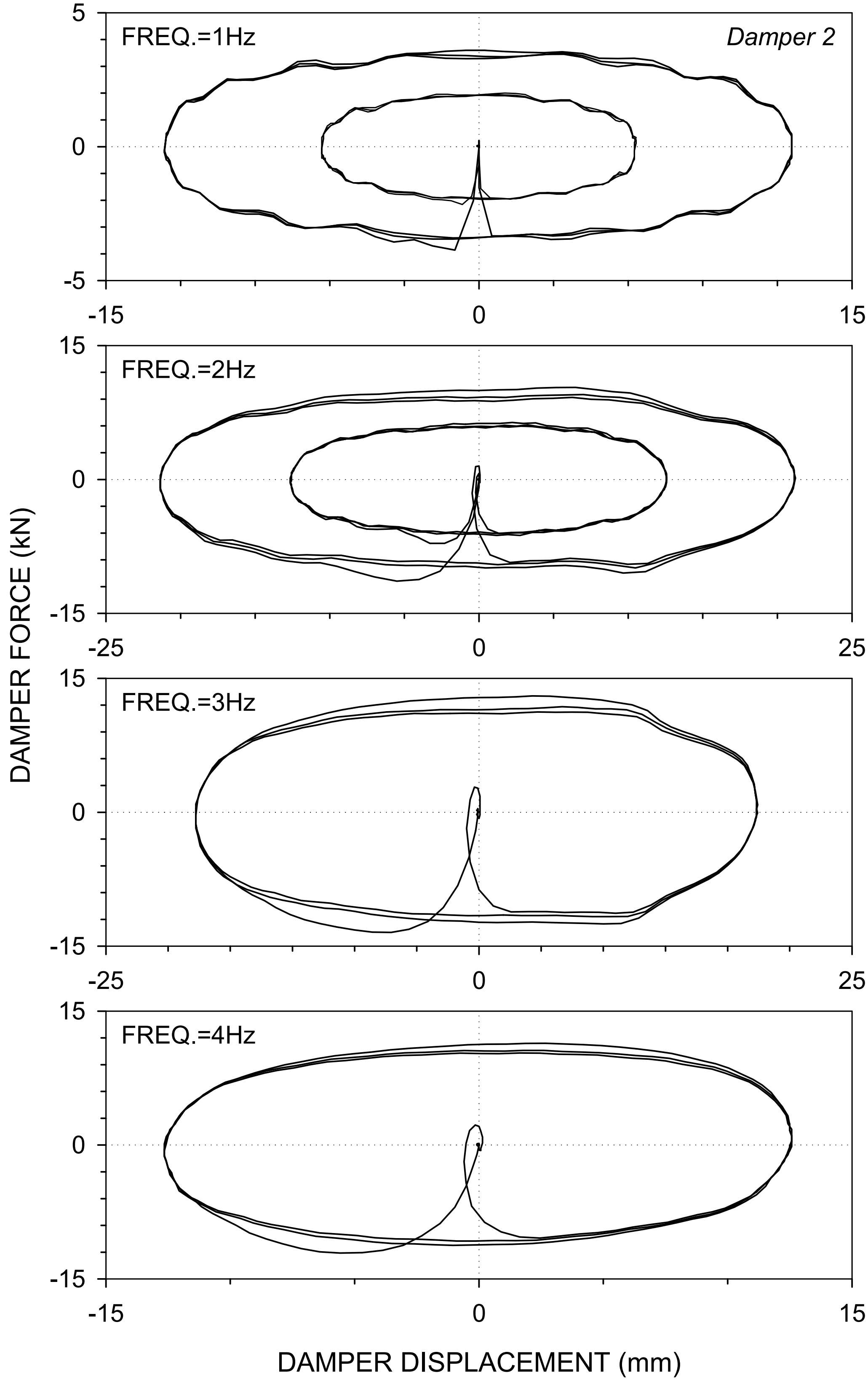

Figure 3-8 (Continued) Recorded Force-Displacement Loops of Fluid Viscous Damper

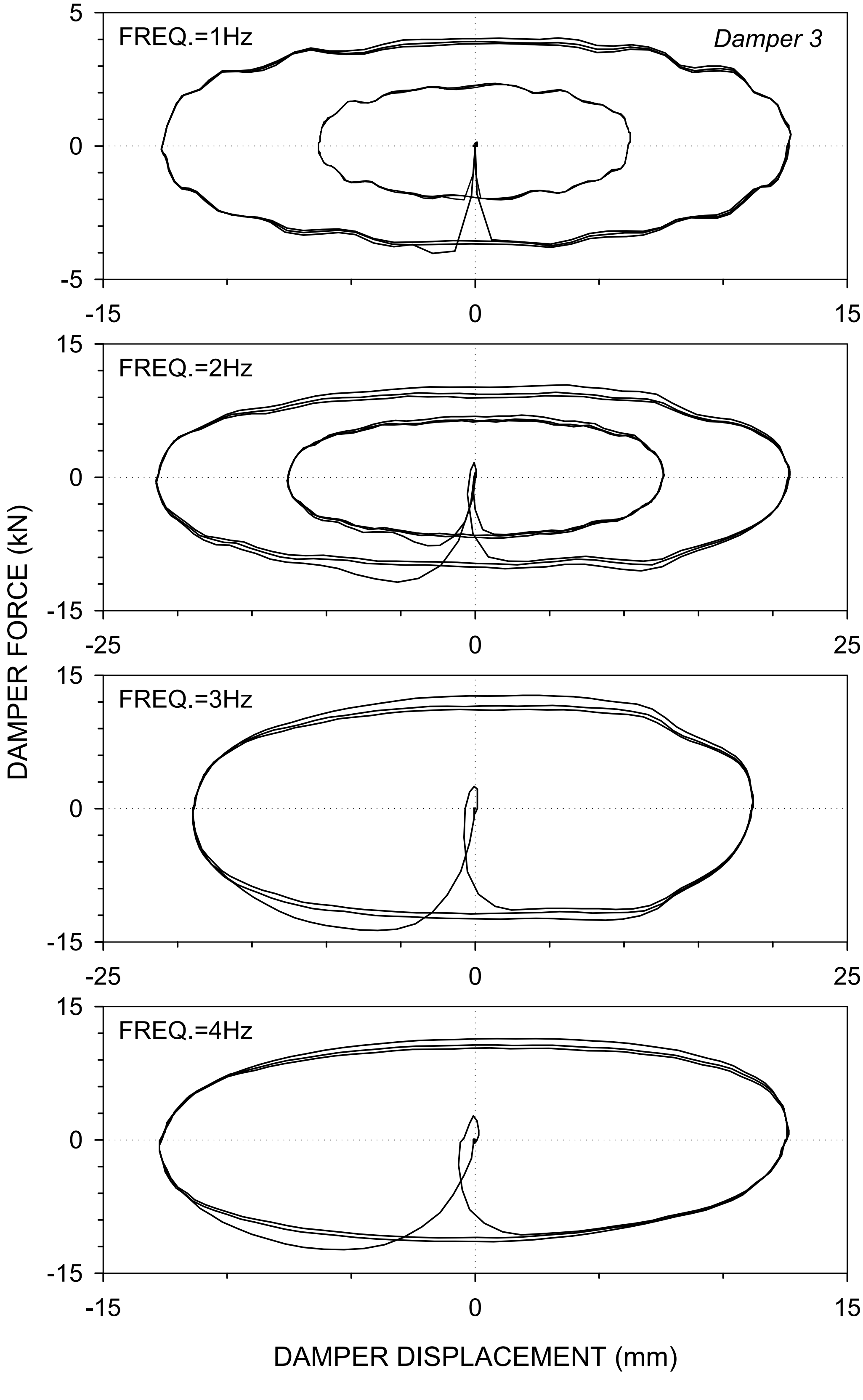

Figure 3-8 (Continued) Recorded Force-Displacement Loops of Fluid Viscous Damper

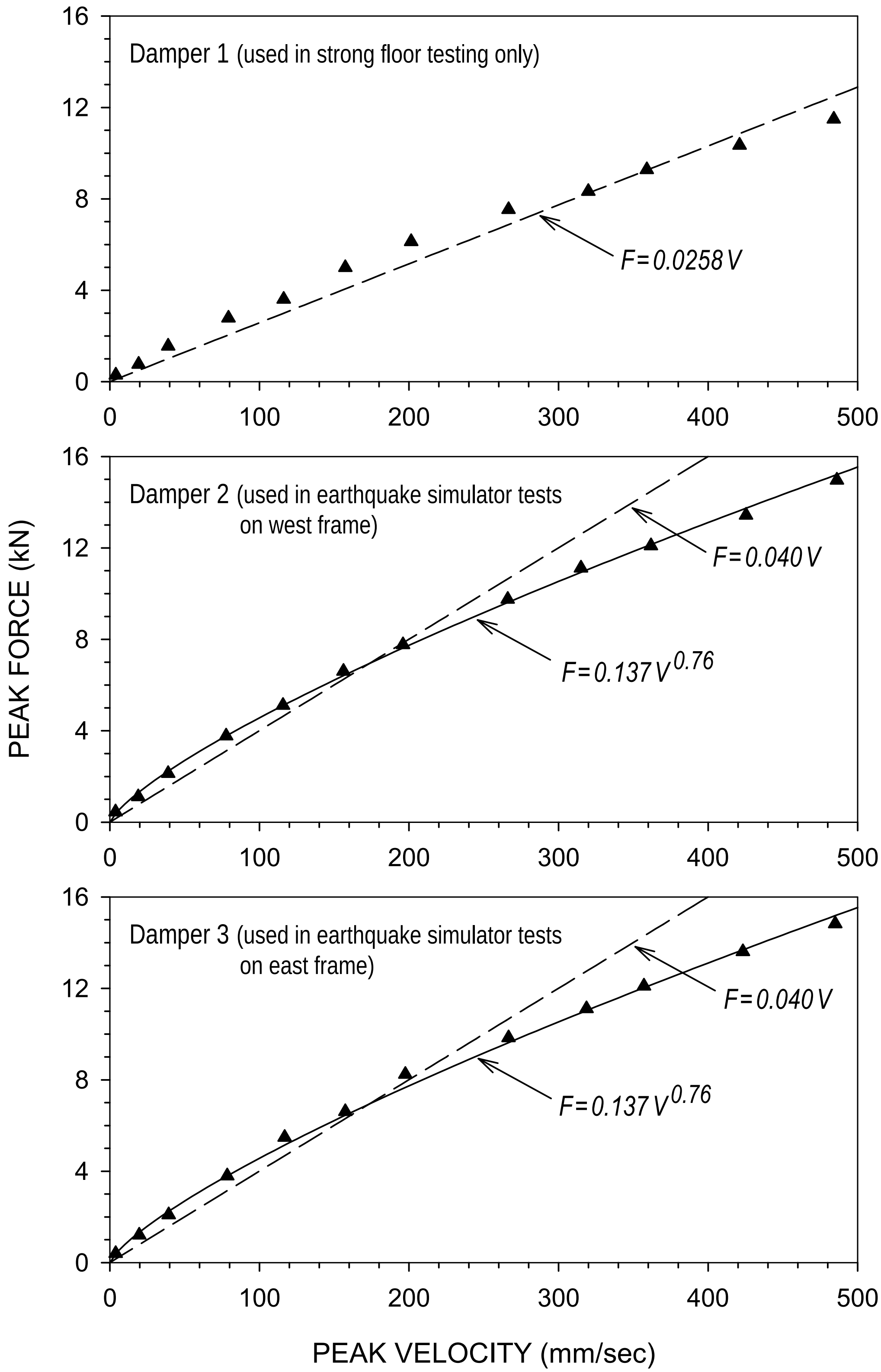

Figure 3-9 Peak Force versus Peak Velocity Relations of Tested Fluid Viscous Dampers

purpose of this testing was to confirm the predictions of the scissor-jack theory described in Section 2. Alternate configurations of beam-to-column connections (rigid-simple, simple-rigid, and rigid-rigid) were tested to observe the effect of frame deformations on the magnification factor f (see Sections 2.3 and 2.5).

As illustrated in Figure 3-10, the tested frame was simply supported on a W21×50 beam that was bolted on the strong floor, and sinusoidal motion was applied through an actuator attached to the frame at one end, and to a reaction frame at the other. Frequency of the imposed displacement varied in the range of 0.01 Hz (quasi-static conditions) to 4 Hz (dynamic conditions), and the amplitudes included 6.35 mm and 8.45 mm (0.25 in and 0.33 in). Lateral displacement, or drift of the frame (displacement of the beam-to-column joint), damper deformation (relative displacement between the two ends of the damper), damper force, and lateral force (force required to impose the displacement) were recorded. The lateral force included the resisting

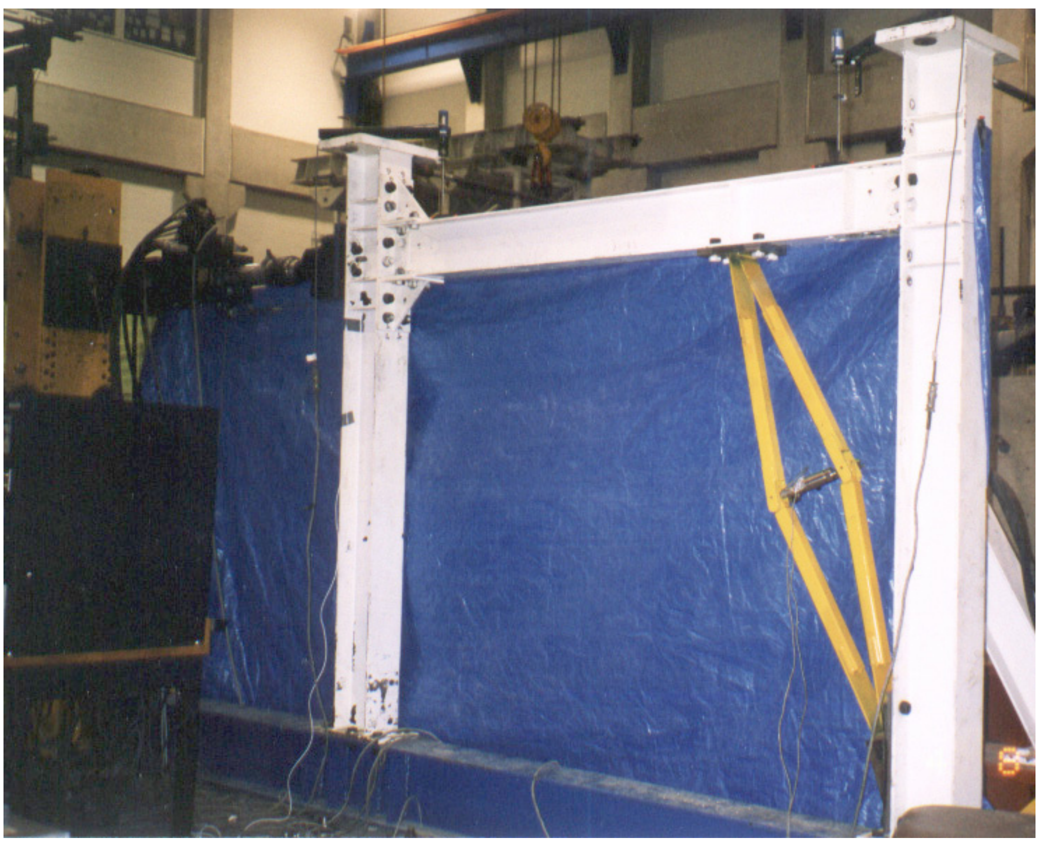

Figure 3-10 View of Frame during Testing under Imposed Lateral Joint Displacement on Strong Floor (Rigid-Simple Connections)

force of the frame (sum of damping force and restoring force) and the inertia force. The inertia force was negligible compared to the resisting force of the frame therefore no corrections were made (peak value of the inertia force in the tests at frequency of 4 Hz was about 4-percent of the lateral force, observed for simple-rigid connections of the frame; lower values of the ratio of peak inertia force to peak lateral force were observed for rigid-simple and rigid-rigid configurations). As mentioned earlier, the strong floor tests utilized damper 1 (see Figure 3-8).

3.4 Earthquake-Simulator Testing Program

Testing of the model structure on the earthquake simulator (see Figure 3-2) consisted of identification of dynamic characteristics using white noise excitations, and of seismic tests using records of actual ground motions (Sections 4.2 and 4.3).

The ground motion records were compressed in time by a factor of $\sqrt{2}$ in accordance with the model's length scale factor of 1/2. These records were also scaled in acceleration amplitude, ranging from 10-percent to 300-percent of the actual value. Seismic tests generally included only horizontal excitations; some tests were repeated with simultaneous application of horizontal and vertical ground motion components.

A list of the ground motions used in the earthquake-simulator testing and their characteristics are presented in Table 3-1. The table provides information on the absolute maxima of acceleration, velocity, and displacement of the prototype (original) record, and the maximum factor used to scale the original records in acceleration amplitude. For example, the El Centro motion was applied in increasing scales up to one and one half times (150-percent) the actual record, that is, with a peak acceleration of 0.52g.

Figure 3-11 compares the 5-percent damped acceleration response spectra of the actual (target) ground motions with the spectra of the motions simulated by the earthquake simulator. In general, the target motions were reproduced satisfactorily, however a close examination reveals higher spectral accelerations of the simulated motions, particularly in the vicinity of the natural period of the structure (~ 0.25 sec – 0.3 sec). The difference in spectral accelerations between target and simulated motions can be attributed mainly to simulator-structure interaction, which becomes more pronounced around the resonant frequency, at which the structure, not the simulator may become the driving component in the test.

Table 3-1 Earthquake Motions Used in Earthquake-Simulator Testing and Characteristics in Prototype Scale (all components are horizontal)

NOTATION	RECORD	PEAK ACCEL. (g)	PEAK VEL. (mm/sec)	PEAK DISPL. (mm)	MAX SCALE FACTOR*
El Centro S00E	Imperial Valley, May 18, 1940, component S00E	0.348	334.5	108.7	150
Taft N21E	Kern County, July 21, 1952 component N21E	0.156	157.2	67.1	300
Pacoima S74W	San Fernando, February 9, 1971, component S74W	1.076	568.2	108.2	50
Pacoima S16E	San Fernando, February 9, 1971, component S16E	1.171	1132.3	365.3	50
Miyagi-Ken-Oki EW	Tohuku Univ., Sendai, Japan, June 12, 1978, component EW	0.164	141.0	50.8	300
Hachinohe NS	Tokachi-Oki earthquake, Japan, May 16, 1968, component NS	0.229	357.1	118.9	150
Mexico N90W	Mexico City, September 19, 1985 SCT Building, component N90W	0.171	605.0	212.0	100
Sylmar 90	Northridge, January 17, 1994, LA Olive View Hosp.-Parking Lot, component 90	0.604	769.4	152.0	100
Newhall 90	Northridge, January 17, 1994, LA County Fire Station, component 90	0.583	748.4	176.0	50
Newhall 360	Northridge, January 17, 1994, LA County Fire Station, component 360	0.589	947.0	305.0	75
Kobe EW	Hyogo-Ken Nanbu Earthquake, Japan, January 17, 1995, JMA-Kobe, component EW	0.629	742.0	191.0	50

* Used in testing as a percentage of the actual record

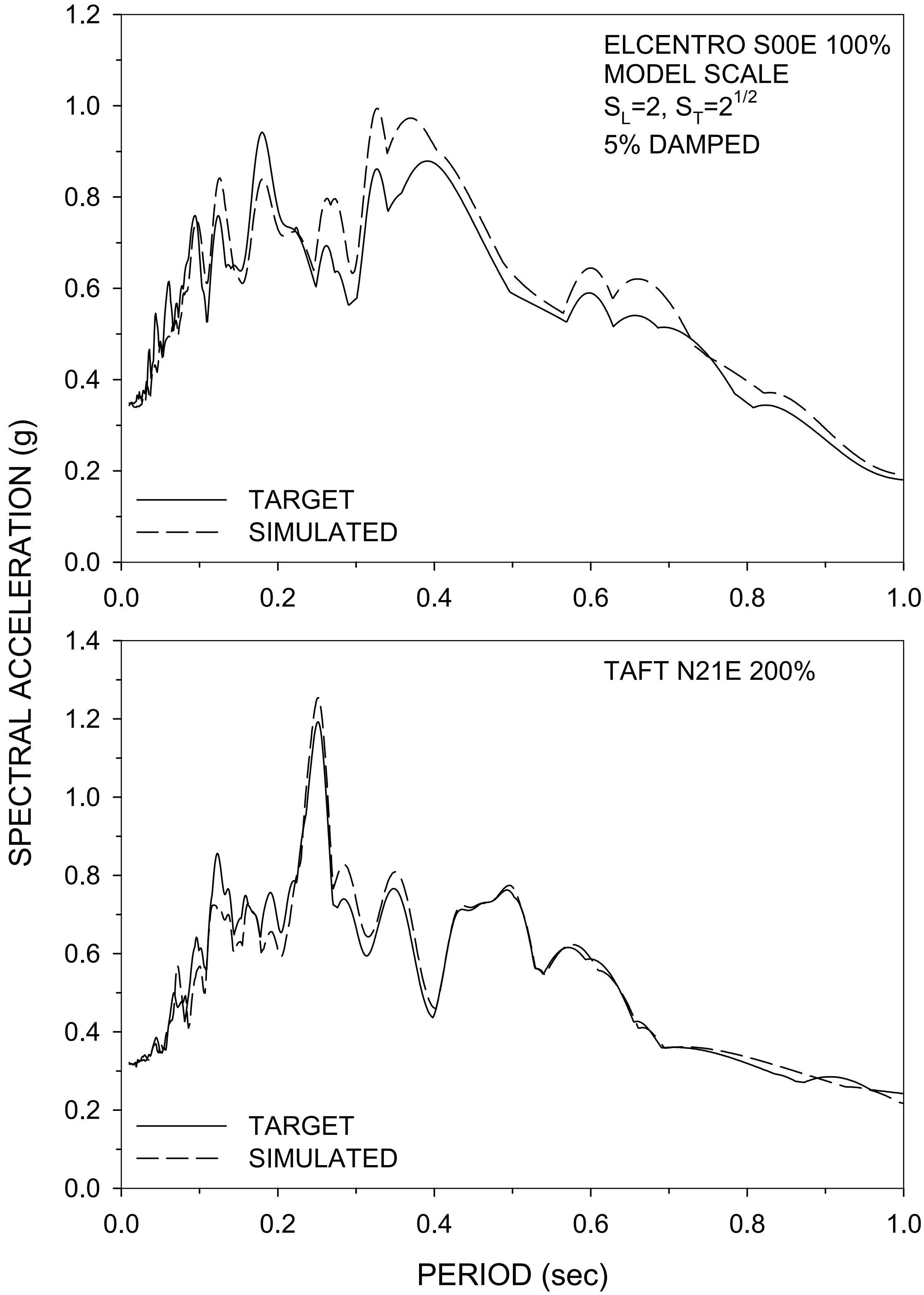

Figure 3-11 Response Spectra in Model Scale of Actual (Target) Ground Motions and Motions Produced by Earthquake Simulator

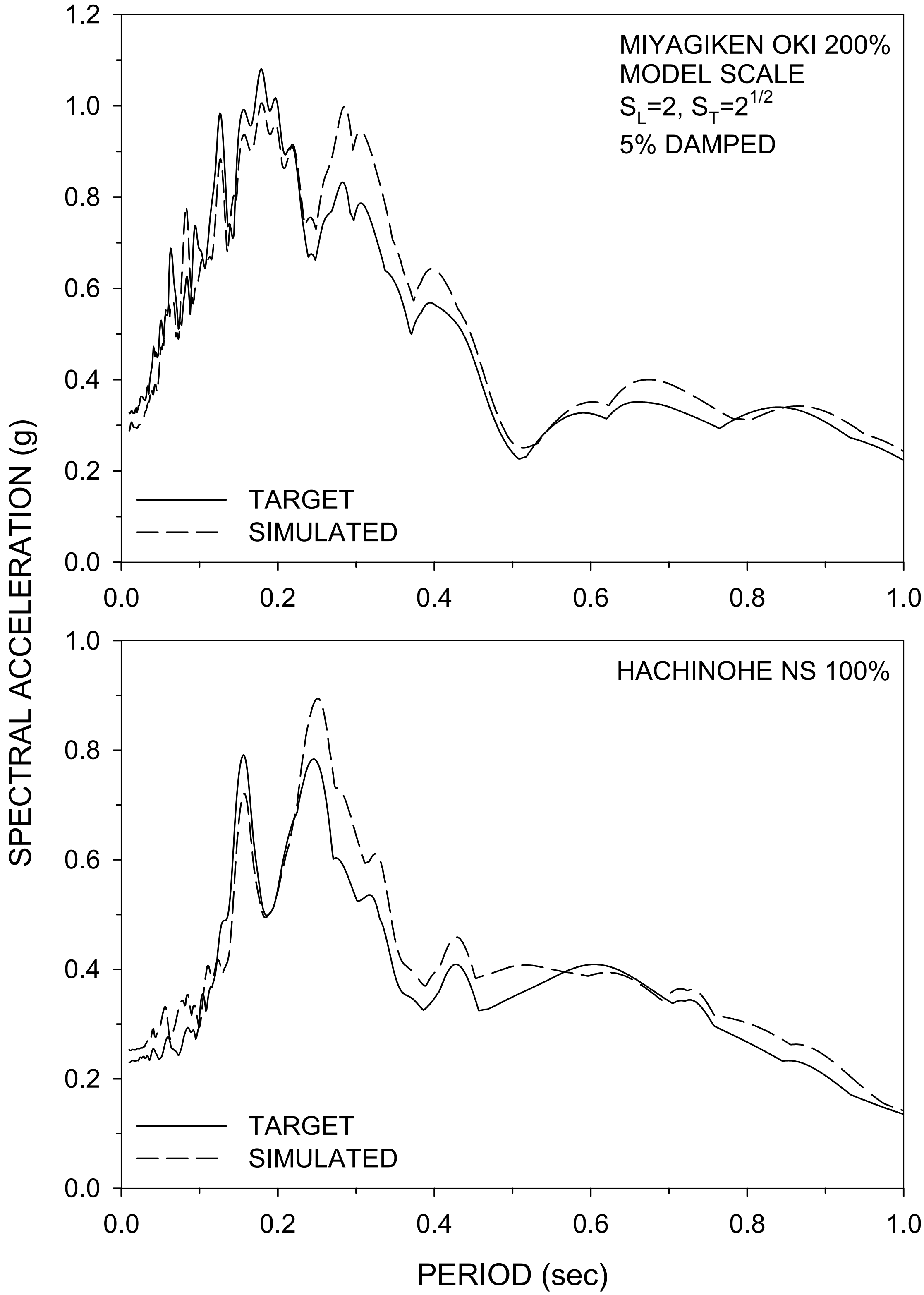

Figure 3-11 (Continued) Response Spectra in Model Scale of Actual (Target) Ground Motions and Motions Produced by Earthquake Simulator

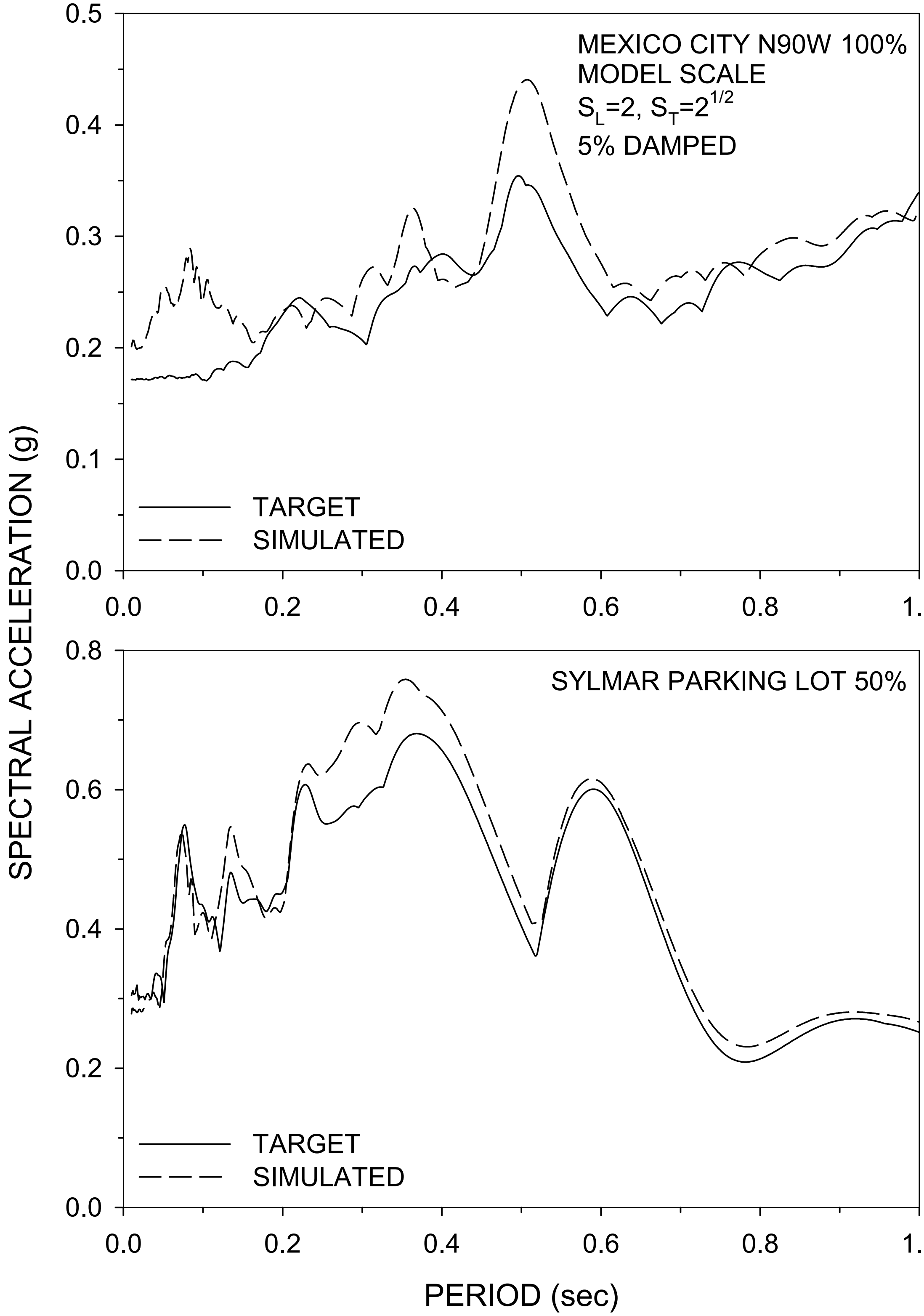

Figure 3-11 (Continued) Response Spectra in Model Scale of Actual (Target) Ground Motions and Motions Produced by Earthquake Simulator

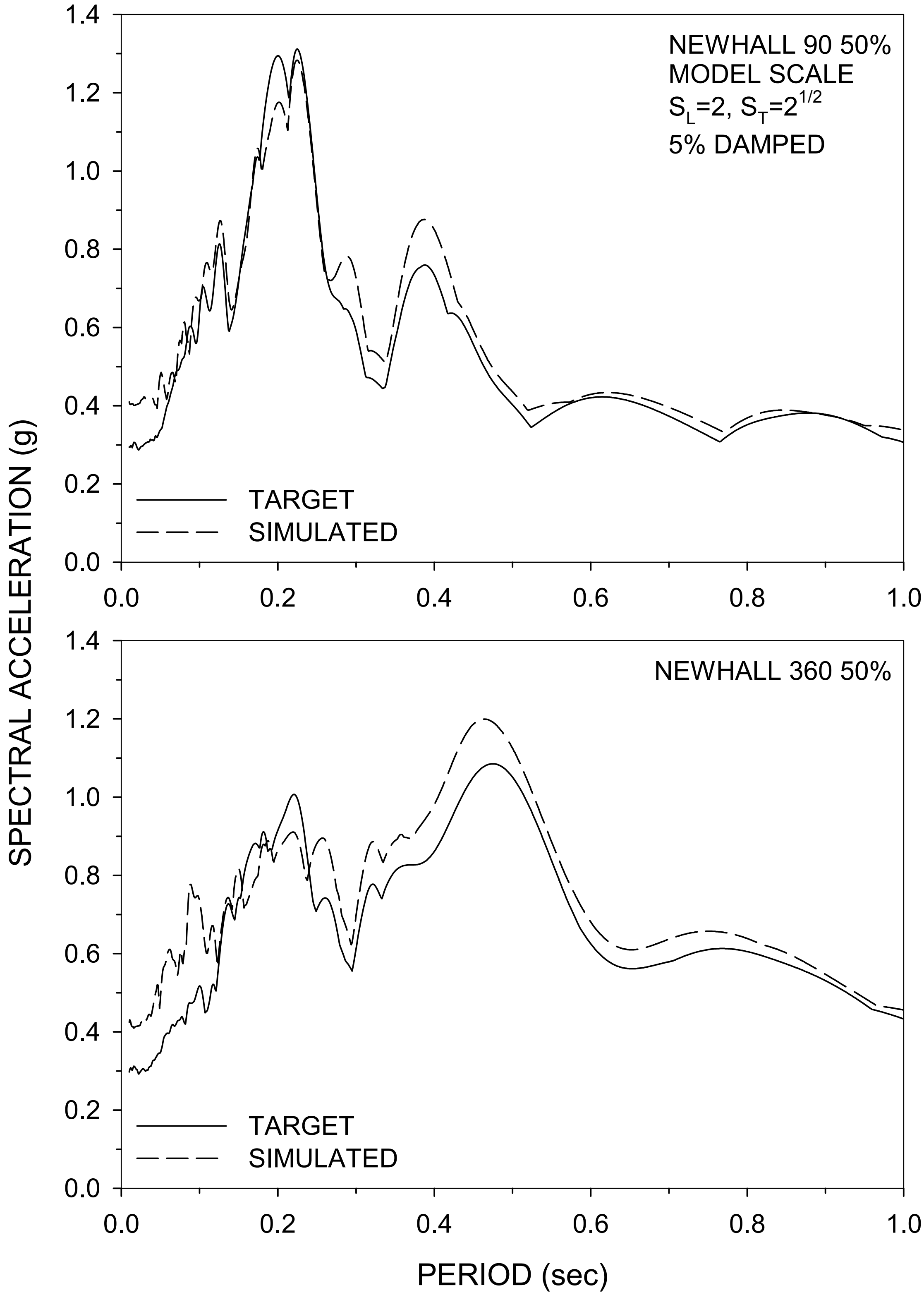

Figure 3-11 (Continued) Response Spectra in Model Scale of Actual (Target) Ground Motions and Motions Produced by Earthquake Simulator

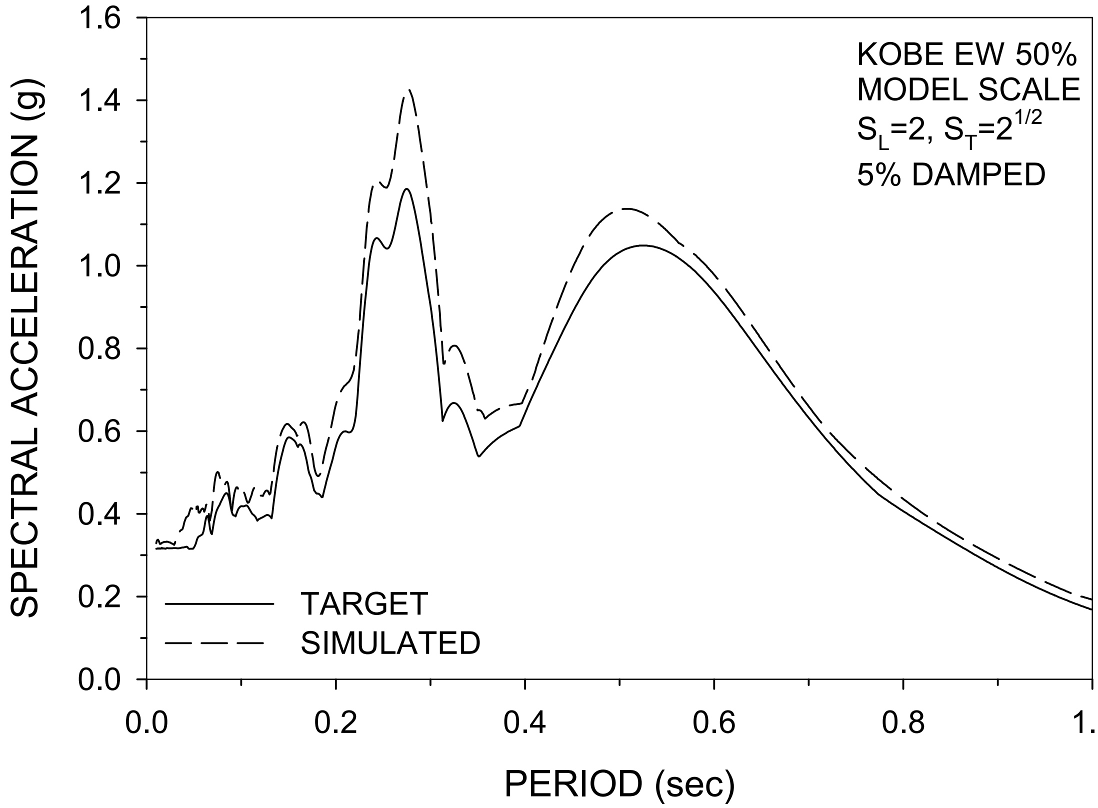

Figure 3-11 (Continued) Response Spectra in Model Scale of Actual (Target) Ground Motions and Motions Produced by Earthquake Simulator

3.5 Instrumentation of Model Structure for Earthquake-Simulator Testing

The data acquisition system consisted of accelerometers, displacement transducers, and load cells, which measured the response of the structure as well as the motion of the earthquake simulator. The instrumentation scheme was similar to that of the previously tested toggle-brace system (Hammel 1997). A list of monitored channels and their descriptions are presented in Table 3-2. Figures 3-12 and 3-13 illustrate the locations of these channels. All measured signals were filtered using a low-pass filter with a cutoff frequency of 25 Hz in the D/A and A/D input.

Table 3-2 List of Channels Utilized in Earthquake-Simulator Testing (refer to Figures 3-12 and 3-13 for locations)

CHANNEL	INSTRUMENT	NOTATION	RESPONSE MEASURED [1]	UNITS
1	/	TIME	Time	sec.
2	Accelerometer	ABEH	Base Horizontal Accel.-E	g
3	Accelerometer	ABWH	Base Horizontal Accel.-W	g
4	Accelerometer	ABSEV	Base Vertical Accel.-SE	g
5	Accelerometer	ABSWV	Base Vertical Accel.-SW	g
6	Accelerometer	ABNEV	Base Vertical Accel.-NE	g
7	Accelerometer	ACTE	Column Top Horiz. Accel.-E	g
8	Accelerometer	ACJE	Column Joint Horiz. Accel.-E	g
9	Accelerometer	ACTW	Column Top Horiz. Accel.-W	g
10	Accelerometer	ACJW	Column Joint Horiz. Accel.-W	g
11	Accelerometer	ACTTN	Column Top Transverse Accel.-N	g
12	Accelerometer	ACTTS	Column Top Transverse Accel.-S	g
13	Accelerometer	ACTVE	Column Top Vertical Accel.-E	g
14	Accelerometer	ACTVW	Column Top Vertical Accel.-W	g
15	Accelerometer	ACJNE	Column Joint Horiz. Accel.-NE	g
16	Accelerometer	ACTNE	Column Top Horiz. Accel.-NE	g
17	Accelerometer	ATBH	Top Block Horiz. Accel.	g
18	Displ. Transducer	DBE	Base Horiz. Displ.-East	in.
19	Displ. Transducer	DBW	Base Horiz. Displ.-West	in.
20	Displ. Transducer	DTE	Top Horiz. Displ.-East	in.
21	Displ. Transducer	DTW	Top Horiz. Displ.-West	in.
22	Load Cell	Dp_Frc_E	Damper Force-East	kips
23	Load Cell	Dp_Frc_W	Damper Force-West	kips
24	Displ. Transducer	Dp_Dsp_E	Damper Displ.-East	in.
25	Displ. Transducer	Dp_Dsp_W	Damper Displ.-West	in.
26 [2]	Accelerometer	ALAT	Table Horiz. Accel	g
27 [2]	Displ. Transducer	DLAT	Table Horiz. Displ.	in.
28 [2]	Accelerometer	AVRT	Table Vertical Accel.	g
29 [2]	Displ. Transducer	DVRT	Table Vertical Displ.	in.

[1] E = East, W = West, N = North, S = South, SE = South East, SW = South West, NE = North East

[2] Channels Used to Control Earthquake Simulator

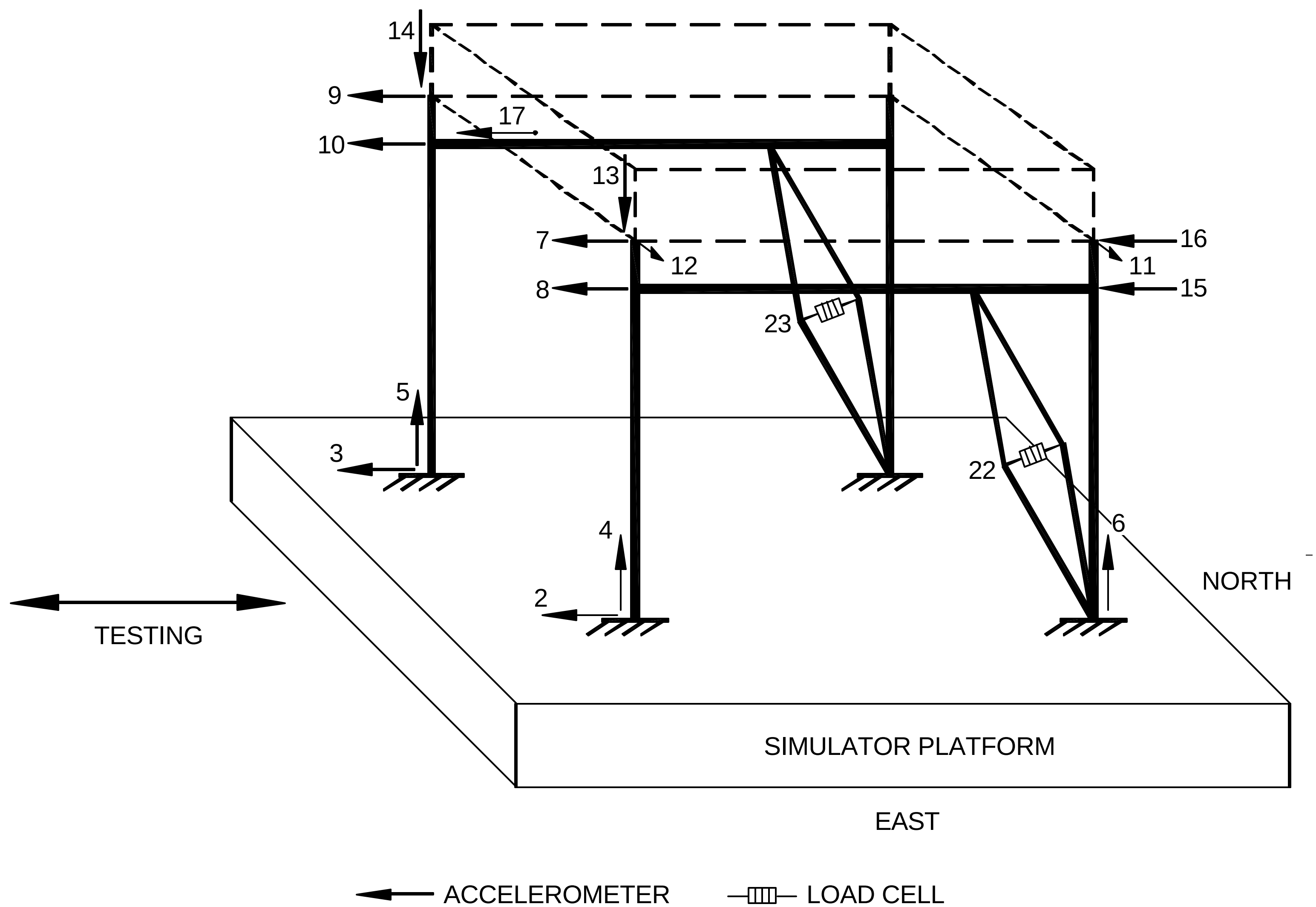

Figure 3-12 Accelerometer and Load Cell Instrumentation Diagram of Tested Structure

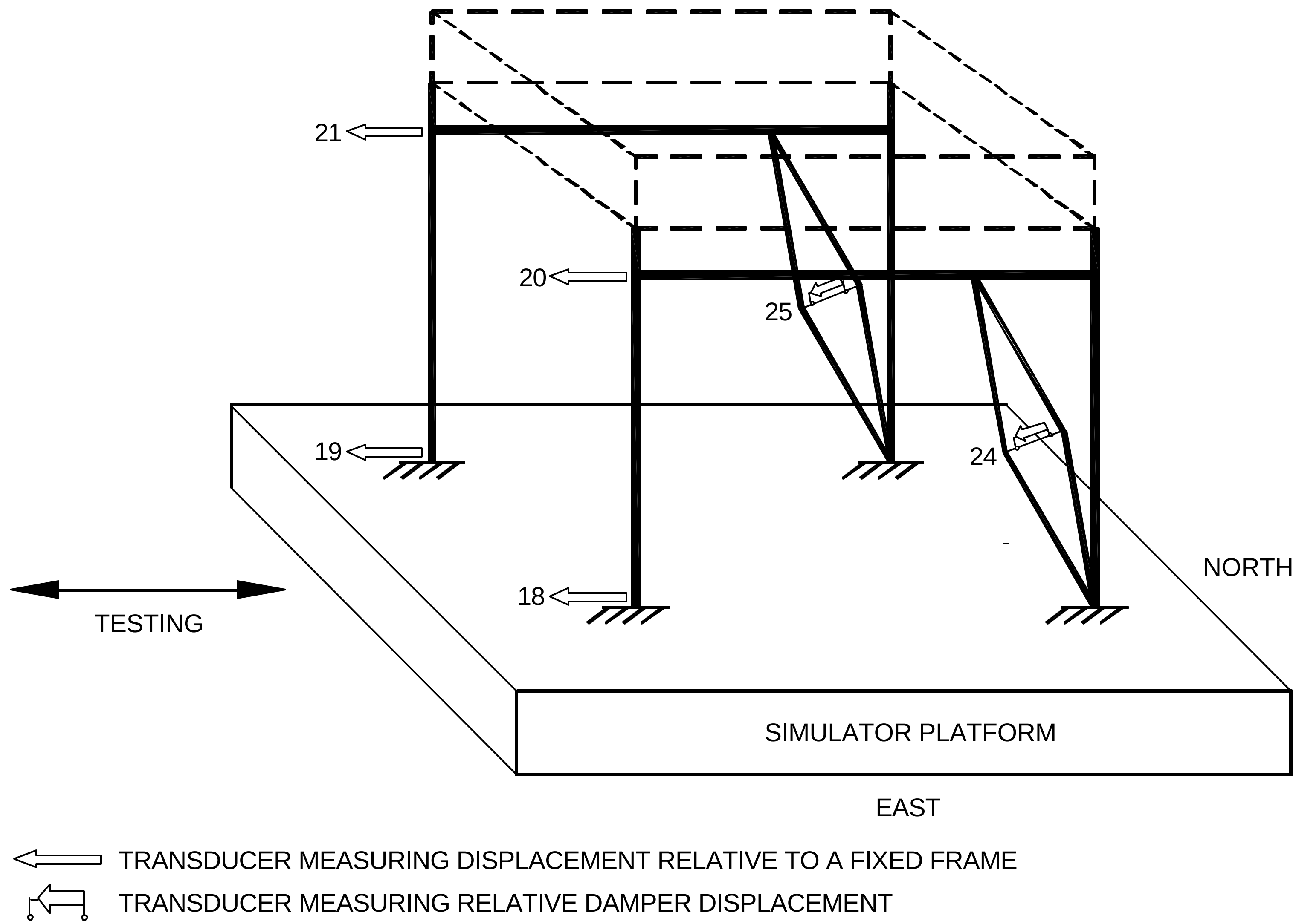

Figure 3-13 Displacement Transducer Instrumentation Diagram of Tested Structure

SECTION 4

TEST RESULTS

4.1 Results of Testing of Frame under Imposed Lateral Joint Displacement

Testing of the frame with the scissor-jack system under harmonic joint displacement was briefly described in the previous section. The experimental program consisted of a series of tests on a single frame with each of the two scissor-brace assemblies. The scissor-braces were labeled as brace 1 and brace 2 for convenience. All tests utilized the same damper, labeled as damper 1. As mentioned previously, testing included various beam-to-column connections, and a range of frequencies and amplitudes of the imposed harmonic displacement (Section 3.3). A view of the test setup is shown in Figure 3-10. This section presents some of the experimental results of this testing to illustrate the key characteristics of the behavior of the frame with the scissor-jack-damper system. Other selected test results are presented in Appendix B. Test results in the appendix include the following information:

1. Test number (label), brace information, beam-to-column connection type, information on the amplitude and frequency of imposed motion, and date and time of test,
2. Graph showing the relation between the lateral force and the lateral displacement (drift) of the frame,
3. Graph of the damper force versus the damper displacement (i.e., deformation between the two ends of the damper),
4. Graph of the damper displacement versus the lateral displacement of the frame (i.e., the magnification factor).

All plots assume the following sign convention: Drift towards the right, resulting increase in damper length, and corresponding forces in the frame and the damper are taken positive.

The behavior of the frame with the scissor-jack-damper system for rigid-simple, simple-rigid and rigid-rigid configurations is presented in Figures 4-1 to 4-3, under quasi-static (0.01 Hz) and dynamic (4 Hz) conditions, and amplitude of 8.45 mm. From these figures, the magnification factors were calculated using the damper displacement – lateral displacement loops. Under quasi-static conditions for which the damper force is negligible, the definition of the magnification factor as the ratio of the peak damper force to the peak lateral displacement can easily be applied. At higher frequencies, the viscoelastic effects due to the finite stiffness of the damping assembly become more apparent (see Section 2.6, eq. 2-23), therefore, the calculation of the magnification factor is rather complicated. The values reported herein for 4 Hz represent the ratio of the peak damper displacement to the peak lateral displacement. This is an average estimate since the absolute maxima of the damper displacement and the lateral displacement do not occur simultaneously, that is, at the point of peak damper displacement, the drift is less than its peak value, and vice versa.

The following observations can be made in the results of Figures 4-1 to 4-3:

1. The rigid-simple configuration, which is shown in Figures 3-1 and 3-10, is, as expected, the most effective (see Sections 2.3 and 2.5), in terms of the value of the magnification factor and the energy dissipated per cycle in the lateral force – lateral displacement loops (energy dissipated per cycle equals the area enclosed by the lateral force – lateral displacement loop in one cycle of motion.
2. Regardless of the beam-to-column joint configuration, the magnification factor attains its largest value under quasi-static conditions (0.01 Hz) when the damping force is practically zero, and decreases with increasing frequency. This behavior is primarily the result of frame deformations under the action of forces in the scissor-jack system. Referring to Figure 2-6 and eqns. (2-12) and (2-13), it can be observed that although the damper forces are low (force F_D), the resultant force on the frame (resultant of forces T acting on the beam equals $F_D / \tan\theta$) is large, due to the magnifying mechanism. For the tested configuration, $\theta = 9^{\circ}$ so that $F_D / \tan\theta = 6.3 \cdot F_D$, causing deflection of the beam.
3. Under quasi-static conditions, the magnification factor is higher than predicted by theory (exclusive of the effect of vertical deformations) for the rigid-simple configuration, and lower for the simple-rigid configuration. For the rigid-rigid configuration, the magnification factor is close to theoretical predictions. It must be noted that for the tested frame, eq. (2-1) takes the form,

   $$u_D = f' \cdot u \tag{4- 1}$$

   where the magnification factor is

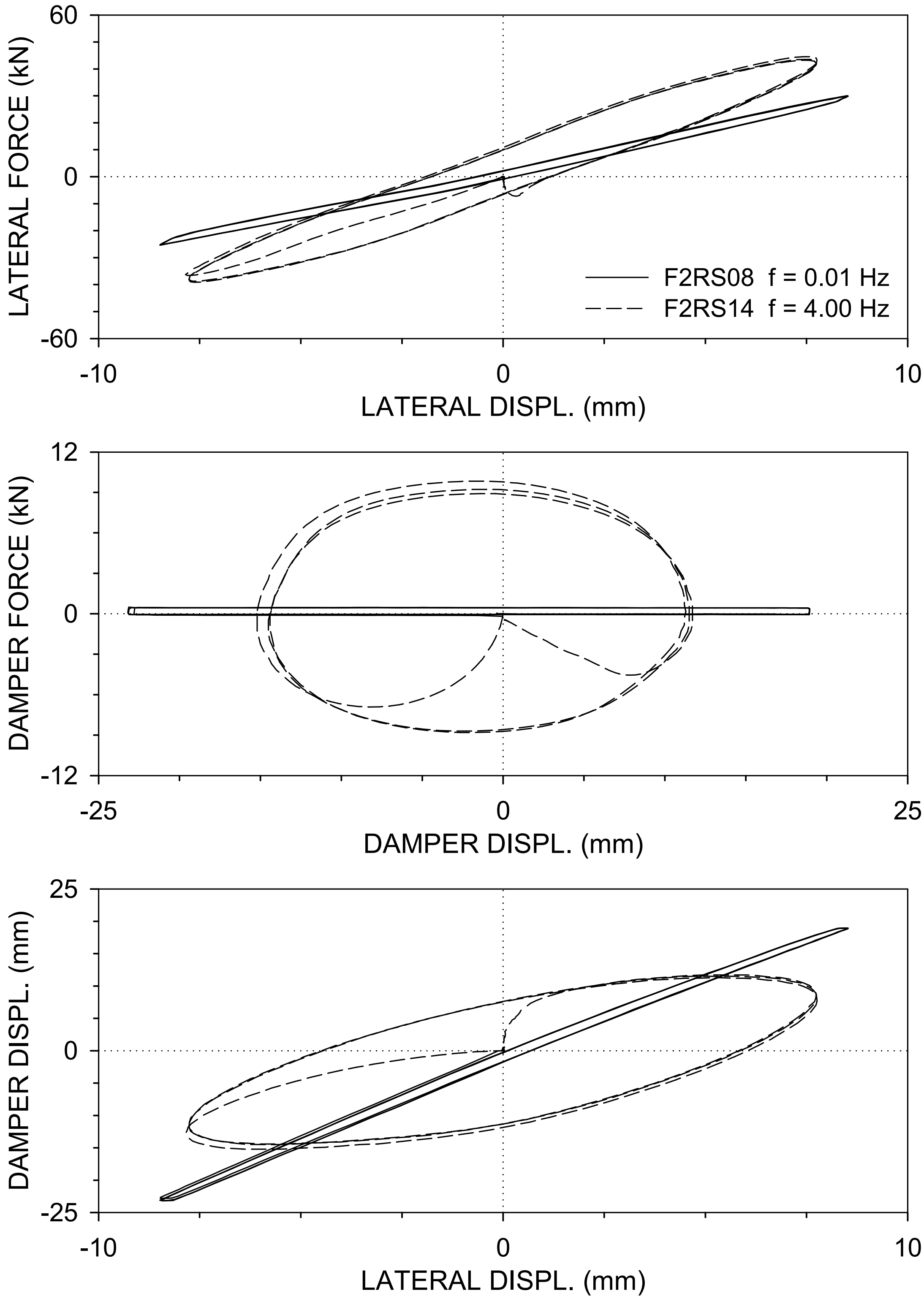

Figure 4-1 Recorded Response of Frame with Brace 2 for Rigid-Simple Beam-to-Column Connections

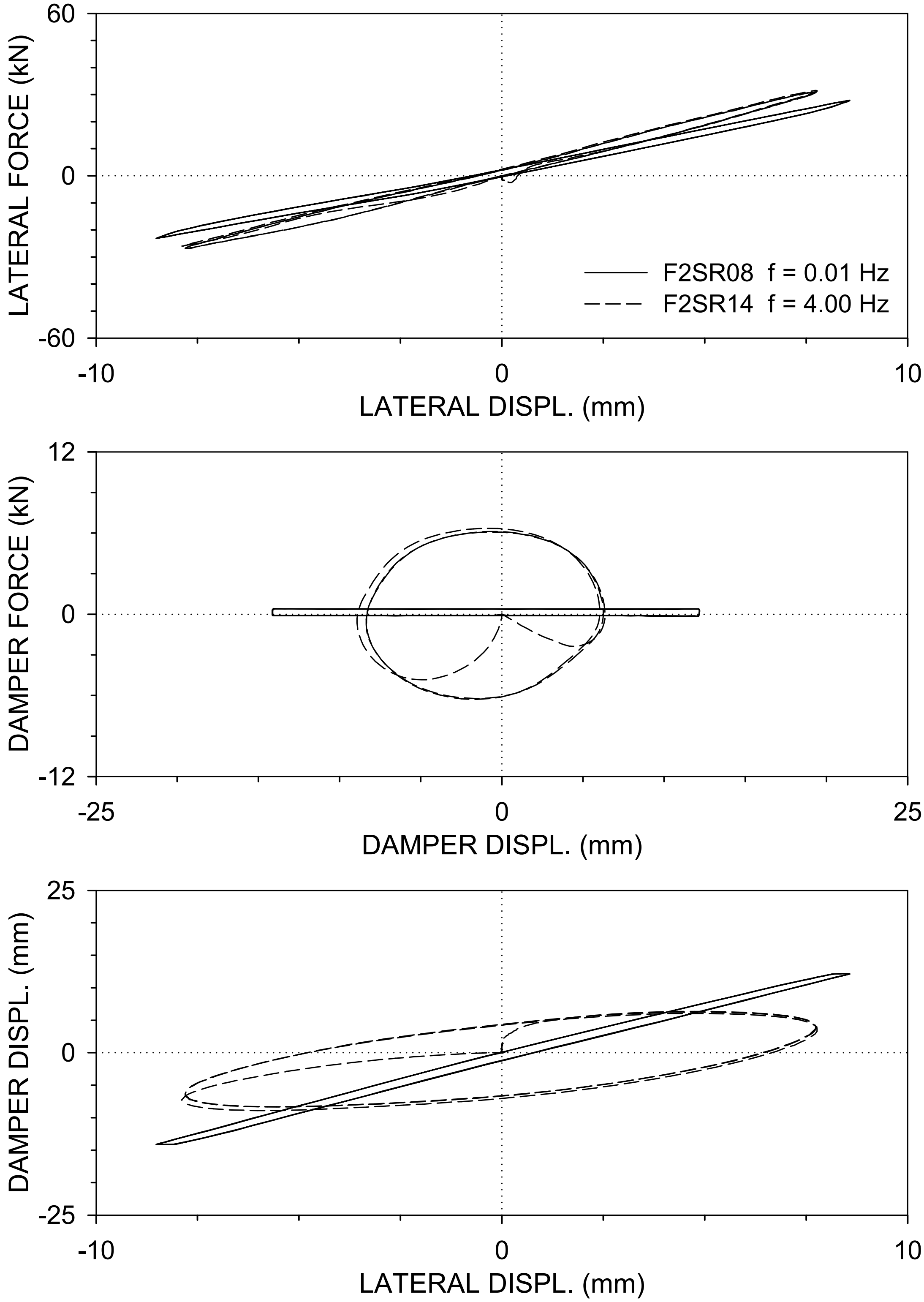

Figure 4-2 Recorded Response of Frame with Brace 2 for Simple-Rigid Beam-to-Column Connections

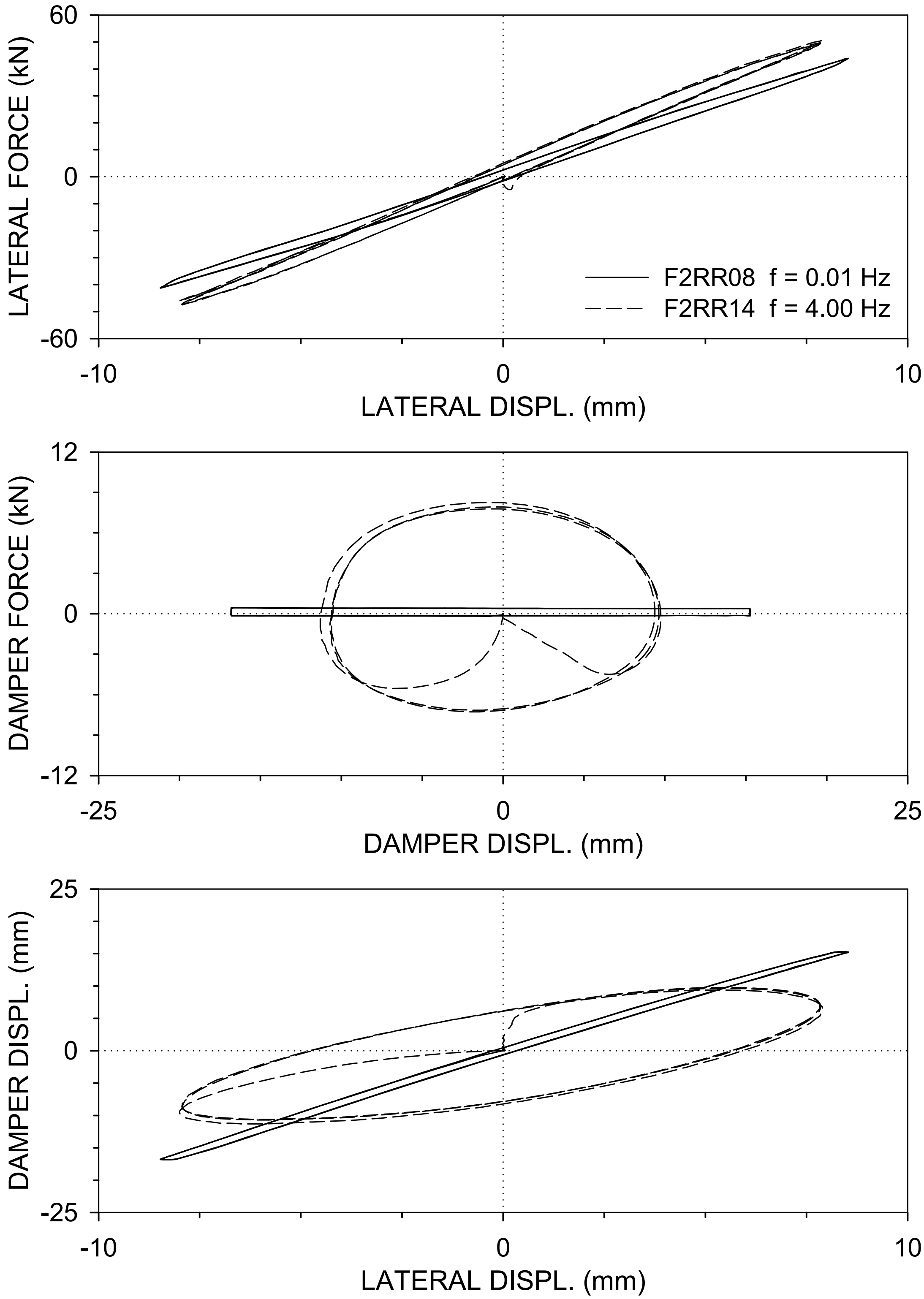

Figure 4-3 Recorded Response of Frame with Brace 2 for Rigid-Rigid Beam-to-Column Connections

$$f' \approx f \cdot (h / h_s) \qquad (4\text{- }2)$$

and h / h_s is a factor accounting for the geometry in which the vertical projection h of the scissor-jack is less than the story height h_s, where drift u takes place (see Figure 3-1). In this case, $h / h_s = 0.838$, $f = 2.16$ (eq. 2-11), and $f' \approx 1.8$. Testing under quasi-static conditions revealed $f' \approx 2.7$ for negative drift (i.e., drift towards the left, damper undergoes compression) and $f' \approx 2.2$ otherwise, for the rigid-simple configuration. For simple-rigid connections, $f' \approx 1.7$ and $f' \approx 1.4$ for damper compression and extension, respectively. The rigid-rigid configuration resulted in $f' \approx 2.0$ for drift to the left, and in $f' \approx 1.8$ for drift to the right. The difference between the predicted and the observed magnification factors is mainly due to frame deformations, as explained in Sections 2.3 and 2.5. For example, with the beam-to-column connections configured as rigid-simple, part of the damper deformation is caused by vertical deflection of the beam (for either direction of drift) – a factor not accounted for in theoretical predictions. The opposite occurs in the case of simple-rigid configuration. The rigid-rigid configuration falls in between these two cases. Calculation of the magnification factor approximately accounting for the effect of vertical deformations (eq. 2-20) yields $f = 2.75$ and $f' \approx 2.3$ for $a \approx 0.1$ (representative of the rigid-simple beam-to-column configuration), and $f = 1.57$ and $f' \approx 1.3$ for $a \approx -0.1$ (representative of the simple-rigid beam-to-column configuration), which are in closer agreement with the experimentally obtained magnification factors in comparison with the predictions of (2-11).

In addition to the effects of frame deformations on the magnification factor, for drift towards the left, as the scissor-braces close, both angles ψ and θ decrease, causing an increase in the instantaneous magnification factor (the opposite occurs for drift towards the right, see Figures 2-7 and 2-8), which cannot be captured by predictions under the assumption of small deformations (eqns. 2-11 and 2-20). The asymmetry in damper deformation and the larger value of f' under negative drift are due to this behavior.

4. Under dynamic conditions for which considerable forces develop in the scissor-jack assembly, the magnification factor attains values that are significantly lower than those

under quasi-static conditions. For example at a frequency of 4 Hz, the rigid-simple configuration results in $f' \approx 1.5$ for positive drift, and $f' \approx 1.9$ for negative drift. In case of the rigid-rigid configuration, $f' \approx 1.2$ and $f' \approx 1.4$ for positive drift and negative drift, respectively. The simple-rigid configuration, on the other hand, yields $f' \approx 0.8$ and $f' \approx 1.1$ for damper extension and compression, respectively, rendering the scissor-jack system ineffective under dynamic conditions for this frame. This is also apparent from comparison of the lateral force versus lateral displacement graphs for frequencies of 1, 2, 3 and 4 Hz in Appendix B, which indicate the small amount of energy dissipated at higher frequencies. A similar observation can also be made for the rigid-rigid configuration. This behavior is the result of frame deformations due to structural system configuration, and deformations caused by the forces in the damping system.

The substantial reduction in the values of the magnification factor with respect to those under quasi-static conditions for all three configurations is due to deformations of the energy dissipation assembly (primarily beam deflections) caused by the damping forces that develop in the damper and in the scissor-braces (see Sections 2.3 and 2.6).

5. There is considerable increase in the effective stiffness of the frame when significant damping forces develop, as is evident in the hysteresis loops of lateral force versus lateral displacement graphs in Figures 4-1 to 4-3. The source of the additional stiffness was explained in Section 2.6. For example, a 60-percent increase in effective stiffness is observed for the rigid-simple configuration, which corresponds to about 25-percent increase in frequency. This is consistent with the earthquake-simulator testing results and the predictions of simplified (approximate) methods of analysis to be presented in the following sections.

4.2 Identification of Dynamic Characteristics

The dynamic characteristics of the model (as depicted in Figure 3-2 with mass) were identified by exciting the structure on the earthquake simulator (with and without the scissor-jack-damper system) with a 0 – 25 Hz stationary band-limited white noise excitation. The peak acceleration of the excitations included 0.05g and 0.10g for the bare structure (without the damping system), and varied from 0.05g to 0.30g for the structure with the damping system. It must be noted that the white noise excitation with a peak acceleration of 0.30g is comparable to earthquake simulator motions in acceleration amplitude (see Table 3-1). Transfer functions were then constructed as the ratio of the Fourier transform of the acceleration at the concrete mass-to-column joint (column-top) to the Fourier transform of the base acceleration (obtained from east frame instruments ACTE and ABEH, see Figure 3-12). Since the rigid concrete mass is simply connected to the top of the frames (see Figure 3-1), the movement of the concrete mass-to-column joint is effectively identical to the movement of the center of mass of the structure. Accordingly, the transfer function calculated on the basis of the description above may be used to obtain the dynamic characteristics of the model structure when it is represented as a single-degree-of-freedom system.

The model structure was identified in two different configurations of the beam-to- column connections: rigid-simple, which amplifies the magnification factor and simple-rigid, which causes an undesirable reduction of the factor. Figure 4-4 presents the amplitudes of the transfer functions of the tested frame with and without the scissor-jack-damper system. The amplitudes of the transfer functions reveal a simple relation that is characteristic of single-degree-of freedom systems. Accordingly, the frequency and damping ratio on the basis of the assumption of linear elastic and linear viscous behavior may be easily determined from the location and magnitude of the primary peak. They are presented in Table 4-1 for each of the tested configurations.

An observation to be made in the results of Table 4-1 and Figure 4-4 is the significant difference in the added damping in the two configurations of the frames, of which the origin has been previously explained. Another important observation is the significant stiffening of the structure, marked by the increase in frequency. For the rigid-simple configuration, the increase in frequency from 3.2 Hz to 4.0 Hz is significant and consistent with the approximately 60-percent increase in stiffness of the frame observed in testing under imposed displacement (Section 4.1). This increase in frequency is the result of viscoelastic behavior caused by frame and energy dissipation assembly deformations under the action of the damping forces as explained in Section 2.

In interpretation of the transfer function amplitudes and associated damping ratios, it must be noted that results of the white noise tests are rather sensitive to the excitation history the structure

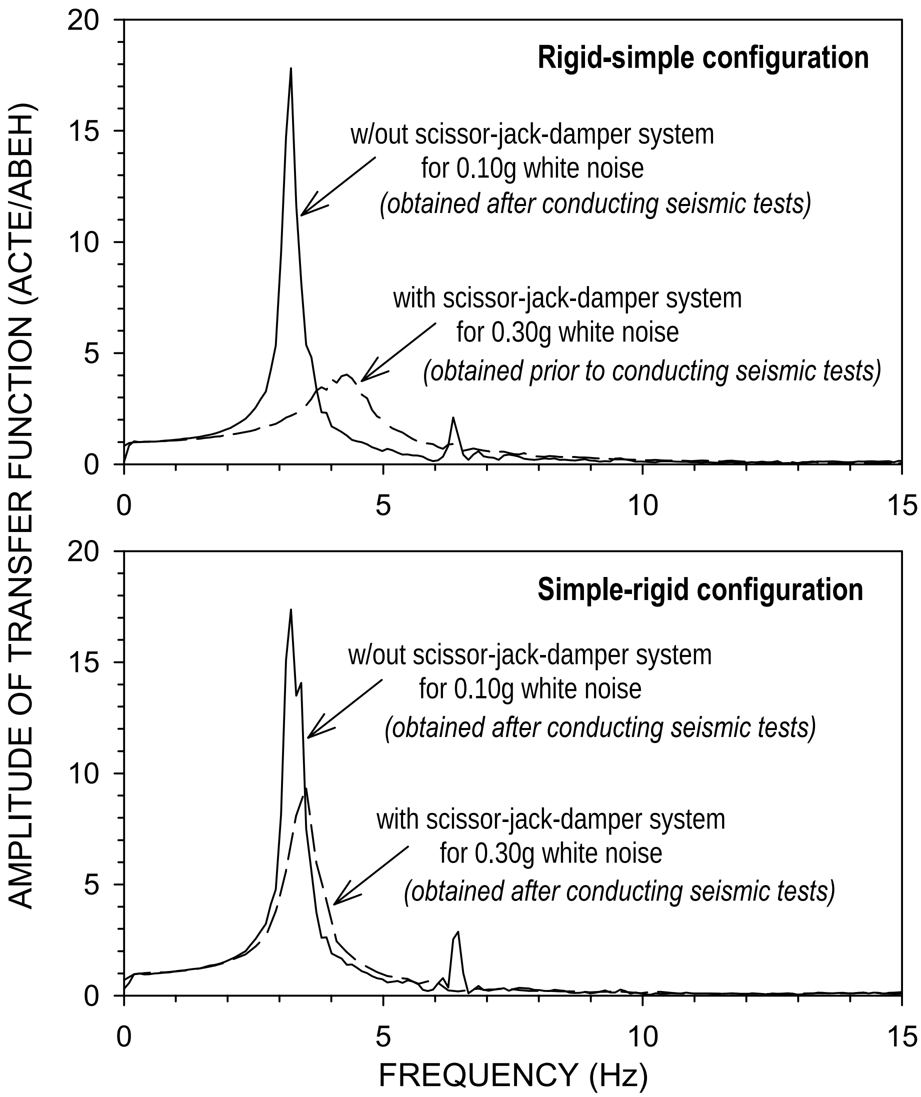

Figure 4-4 Amplitude of Transfer Function of Model Structure with Rigid-Simple and Simple-Rigid Connections

Table 4-1 Identified Dynamic Characteristics of Model Structure with and without Scissor-Jack-Damper System

Beam-to-Column Connections	Configuration	Fundamental Frequency (Hz)	Damping Ratio
Rigid-Simple	No Dampers	3.2	0.028
	Scissor-Jack-Damper	4.0	0.130
Simple-Rigid	No Dampers	3.2	0.029
	Scissor-Jack-Damper	3.5	0.055

was subjected to, prior to being identified. That is, white noise tests performed after a number of high-amplitude seismic tests may give slightly lower damping ratios compared to those obtained before seismic tests. In relation to this behavior, Figure 4-5 shows the amplitudes of transfer functions of the rigid-simple structure with the scissor-jack-damper system for the case of 0.30g white noise, obtained before (duplicate from Figure 4-4) and after conducting seismic tests. The figure reveals a reduction in the damping ratio after seismic tests, as implied by higher amplitude of the transfer function. The same trend was observed for lower amplitudes of white noise. The difference is mainly due to elevated temperature of the dampers from immediate prior testing, reduction in friction (at connections, supports, etc.) as a result of repetitive testing and occasional disassembly of the model, and deterioration of damper behavior due to repeated testing. It must be added that identifications of the structure with the scissor-jack-damper system with simple-rigid beam-to-column configuration and identifications without the damping system (bare frame) in both configurations were performed after conducting the seismic tests (as noted in all figures of transfer function amplitudes).

Amplitudes of transfer functions of the structure with the damping system for various levels of excitations are presented in Figure 4-6, to reveal further observations. As the figure suggests, the damping ratio increases significantly with increasing level of excitation. For example, for the

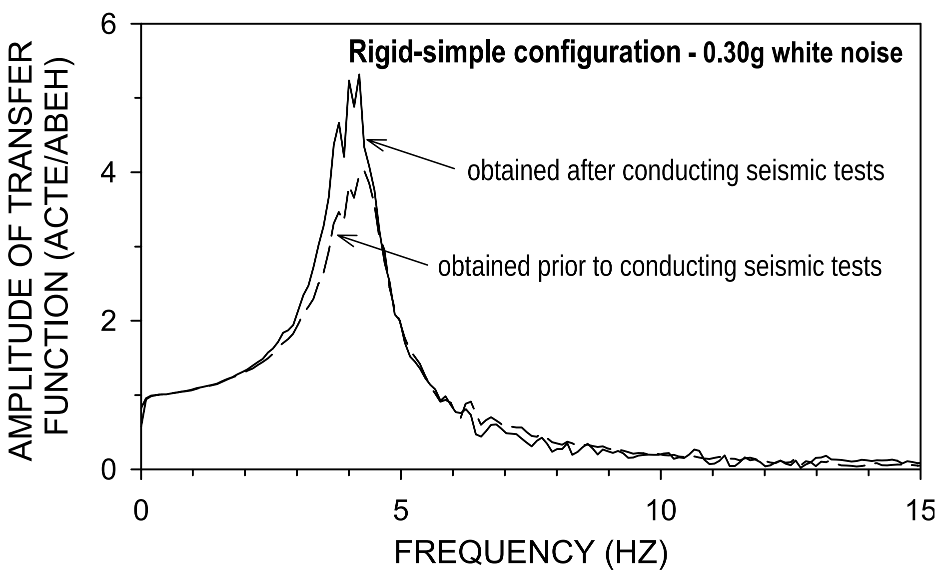

Figure 4-5 Amplitude of Transfer Function of Rigid-Simple Structure with Scissor-Jack-Damper System for 0.30g White Noise, prior to and after Seismic Tests

excitation with a peak acceleration of 0.05g, the damping ratios are approximately 8.5-percent and 3.5-percent for the rigid-simple and the simple-rigid configurations, respectively. The damping ratios are 13-percent and 5.5- percent for the rigid-simple and the simple-rigid configurations, respectively, for the white noise excitation with 0.30g peak acceleration. Contributing mechanisms for this behavior include the amplitude dependence of inherent damping, the ineffectiveness of fluid dampers at very small amplitude movements, mild inelastic action in the scissor-jack system, and dependence of the magnification factor of the scissor-jack system on the amplitude of motion due to small imperfections (such as slightly oversized holes

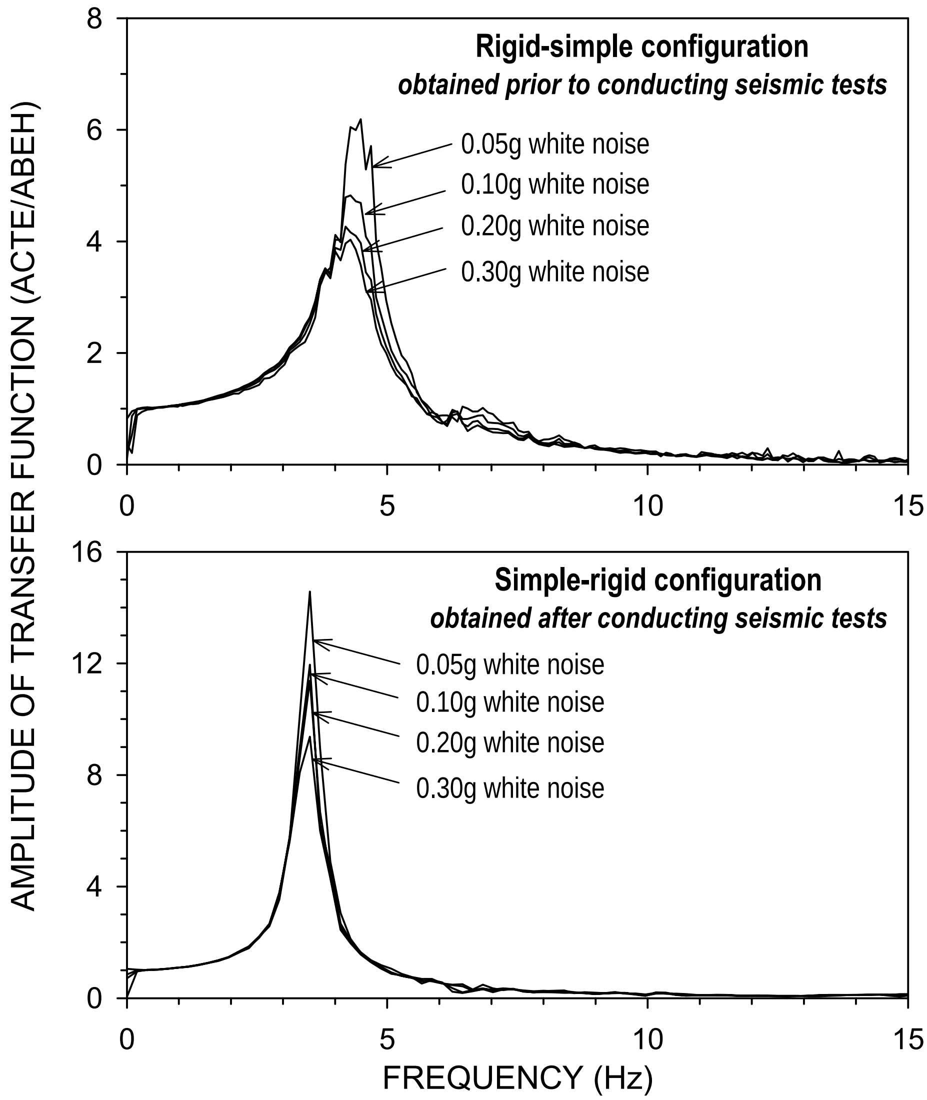

Figure 4-6 Amplitude of Transfer Function of Model Structure with Scissor-Jack-Damper System under Various Levels of Excitation

that allow for some rigid body motion, use of plates for connecting the scissor-braces to the frame rather than utilizing spherical bushings, etc.). This latter mechanism is the major contributor to the dependency of damping ratio since lower magnification factors were recorded in earthquake-simulator testing with weak excitation (Section 4.3).

The structure was also identified without the dampers only (inclusive of the braces) in both beam-to-column configurations. The resulting transfer functions confirmed the purely viscous behavior of the dampers.

4.3 Earthquake-Simulator Testing Results

A summary of the earthquake-simulator (seismic) testing results is presented in Table 4-2. Tests are tabulated in the order in which they were conducted (white noise tests are excluded). The table contains the following:

a. Test number.
b. Description of seismic excitation, which includes the excitation name, component, and acceleration amplitude scale. For example, EL CENTRO S00E 50% implies that the record was component S00E of the El Centro earthquake, scaled in amplitude of acceleration to 50-percent of the actual value.
c. Peak values of the earthquake simulator displacement, velocity and acceleration records. The peak simulator displacement was obtained from displacement transducer DBE, the peak velocity was derived from numerical differentiation of the displacement record, and the peak acceleration was obtained from accelerometer ABEH (see Table 3-2, and Figures 3-12 and 3-13).
d. Peak frame response in terms of drift (displacement of the beam-to-column joint with respect to the column base), beam-to-column joint acceleration, damper relative displacement, and damper force. The peak frame output values are given for the east and west side frames in order to identify any torsional motion of the structure.
e. Information as to whether the structure is tested with or without the scissor-jack-damper system.
f. Values of the magnification factor for east and west frames, determined as the ratio of the peak damper displacement to the peak drift.

Table 4-2 Peak Response of Model Structure in Earthquake-Simulator Testing

Test No	Excitation	Earthquake Simulator			Frame Peak Values								Scissor Damper	Magnification Factor	
		Displ. (mm)	Veloc. (mm/sec)	Accel. (g)	Drift (mm)		Accel. (g)		Damper Displ. (mm)		Damper Force (kN)				
					East	West	East	West	East	West	East	West		East	West
ELRSBD025	EL CENTRO S00E 25%	10.3	55.6	0.103	1.5	1.6	0.117	0.127	2.2	2.2	2.10	2.38	YES	1.5	1.7
ELRSBD050	EL CENTRO S00E 50%	20.7	112.1	0.187	3.1	3.2	0.232	0.247	4.9	4.9	4.30	4.59	YES	1.7	1.9
ELRSBD100	EL CENTRO S00E 100%	41.5	219.7	0.340	6.3	6.6	0.446	0.472	10.7	10.8	8.72	8.60	YES	1.8	2.0
ELRSBD150	EL CENTRO S00E 150%	62.4	332.7	0.573	10.0	10.7	0.659	0.656	16.0	16.9	11.02	11.72	YES	1.9	2.0
ELRSBD150.2	EL CENTRO S00E 150%	62.4	335.3	0.582	9.7	10.6	0.619	0.663	16.3	16.9	12.31	11.89	YES	1.9	2.0
ELRSBD150.3	EL CENTRO S00E 150%	62.0	334.0	0.549	9.7	10.3	0.655	0.719	16.5	17.0	12.71	12.81	YES	1.8	2.0
EVRSBD050	EL CENTRO S00E H+V 50%	20.6	110.2	0.183	3.3	3.3	0.236	0.253	5.0	4.9	3.89	4.56	YES	1.6	1.8
EVRSBD100	EL CENTRO S00E H+V 100%	41.3	221.0	0.338	6.4	6.7	0.460	0.481	10.3	10.9	8.46	8.63	YES	1.8	1.8
EVRSBD150	EL CENTRO S00E H+V 150%	62.1	329.6	0.558	10.0	10.3	0.660	0.717	16.3	16.8	13.33	12.91	YES	1.8	2.0
TARSBD075	TAFT N21E 75%	16.2	78.7	0.123	3.3	3.2	0.252	0.240	4.6	4.5	3.77	4.72	YES	1.6	1.4
TARSBD100	TAFT N21E 100%	21.9	106.0	0.156	4.2	4.1	0.316	0.306	6.0	5.9	4.93	6.01	YES	1.6	1.5
TARSBD200	TAFT N21E 200%	43.6	207.6	0.316	7.5	7.6	0.557	0.563	11.7	11.7	8.88	10.65	YES	1.7	1.7
TARSBD300	TAFT N21E 300%	65.3	315.9	0.564	10.6	10.6	0.731	0.746	16.2	16.4	12.22	13.80	YES	1.8	1.7
TARSBD300.2	TAFT N21E 300%	65.3	315.0	0.553	10.6	10.7	0.726	0.752	16.0	16.4	12.08	13.80	YES	1.8	1.7
TARSBD300.3	TAFT N21E 300%	65.7	318.5	0.612	10.4	10.5	0.679	0.733	14.9	15.2	13.73	13.81	YES	1.7	1.7
TVRSBD200	TAFT N21E H+V 200%	43.8	205.7	0.330	7.9	8.0	0.554	0.576	11.2	12.9	9.87	10.35	YES	1.7	1.7
HARSBD050	HACHINOHE NS 50%	25.1	107.0	0.134	3.1	3.3	0.228	0.245	4.3	5.1	3.87	4.28	YES	1.3	1.5
HARSBD100	HACHINOHE NS 100%	50.0	212.1	0.252	5.7	6.2	0.418	0.445	8.4	9.5	7.46	7.48	YES	1.6	1.6
HARSBD150	HACHINOHE NS 150%	75.1	321.3	0.371	8.4	8.9	0.593	0.606	11.7	12.5	9.86	10.02	YES	1.6	1.7
MIRSBD100	MIYAGIKEN EW 100%	17.4	100.7	0.161	3.5	3.8	0.254	0.277	5.1	5.3	4.64	4.72	YES	1.4	1.6
MIRSBD200	MIYAGIKEN EW 200%	34.7	203.2	0.284	6.6	7.2	0.479	0.509	10.6	11.0	8.67	8.60	YES	1.6	1.6

Table 4-2 Continued

Test No	Excitation	Earthquake Simulator			Frame Peak Values								Scissor Damper	Magnification Factor	
		Displ. (mm)	Veloc. (mm/sec)	Accel. (g)	Drift (mm)		Accel. (g)		Damper Displ. (mm)		Damper Force (kN)				
					East	West	East	West	East	West	East	West		East	West
MIRSBD300	MIYAGIKEN EW 300%	52.4	30.8	0.456	9.9	10.7	0.662	0.704	15.7	16.2	11.81	11.30	YES	1.6	1.6
MXRSBD100	MEXICO CITY N90W 100%	101.1	417.5	0.199	2.8	3.6	0.189	0.195	5.8	7.0	2.48	2.31	YES	2.1	1.9
PWRSBD025	PACOIMA S74W 25%	14.0	103.8	0.265	4.8	4.8	0.359	0.378	6.7	7.4	6.30	6.67	YES	1.4	1.5
PWRSBD050	PACOIMA S74W 50%	27.9	219.4	0.486	9.0	9.1	0.672	0.705	15.0	16.4	12.26	12.29	YES	1.6	1.8
PERSBD010	PACOIMA S16E 10%	14.8	62.6	0.092	2.3	2.3	0.172	0.178	2.6	3.1	2.76	2.87	YES	1.1	1.3
PERSBD025	PACOIMA S16E 25%	37.3	154.0	0.242	5.0	5.1	0.370	0.384	7.2	7.7	6.24	6.58	YES	1.4	1.5
PERSBD050	PACOIMA S16E 50%	74.4	307.6	0.505	9.4	9.6	0.655	0.685	15.2	15.8	11.66	11.96	YES	1.6	1.7
SYRSBD025	SYLMAR 90 25%	25.4	105.1	0.149	2.9	3.0	0.208	0.232	3.6	4.2	3.55	3.76	YES	1.4	1.7
SYRSBD040	SYLMAR 90 40%	40.7	168.0	0.223	4.5	4.5	0.317	0.345	5.9	7.1	5.43	5.66	YES	1.5	1.8
SYRSBD050	SYLMAR 90 50%	50.8	209.9	0.276	5.4	5.4	0.380	0.412	7.6	8.9	6.69	6.92	YES	1.6	1.8
SYRSBD010	SYLMAR 90 10%	10.0	40.6	0.067	1.3	1.3	0.096	0.098	1.3	1.5	1.36	1.54	YES	1.0	1.4
SYRSBD075	SYLMAR 90 75%	76.2	317.5	0.413	7.8	7.9	0.539	0.582	12.3	13.7	9.84	9.90	YES	1.8	1.9
SYRSBD100	SYLMAR 90 100%	101.0	423.5	0.548	10.2	10.2	0.683	0.730	16.7	18.2	13.10	12.96	YES	1.8	1.9
SYRSBD100.2	SYLMAR 90 100%	101.1	420.1	0.543	10.1	10.1	0.677	0.718	18.1	18.5	12.88	12.58	YES	2.0	1.9
N3RSBD025	NEWHALL 360 25%	30.1	146.1	0.200	3.6	3.9	0.281	0.286	5.4	6.2	4.64	4.83	YES	1.5	1.6
N3RSBD040	NEWHALL 360 40%	48.0	235.9	0.330	5.6	6.0	0.416	0.447	9.2	10.2	7.52	7.65	YES	1.6	1.7
N3RSBD050	NEWHALL 360 50%	60.0	298.5	0.414	7.0	7.4	0.518	0.553	11.6	13.1	9.41	9.31	YES	1.7	1.7
N3RSBD075	NEWHALL 360 75%	89.9	466.1	0.663	10.9	11.4	0.736	0.809	19.1	20.1	14.02	13.22	YES	1.8	1.8
N9RSBD025	NEWHALL 90 25%	17.9	100.3	0.173	4.7	5.0	0.349	0.356	6.7	7.3	4.55	5.57	YES	1.4	1.5
N9RSBD040	NEWHALL 90 40%	28.6	161.6	0.301	7.1	7.5	0.529	0.556	10.8	12.6	7.93	8.49	YES	1.5	1.7
N9RSBD050	NEWHALL 90 50%	35.8	203.2	0.402	8.9	9.1	0.634	0.675	14.3	15.6	9.79	10.30	YES	1.6	1.7

Table 4-2 Continued

Test No	Excitation	Earthquake Simulator			Frame Peak Values								Scissor Damper	Magnification Factor	
		Displ. (mm)	Veloc. (mm/sec)	Accel. (g)	Drift (mm)		Accel. (g)		Damper Displ. (mm)		Damper Force (kN)				
					East	West	East	West	East	West	East	West		East	West
KORSBD025	KOBE EW 25%	17.8	144.1	0.188	4.9	5.1	0.371	0.370	6.7	8.0	6.55	6.49	YES	1.3	1.5
KORSBD040	KOBE EW 40%	28.6	232.7	0.269	7.5	7.7	0.541	0.571	11.1	12.7	9.95	9.56	YES	1.5	1.6
KORSBD050	KOBE EW 50%	35.7	292.1	0.327	9.1	9.3	0.643	0.689	14.5	15.9	11.85	11.33	YES	1.6	1.7
SYRSBD050.2*	SYLMAR 90 50%	50.0	209.2	0.262	5.5	5.4	0.388	0.415	7.3	8.5	5.96	6.98	YES	1.6	1.7
SYRSBD075.2*	SYLMAR 90 75%	74.9	313.7	0.382	7.8	7.8	0.542	0.578	11.6	13.1	8.63	9.79	YES	1.7	1.8
TARSBD200.2*	TAFT N21E 200%	43.1	202.9	0.315	7.9	7.9	0.565	0.593	11.7	12.3	9.81	11.05	YES	1.7	1.6
ELRSBD100.2*	EL CENTRO S00E 100%	40.7	215.9	0.320	6.8	7.0	0.469	0.486	10.8	11.4	7.54	8.40	YES	1.6	1.8
ELRSNN025	EL CENTRO S00E 25%	10.0	59.7	0.107	6.1	6.1	0.286	0.292	–	–	–	–	NO	–	–
ELRSNN050	EL CENTRO S00E 50%	20.3	115.6	0.201	13.3	13.0	0.563	0.574	–	–	–	–	NO	–	–
TARSNN100	TAFT N21E 100%	21.8	103.5	0.156	7.4	7.2	0.329	0.342	–	–	–	–	NO	–	–
TARSNN100.2#	TAFT N21E 100%	21.8	104.8	0.154	7.1	7.1	0.322	0.335	–	–	–	–	NO	–	–
ELRSNN050.2#	EL CENTRO S00E 50%	20.2	115.6	0.200	14.5	14.1	0.604	0.607	–	–	–	–	NO	–	–
ELRSNN025.2#	EL CENTRO S00E 25%	10.1	61.0	0.112	7.4	7.2	0.337	0.332	–	–	–	–	NO	–	–
MIRSNN100	MIYAGIKEN EW 100%	17.3	94.6	0.146	10.6	10.7	0.426	0.475	–	–	–	–	NO	–	–
MXRSNN100	MEXICO CITY N90W 100%	100.1	412.8	0.196	6.4	7.2	0.304	0.338	–	–	–	–	NO	–	–
SYRSNN025	SYLMAR 90 25%	24.9	115.6	0.165	8.6	8.5	0.377	0.393	–	–	–	–	NO	–	–
HARSNN050	HACHINOHE NS 50%	25.1	108.0	0.127	8.3	8.6	0.349	0.407	–	–	–	–	NO	–	–
N9RSNN025	NEWHALL 90 25%	17.6	105.4	0.171	7.2	7.1	0.318	0.312	–	–	–	–	NO	–	–
N3RSNN025	NEWHALL 360 25%	29.6	153.7	0.188	10.1	9.8	0.438	0.462	–	–	–	–	NO	–	–

* Tests conducted to check the behavior prior to identification of the structure in simple-rigid configuration

Tests repeated due to misplaced accelerometer ABNEV

All tabulated peak values represent the maximum absolute value for either the positive or negative direction of drift.

It should be noted that seismic testing was conducted with the effective rigid-simple frame configuration only (identification tests included both rigid-simple and simple-rigid configurations). As mentioned earlier, the scissor-jack systems included damper 3 (and brace 1) on the east frame, and damper 2 (and brace 2) on the west frame (see Fig. 3-9). Also, the frame that was tested on the strong floor was used as the east frame in the earthquake simulator tests.

The results of Table 4-2 demonstrate that the scissor-jack system operates as an effective damping system. Drift is substantially reduced. As an example, consider the results of the El Centro motion: without the scissor-jack system, the structure (which is essentially elastic with damping ratio of 0.03) undergoes drift of 14.3 mm (average of east and west frames, test ELRSNN050.2). The damped structure undergoes less than half that drift when excited by the full-scale El Centro motion (test ELRSBD100). Interestingly in this case of elastic response, the peak-recorded acceleration is also smaller in the damped structure despite the stronger input. The responses of the undamped and damped structures in the Mexico City motion reveal similar observations (tests MXRSBD100 and MXRSNN100, respectively). For the same input, the damped structure undergoes 50-percent lesser drift and 40-percent lesser acceleration.

Measured values of the magnification factor for east and west frames vary in the range of 1.3 to 2.1 and are dependent on the excitation type and amplitude. As noted earlier, the magnification factor is also dependent on the direction of movement due to changes in the geometry of the scissor-jack system. In comparison to the measured values, the theoretical value (exclusive of the vertical deformation effects) is 1.8, whereas values measured in the testing of the frame in rigid-simple configuration under imposed harmonic displacement varied between 1.5 and 1.9. It must be noted that lower magnification factors of 1.0 and 1.1 were observed (tests PERSBD010 and SYRSBD010) as tabulated in Table 4-2, when the structure was subjected to earthquake motions of small amplitudes. While the lower magnification factors explain the reduction in damping ratio in low amplitude excitations (see previous discussion in conjunction with Figure 4-6), they also shed light on the origin of this phenomenon. As discussed earlier in Section 4.2, the lower magnification factors are likely caused by small imperfections in the scissor-jack system.

As mentioned previously, some of the tests were conducted with simultaneous application of horizontal and vertical components of the ground motions. The results of Table 4-2 show that the influence of the vertical component is generally trivial. This is in part because the gravity load on the structure was applied directly to the columns and not on the beams (see Figures 3-1 and 3-2), therefore vertical ground excitations could not cause significant vibration of the beams, which in turn could affect the scissor-jack system performance.

Table 4-2 also reveals that there is slight torsional response of the structure, apparent by the higher peak response parameters of the west frame. The reason for this torsional behavior may be due to differences in the stiffness and damping properties of the two frames and the scissor-jack-damper assemblies, although the frames and the damping systems were designed to be identical. In addition, the control of the earthquake simulator might have been imperfect, causing unwanted torsional motion, which may also have contributed to the torsional response of the structure.

Based on the results of Table 4-2, Figure 4-7 was developed, which presents a comparison of the performances of the structure without and with the damping system. The recorded peak drift ratio (peak drift divided by the height of the beam-to-column joint), normalized peak structural acceleration (peak acceleration of the beam-to-column joint divided by the peak simulator acceleration), and normalized peak damper force (peak damper force divided by the tributary weight per frame) are plotted against the peak simulator acceleration. The peak response quantities of drift, acceleration and damper force in Figure 4-7 are the greater of the east and west frame peak values from Table 4-2. Note the use of the peak simulator acceleration as representative of the intensity of the seismic excitation, given the low period of the tested model. The benefits offered by the damping system are clearly evident in this figure: lower drift and lower acceleration for a given intensity of seismic excitation. These benefits are typical of what damping systems may offer, thus Figure 4-7 demonstrates the equivalence of the scissor- jack-damper configuration to more conventional configurations. In addition, the normalized peak damper force plot suggests that the required peak damper force as portion of the tributary weight in the scissor-jack-damper configuration is smaller in comparison to other tested damper configurations (e.g., Constantinou and Symans 1992, Seleemah and Constantinou 1997).

Of interest is to discuss the effect of the stiffening of the structure on the reduction of response.

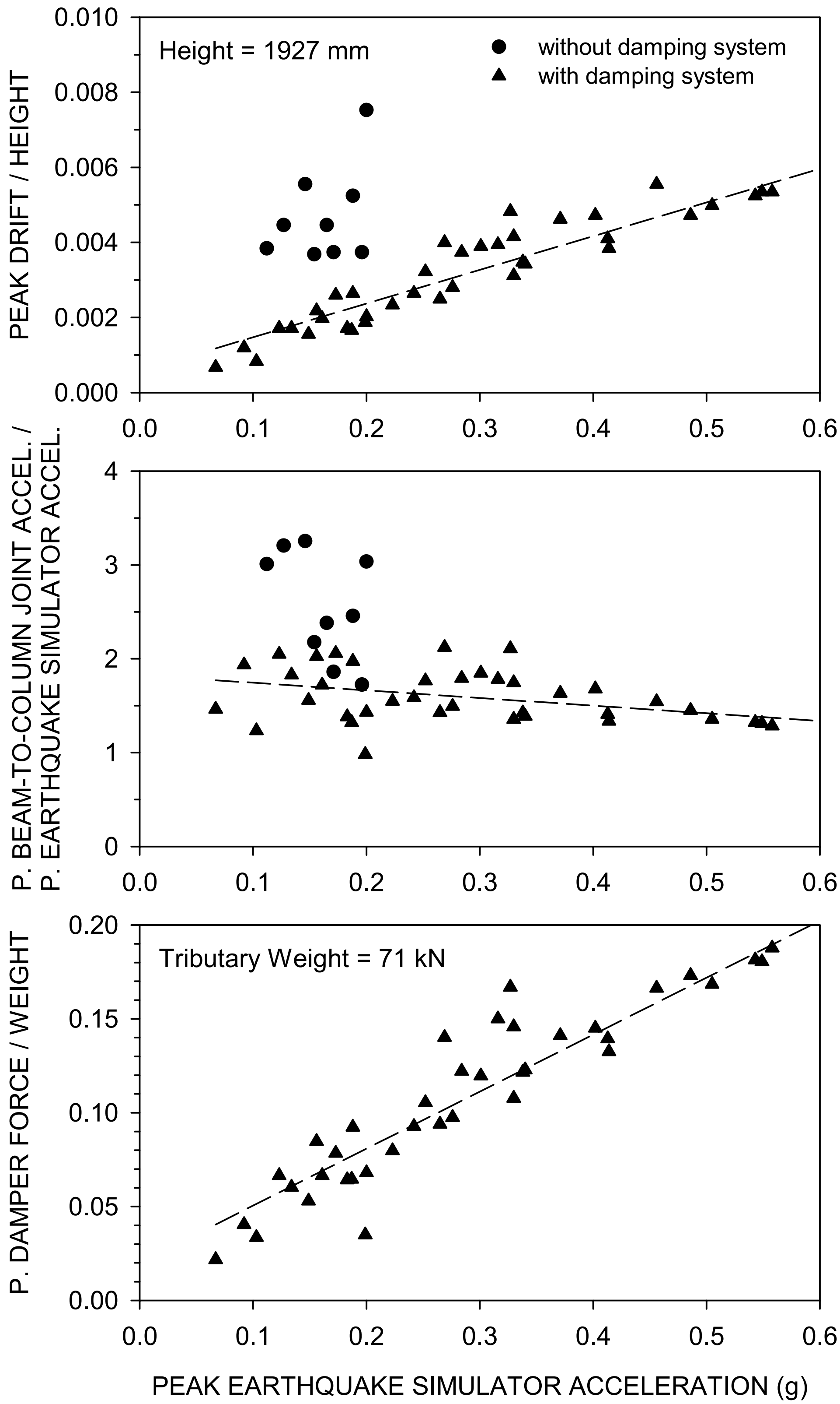

Figure 4-7 Peak Response of Model Structure as Function of Peak Earthquake Simulator Acceleration (Rigid-Simple Configuration)

The reduction in displacement response is certainly the combined result of stiffening of the structure and of increased damping. However, the reduction of acceleration response is primarily the result of increased damping. It should be noted that the model structure is stiff with a fundamental period that falls within the acceleration-sensitive region of the spectrum for all of the earthquake motions used in the testing (see Figure 3-11 and Table 4-1), for which, reductions in period (stiffening) do not result in reduction of acceleration.

Detailed results of each test are presented in Appendix C in the form of histories of drift and acceleration, and damper force versus damper deformation loops. In accordance with previous sign conventions, drift towards the right and associated damper extension and damper force are taken positive.

SECTION 5

ANALYTICAL PREDICTION OF RESPONSE-HISTORY

5.1 Introduction

Dynamic analysis of the tested structure was performed using the computer program SAP2000 (Computers and Structures, Inc. 2000 and 2003). Two different solution methods were used; nonlinear modal time-history analysis (also called fast nonlinear analysis, or FNA), and nonlinear direct-integration time-history analysis. The latter became available in the latest version (at the time of writing of this report) of SAP2000 (version 8). Initially, the model was created with version 7.4 and analyzed using FNA. While detailed information on the two procedures is available in the program manuals, a brief description of each will be presented herein.

The FNA is suitable and very efficient for analyzing structures that are primarily linear elastic, but may have a number of predefined nonlinear elements (that is, geometric nonlinearities are not taken into account). This analysis option is thus expected to replicate the dynamic behavior of the structure under the assumption of small deformations. The method involves solution of uncoupled modal equations and modal superposition with the use of Load Dependent Ritz (LDR) vectors, which include the effects of nonlinear forces. On the other hand, the nonlinear direct-integration time-history analysis utilizes direct integration of the full equations of motion, in which, material and geometric nonlinearities may be included.

5.2 Analytical Model

Due to symmetry of the structure, only one of the two frames was modeled. Figure 5-1 illustrates the 2-dimensional model used to simulate the behavior of the structure under earthquake excitation. Masses, calculated from the added concrete blocks and tributary lengths of the elements, were lumped at the joints, as shown in Figure 5-2. Joint coordinates including lumped masses, and a summary of member properties are listed in Tables 5-1 and 5-2, respectively. In Figure 5-1, single lines denote frame elements (beam, columns and braces), and triple lines represent rigid elements (frame elements with large section properties), which were

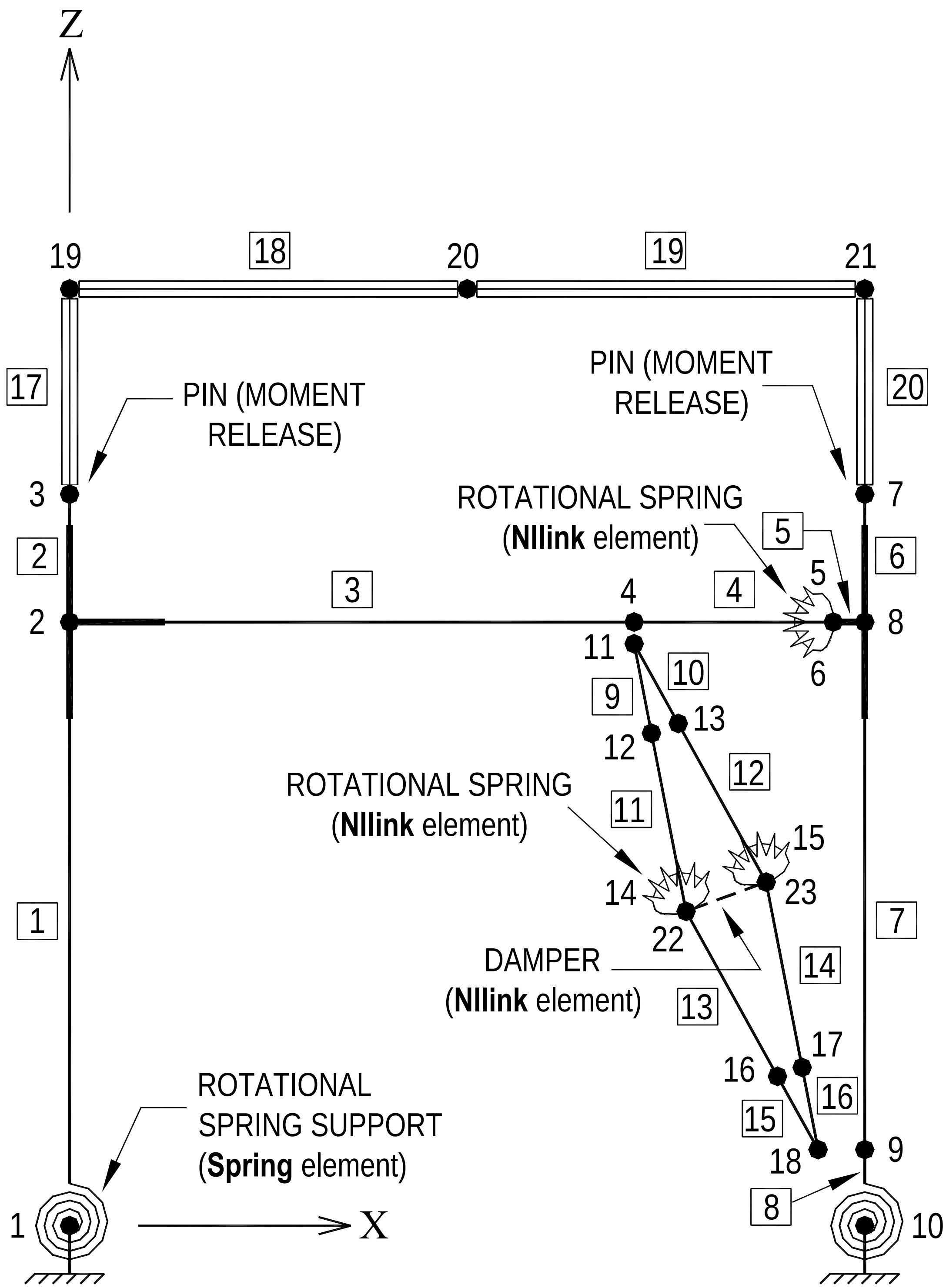

Figure 5-1 Schematic Illustrating Joints and Elements in SAP2000 Model of Frame with Rigid-Simple Connections (see Tables 5-1 and 5-2 for joint coordinates and member properties)

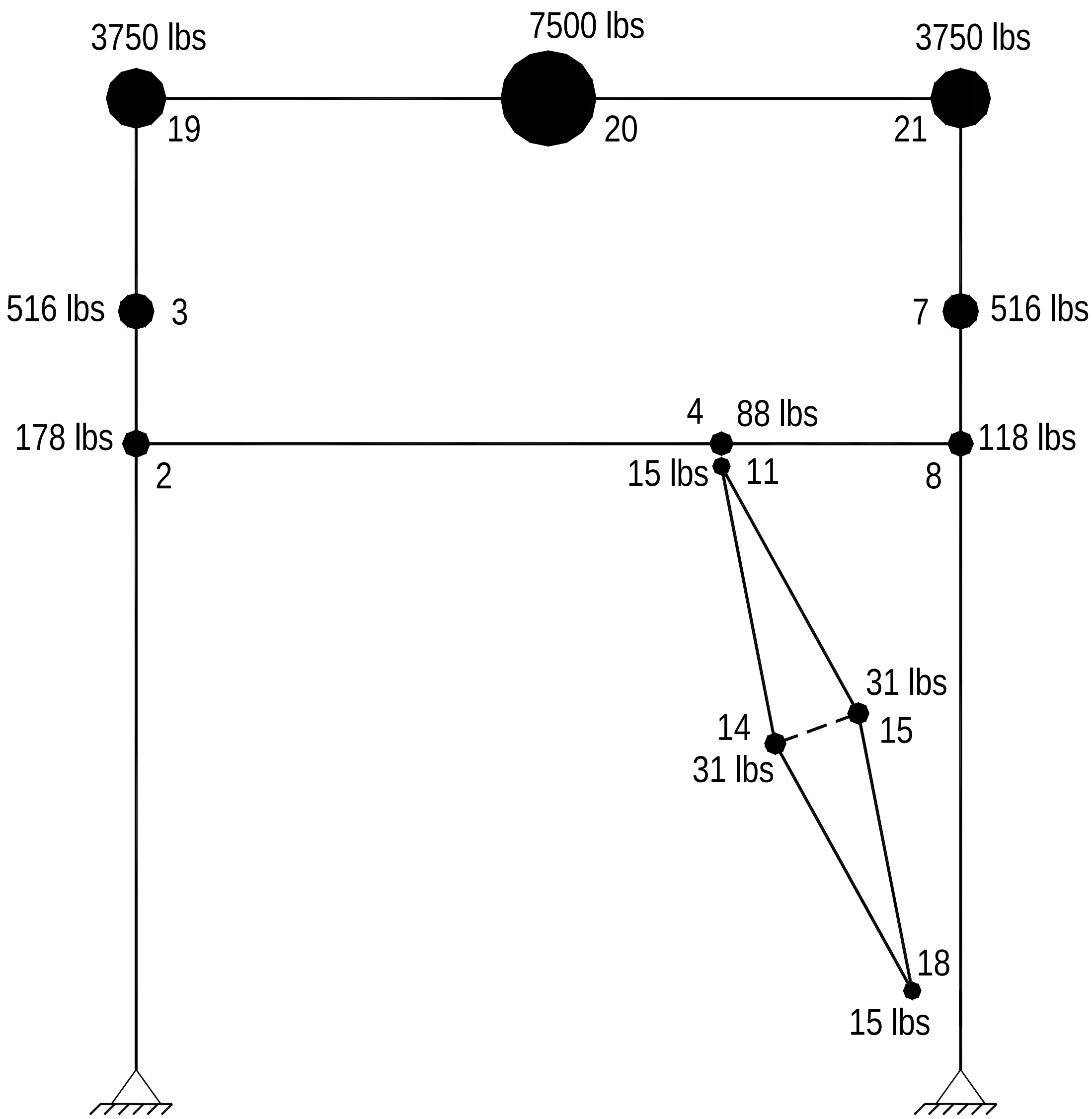

Figure 5-2 Schematic Illustrating Lumped Weights in SAP2000 Model of Frame (1 lb = 4.45 N)

used to model the behavior of the concrete blocks. Joints and frame elements are numbered as they appear in the sample input file, which is included in Appendix D.

The connections of the columns to the base plates were modeled as pins with rotational springs, to simulate their semi-rigid behavior. The connection at the interface between the beam and the right column was also modeled as a pin with a rotational spring. The values of these rotational springs were assigned such that the calculated fundamental frequency of the analytical model

Table 5-1 Joint Coordinates and Lumped Masses in SAP2000 Model (1 in = 25.4 mm)

Joint No	X (in)	Z (in)	Mass (kips×sec^2/in)	Joint No	X (in)	Z (in)	Mass (kips×sec^2/in)
1	0	0	–	13	76.54	63.13	–
2	0	75.88	4.61×10^{-4}	14	77.52	39.52	7.94×10^{-5}
3	0	91.94	1.34×10^{-3}	15	87.59	43.18	7.94×10^{-5}
4	70.99	75.88	2.29×10^{-4}	16	89.02	18.77	–
5	96.04	75.88	–	17	92.12	19.90	–
6	96.04	75.88	–	18	94.13	9.56	3.97×10^{-5}
7	100	91.94	1.34×10^{-3}	19	0	117.74	9.71×10^{-3}
8	100	75.88	3.05×10^{-4}	20	50	117.74	1.94×10^{-2}
9	100	9.56	–	21	100	117.74	9.71×10^{-3}
10	100	0	–	22	77.52	39.52	–
11	70.99	73.14	3.97×10^{-5}	23	87.59	43.18	–
12	73.17	61.90	–				

matched that obtained from testing. Rotational springs were also introduced at the joints where the scissor-braces and the damper were connected. These connections were not true pins so that they exhibited a finite amount of fixity. (Rotational springs are not needed when spherical bushings are used – a situation most likely to occur in applications of the technology.) It must be noted that in version 8, it is also possible to use **frame releases** with **partial fixity** in lieu of the rotational springs at the beam-to-column interface and damper-brace connections.

The dampers were modeled as nonlinear viscous elements, using the **Nllink** element (**Link** element in versions 8 of SAP2000), **damper** property, with force-velocity relation given by $F_D = C_{No} \cdot \dot{u}_D{}^{\alpha}$ with parameters $C_{No} = 137.3$ N-(sec/mm)$^{\alpha}$, and α = 0.76 to simulate their behavior for a large range of damper velocities (see Figure 3-9). Beam-to-column joints were modeled using **end offsets** and **rigid-end factor**s, to represent the rigid zone at the connections (shown with thick single lines in Figure 5-1).

As seen in Figure 5-1, no elements were explicitly defined between joints 4 and 11, and between joints 18 and 9. Instead, each pair of these joints was constrained in the two translational (X and Z), and one rotational (Y) degrees of freedom. **Constraints** in translational degrees of freedom

TABLE 5-2 Element Properties in SAP2000 Model (1 in = 25.4 mm, 1 kip = 4.45 kN)

Element	Joint i	Joint j	Section	Area (in^2)	I_{y-y} (in^4)	Shear Area (in^2)
1	1	2	W8×24	7.08	82.8	1.94
2	2	3	W8×24	7.08	82.8	1.94
3	2	4	W8×21	6.16	75.3	2.07
4	4	5	W8×21	6.16	75.3	2.07
5	6	8	W8×24	7.08	82.8	1.94
6	7	8	W8×24	7.08	82.8	1.94
7	8	9	W8×24	7.08	82.8	1.94
8	9	10	W8×24	7.08	82.8	1.94
9	11	12	PLATE	1	0.0052	0.83
10	11	13	PLATE	1	0.0052	0.83
11	12	14	TS2×2×1/4	1.59	0.766	1
12	13	15	TS2×2×1/4	1.59	0.766	1
13	22	16	TS2×2×1/4	1.59	0.766	1
14	23	17	TS2×2×1/4	1.59	0.766	1
15	16	18	PLATE	1	0.0052	0.83
16	17	18	PLATE	1	0.0052	0.83
17	3	19	RIGID	100	1000	0 *
18	19	20	RIGID	100	1000	0 *
19	20	21	RIGID	100	1000	0 *
20	21	7	RIGID	100	1000	0 *
SPRING	1	–	K_{rot} = 45000 kips×in/radian			
SPRING	10	–	K_{rot} = 45000 kips×in/radian			
NLLINK **	14	15	C = 0.36 kips-(sec/in)$^{\alpha}$, and α = 0.76			
NLLINK **	5	6	K_{rot} = 1660 kips×in/radian			
NLLINK **	14	22	K_{rot} = 1000 kips×in/radian			
NLLINK **	15	23	K_{rot} = 1000 kips×in/radian			

* A zero shear area is interpreted, as being infinite in SAP2000, such that the corresponding shear deformation is zero.

** Nllink elements are referred to as Link in SAP2000 version 8.

were also used at coincident joint pairs (i.e., joints 5-6, 14-22, and 15-23), where zero-length link elements provided for rotational stiffness. Additional details regarding the model may be found in the input file provided in Appendix D.

It must be noted that the text input file in Appendix D was created for SAP2000 version 7.4 (and uses FNA method), and it must be translated to run in version 8. Versions earlier than 8 support text input files besides graphical input, whereas version 8 is more graphical user interface (GUI) oriented. However it is possible to edit the input once the model is created. All input files, prepared for version 7.4 (with FNA analysis) and 8.2.3 (with FNA and nonlinear direct-integration time-history analysis options) can also be provided electronically.

5.3 Dynamic Response-History Analysis Results

Sample comparisons of experimental results to analytical predictions using the FNA method are presented in Figures 5-3 to 5-8. The compared responses are histories of drift (displacement of joint 2 with respect to joint 1) and of absolute acceleration of joint 2, and damper force-displacement loops (experimental data were obtained from east frame instruments). As evident in the figures, the analytical model is well capable of capturing significant characteristics of the behavior of the system, such as the stiffening effect (evident by matching frequency contents of the experimental and analytical response-histories) and peak values of drift and acceleration. Also, the analysis tended to slightly overestimate the damper displacements and forces in some tests, and underestimated them in others (it is easier to observe the match/mismatch in the damper output by looking at histories of damper force and damper displacement, rather than loops). The discrepancies between the experimental and the analytically predicted damper force and damper displacement are mainly due to:

1. Uncertainties in the exact geometry of the scissor-braces during testing (the damper output is sensitive to changes in the geometry of the scissor-braces as seen in Figure 2-7).
2. Changes in the temperature of the dampers during continuous testing can cause changes in their properties.
3. Deformations as a result of any minor slippage (or reduction in friction) in the joints are magnified in the scissor-braces, which can affect the damper output.

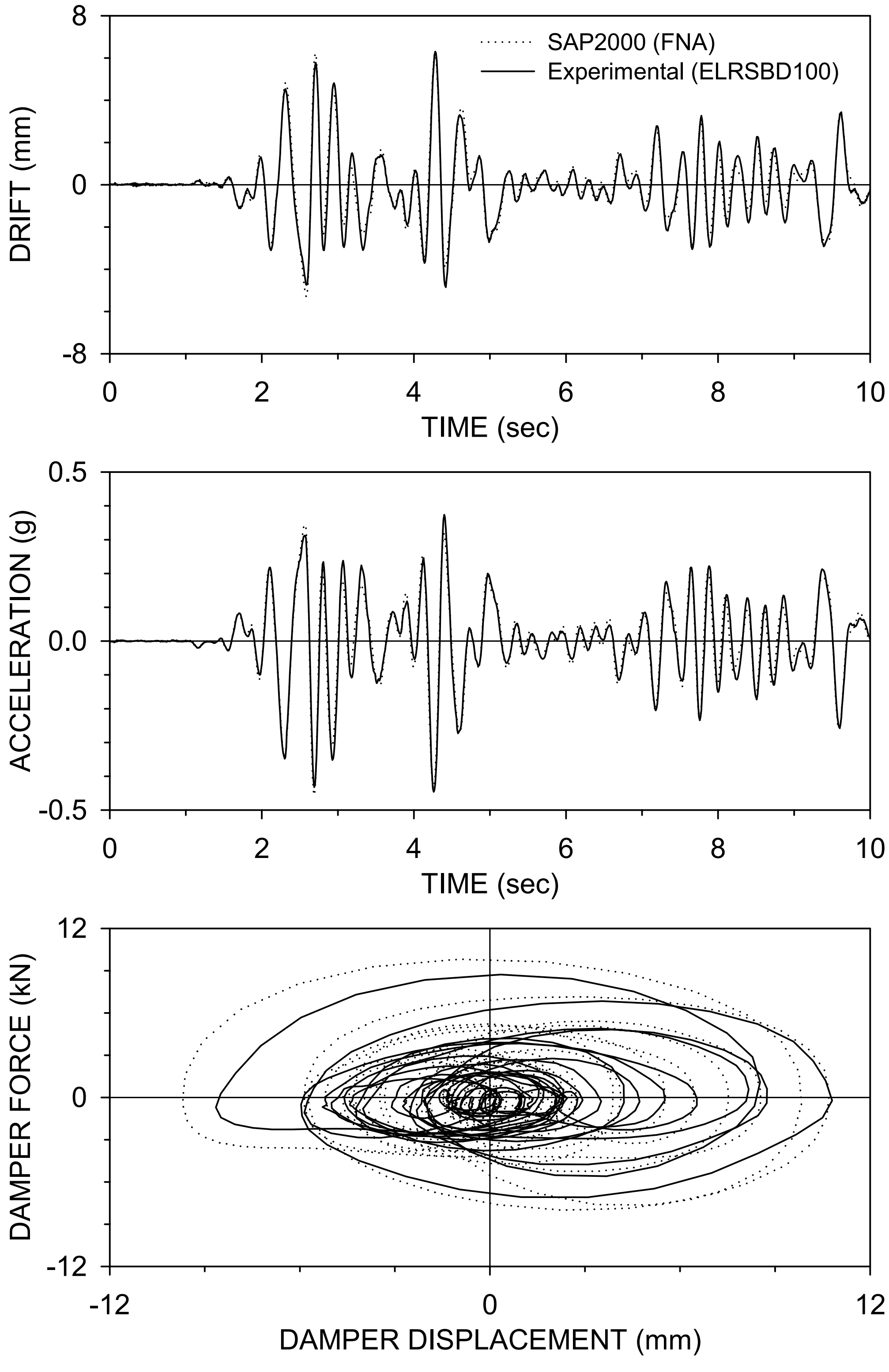

Figure 5-3 Comparison of Analytical (SAP2000, FNA) and Experimental Response of Model Structure with Rigid-Simple Beam-to-Column Connections for El Centro 100% Input

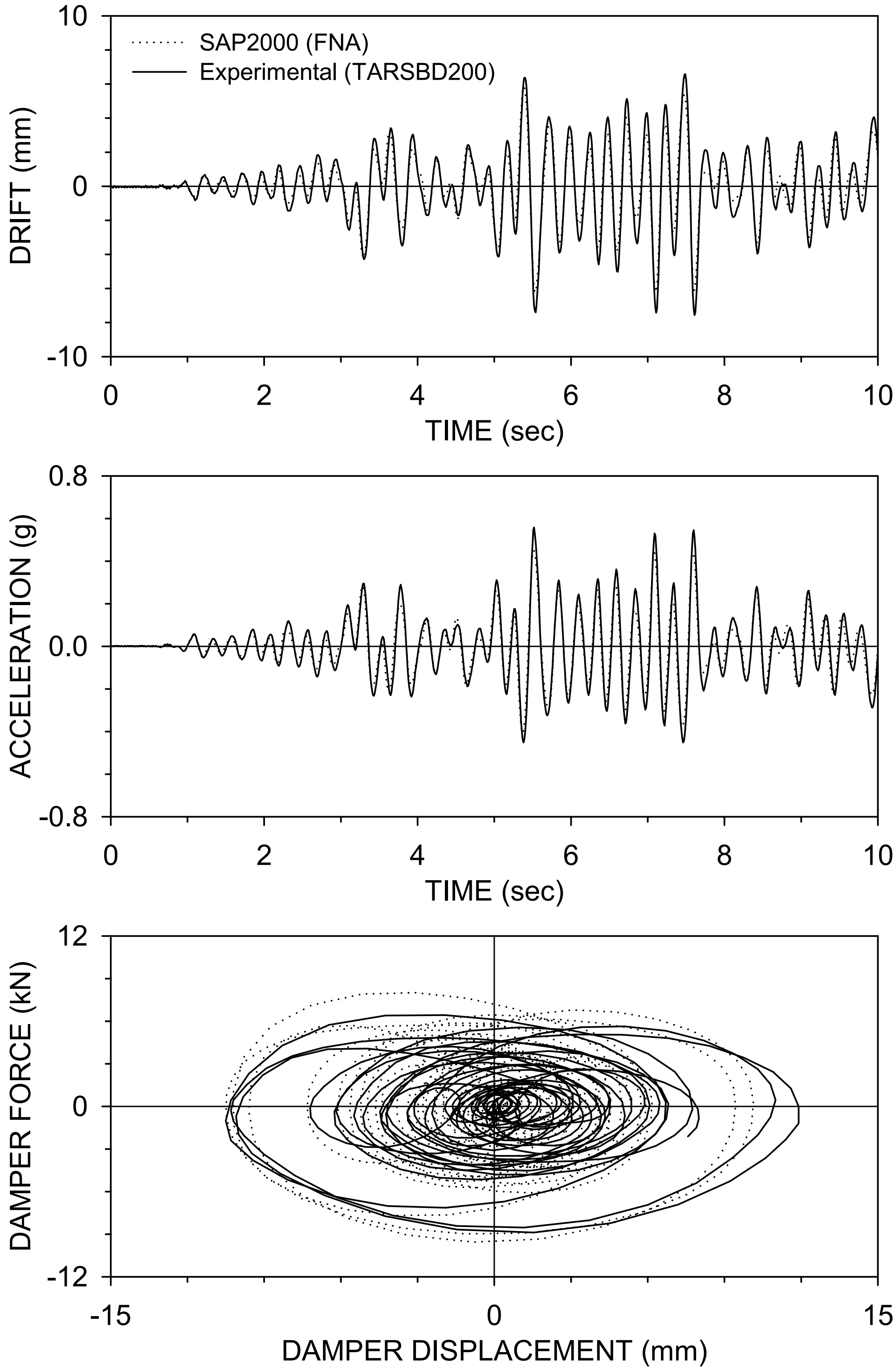

Figure 5-4 Comparison of Analytical (SAP2000, FNA) and Experimental Response of Model Structure with Rigid-Simple Beam-to-Column Connections for Taft 200% Input

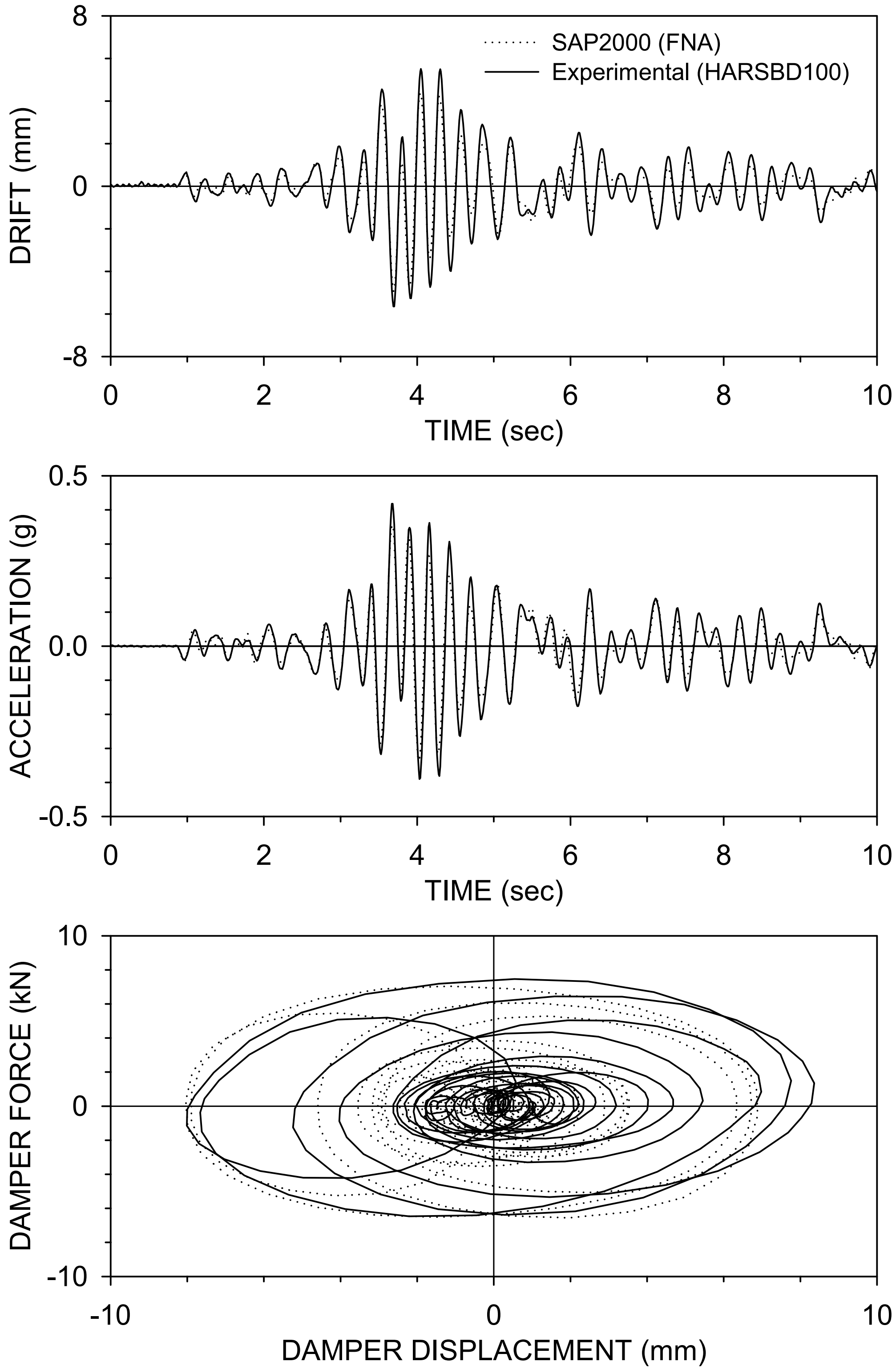

Figure 5-5 Comparison of Analytical (SAP2000, FNA) and Experimental Response of Model Structure with Rigid-Simple Beam-to-Column Connections for Hachinohe 100% Input

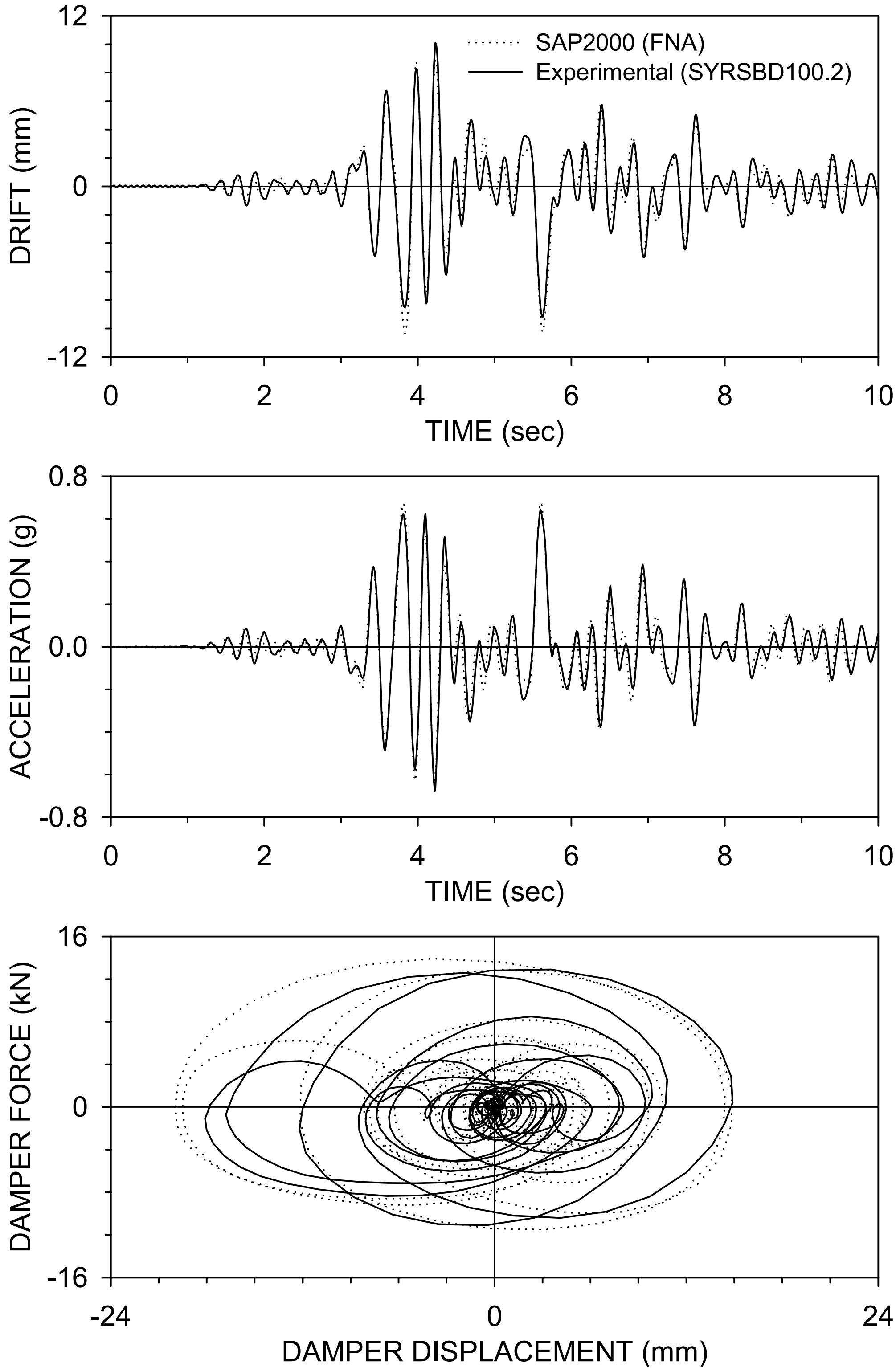

Figure 5-6 Comparison of Analytical (SAP2000, FNA) and Experimental Response of Model Structure with Rigid-Simple Beam-to-Column Connections for Sylmar 100% Input

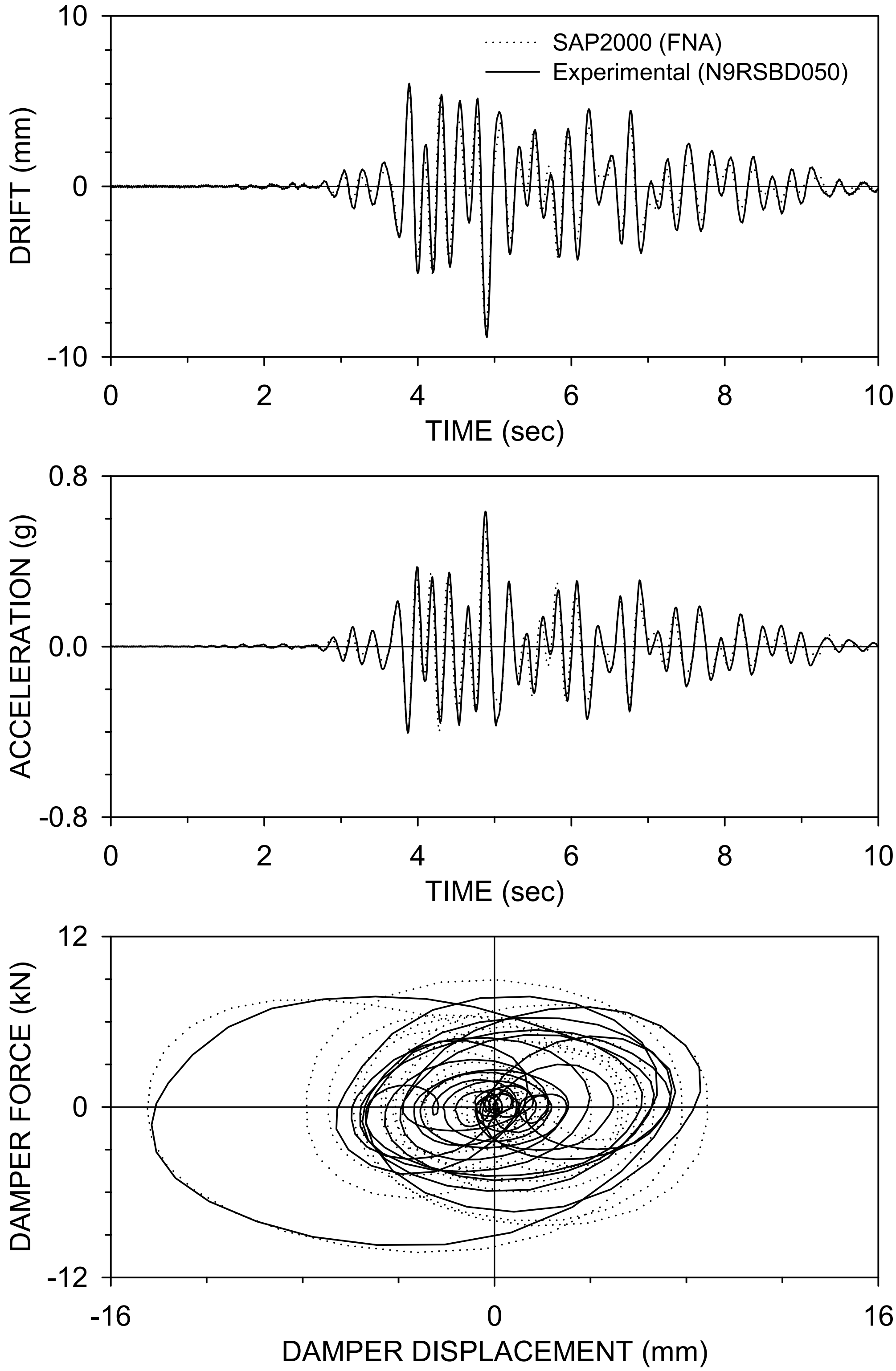

Figure 5-7 Comparison of Analytical (SAP2000, FNA) and Experimental Response of Model Structure with Rigid-Simple Beam-to-Column Connections for Newhall 90 50% Input

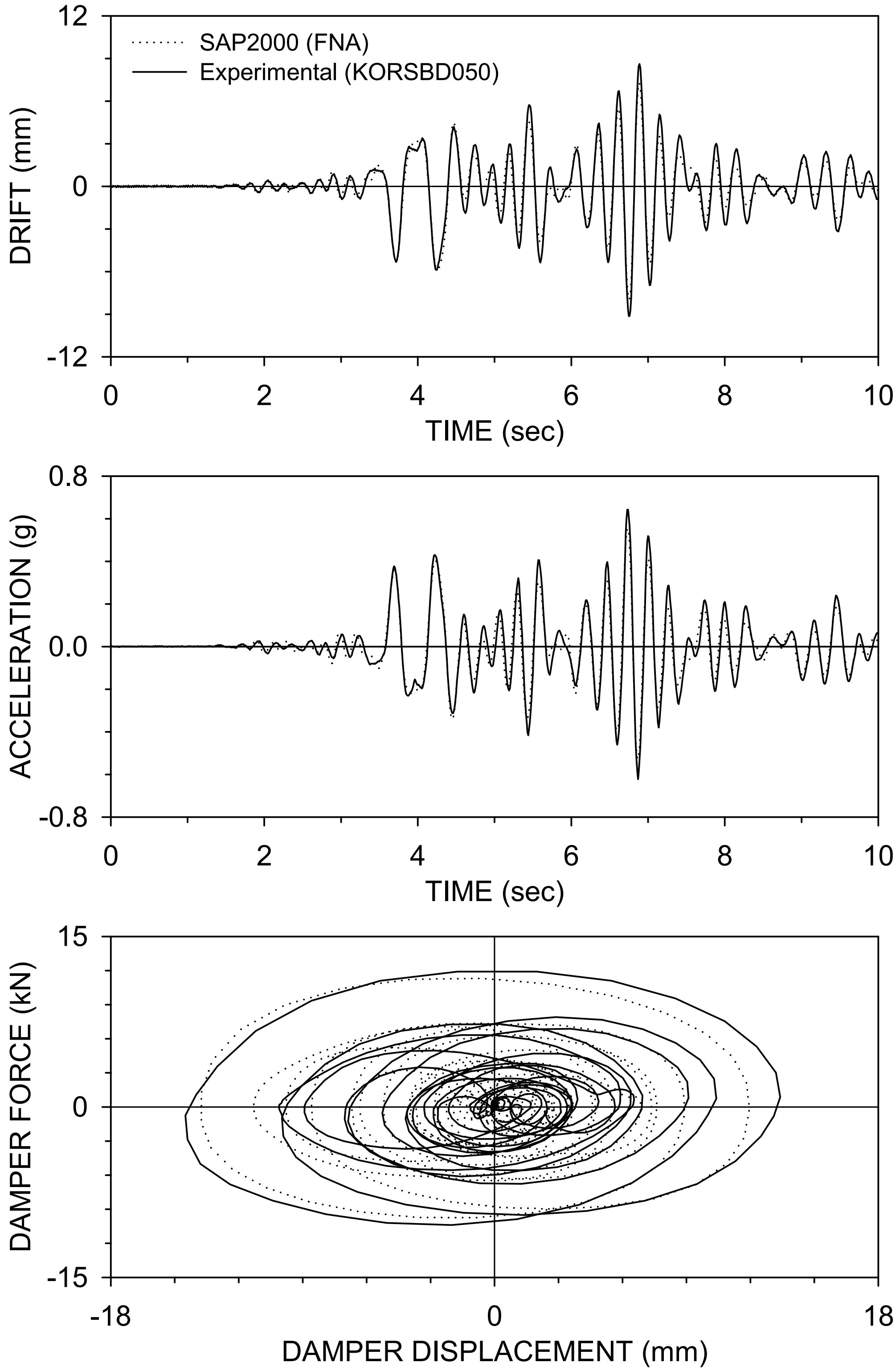

Figure 5-8 Comparison of Analytical (SAP2000, FNA) and Experimental Response of Model Structure with Rigid-Simple Beam-to-Column Connections for Kobe 50% Input

4. Dependence of magnification factor on amplitude of motion due to scissor-jack imperfections.

As mentioned earlier, analysis of the model using the FNA method is representative of its behavior under the small deformation theory. Results of analysis under the assumption of small deformations are compared to large deformation analysis results in Figure 5-9, where the latter are obtained by the nonlinear direct-integration time-history analysis method. As the figure suggests, the difference between the two sets of results is insignificant, which is in agreement with the analysis presented in Figure 2-8 (note, in the figure, that the two methods start diverging at approximately ±15 mm of lateral displacement, whereas the largest drift observed in the earthquake simulator tests with the damping system was about 11 mm, see Table 4-2).

It should be noted that the nonlinear direct-integration time-history analysis lasted over 30 hours for a 30-second portion of the El Centro motion, on an Intel Pentium computer (with two CPU's of 3.05 GHz each, and a 1 GB RAM), with and without the large displacement effects, whereas the FNA took only about 2 minutes for the full-length motion.

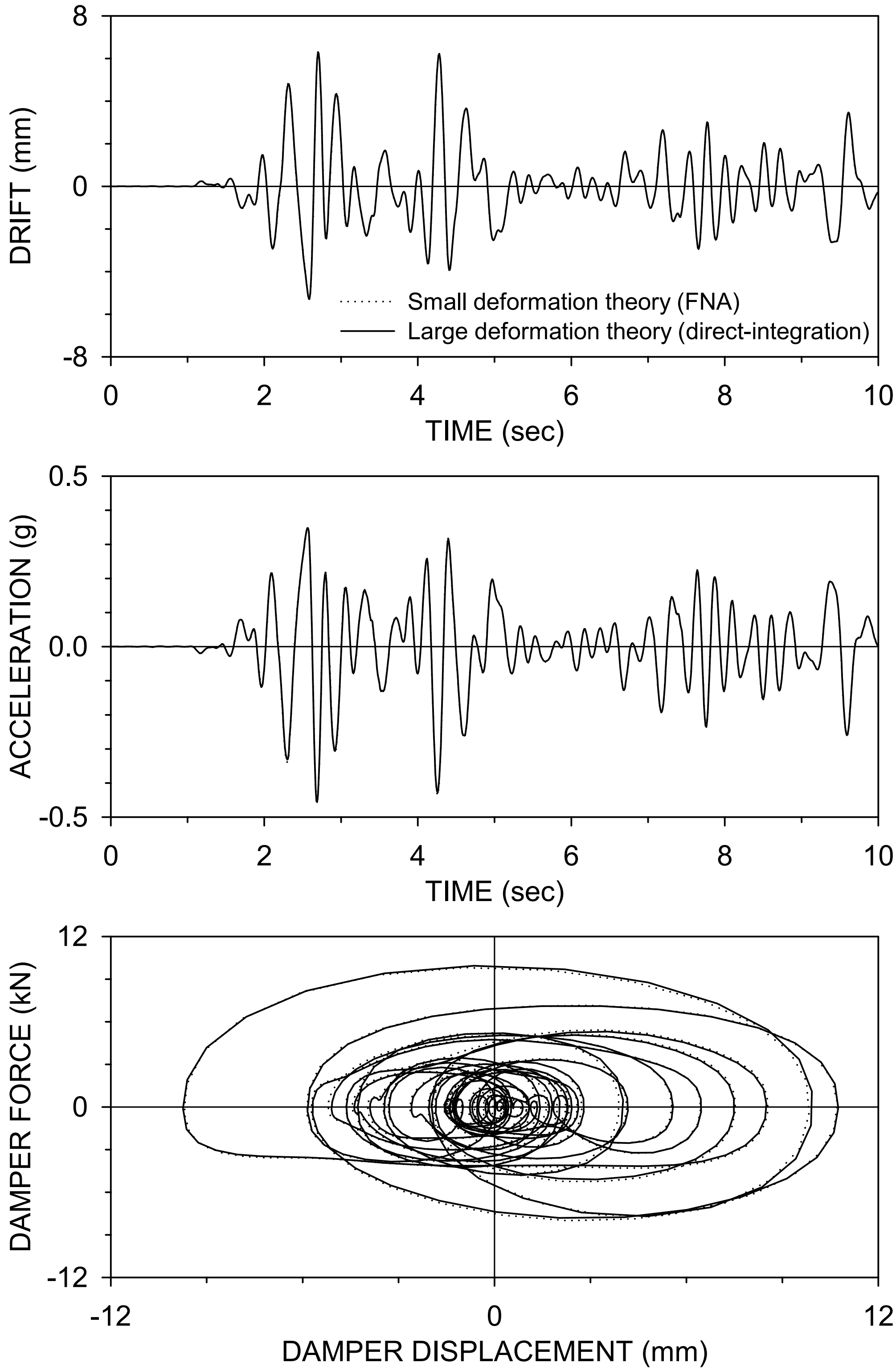

Figure 5-9 Comparison of Analytical Response of Model Structure by SAP2000 for El Centro 100% Input (Test ELRSBD100) Using Small and Large Deformation Theories

SECTION 6

SIMPLIFIED ANALYSIS

6.1 Introduction

The effects of adding an energy dissipation system to a structure, accounting for the flexibility of the damping assembly were explained in Section 2.6. This section presents an approximate analysis method based on energy principles, and illustrates its application on the tested structure utilizing the information given in Section 2.6.

The addition of energy dissipation devices to a building results in a nonclassically damped structure even if the structure itself has classical damping. Exact methods to determine the dynamic properties (e.g., frequencies of free vibration, mode shapes, and damping ratios) of the damped structure are available, but may become involved since they necessitate complex eigenvalue analysis. The interested reader is referred to Veletsos and Ventura (1986) for a comprehensive treatment of the complex eigenvalue problem and Constantinou and Symans (1992) for an illustration of the exact analysis for the case of linear viscous and viscoelastic fluid dampers.

Also, as explained in Section 2.6, addition of energy dissipation devices to a building causes an increase in stiffness and a reduction in period (see eq. 2-23). This phenomenon is well understood for devices with viscoelastic behavior (e.g., see Soong and Dargush 1997, Constantinou et al. 1998, and Hanson and Soong 2001).

An alternative to the exact methods is the use of approximate methods of analysis based on energy principles. Such methods are very simple to apply and, accordingly, have been utilized in analysis and design provisions and guidelines (Federal Emergency Management Agency 1997, 2000, and 2003). The approximate methods of analysis typically provide results of acceptable accuracy when complete vertical distributions of damping devices are used.

The approximate energy method starts with the assumption that the frequencies and mode shapes of the nonclassically damped structure are identical to those of the undamped structure with the added effect of storage stiffness (k'), but not of damping (c'), from the energy dissipation assembly (see eq. 2-23). This assumption implies that the added damping is proportional – that is, the undamped mode shapes f of the structure with added stiffnesses that are due to the damping devices diagonalize the structure's damping matrix; namely the product $f^T \cdot C \cdot f$, where C is the damping matrix, is diagonal. Thus, the frequencies and mode shapes can be determined from standard eigenvalue analysis. Figure 6-1 depicts a multi-story structural system with linear viscous dampers in scissor-jack assemblies. Assuming that the structure undergoes vibration in the k^{th} mode with period T_k (or with frequency of vibration in the k^{th} mode equal to w_k), the damping ratio at the j^{th} story may be expressed as (Constantinou and Symans 1992, Federal Emergency Management Agency 1997, 2000, and 2003)

$$b_k = \frac{g}{4 \cdot p} \cdot \frac{T_k \cdot \sum_j c'_j(w_k) \cdot f_j^2 \cdot f_{rj}^2}{\sum_i W_i \cdot f_i^2} \tag{6- 1}$$

where f_{rj} is the k^{th} modal interstory drift of the j^{th} story (equal to the relative modal displacement between the ends of damper system j in the horizontal direction); W_i = lumped weight at the i^{th} floor level; f_i = modal displacement of floor level i in the k^{th} mode of vibration; and c'_j is the damping coefficient of damper system j inclusive of the effect of energy dissipation assembly flexibility, given by (2-23). Summation j extends over all stories and summation i extends over all lumped weights. It must be noted that the magnification factor f_j is equal to $cos q_j$ (q_j = inclination angle of the dampers) for devices installed diagonally; is unity for the case of chevron brace configuration of Figure 2-4; and $cos y_j / tan q_j$ (refer to Figure 2-4 for angles y_j and q_j) for the scissor-jack system. For a single-story structure, $f_{rj} = f_i = 1$, $i = j = 1$ and (6-1) simplifies, for the case of rigid energy dissipation assembly, to (2-5).

It can be seen that the calculation of b_k using (6-1) takes into account the lateral interstory drift only (i.e., the horizontal displacement of each floor represents a degree of freedom in Figure 6-1). However, vertical displacements (due to column rotation, axial flexibility of supporting columns and frame deformations) may also affect the damper deformation, as explained in Sections 2.3 and 2.5. In such cases, it is useful to express b_k in its general form, which is given as (Constantinou and Symans 1992, Federal Emergency Management Agency 1997 and 2000)

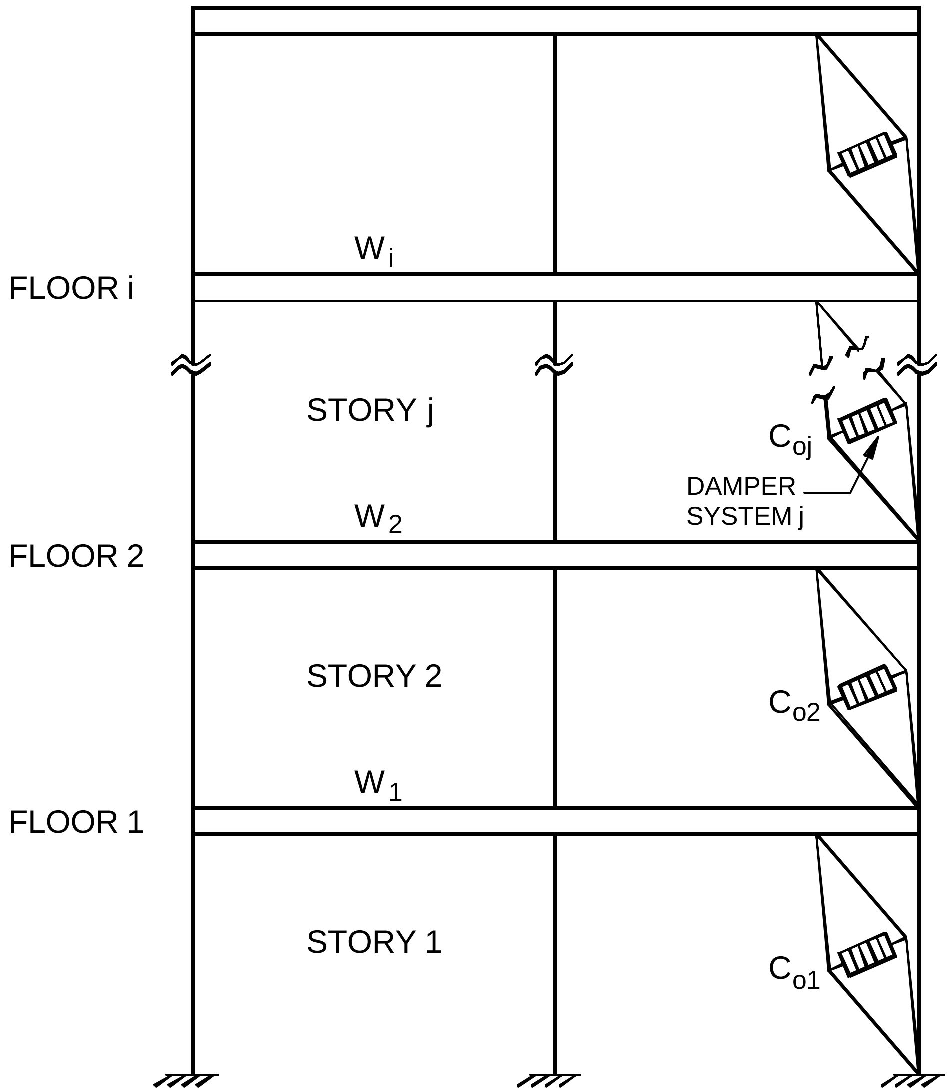

Figure 6-1 Structural System with Linear Dampers

$$b_k = \frac{g}{4 \cdot p} \cdot \frac{T_k \cdot \sum_j c'_j(w_k) \cdot f_{rjD}^2}{\sum_i W_i \cdot f_i^2} \qquad (6\text{- }2)$$

where f_{rjD} is the k^{th} modal relative displacement between the ends of the device along the axis of the device at the j^{th} story, which implicitly accounts for the effect of vertical displacements.

Within the context of approximate methods of analysis (as, for example, those described in Federal Emergency Management Agency 2000), the mode shapes may be assumed or calculated for the undamped structure without the effect of the storage stiffness resulting from the viscoelastic nature of the energy dissipation assembly. Such an approximation produces acceptable results when the distribution of damping devices is complete over the building height. In such cases, it is of interest to develop a simple approximate method of estimating the periods of vibration of the damped structure. In arriving at an approximate method, one recognizes that

$$T_k' = 2 \cdot p \cdot \left[\frac{\sum_i W_i \cdot f_i^2}{g \cdot \sum_j K_j \cdot f_{rj}^2} \right]^{1/2} \tag{6- 3}$$

where T_k' is the k^{th} mode period of the undamped structure (exclusive of the damping system) and K_j is the horizontal stiffness of story j. Similarly, the period T_k of the structure with the damping system may be written as

$$T_k = 2 \cdot p \cdot \left[\frac{\sum_i W_i \cdot f_i^2}{g \cdot \sum_j (K_j + c_j' \cdot t_j \cdot w_k^2 \cdot f_j^2) \cdot f_{rj}^2} \right]^{1/2} \tag{6- 4}$$

where t_j is the relaxation time, calculated as the ratio of the damping constant to the stiffness of the damping assembly at story j (see Section 2.6). Equations (6-1) to (6-4) may be combined to arrive at the following relation provided that the mode shape is the same for the undamped and the damped structure:

$$T_k = T_k' \cdot \left[1 - \frac{4 \cdot p \cdot t \cdot b_k}{T_k} \right]^{1/2} \tag{6- 5}$$

where parameter t is assumed to be the same for all stories of the structure, or t is an average representative value for all stories. Equation (6-5) is implicit in period T_k and can be solved using an iterative procedure, or by the solution of a cubic equation. However, given the approximate nature of the calculation, the following equation, representing the result of the first iteration, may be used.

$$T_k \approx T_k' \cdot \left[1 - \frac{4 \cdot p \cdot t \cdot b_k}{T_k'} \right]^{1/2} \tag{6- 6}$$

6.2 Simplified Analysis of Tested Structure

Response-history analysis represents the best means of calculating the seismic response of a structure with the scissor-jack system. Illustrated in Figure 6-2(a) is the complete structural representation of the tested model that was used in the response-history analysis reported in Section 5 (only one of the two frames of Figure 3-2 was analyzed due to symmetry), with the exception that the damper is linear viscous as described by (2-3). This representation may be simplified for ease in the dynamic analysis by replacing the scissor-jack assembly by an equivalent spring and dashpot system as shown in Figure 6-2(b). It must be noted that the quantity K_a represents the stiffness of the assembly only, which is typically very large. It is determined by the procedure illustrated in Figure 6-2(b). In the calculation of stiffness, the damper is considered "locked" so that it acts as a spring with stiffness equal to that of the oil column in the damper. This stiffness is given by $A_r^2 \cdot B / V$, where A_r is the piston rod area, V is the effective volume of fluid, and B is its bulk modulus. In the case of the dampers in the tested model, the stiffness of the locked damper was represented by a steel element having a diameter of 10 mm and length equal to that of the damper.

Simplified analysis is based on the premise that a linear elastic and proportional linear viscous representation of the structural system produces estimates of the seismic response that are of acceptable accuracy. A discussion on the subject may be found in Hanson and Soong (2001); several examples of application of simplified methods of analysis and evaluation of the accuracy of the methods may be found in Ramirez et al. (2001). Herein, it is of interest to predict the fundamental period and associated damping ratio of the tested model using simplified methods of analysis described by eqns. (6-1) and (6-5).

The tested model is simple in the sense that it essentially is a single-degree-of-freedom system undergoing elastic deformations. Yet, application of the simplified methods for predicting the period and damping ratio are complicated by the effect of the deformations of each frame under the action of the damping forces, which results in a substantial increase in stiffness. Prediction of this increase in stiffness is important in the application of simplified analysis.

Figure 6-2(c) illustrates the procedure for calculating stiffness parameter K_b. As in the case of the response-history analysis, half of the structure is analyzed (due to symmetry) with the lateral degree of freedom restrained, the scissor-jack assembly disconnected from the column and a

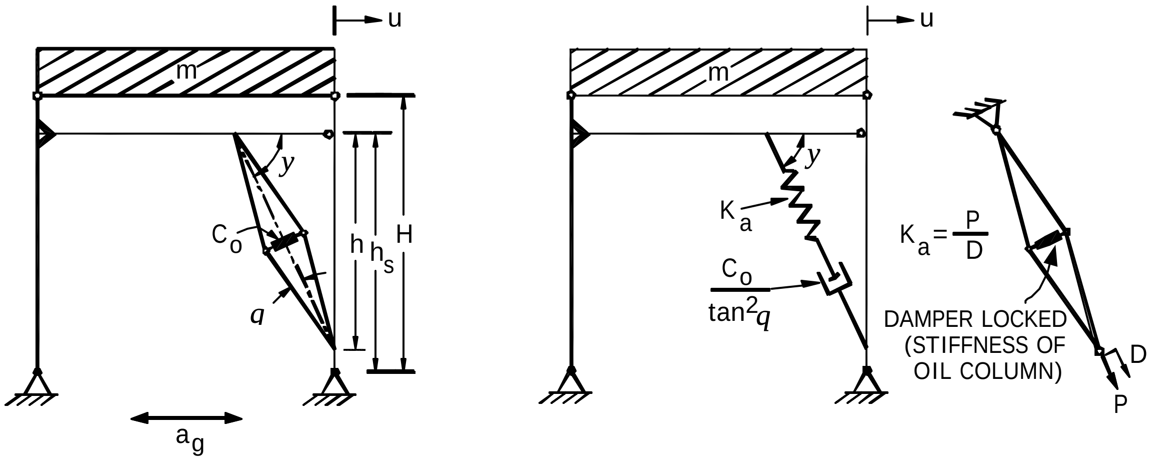

(a) Complete Structural Representation

(b) Representation with Scissor-Jack Replaced by Equivalent Spring/Dashpot

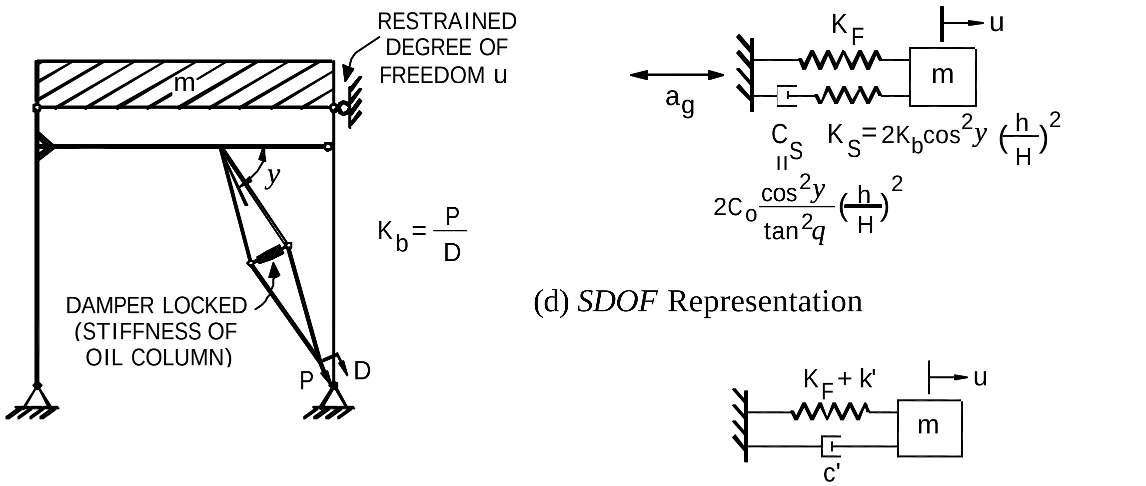

(c) Determination of Stiffness K_b

(e) *SDOF* Representation using Kelvin Element

Figure 6-2 Representation of Structure for Simplified Analysis

displacement D applied along the axis of the scissor-jack. The force P needed to produce displacement D is calculated and the stiffness parameter is computed as $K_b = P/D$. This stiffness is simply related to the added stiffness provided by the energy dissipation assembly. Stiffness K_b was calculated to be 34.5 kN/mm (per frame).

Shown in Figure 6-2(d) is a single-degree-of-freedom representation of the tested model, in which, the structure is considered in its entirety (i.e., two frames, two scissor-jacks). In this representation, K_F is the lateral stiffness of the frames exclusive of the energy dissipation system, and K_S and C_S are the stiffness and damping constant, respectively, contributed by the two scissor-jack-damper systems inclusive of the effect of interaction between each frame and the scissor-jack-damper system connected to it. These parameters are given by

$$K_S = 2 \cdot K_b \cdot cos^2 y \cdot \left(\frac{f_{r1}}{f_1} \right)^2 \approx 2 \cdot K_b \cdot cos^2 y \cdot \left(\frac{h}{H} \right)^2 \tag{6- 7}$$

$$C_S = 2 \cdot \frac{C_o \cdot cos^2 y}{tan^2 q} \cdot \left(\frac{f_{r1}}{f_1} \right)^2 \approx 2 \cdot \frac{C_o \cdot cos^2 y}{tan^2 q} \cdot \left(\frac{h}{H} \right)^2 \tag{6- 8}$$

where f_{r1} is the relative modal horizontal displacement of the two ends of the scissor-braces and f_1 is the modal displacement of the center of mass of the concrete block. The mode shape can easily be determined from the analytical model of the structure developed for response-history analysis (Section 5). One can also recognize that for the model structure, $f_{r1} / f_1 \approx h / H$, as illustrated in Figure 6-3 (also see Figure 3-1). It must be noted, in Figure 6-3, that f_1 is the same as the modal displacement of the points of connection of the concrete block to the columns (pins).

Analysis of the single-degree-of-freedom representation of Figure 6-2(d) is itself complicated given the viscoelastic nature of the system. For example, calculation of the period and damping

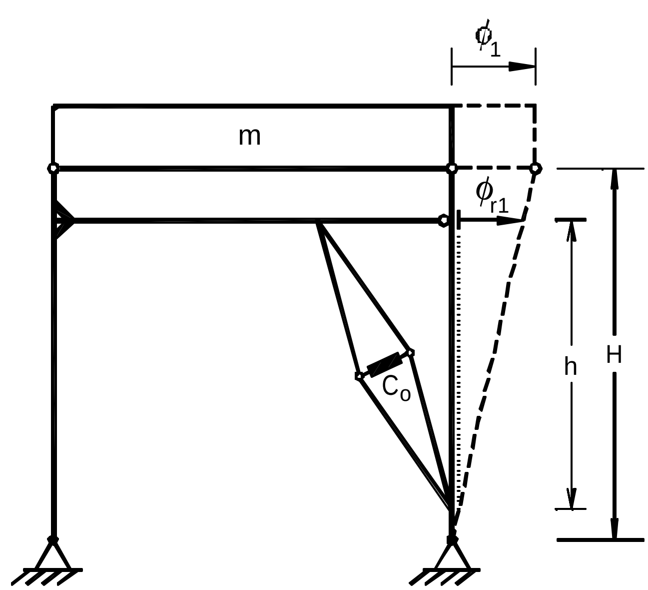

Figure 6-3 Schematic of Tested Model Showing Modal Displacements

ratio requires complex eigenvalue analysis (Constantinou and Symans 1992). Simplified analysis would require a further step of replacing the Maxwell element in Figure 6-2(d) by an equivalent Kelvin element of stiffness k' and damping constant c' (Constantinou et al. 1998) as shown in Figure 6-2(e), where (see eq. 2-23)

$$k' = \frac{C_S \cdot t \cdot w^2}{1 + t^2 \cdot w^2} \tag{6- 9}$$

$$c' = \frac{C_S}{1 + t^2 \cdot w^2} \tag{6- 10}$$

$$t = \frac{C_S}{K_S} = \frac{C_o}{tan^2 q \cdot K_b} \tag{6- 11}$$

Parameter $w = 2 \cdot p \,/\, T_1$ is the frequency of vibration of the damped structure, and parameter t is the relaxation time, which also appears in eqns. (6-5) and (6-6).

On the basis of the representations shown in Figures 6-2(e) and 6-3, the period T_1 and damping ratio b_1 of the damped structure are:

$$T_1 = 2 \cdot p \cdot \left[\frac{m}{K_F + k'} \right]^{1/2} = T_1' \cdot \left[1 - \frac{4 \cdot p \cdot t \cdot b_1}{T_1} \right]^{1/2} \tag{6- 12}$$

$$b_1 = \frac{c' \cdot T_1}{4 \cdot p \cdot m} = \frac{C_o \cdot cos^2 y \cdot T_1}{2 \cdot p \cdot m \cdot (1 + t^2 \cdot w^2) \cdot tan^2 q} \cdot \left(\frac{h}{H} \right)^2 \tag{6- 13}$$

where T_1' is the period of vibration of the structure exclusive of the energy dissipation system given by (see eq. 6-3)

$$T_1' = 2 \cdot p \cdot \left[\frac{m}{K_F} \right]^{1/2} \tag{6- 14}$$

It must be noted that eqns. (6-12) and (6-13) are identical to eqns. (6-5) and (6-1), respectively, for the model structure with the exception that f_{r1} / f_1 appears instead of h / H. Also, the quantities f^2 and $\left(f_{r1} / f_1 \right)^2$ are implicit in the calculation of c' (see eqns. 6-8 and 6-10).

In order to perform calculations, C_o = 40.0 N-sec/mm was used. This value represents well the behavior of the dampers for velocities less than about 250 mm/sec (see Figure 3-9). Also, m = 14.5 N-sec/mm^2 (W = 142.3 kN). Parameters K_S and C_S are calculated using eqns. (6-7) and (6-8). Equation (6-11) then results in t = 0.046 sec. Based on the model identification (frequency of 3.2 Hz, see Table 4-1), period $T_1' = 0.31$ sec. Additionally, $f_{r1}/f_1 \approx h/H$ = 0.68 and eqns. (6-12) and (6-13) are iteratively solved to result in T_1 = 0.27 sec and b_1 = 0.12. One can also calculate w (thus T_1) by solving (from eqns. 6-12 and 6-9)

$$K_F + \frac{C_S \cdot t \cdot w}{1 + t^2 \cdot w^2} = m \cdot w^2 \qquad (6\text{-}15)$$

where K_F is calculated using (6-14). Note that the period of 0.27 sec corresponds to a frequency of 3.7 Hz, which is less than the identified value of 4.0 Hz (see Table 4-1) but sufficiently close for practical purposes. Also, the calculated damping ratio of 0.12 represents the added damping supplied by the damping system. Since the inherent damping was of the order of 0.03, the total damping ratio is about 0.15. Identification of the structure showed a total damping ratio of 0.13 (see Table 4-1).

As an alternative to using (6-13) to predict T_1 and b_1, (6-2) can be used, which takes into account the vertical deflections due to frame deformations. For the tested structure, (6-2) can be written as

$$b_1 = \frac{C_o \cdot T_1}{2 \cdot p \cdot m \cdot (1 + t^2 \cdot w^2)} \cdot \left(\frac{f_{r1D}}{f_1} \right)^2 \qquad (6\text{-}16)$$

Equation (6-16) necessitates modal analysis for calculation of f_{r1D} and f_1. Using the analytical model of the structure developed for response-history analysis (Section 5), $f_{r1D}/f_1 = 1.82$. Iterative solution of eqns. (6-12) and (6-16) result in T_1 = 0.25 sec (frequency of 4 Hz) and b_1 = 0.155. The predicted frequency is the same with that obtained from identification tests, but the damping ratio is overestimated (see Table 4-1). In general however, simplified analysis predicts the dynamic properties of the model satisfactorily.

The peak dynamic response of the tested model can be estimated by use of response spectra, for the purpose of comparison to experimental results (tabulated in Table 4-2). As an example,

Figure 6-4 presents acceleration and displacement spectra for the El Centro motion for various damping ratios, generated using the earthquake simulator motion. It must be noted that the acceleration spectra in Figure 6-4 represent the actual maximum accelerations, not the pseudo-accelerations, which were shown in Figure 3-11. The peak response obtained from Figure 6-4 corresponds to that of the center of mass of the concrete blocks, and must be multiplied by the factor $h_s / H = 0.81$ (see Figures 3-1 and 6-2a) in order to approximately calculate the peak response of the beam-to-column joint (for comparison with the peak frame values reported in Table 4-2).

Table 6-1 presents a summary of the peak dynamic response calculated based on Figure 6-4 together with the experimental response from Table 4-2. In estimating the maximum acceleration and the maximum displacement, T = 0.27 sec and damping ratio = 0.15 were used (based on simplified calculations where the damping ratio was calculated as 0.12 and 0.03 was added for the inherent damping). The peak damper displacement u_{Dmax} was calculated from

$$u_{Dmax} = f \cdot \frac{h}{H} \cdot u_{max} \tag{6- 17}$$

where u_{max} is the maximum displacement from Figure 6-4 and f is given by (2-11). The peak damper force F_{Dmax} was calculated using

$$F_{Dmax} = C_o \cdot \frac{2 \cdot p}{T} \cdot u_{Dmax} \cdot CFV \tag{6- 18}$$

The quantity $(2 \cdot p / T) \cdot u_{Dmax}$ in (6-18) is the damper pseudo-velocity, and CFV is a correction factor so that the product of CFV and the pseudo-velocity is a good approximation to the peak damper velocity. Values of CFV have been presented in Ramirez et al. (2001). They are dependent on period and damping ratio. For period of 0.27 sec and damping ratio of about 0.15, CFV is equal to 0.70. It can be seen in Table 6-1 that the predicted response is in good agreement with the experimentally obtained peak response.

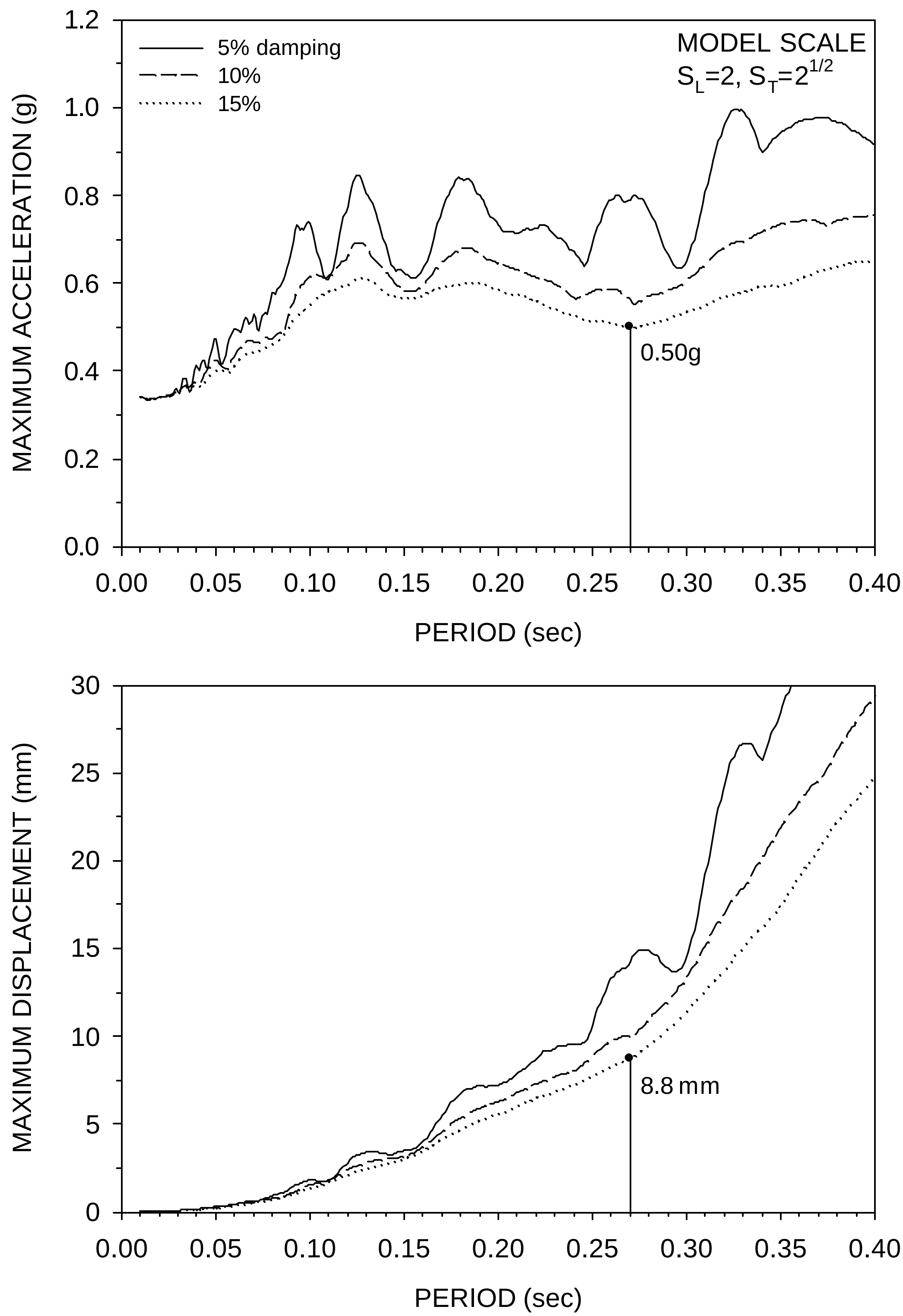

Figure 6-4 Response Spectra for El Centro S00E (100%) at Damping Ratios of 0.05, 0.10 and 0.15

TABLE 6-1 Peak Response of Tested Structure Calculated by Simplified Analysis and Comparison to Results of Earthquake-Simulator Tests (El Centro 100 % Input)

Peak Response Quantity	Analytical	Experimental *
Drift (mm)	7.1	6.3
Joint Acceleration (g)	0.41	0.45
Peak Damper Displacement (mm)	12.9	10.7
Peak Damper Force (kN)	8.4	8.7

* East frame response, test ELRSBD100

SECTION 7

APPLICATION OF SCISSOR-JACK-DAMPER SYSTEM

The scissor-jack-damper system has been implemented in the design of a new, 3-story building structure in Cyprus, which is currently under construction. The building will serve as the headquarters of the Cyprus Olympic Committee. The scissor-jack-damper system was determined to be advantageous with respect to other economically feasible supplemental damping systems due to open-space requirements for the structure. Figure 7-1 illustrates the plan view of the 1st floor of this building, where "S" demarks the locations of the scissor-jack-damper systems. Also included in this figure is a cross-sectional view of the building (cut along the dashed line shown in the 1st floor plan view) illustrating the scissor-jack-damper installation. Details regarding the geometry and dimensions of the damper assembly are given in Figure 7-2. The structure utilizes 52 scissor-jack-damper assemblies equipped with linear fluid viscous damping devices.

Modeling and analysis of the building was performed using SAP2000. Response-history analyses were conducted with the 1940 El Centro S00E, 1986 Kalamata-Nomarhia NS (Greece) and 1952 Taft N21E ground motions, scaled at various amplitudes in order to represent the site response spectrum. Figure 7-3 presents the average of the pseudo-acceleration spectra of the scaled motions, superposed upon the site-specific design spectrum. The analytical model of the structure resembles that of the tested scissor-jack-damper system (Section 5). Figure 7-4 illustrates the SAP2000 model, which represents a portion of the structure. Sample results from response-history analysis, using the model shown in Figure 7-4 with and without the scissor-jack-damper system are presented in Figures 7-5 and 7-6, for the controlling-scaled (scale factor 100%) Taft N21E record. The effectiveness of the damping system is evident in the reduced displacement (and slightly reduced acceleration) response of the structure with the scissor-jack-damper system.

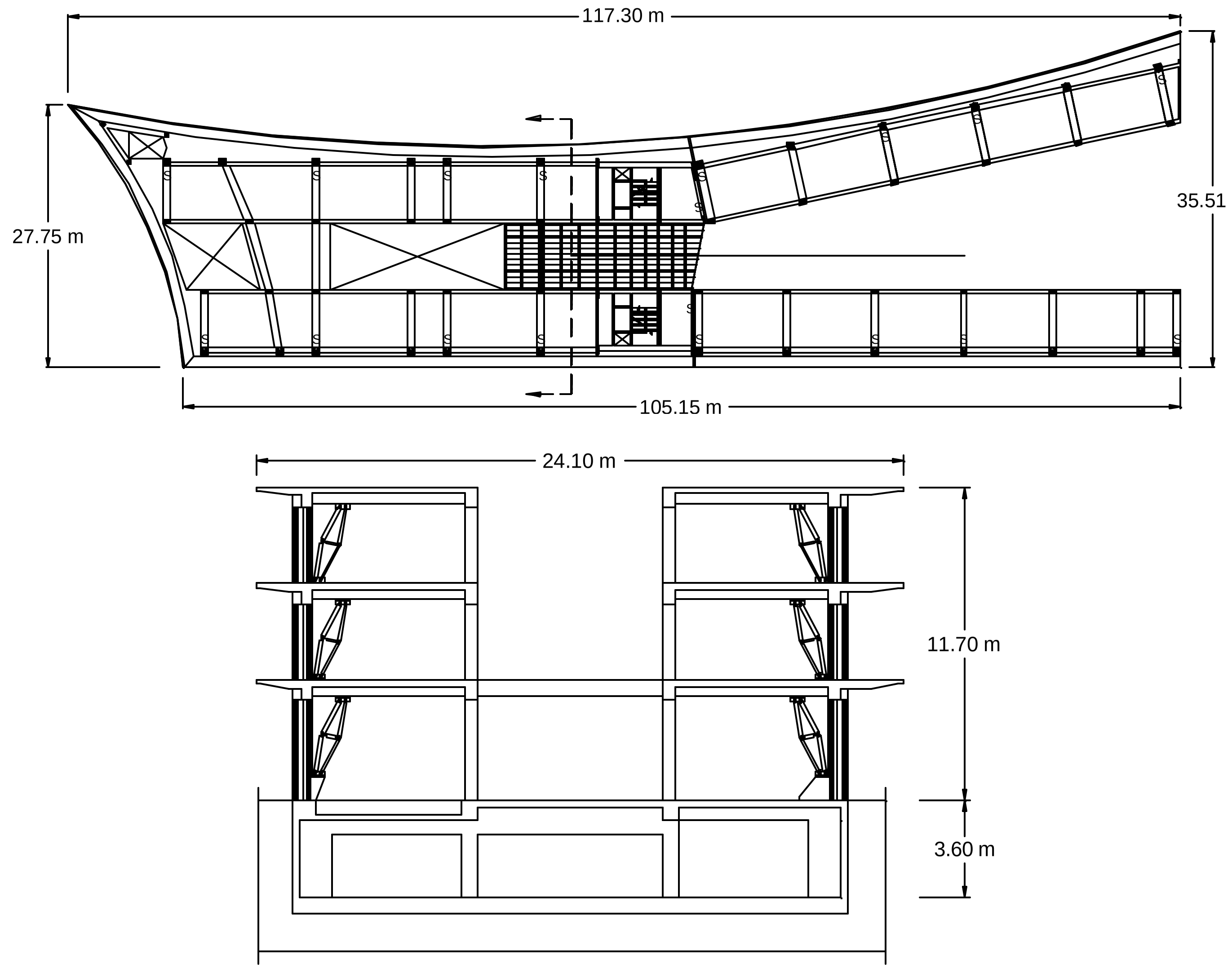

Figure 7-1 **Plan View of 1st Floor *(above)* and Elevation View of Building Showing Scissor-Jack-Damper System *(below)***

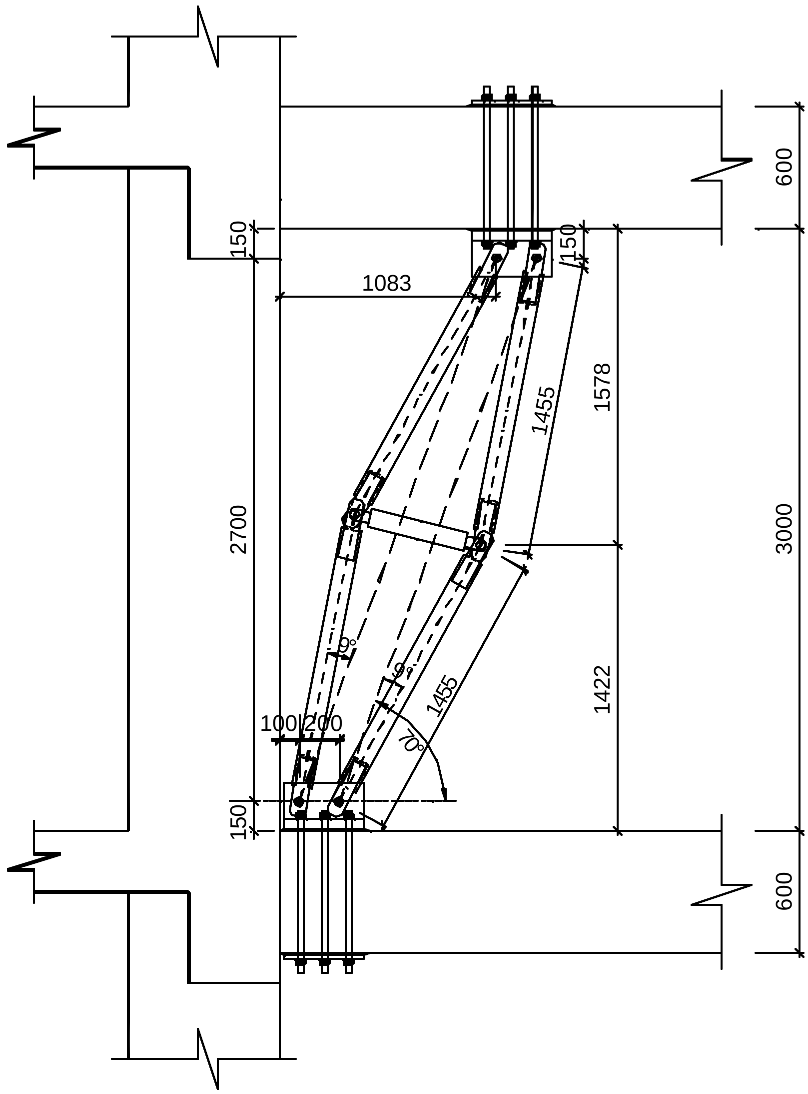

Figure 7-2 Details of Scissor-Jack-Damper System for Building in Cyprus (typical for 2nd and 3rd floors; dimensions in mm)

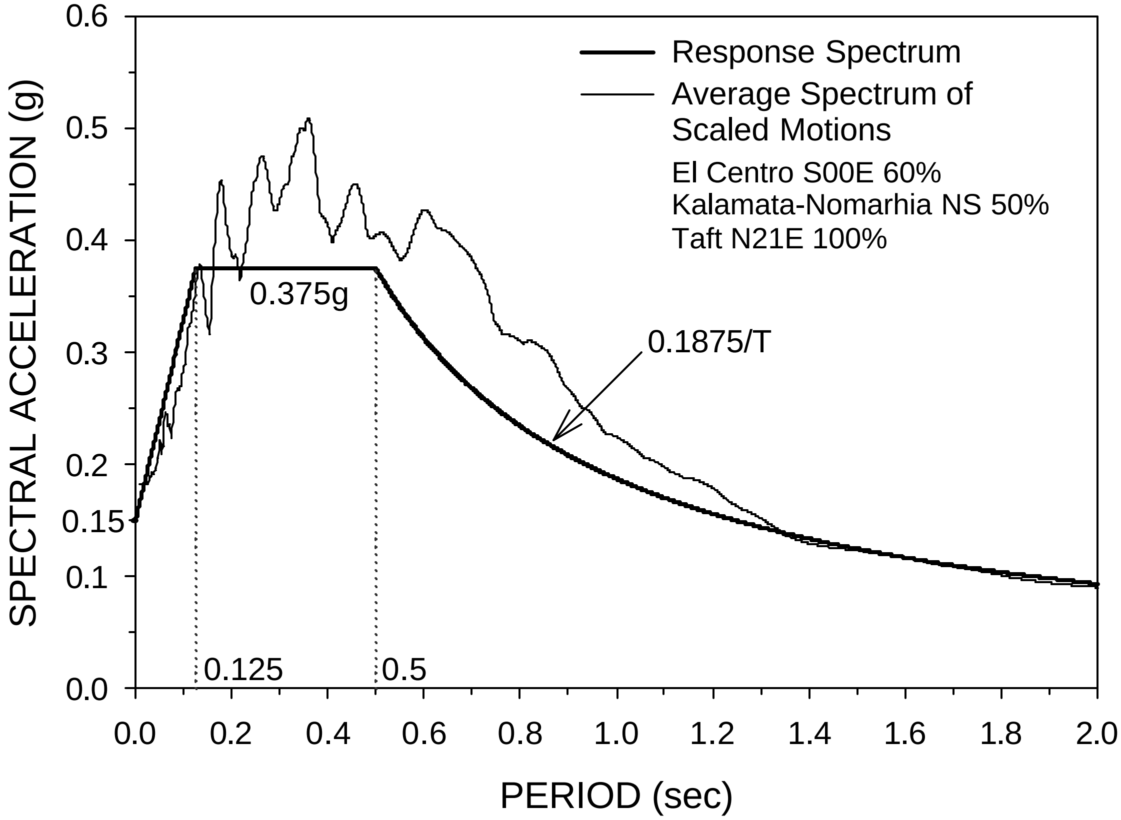

Figure 7-3 Response Spectra of Scaled Motions used in Response-History Analysis

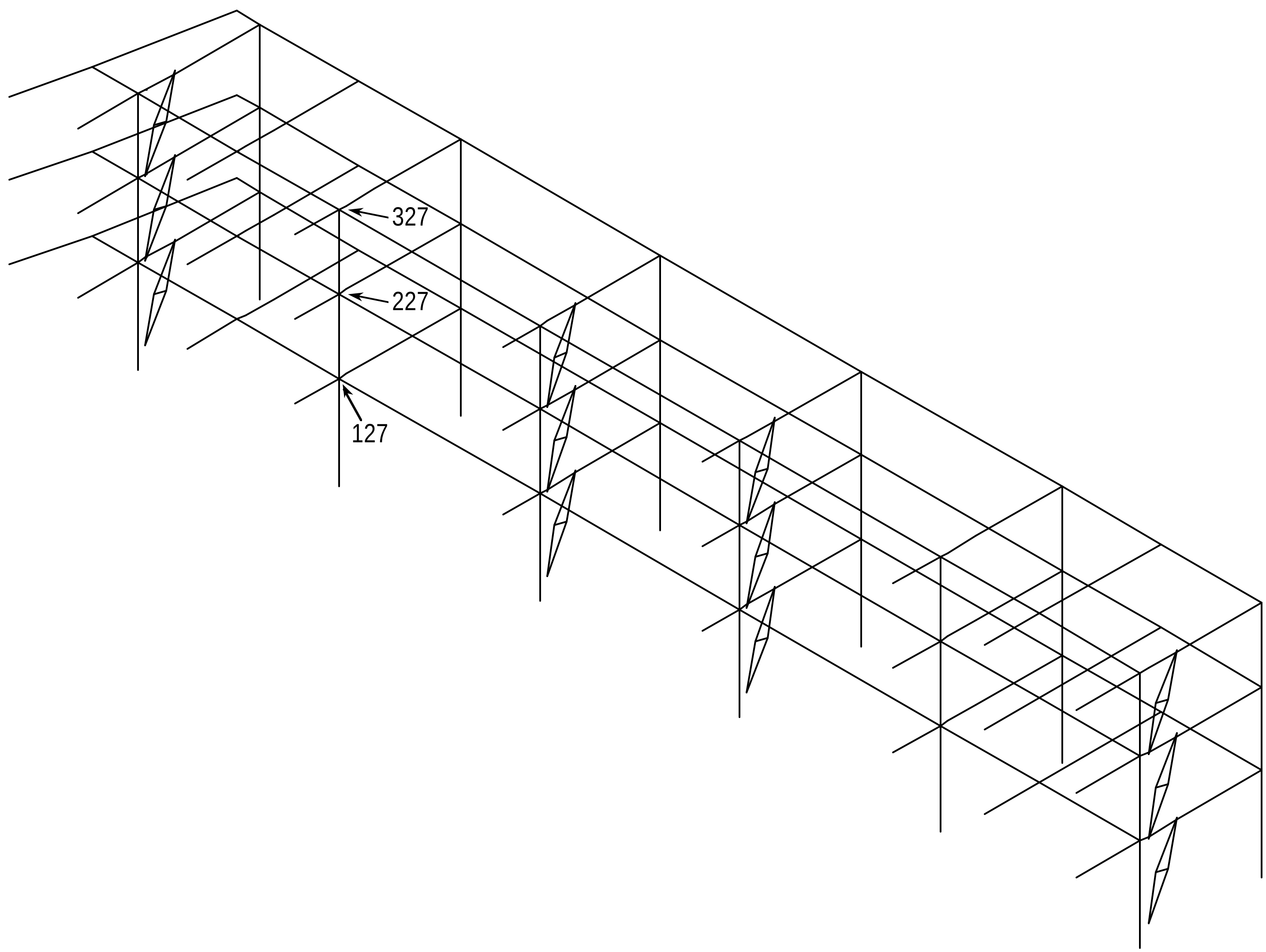

Figure 7-4 SAP2000 Model for Response-History Analysis

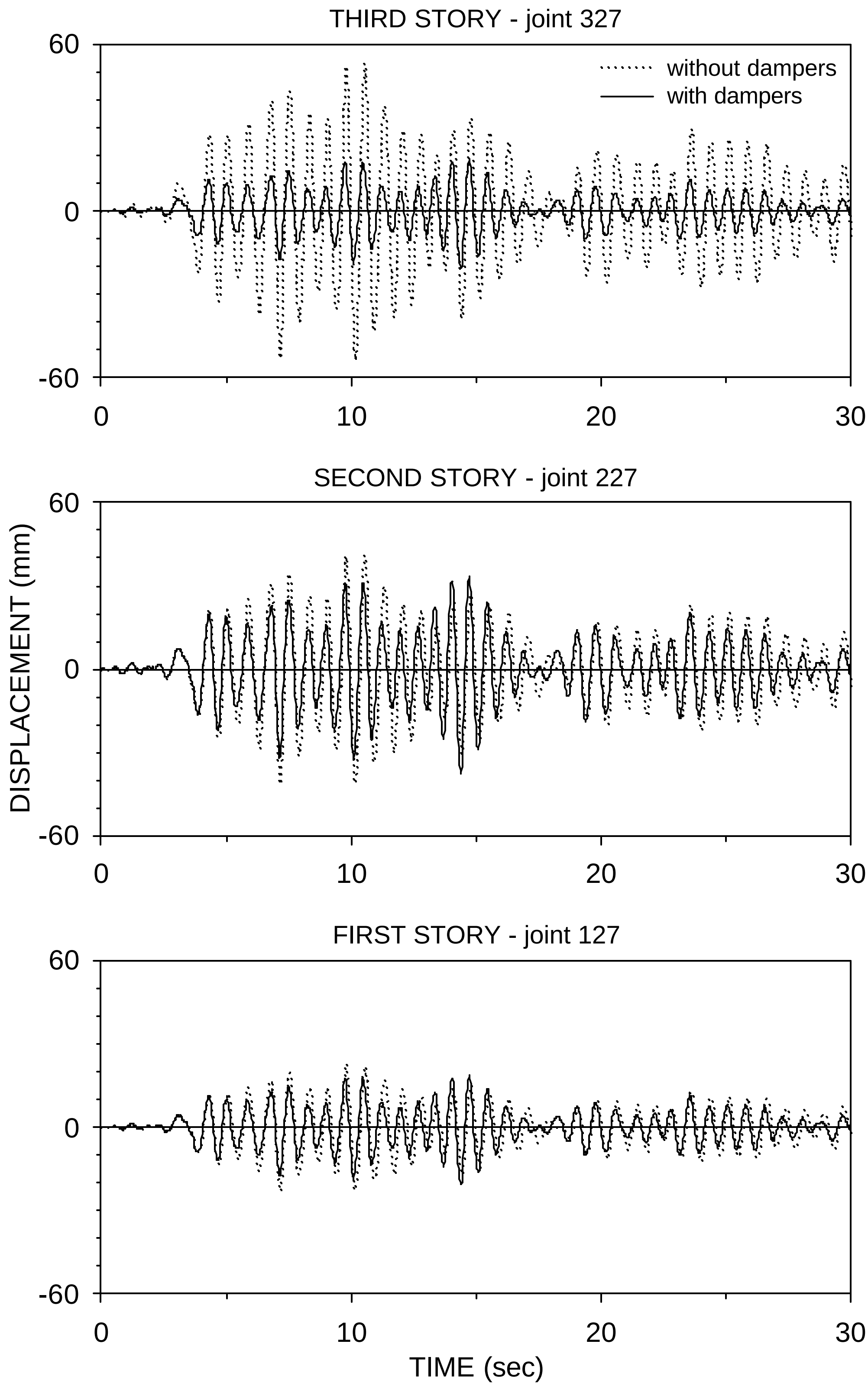

Figure 7-5 Displacement Response of Structure from Response History Analysis for Taft N21E 100% Input (see Figure 7-4 for joint locations)

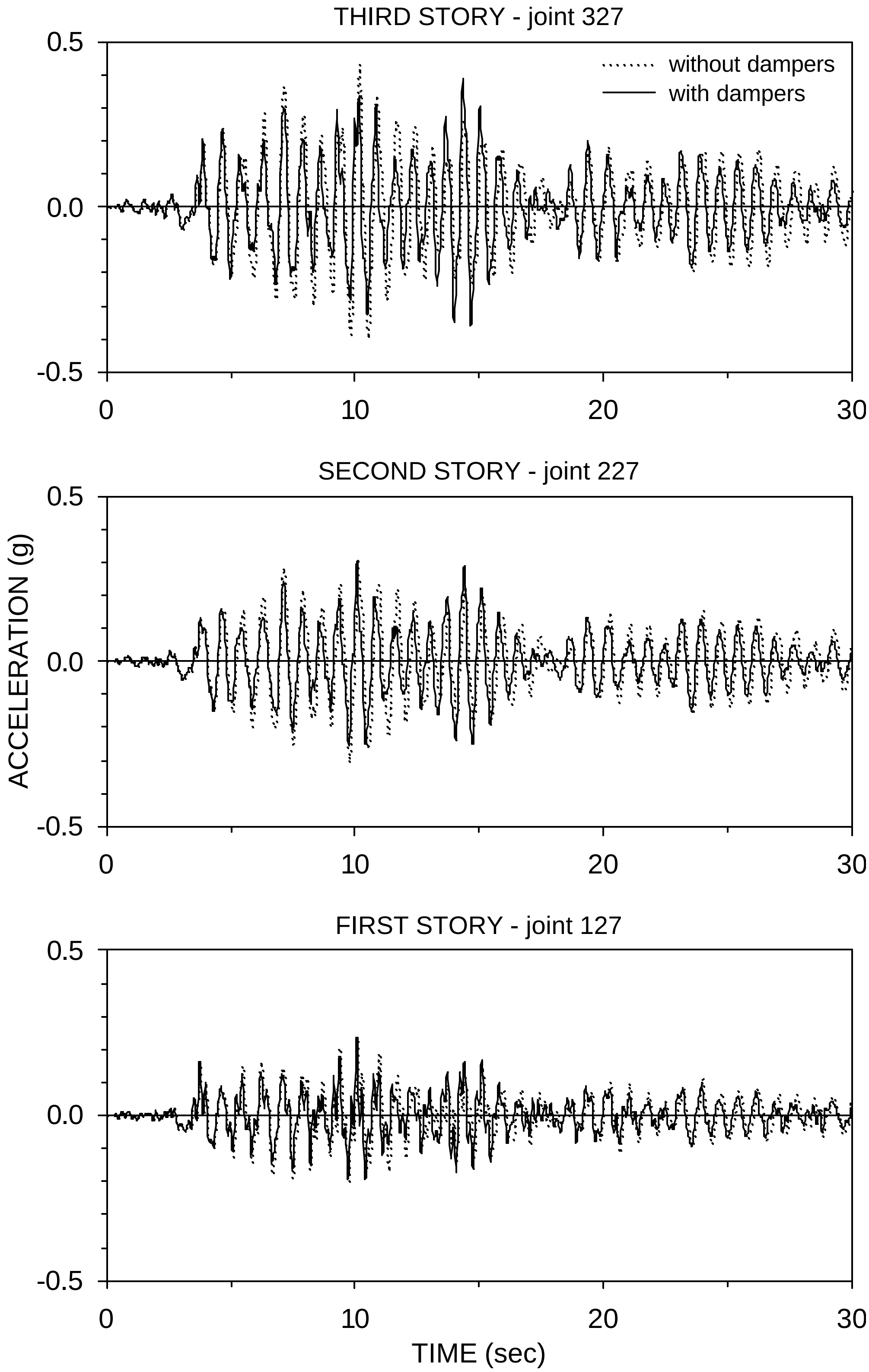

Figure 7-6 Acceleration Response of Structure from Response History Analysis for Taft N21E 100% Input (see Figure 7-4 for joint locations)

SECTION 8

SUMMARY AND CONCLUSIONS

Scissor-jack-damper energy dissipation system offers structural systems with small drifts an opportunity to benefit from supplemental damping. Similar to the toggle-brace-damper system that preceded its development, the scissor-jack-damper system utilizes shallow trusses to magnify the damper displacement for a given interstory drift, and to magnify the damper force output delivered to the structural frame. The system thus extends the applicability of damping devices to cases of small interstory drifts, such as stiff structures under seismic loading and structures subject to wind loading. Additionally, the scissor-jack damping system can be configured to allow for open space through its compactness and near-vertical installation, a feature that is often desired for architectural purposes.

This report presented a theoretical treatment of the scissor-jack-damper system and demonstrated its utility via experimental results. Analysis of the kinematics of the scissor-jack configuration was illustrated. The equations that described the behavior were reduced to the case of small rotations to yield simple expressions for the magnification factor, which is defined as the ratio of the damper deformation to the lateral interstory drift. The effect of frame deformations on the damper deformation and the magnification factor was also presented. In addition, the effects of the flexibility of the energy dissipation assembly were discussed.

The experimental study included testing of a half-scale steel model structure equipped with a scissor-jack-damper system on the strong floor under imposed cyclic displacement and on the earthquake simulator. The strong floor tests confirmed the theoretically predicted behavior. The effect of various beam-to-column connection configurations was also demonstrated. The earthquake-simulator testing indicated a significant increase in the damping ratio, accompanied with reduction in drift and acceleration responses, in comparison with the same structure without the energy dissipation system. The scissor-jack-damper system also stiffened the structure, marked by an increase in frequency. This viscoelastic behavior occurred as a result of frame and energy dissipation assembly deformations under the action of damping forces. Testing of the scissor-jack-damper system also pointed out important issues that can affect the performance of the system, such as sensitivity of the system's behavior to repetitive testing and small imperfections.

The response of the model structure to seismic excitation was reproduced analytically by response-history analysis using SAP2000. Two different analysis methods, namely nonlinear modal time-history analysis and nonlinear direct-integration time-history analysis, were utilized. In addition to using a different solution procedure, the modal method predicted the dynamic response of the structure under the assumption of small deformations, whereas the direct-integration method allowed for large deformations. It was shown that analysis of the structure using the small deformation theory produces results that are identical to those of the large deformation theory and that the modal method is more efficient than the direct-integration method, which requires substantial amount of computational time. The analytical model produced response-history results of acceptable accuracy and satisfactorily captured the significant characteristics of the model such as the stiffening effect, and peak values of drift and acceleration.

In addition, application of simplified analysis methods for predicting the period and damping ratio of the model structure, based on information on the dynamic characteristics of the undamped structure and the geometry of the scissor-jack-damper system, was presented. Simplified analysis requires a proper presentation of the increase in stiffness of the structure due to the damping system. Results of this analysis were in close agreement with those of the experiments. Also, the peak dynamic response of the tested structure was estimated utilizing response spectra of ground motions, which matched closely with experimental results.

An important outcome of this study is that structures with the scissor-jack-damper system can conveniently be analyzed using code-oriented procedures such as those outlined in Federal Emergency Management Agency (1997, 2000, and 2003), with the appropriate modification for the magnification factor, which relates the lateral interstory drift to the damper deformation. This is also true for structures with toggle-brace-damper systems. The simplicity of both configurations lies in the fact that the magnification factors are related to simple geometry of the systems. In cases where vertical deflections may affect the damper deformation, these equations may still be utilized with the appropriate adjustment to account for the vertical motion effects.

The effectiveness of the scissor-jack-damper system was demonstrated on a linear elastic structure. This system can also be implemented in building structures that are expected to respond beyond the elastic limit. Simplified methods for the analysis of yielding structures with energy dissipation systems are presented in Federal Emergency Management Agency (1997, 2000, and 2003). Evaluation and application of these methods can be found in Ramirez et al. (2001) and Tsopelas et al. (1997). In a yielding structure with the scissor-jack-damper configuration, the frame deformations due to structural system configuration are likely to be different than before beyond the elastic limit. Changes in the boundary conditions at the beam-to-column connections are important due to their effect on the magnification factor. Such changes must be considered. In addition, since the connection details and sensitivity to imperfections are important in ensuring magnification and proper load transfer, the components and connections in the vicinity of the scissor-jack-damper system should be designed to remain elastic for all levels of earthquake shaking.

The scissor-jack-damper system is a viable solution for supplemental damping in stiff structural systems and for reducing wind-induced vibrations. The versatility of the system is enhanced by its compact size and geometry, which allow for configurations that offer open space for architectural components. Indeed, the decision to use the scissor-jack-damper system for supplemental damping for a building in Cyprus was in the large part related to architectural considerations. The system can also be installed in various arrangements depending on damping and open space requirements. Moreover, the scissor-jack configuration can be used in conjunction with other magnifying mechanisms, such as the coupled truss and damping system used in the Torre Mayor. As with all supplemental damping mechanisms, the scissor-jack-damper system is replaceable following a major event; the fact that the scissor-jack system permits the use of standard connection details makes the post-earthquake maintenance and replacement relatively simple.

SECTION 9

REFERENCES

Chironis, N.P., (1991), “Mechanisms and Mechanical Devices Sourcebook,” McGraw-Hill, Inc., N.Y., USA.

Computers and Structures Inc., (2000), “SAP2000: Static and Dynamic Finite Element Analysis of Structures (Nonlinear Version 7.40),” Computers and Structures Inc., Berkeley, CA.

Computers and Structures Inc., (2003), “SAP2000: Static and Dynamic Finite Element Analysis of Structures (Nonlinear Version 8.2.3),” Computers and Structures Inc., Berkeley, CA.

Constantinou, M.C., (2000), “Damping Systems for Structural Design and Retrofit,” *Presentation, EERI 52nd Annual Meeting,* St. Louis, MI.

Constantinou, M.C. and Sigaher, A.N., (2000), “Energy Dissipation System Configurations for Improved Performance,” *Proceedings of 2000 Structures Congress & Exposition,* ASCE, Philadelphia, PA.

Constantinou, M.C., Soong, T.T., and Dargush, G.F., (1998), “Passive Energy Dissipation Systems for Structural Design and Retrofit,” *Monograph Series No. 1*, Multidisciplinary Center for Earthquake Engineering Research (MCEER), State University of New York at Buffalo, Buffalo, N.Y.

Constantinou, M.C., and Symans, M.D., (1992), “Experimental and Analytical Investigation of Seismic Response of Structures with Supplemental Fluid Viscous Dampers,” *Technical Report NCEER-92-0032*, National Center for Earthquake Engineering Research (NCEER), State University of New York at Buffalo, Buffalo, N.Y.

Constantinou, M.C., Tsopelas, P., and Hammel, W., (1997), “Testing and Modeling of an Improved Damper Configuration for Stiff Structural Systems,” Center for Industrial Effectiveness, State University of New York at Buffalo, Buffalo, N.Y., <*http://civil.eng.buffalo.edu/users_ntwk/*>.

Constantinou, M.C., Tsopelas, P., Hammel, W., and Sigaher, A.N., (2000), “New Configurations of Fluid Viscous Dampers for Improved Performance,” *Proceedings of Passive Structural Control Symposium 2000*, Tokyo Institute of Technology, Yokohama, Japan.

Constantinou, M.C., Tsopelas, P., Hammel, W., and Sigaher, A.N., (2001), “Toggle-Brace-Damper Seismic Energy Dissipation Systems,” *Journal of Structural Engineering*, ASCE, Vol. 127 No. 2, pp.105-112.

Federal Emergency Management Agency (FEMA), (1997), "NEHRP Guidelines for the Seismic Rehabilitation of Buildings," and "NEHRP Commentary on the Guidelines for the Seismic Rehabilitation of Buildings," *Reports No. FEMA 273 and FEMA* 274, Washington, D.C.

Federal Emergency Management Agency (FEMA), (2000), "Prestandard and Commentary for the Seismic Rehabilitation of Buildings," *Report No. FEMA 356*, Washington, D.C.

Federal Emergency Management Agency (FEMA), (2000), "NEHRP Recommended Provisions for Seismic Regulations for New Buildings and Other Structures, Part 1 Provisions and Part 2 Commentary)," *Reports No. FEMA 368 and FEMA 369*, Washington, D.C.

Federal Emergency Management Agency (FEMA), (2003), "NEHRP Recommended Provisions for Seismic Regulations for New Buildings and Other Structures," Washington, D.C. *(in publication)*.

Hammel, W., (1997), "Testing and Modeling of an Improved Damper Configuration for Stiff Structural Systems," *Master of Science Thesis*, Department of Civil, Structural and Environmental Engineering, State University of New York at Buffalo, Buffalo, N.Y.

Hanson, R.D., and Soong, T.T., (2001), "Seismic Design with Supplemental Energy Dissipation Devices," *Monograph No. 8*, Earthquake Engineering Research Institute (EERI), Oakland, CA.

Hibino, H., Kawamura, S., Hisano, M., Yamada, M., Kawamura, H., and Morita, H., (1989), "A Study on Response Control System on Structures Utilizing Damping Amplifier," *Taisei Technical Research Journal*, Vol. 22 (November), pp. 155-162 (in Japanese).

Kani, N., Ogura, K., Tsujita, O., Hosozawa, O., and Shinozaki, Y., (1992), "A Design Method and Development of Damping Amplifier System for Passive Response Controlled Structure," *Proceedings of 10th World Conference on Earthquake Engineering*, Madrid, Spain, Vol. 7, pp. 4165-4170.

Rahimian, A.A., (2002), "Coupled Truss Systems with Damping for Seismic Protection of Buildings," *U.S. Patent 6,397,528 B1*, assigned to the Cantor Seinuk Group, P.C., New York, N.Y.

Ramirez, O.M., Constantinou, M.C., Kircher, C.A., Whittaker, A.S., Johnson, M.W., Gomez, J.D., and Chrysostomou, C.Z., (2001), "Development and Evaluation of Simplified Procedures for Analysis and Design of Buildings with Passive Energy Dissipation Systems," *Technical Report MCEER-00-0010, Revision 1*, Multidisciplinary Center for Earthquake Engineering Research (MCEER), State University of New York at Buffalo, Buffalo, N.Y.

Seleemah, A.A., and Constantinou, M.C., (1997), "Investigation of Seismic Response of Buildings with Linear and Nonlinear Fluid Viscous Dampers," *Technical Report NCEER-97-0004*, National Center for Earthquake Engineering Research (NCEER), State University of New York at Buffalo, Buffalo, N.Y.

Sigaher, A.N., and Constantinou, M.C., (2003), “Scissor-Jack-Damper Energy Dissipation System,” *Earthquake Spectra*, EERI, Volume 19, No. 1, pp. 133–158.

Soong, T.T., and Dargush, G.F., (1997), “Passive Energy Dissipation Systems in Structural Engineering,” John Wiley & Sons Ltd., London, UK and New York, USA.

Taylor, D.P., (2003), “Mega Brace Seismic Dampers for the Torre Mayor Project at Mexico City,” <*http://www.taylordevices.com/papers/*>.

Tsopelas, P., Constantinou, M.C., Kircher C.A., and Whittaker, A.S., (1997), “Evaluation of Simplified Methods of Analysis for Yielding Structures,” *Technical Report NCEER-97-0012*, National Center for Earthquake Engineering Research (NCEER), State University of New York at Buffalo, Buffalo, N.Y.

Veletsos, A.S., and Ventura, C.E., (1986), “Modal Analysis of Non-Proportionally Damped Linear Systems,” *Earthquake Engineering and Structural Dynamics*, Vol. 14, pp. 217-243.

Whittaker, A.S., and Constantinou, M.C., (1999a), “Advances in Supplemental Damping Systems for Civil Infrastructure,” *Proceedings of VIIth Mexican Conference on Earthquake Engineering,* Morelia, Mexico.

Whittaker, A.S., and Constantinou, M.C., (1999b), “Supplemental Damping for New and Retrofit Construction,” *Revista de Ingenieria Sismica*, Vol. 61, Sociedad Mexicana de Ingenieria Sismica A. C., Mexico City.

Whittaker, A.S., and Constantinou, M.C., (2000), “Fluid Viscous Dampers for Building Construction,” *Proceedings of Passive Structural Control Symposium 2000,* Tokyo Institute of Technology, Yokohama, Japan.

APPENDIX A

DRAWINGS OF TESTED STRUCTURE

Notes: 1. Drawings are as provided to fabricator.
2. Refer to Hammel (1997) for information on existing frame connection details.

(1 foot = 304.8 mm, 1 in = 25.4 mm)

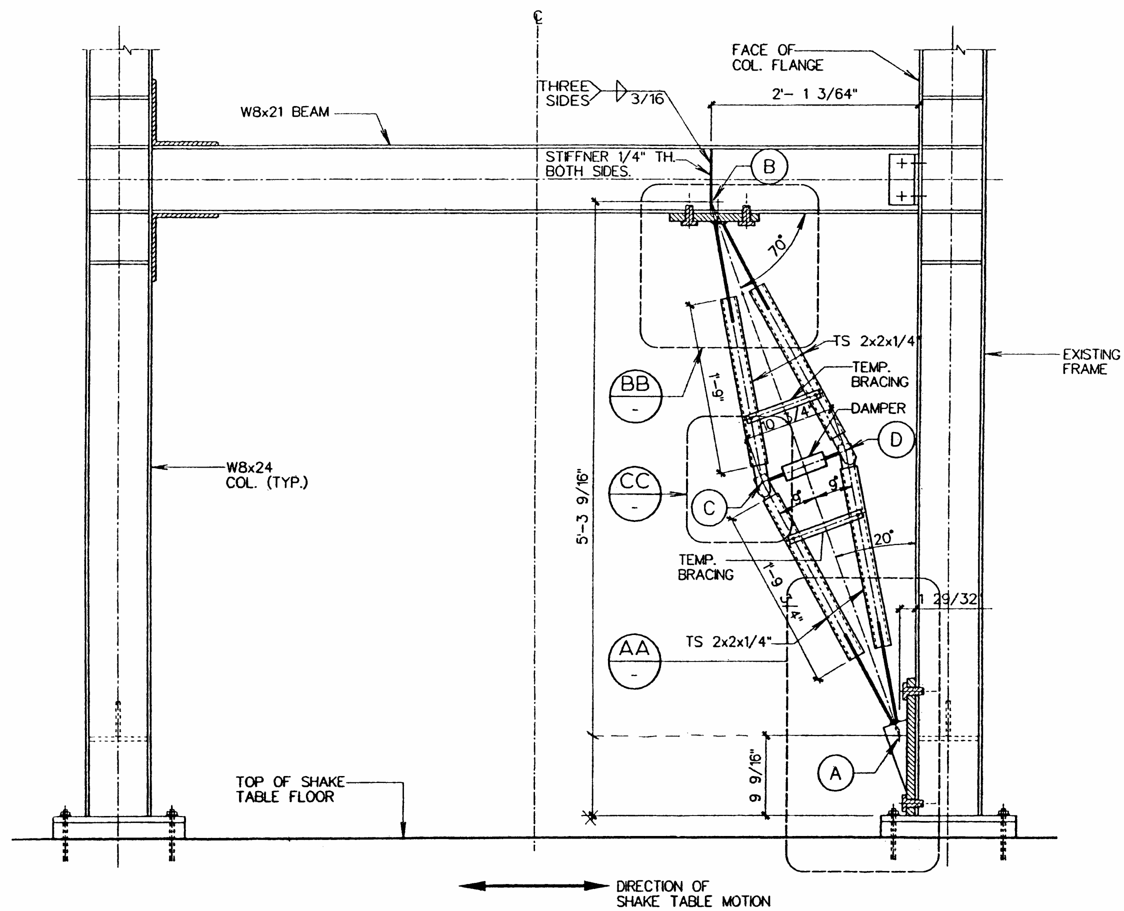

THREE SIDES
3/16
FACE OF COL. FLANGE
2'- 1 3/64"
W8x21 BEAM
STIFFNER 1/4" TH. BOTH SIDES.
B
70°
TS 2x2x1/4"
EXISTING FRAME
TEMP. BRACING
BB
1'-9"
DAMPER
D
W8x24 COL. (TYP.)
CC
C
5'-3 9/16"
20°
TEMP. BRACING
1'-9 3/4"
1 29/32
AA
TS 2x2x1/4"
9 9/16"
A
TOP OF SHAKE TABLE FLOOR
DIRECTION OF SHAKE TABLE MOTION

1 ELEVATION

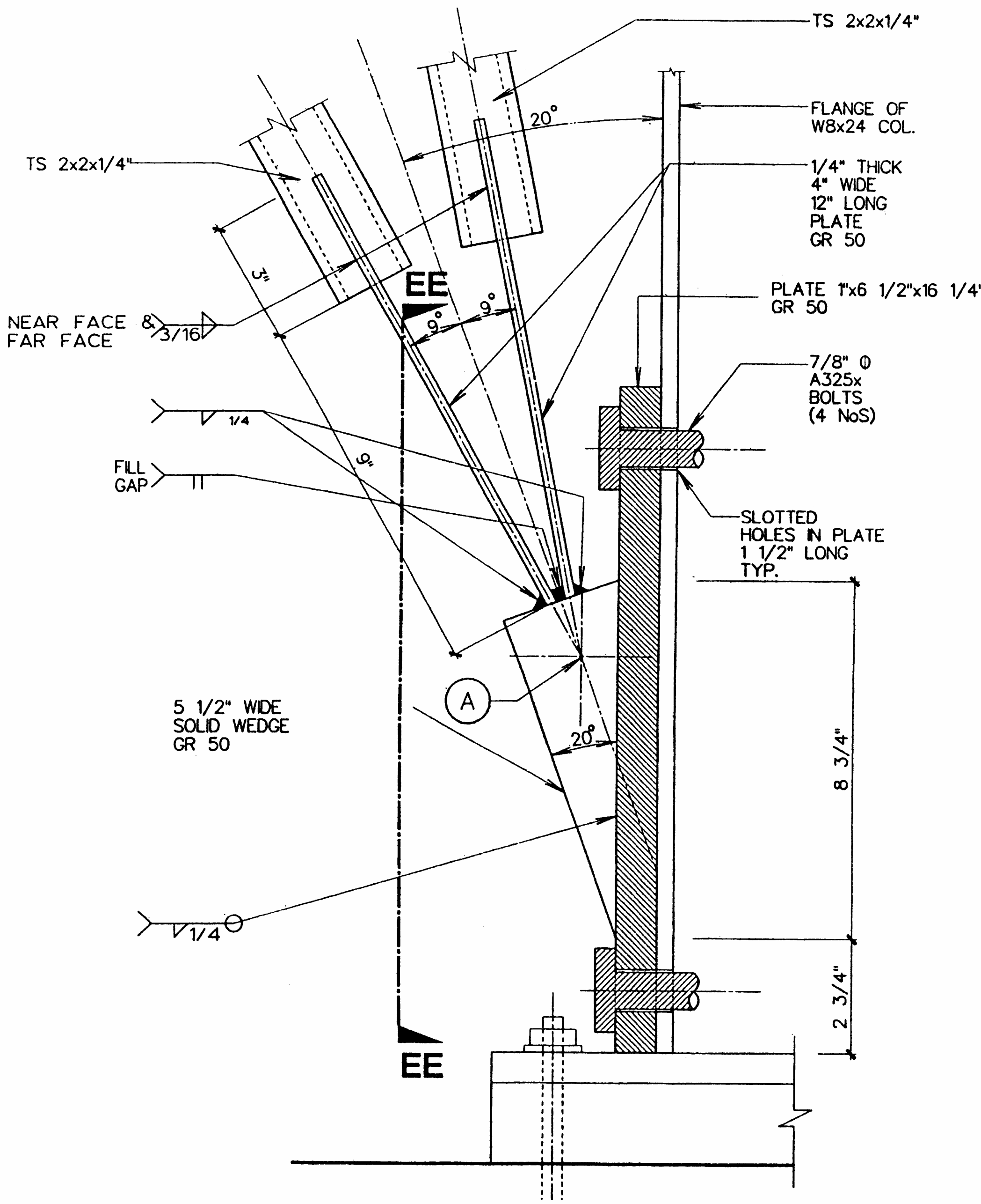

AA SECTION AT JOINT A

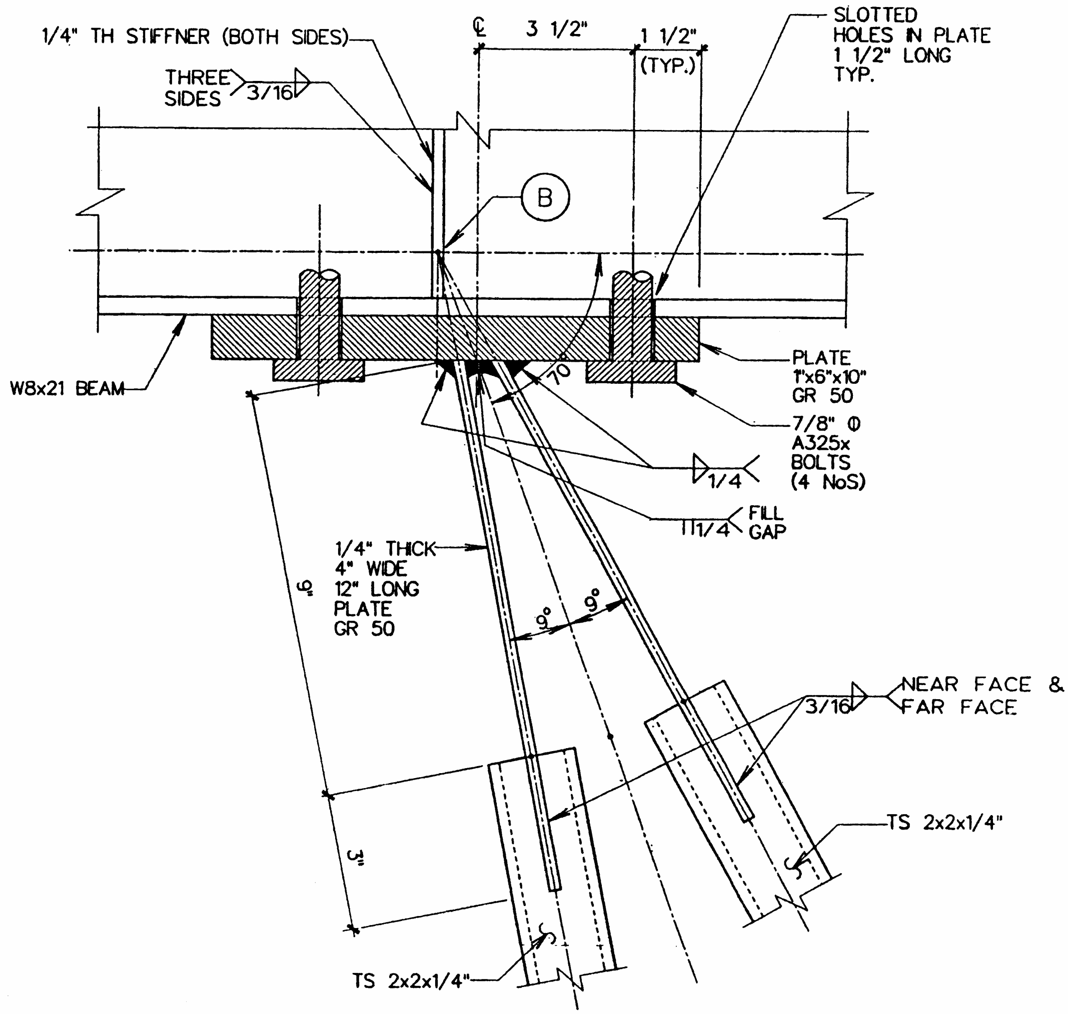

BB SECTION AT JOINT **B**

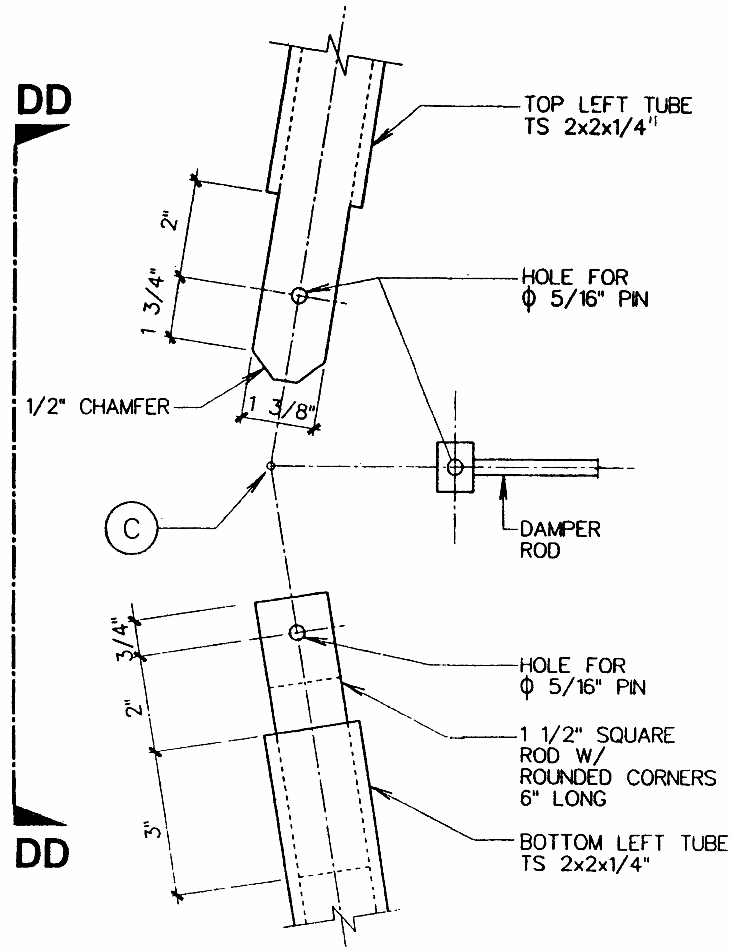

CC ASSEMBLY AT JOINT C

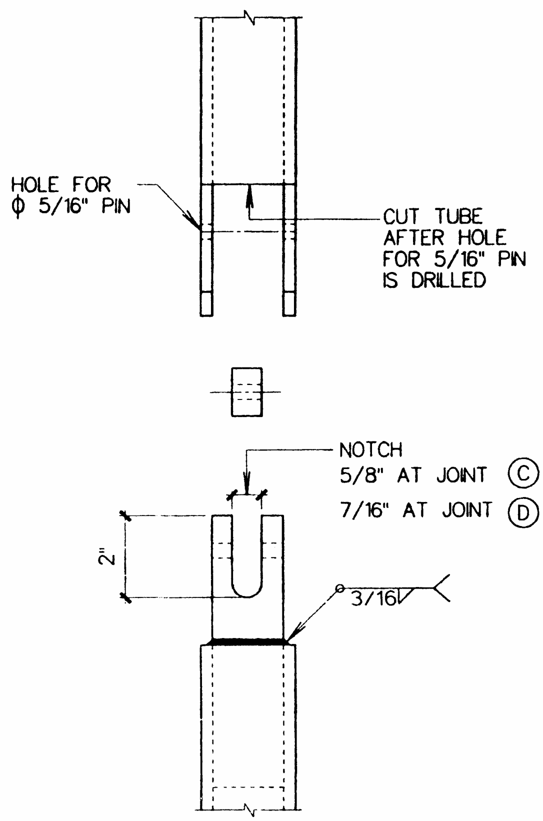

DD SECTION - DD

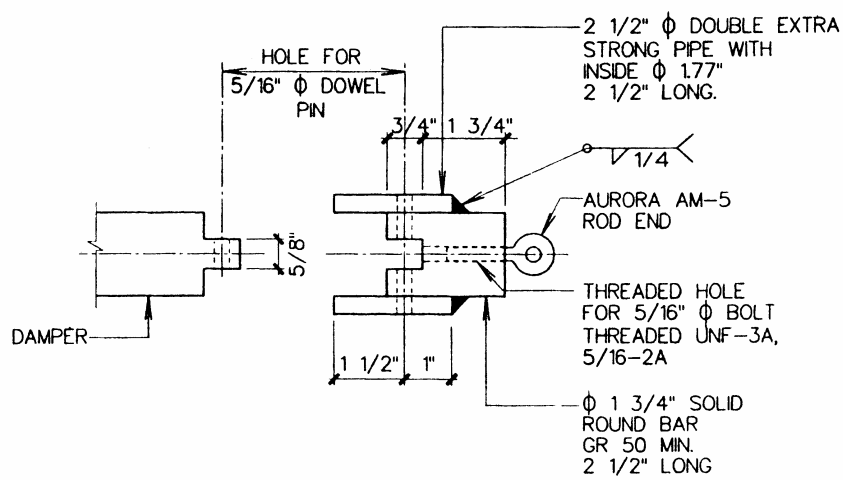

FF DAMPER END CONNECTION AT JOINT D

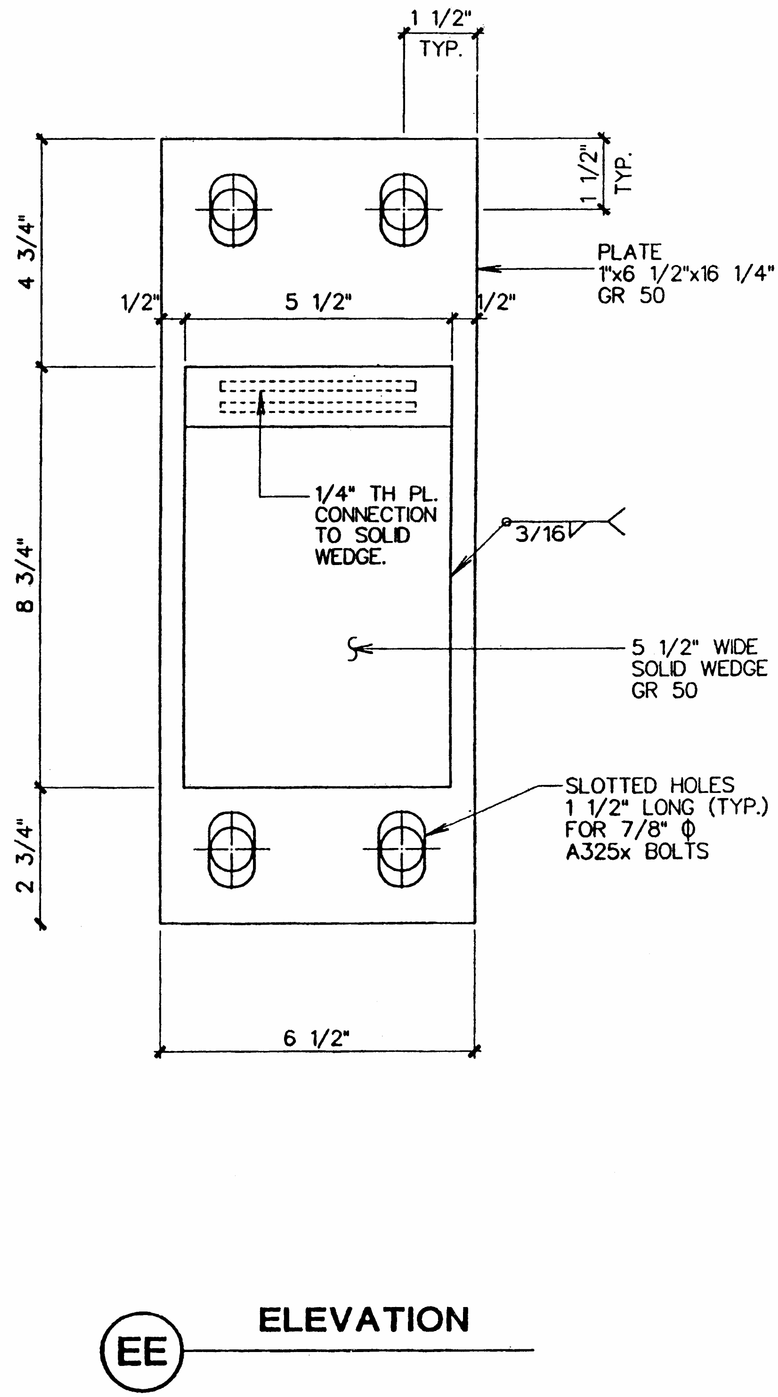
1 1/2"
TYP.
1 1/2"
TYP.
PLATE
1"x6 1/2"x16 1/4"
GR 50
4 3/4"
1/2"
5 1/2"
1/2"
1/4" TH PL.
CONNECTION
TO SOLID
WEDGE.
3/16
8 3/4"
5 1/2" WIDE
SOLID WEDGE
GR 50
SLOTTED HOLES
1 1/2" LONG (TYP.)
FOR 7/8" Φ
A325x BOLTS
2 3/4"
6 1/2"
EE
ELEVATION

APPENDIX B

RESULTS OF TESTING OF FRAME UNDER IMPOSED LATERAL JOINT DISPLACEMENT

F2SR01 : BRACE 2, SIMPLE-RIGID CONNECTIONS
U_O=6.35 mm, f=0.01 Hz (03/19/99, 09:55:07)

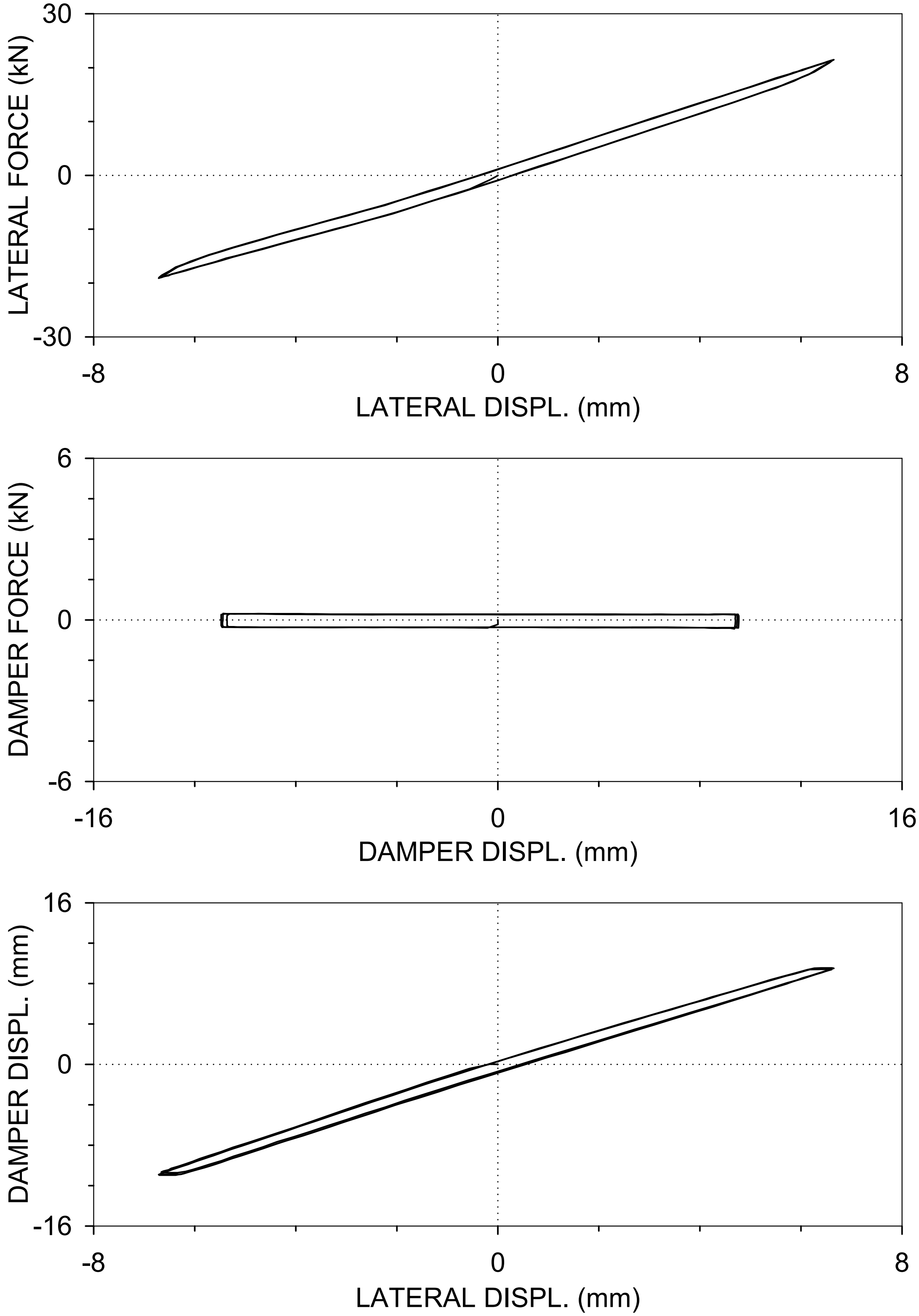

F2SR02 : BRACE 2, SIMPLE-RIGID CONNECTIONS
U_O=6.35 mm, f=0.05 Hz (03/19/99, 10:02:21)

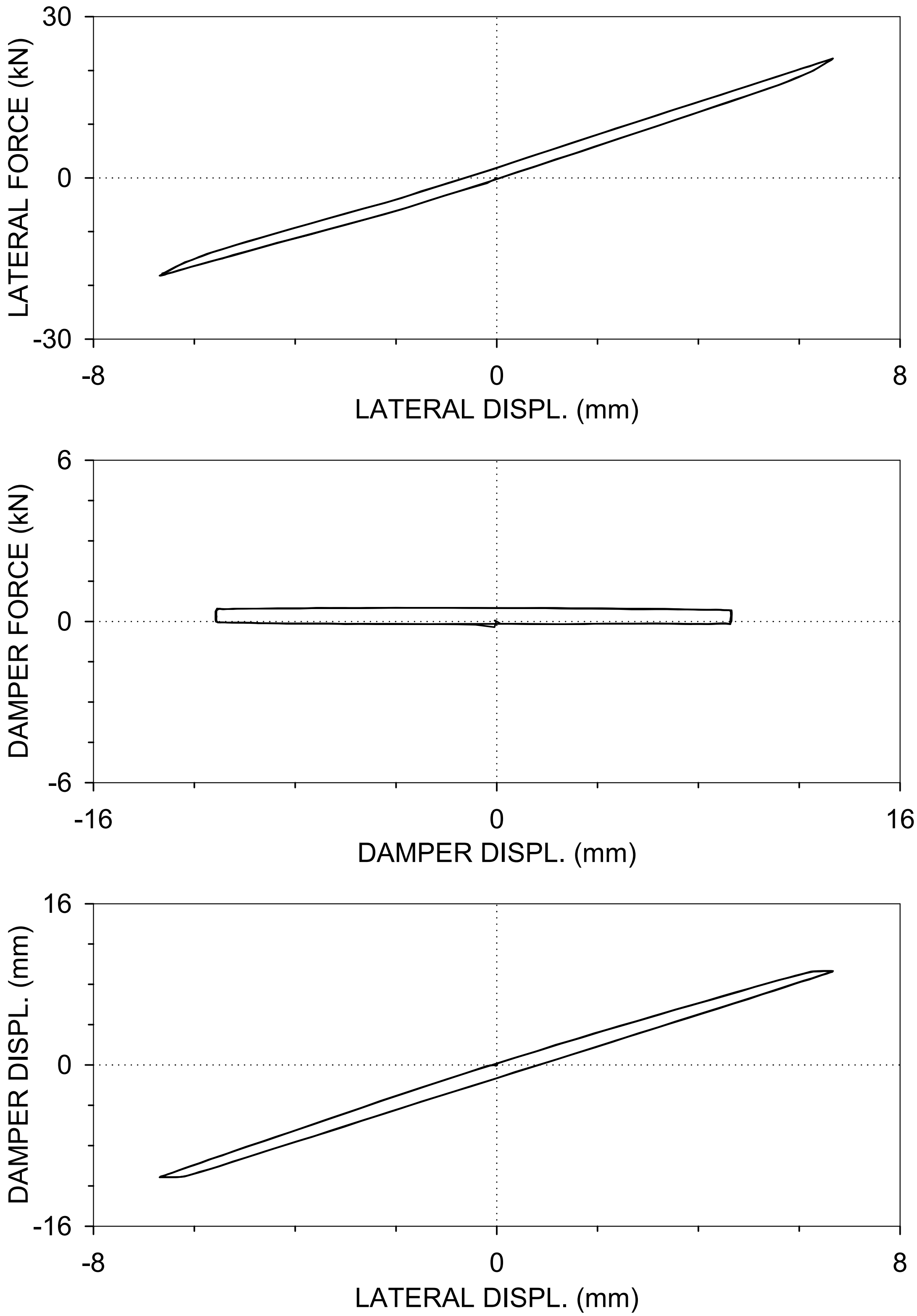

F2SR03 : BRACE 2, SIMPLE-RIGID CONNECTIONS
U_O=6.35 mm, f=0.5 Hz (03/19/99, 10:05:54)

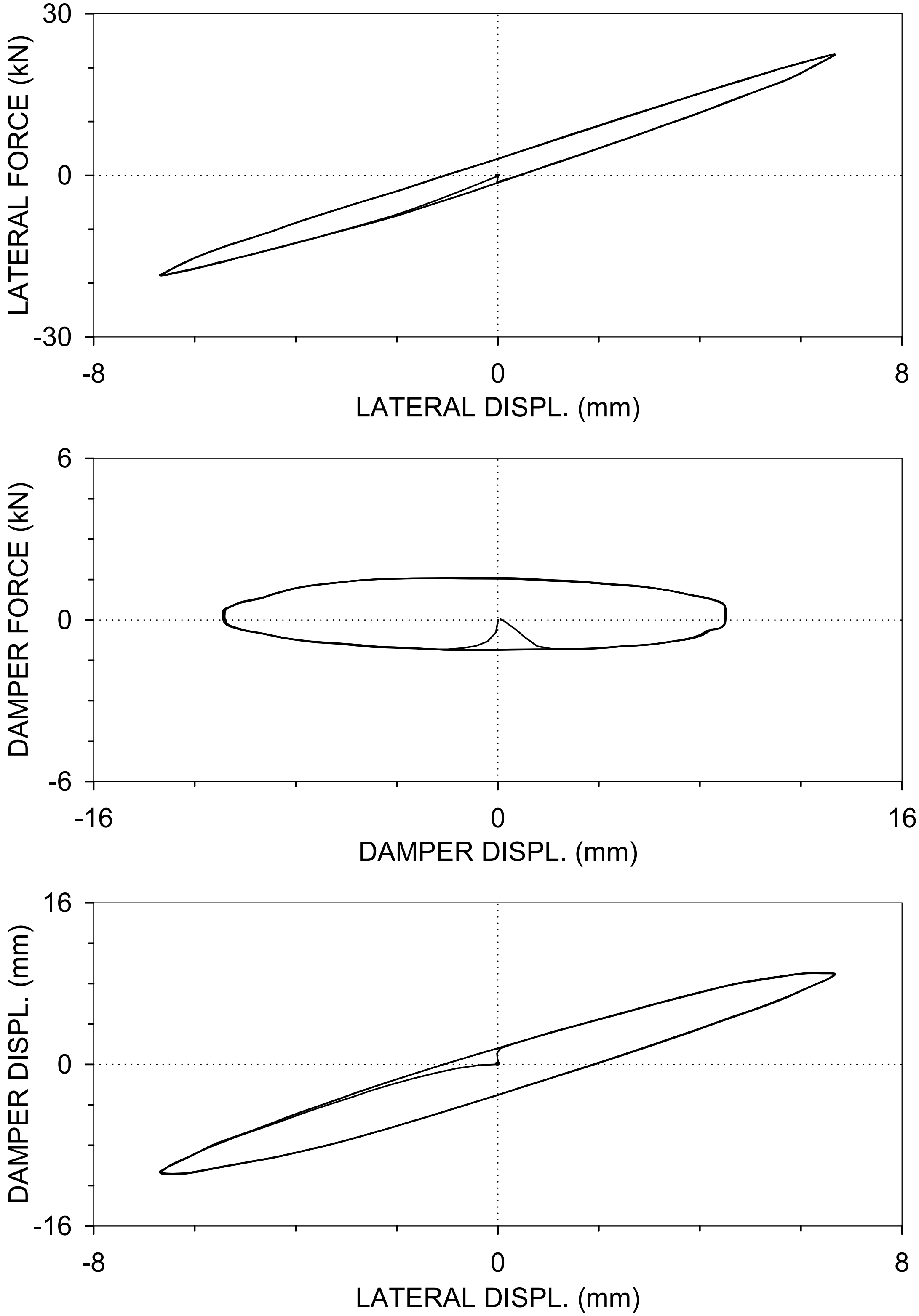

F2SR04 : BRACE 2, SIMPLE-RIGID CONNECTIONS
U_O=6.35 mm, f=1 Hz (03/19/99, 10:20:14)

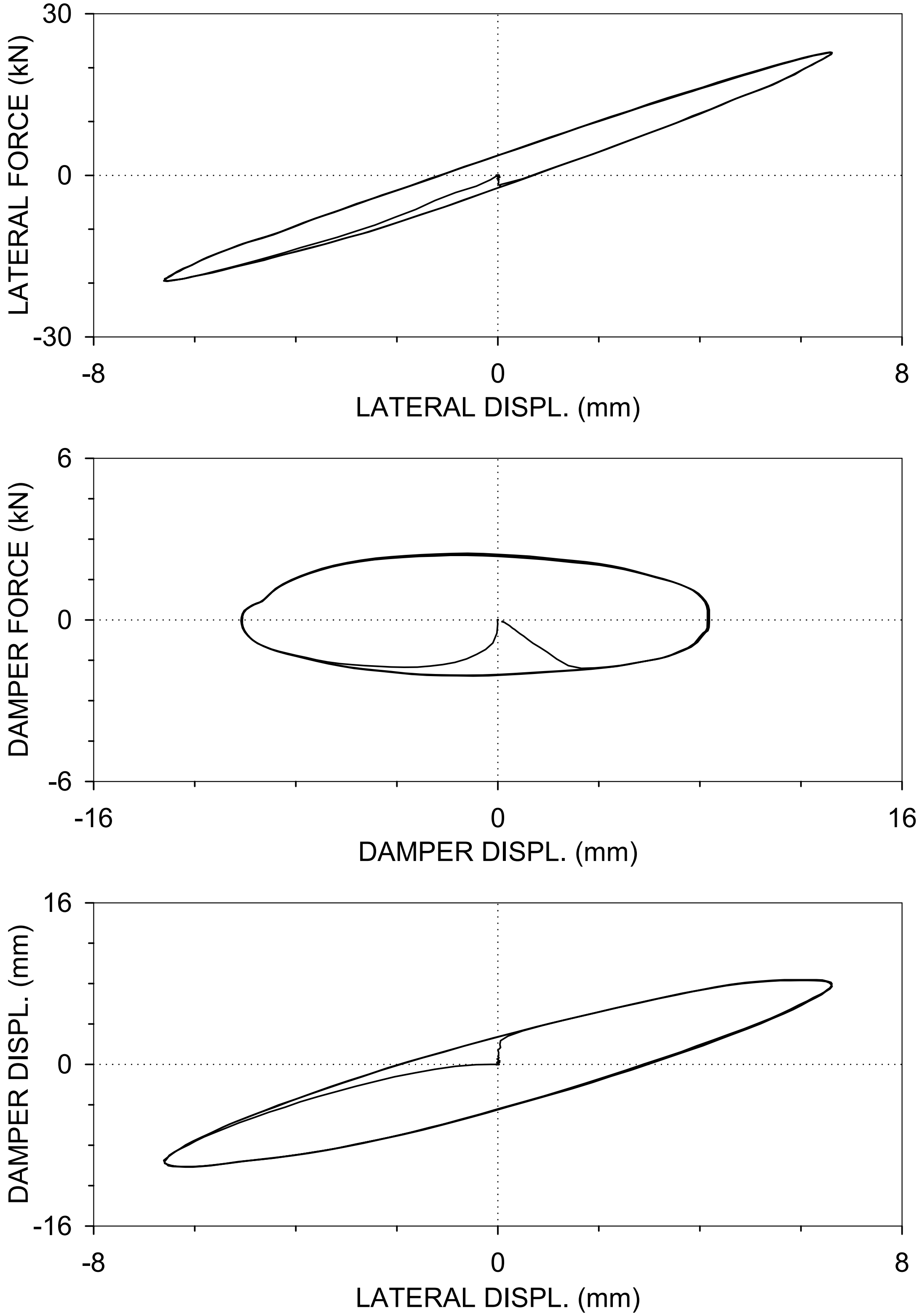

F2SR05 : BRACE 2, SIMPLE-RIGID CONNECTIONS
U_O=6.35 mm, f=2 Hz (03/19/99, 10:22:12)

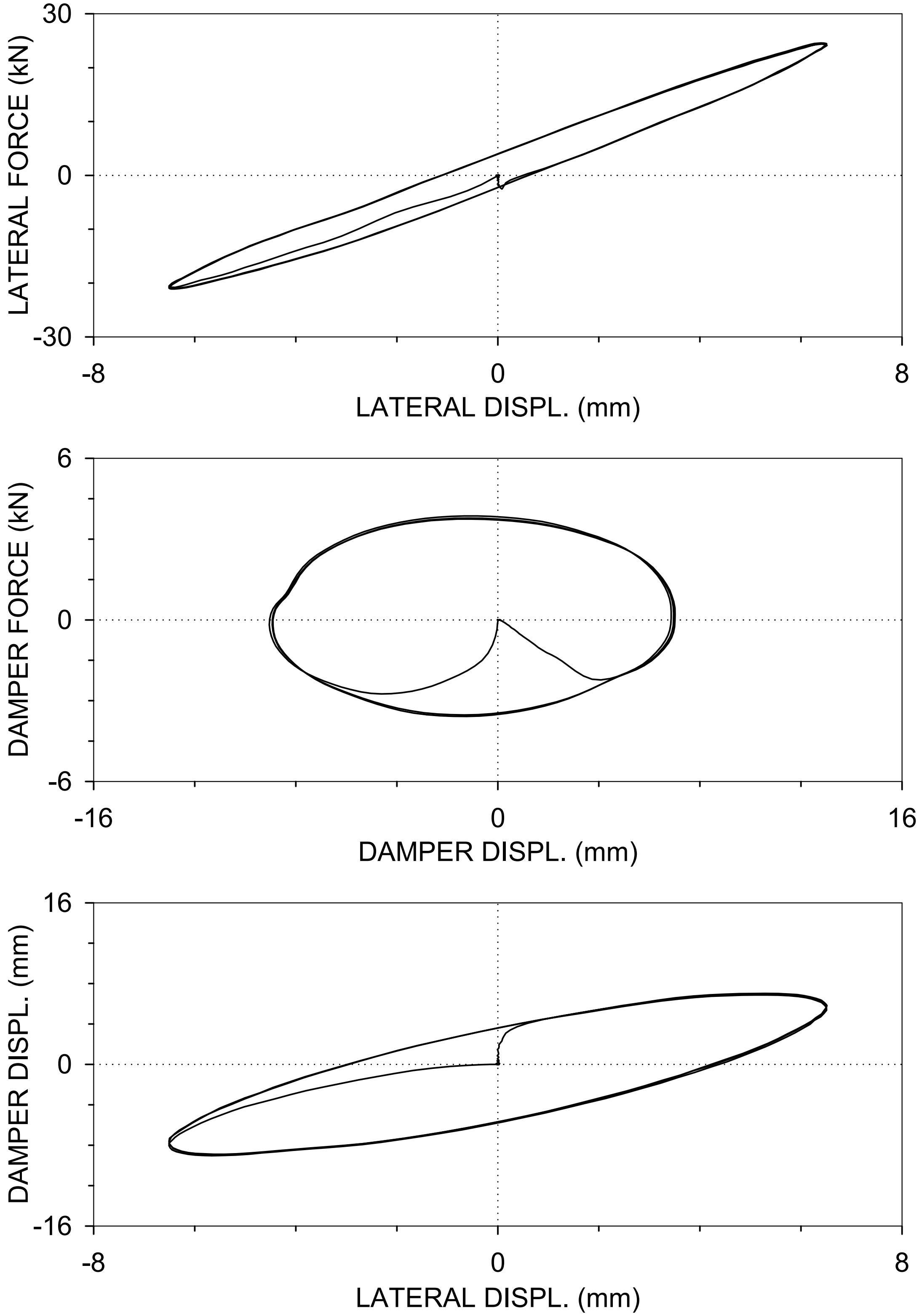

F2SR06 : BRACE 2, SIMPLE-RIGID CONNECTIONS
U_O=6.35 mm, f=3 Hz (03/19/99, 10:08:07)

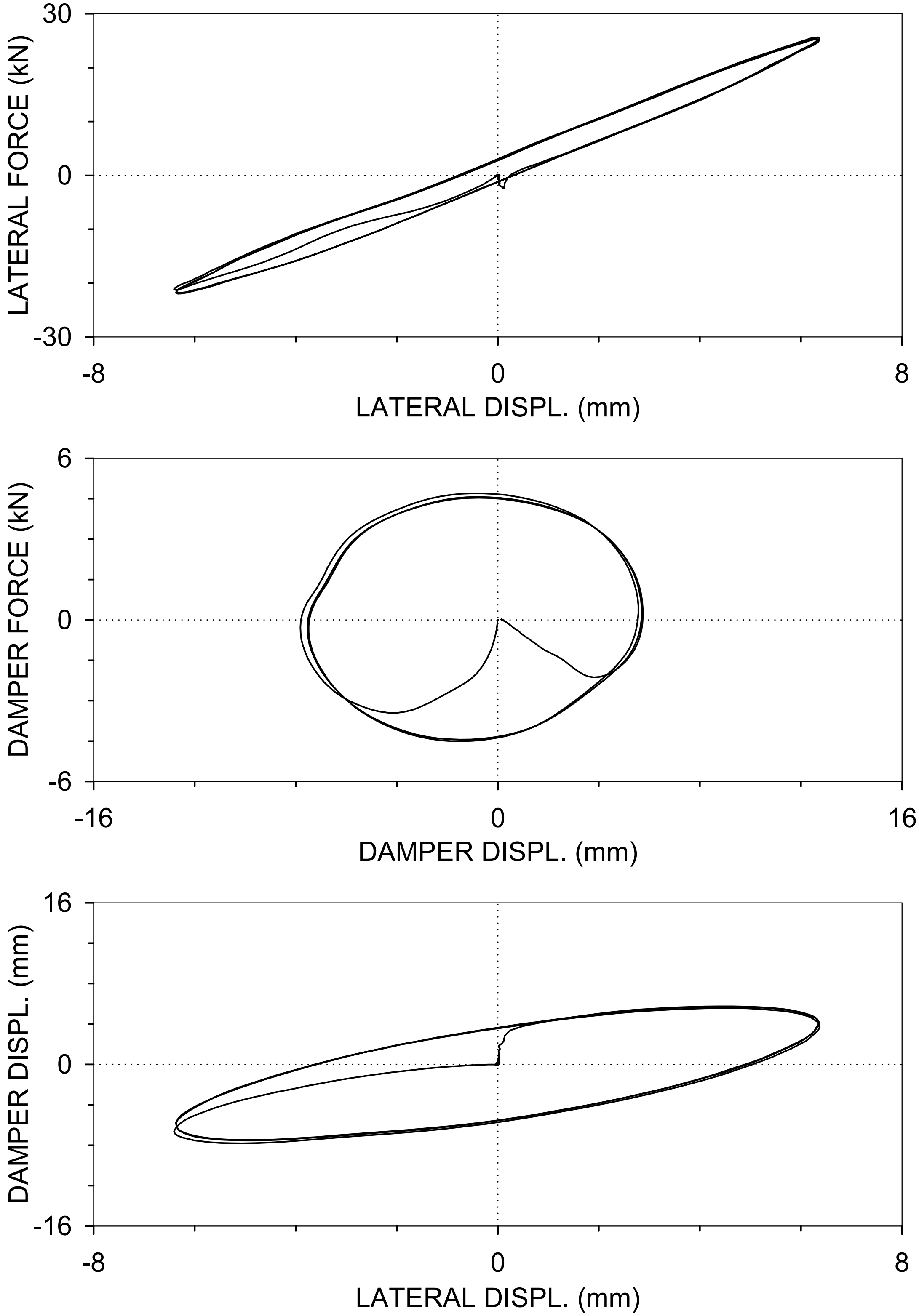

F2SR07 : BRACE 2, SIMPLE-RIGID CONNECTIONS
U_O=6.35 mm, f=4 Hz (03/19/99, 10:10:34)

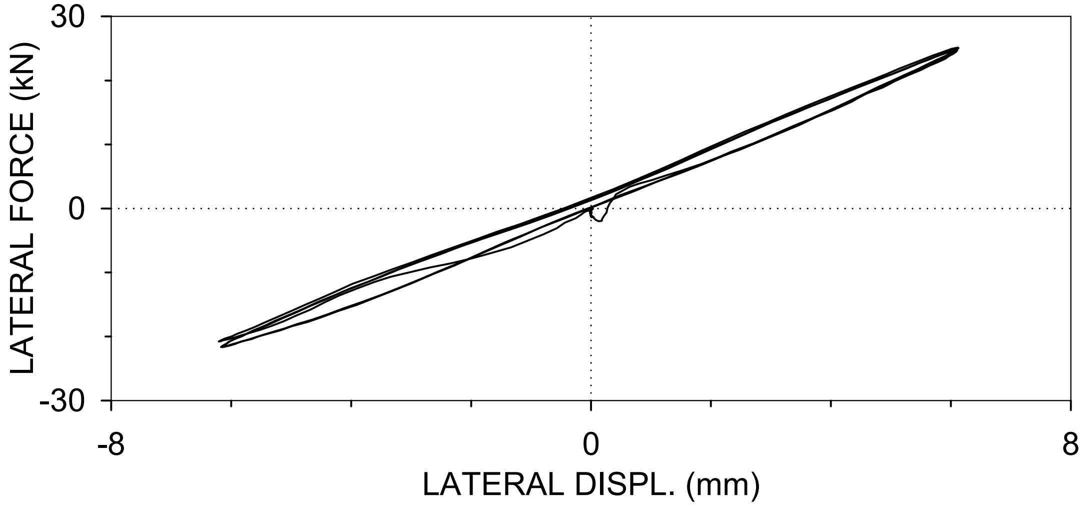

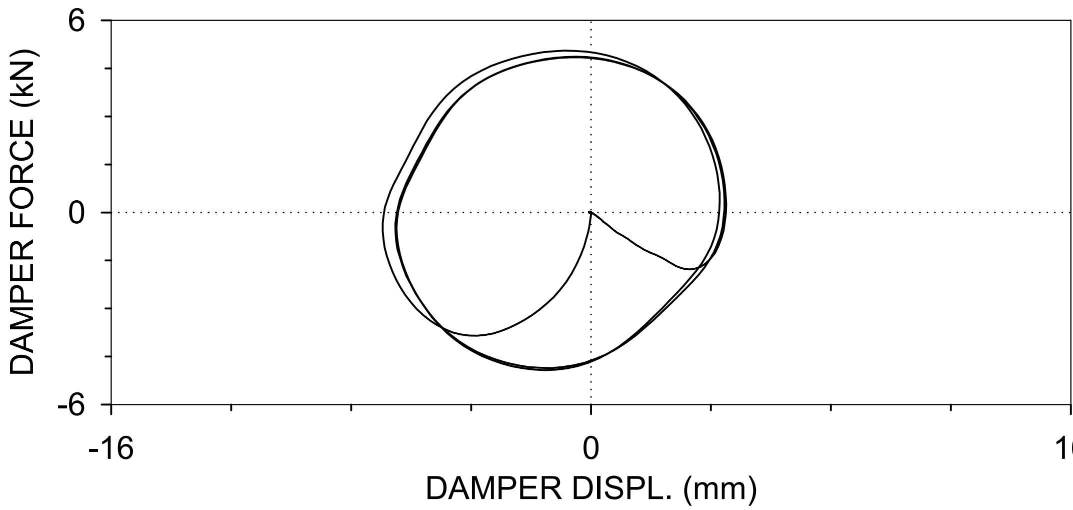

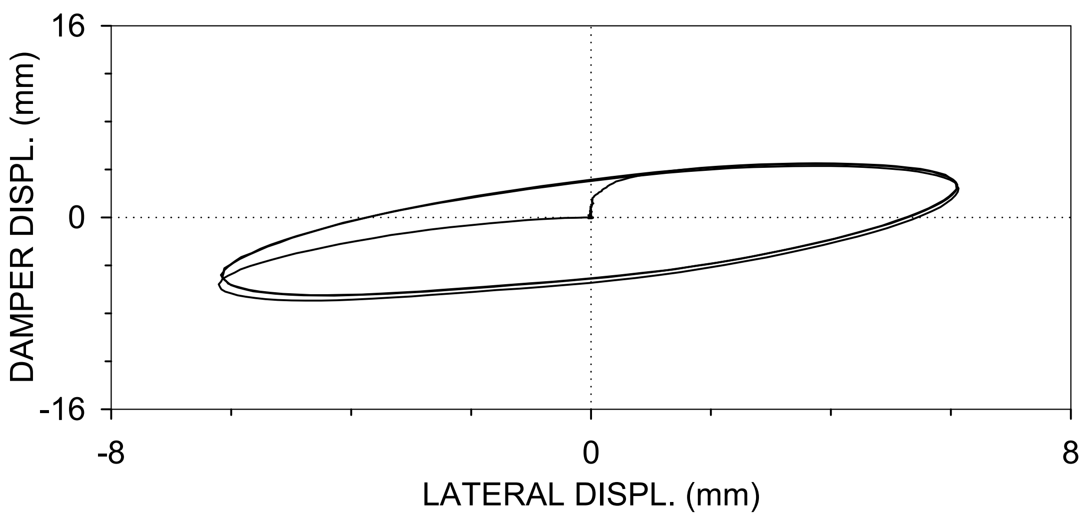

F2SR08 : BRACE 2, SIMPLE-RIGID CONNECTIONS
U_O=8.45 mm, f=0.01 Hz (03/19/99, 10:37:20)

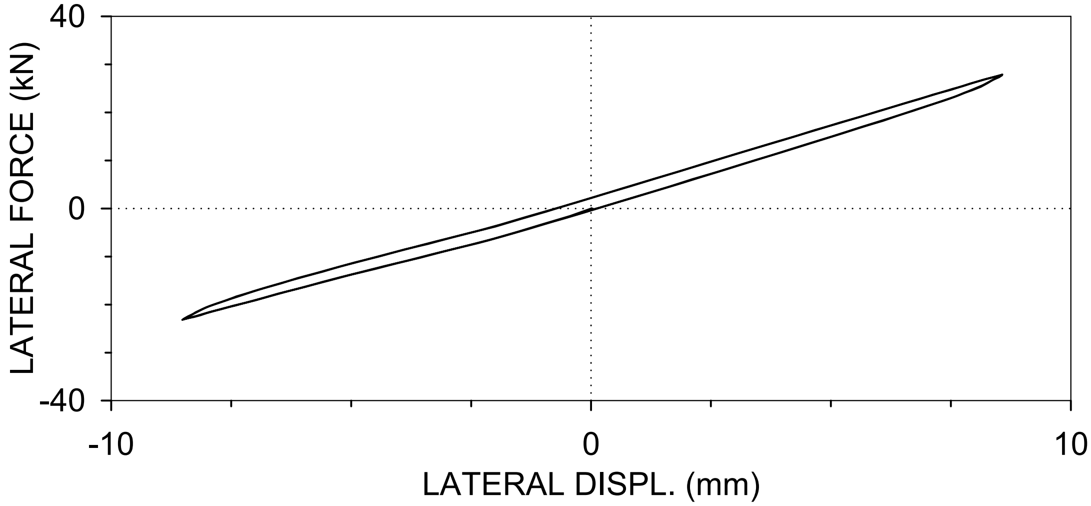

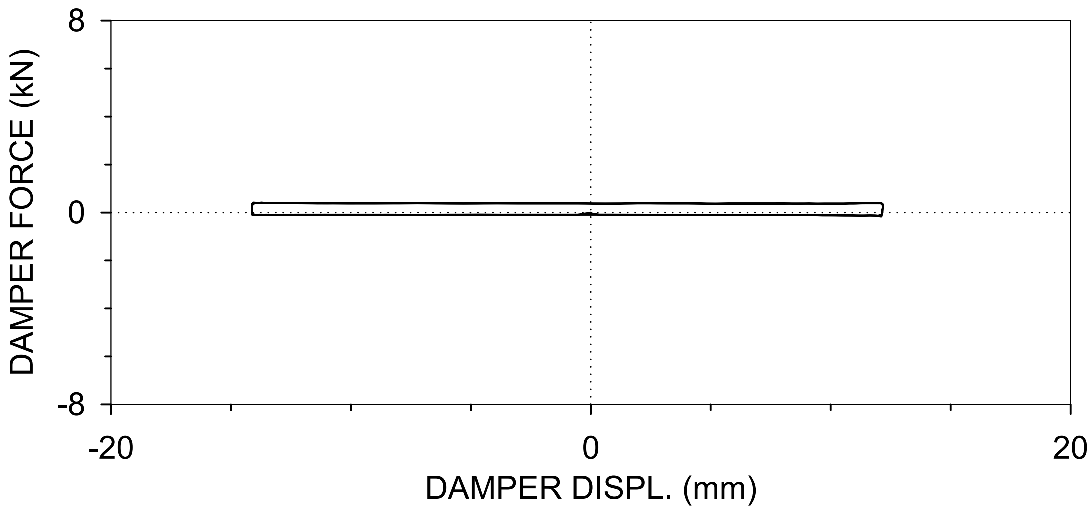

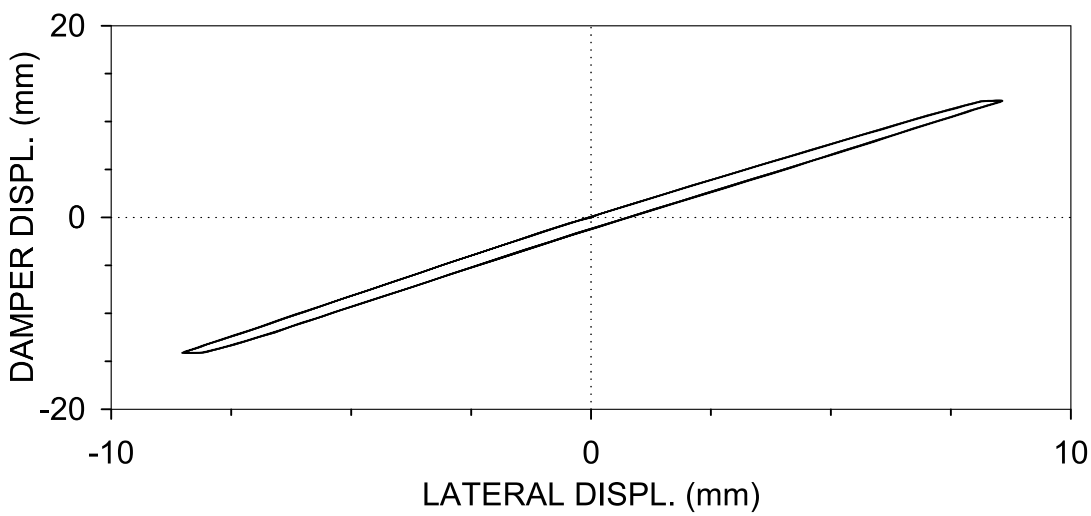

F2SR09 : BRACE 2, SIMPLE-RIGID CONNECTIONS

U_O=8.47 mm, f=0.05 Hz (03/19/99, 10:34:29)

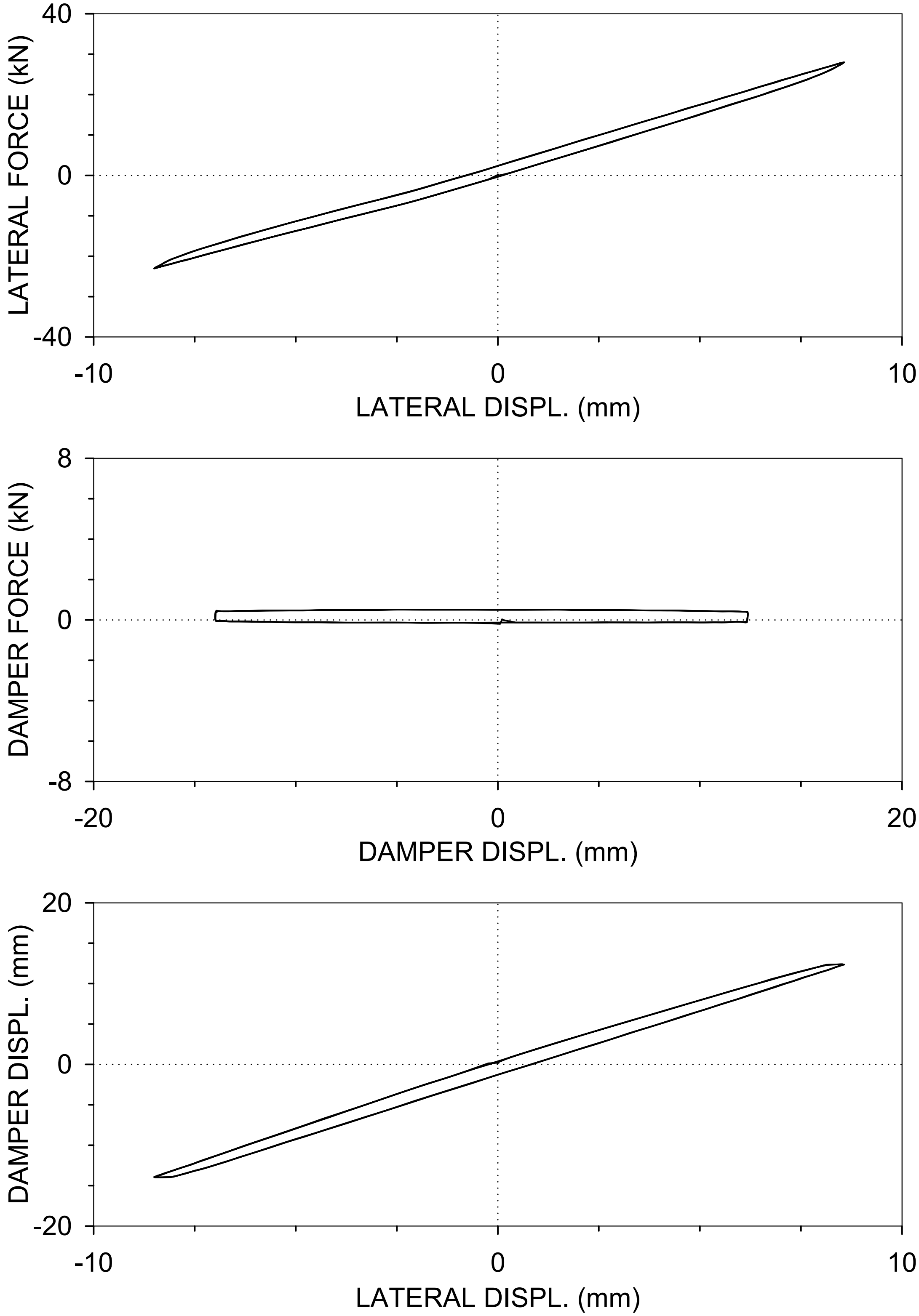

F2SR10 : BRACE 2, SIMPLE-RIGID CONNECTIONS
U_O=8.45 mm, f=0.5 Hz (03/19/99, 10:44:25)

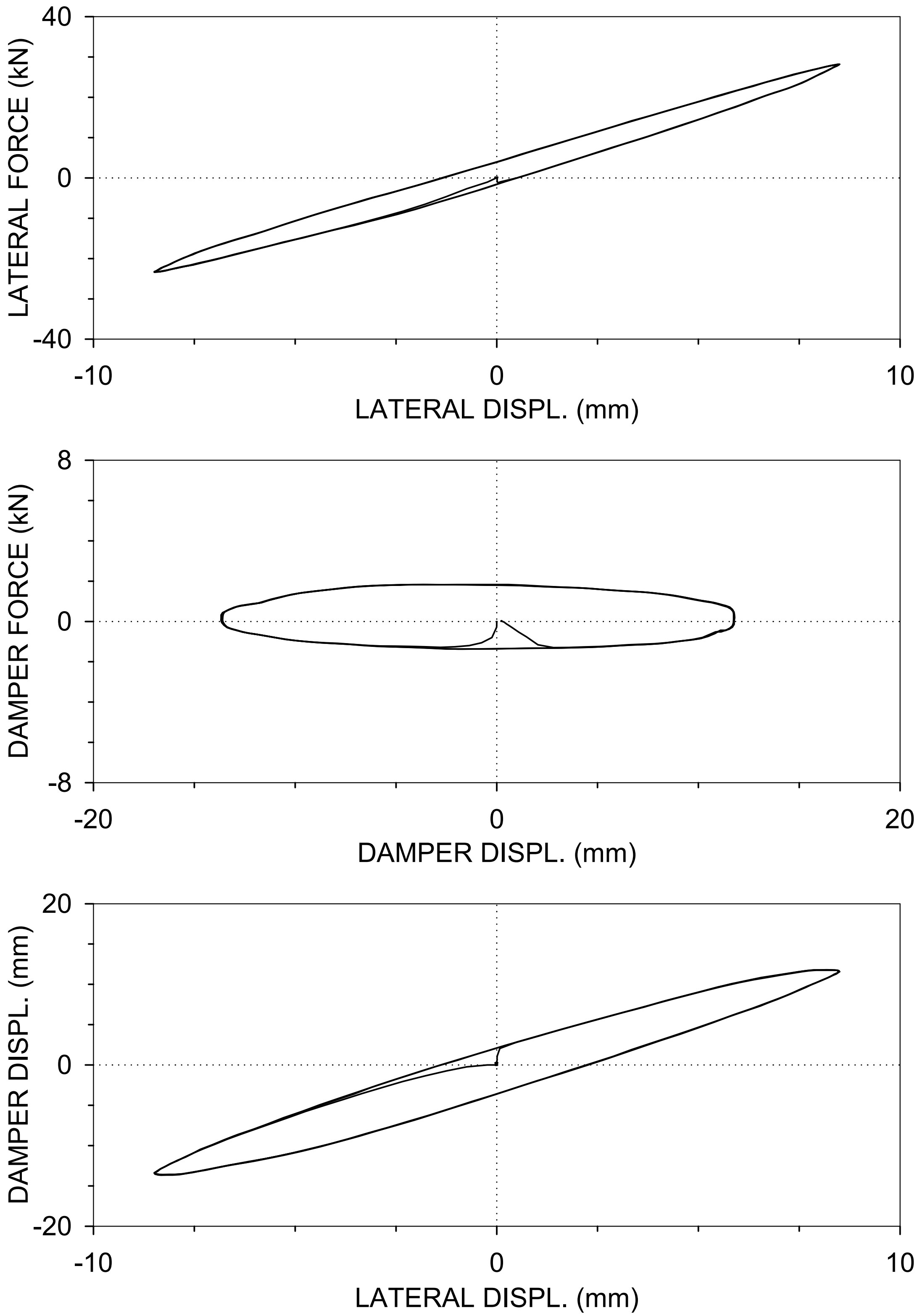

F2SR11 : BRACE 2, SIMPLE-RIGID CONNECTIONS
U_O=8.45 mm, f=1 Hz (03/19/99, 10:50:57)

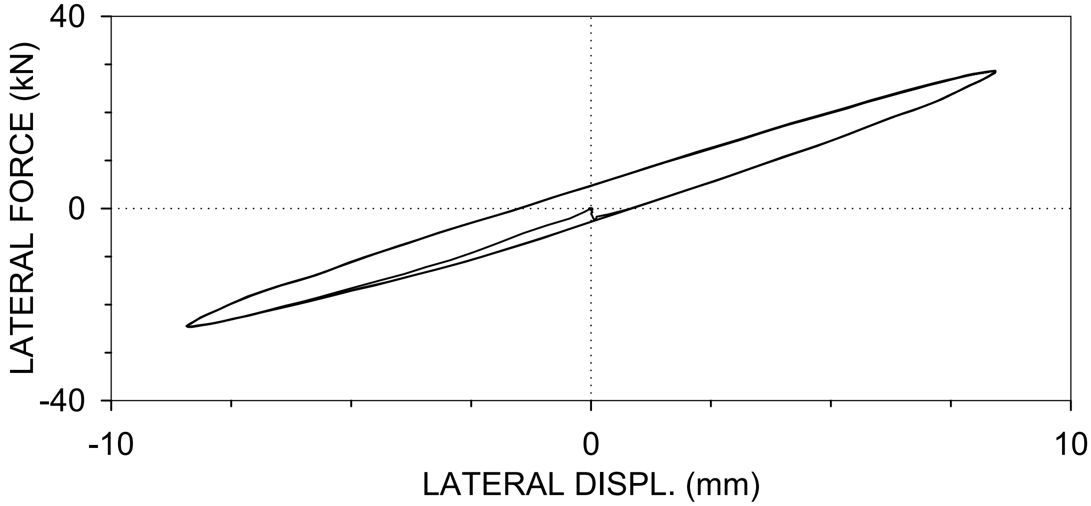

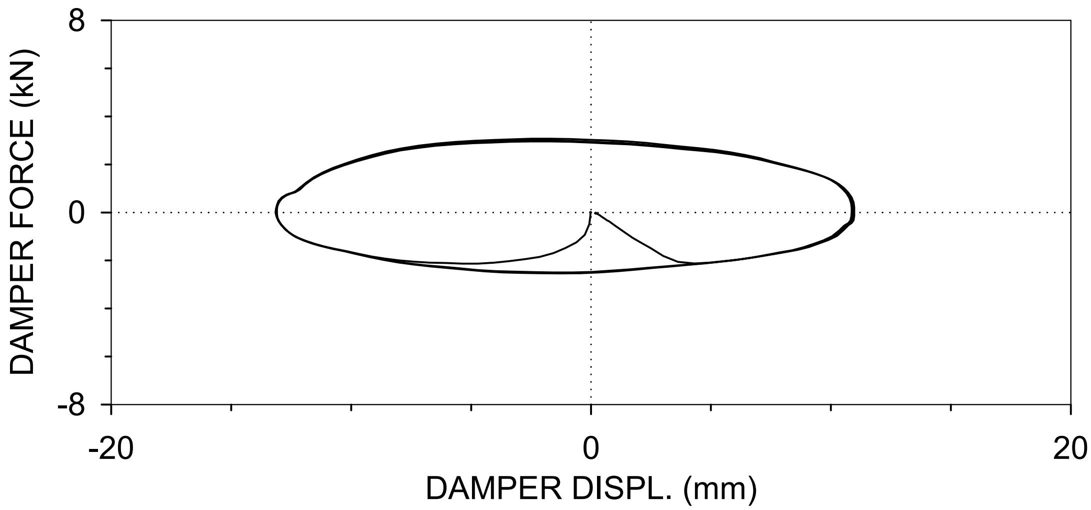

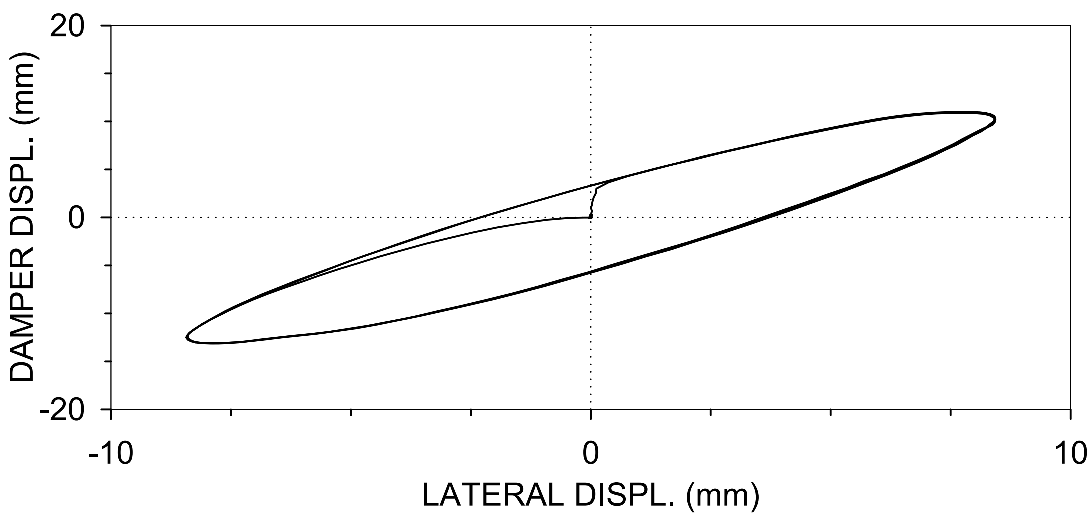

F2SR12 : BRACE 2, SIMPLE-RIGID CONNECTIONS
U_O=8.45 mm, f=2 Hz (03/19/99, 10:52:25)

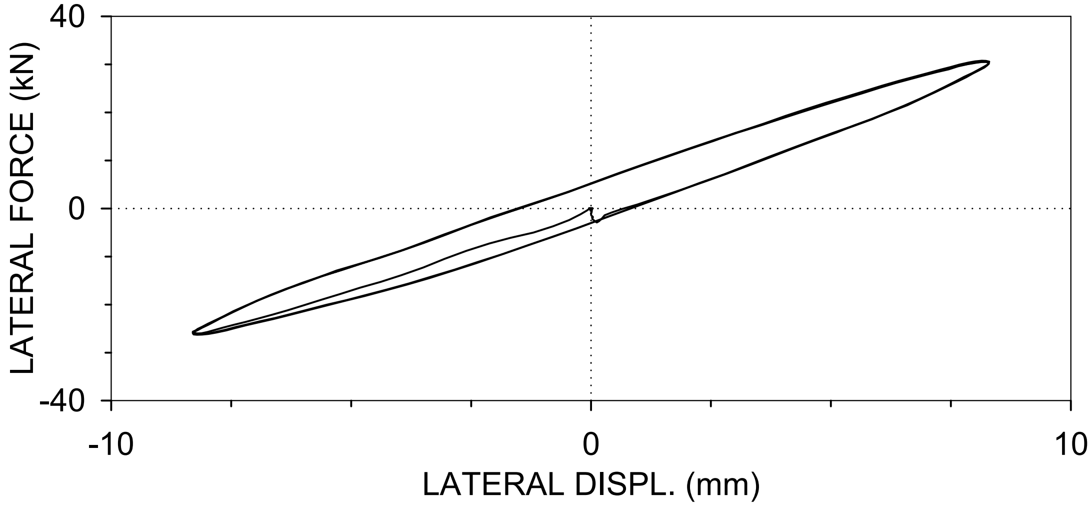

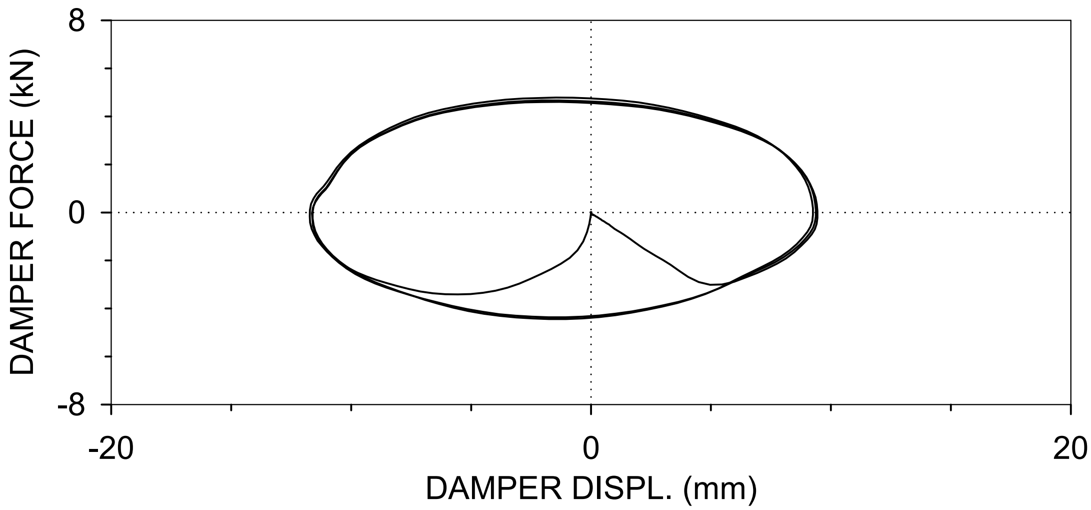

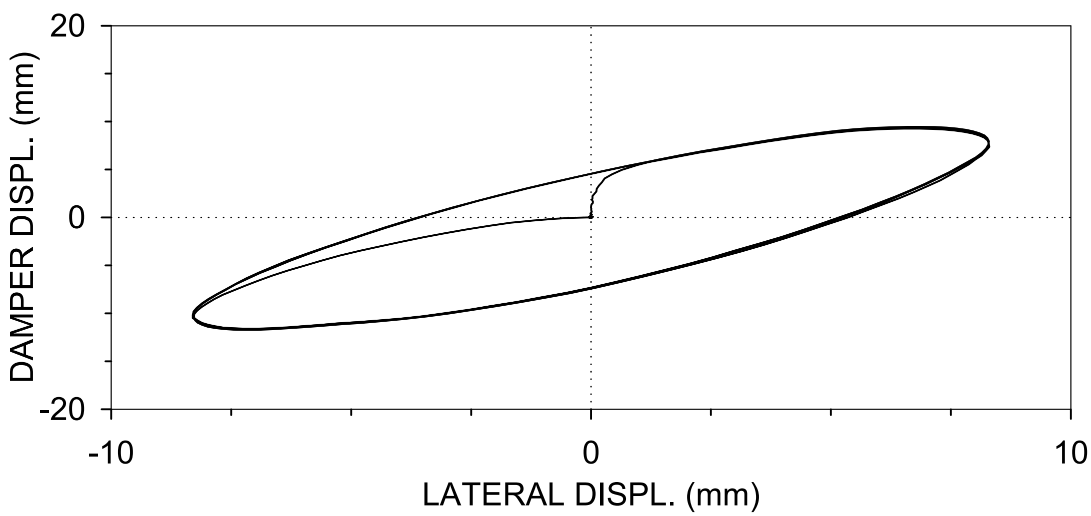

F2SR13 : BRACE 2, SIMPLE-RIGID CONNECTIONS
U_O=8.45 mm, f=3 Hz (03/19/99, 10:46:27)

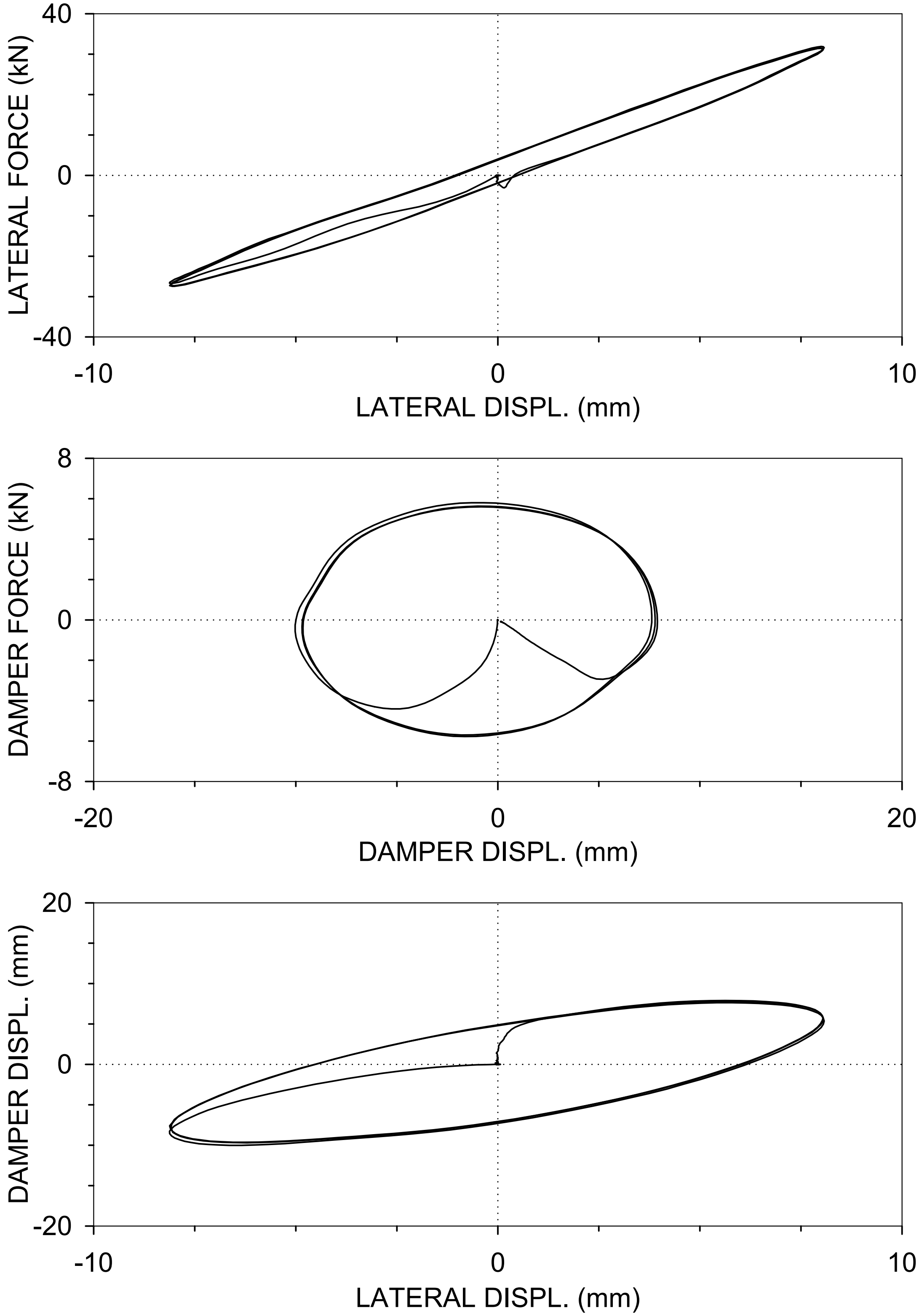

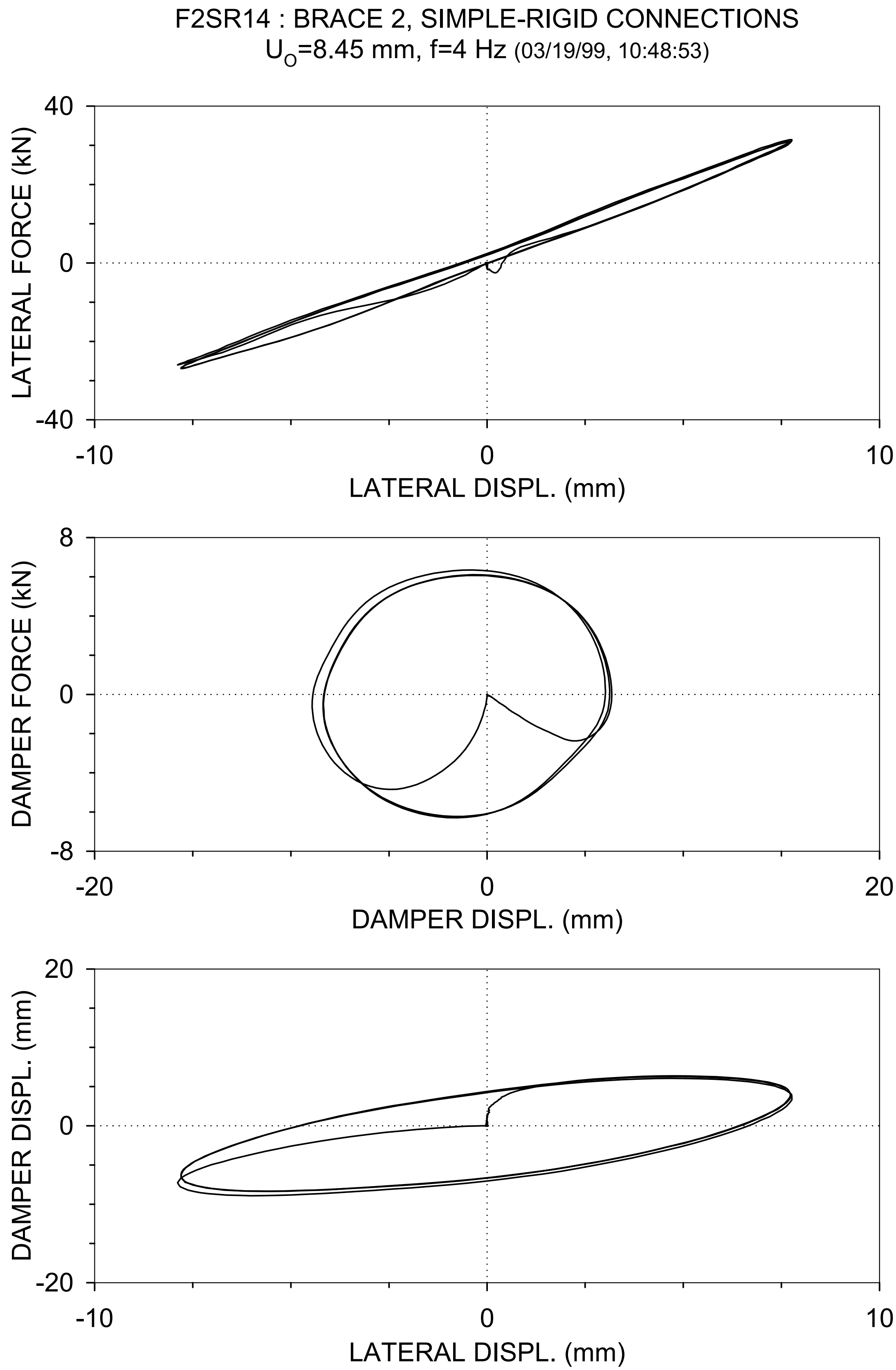
F2SR14 : BRACE 2, SIMPLE-RIGID CONNECTIONS
U_O=8.45 mm, f=4 Hz (03/19/99, 10:48:53)
LATERAL FORCE (kN)
40
0
-40
-10
0
10
LATERAL DISPL. (mm)
DAMPER FORCE (kN)
8
0
-8
-20
0
20
DAMPER DISPL. (mm)
DAMPER DISPL. (mm)
20
0
-20
-10
0
10
LATERAL DISPL. (mm)

F2RS01 : BRACE 2, RIGID-SIMPLE CONNECTIONS
U_O=6.35 mm, f=0.01 Hz (03/19/99, 13:46:53)

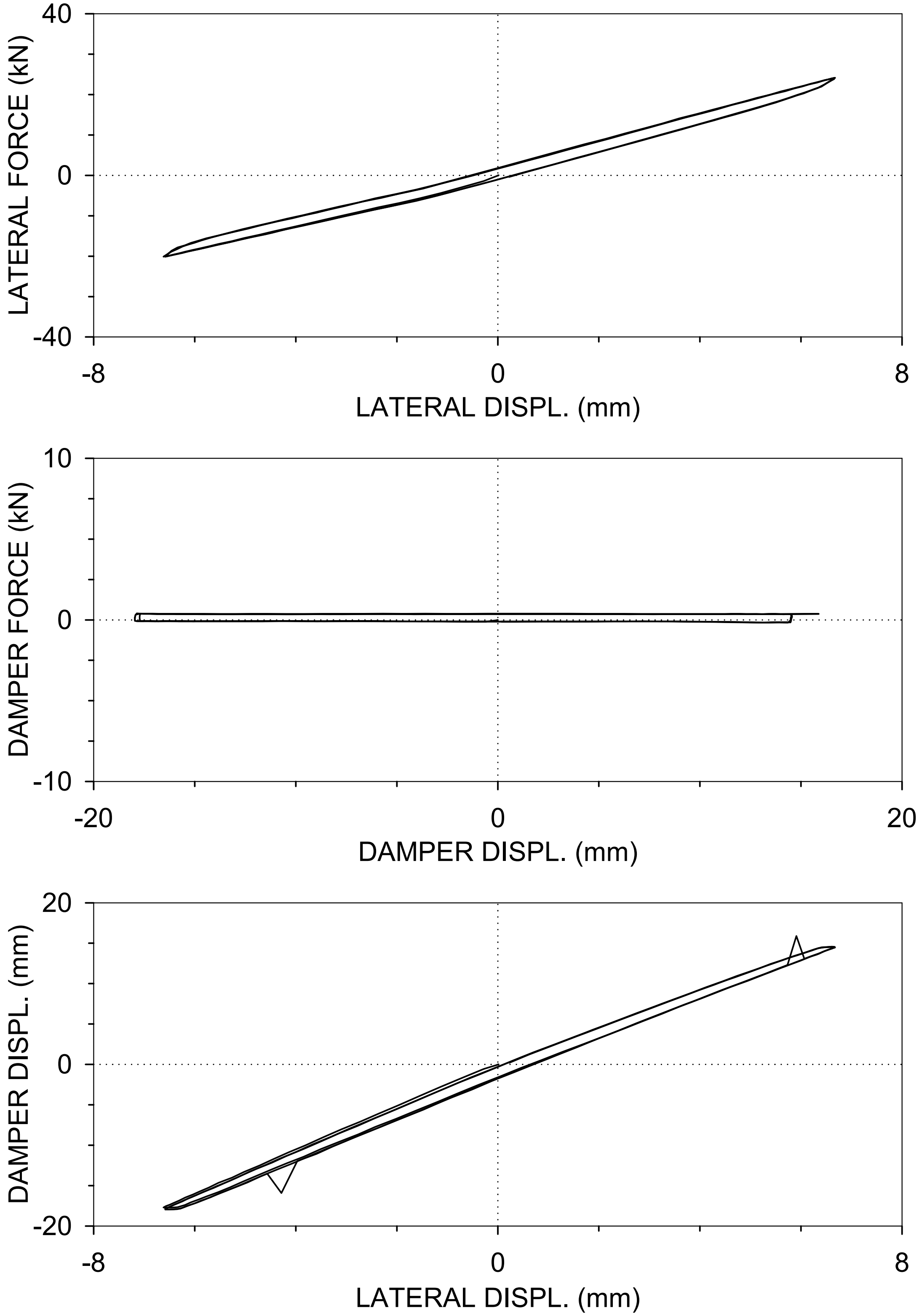

F2RS02 : BRACE 2, RIGID-SIMPLE CONNECTIONS
U_O=6.35 mm, f=0.05 Hz (03/19/99, 13:54:47)

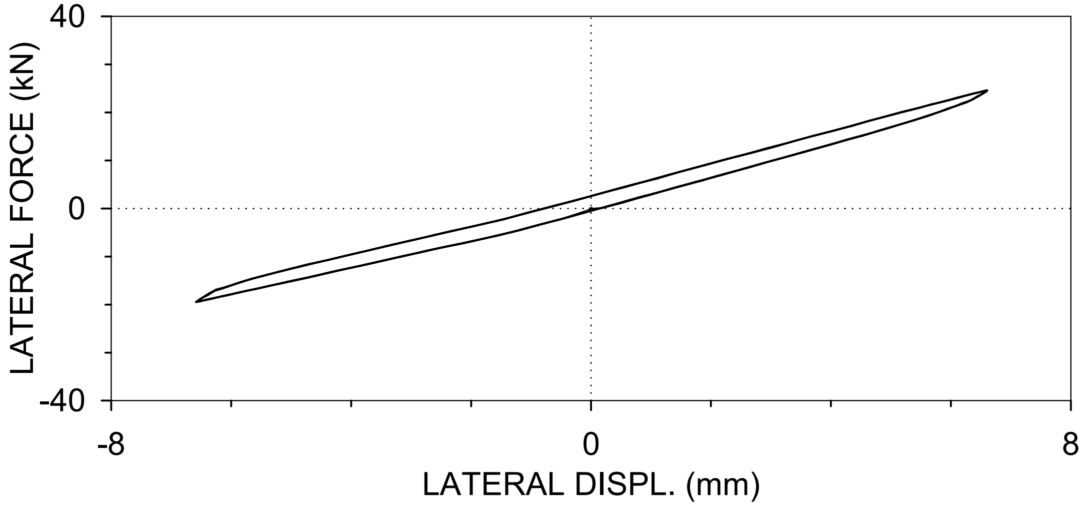

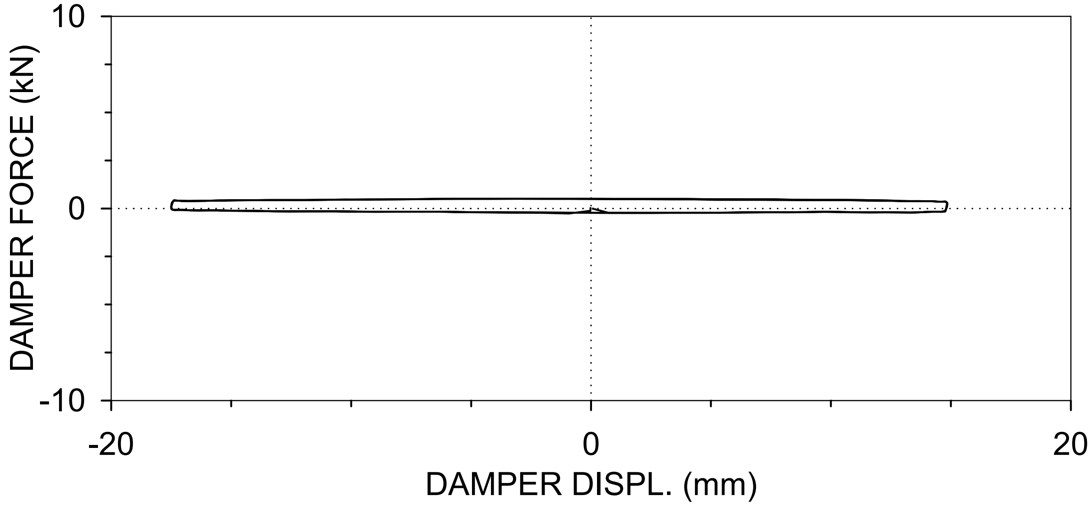

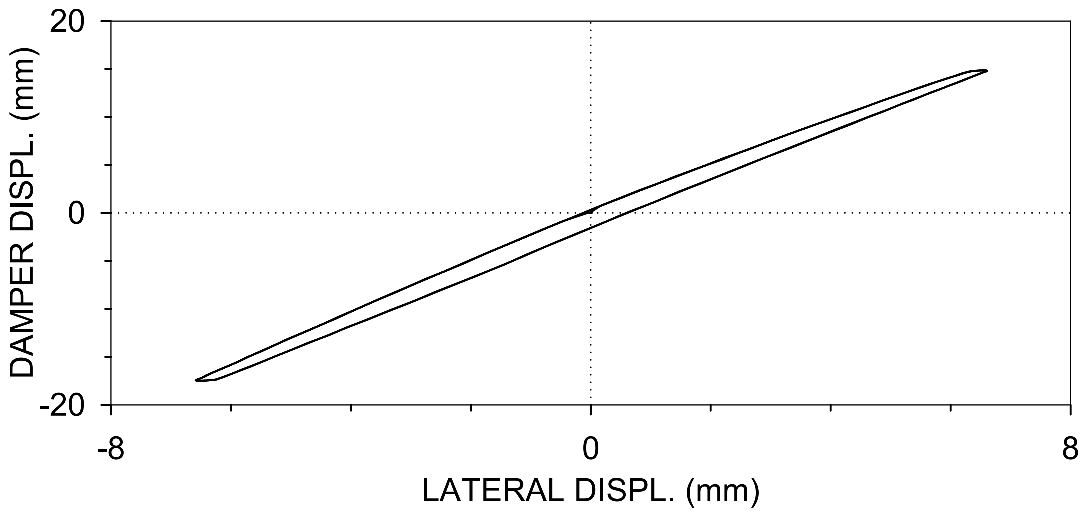

F2RS03 : BRACE 2, RIGID-SIMPLE CONNECTIONS
U_O=6.35 mm, f=0.5 Hz (03/19/99, 14:00:01)

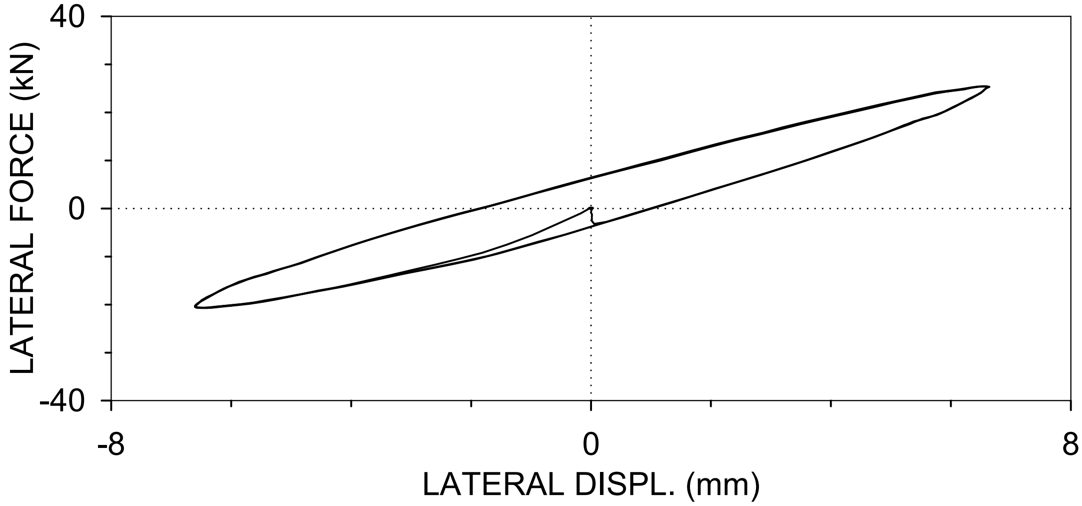

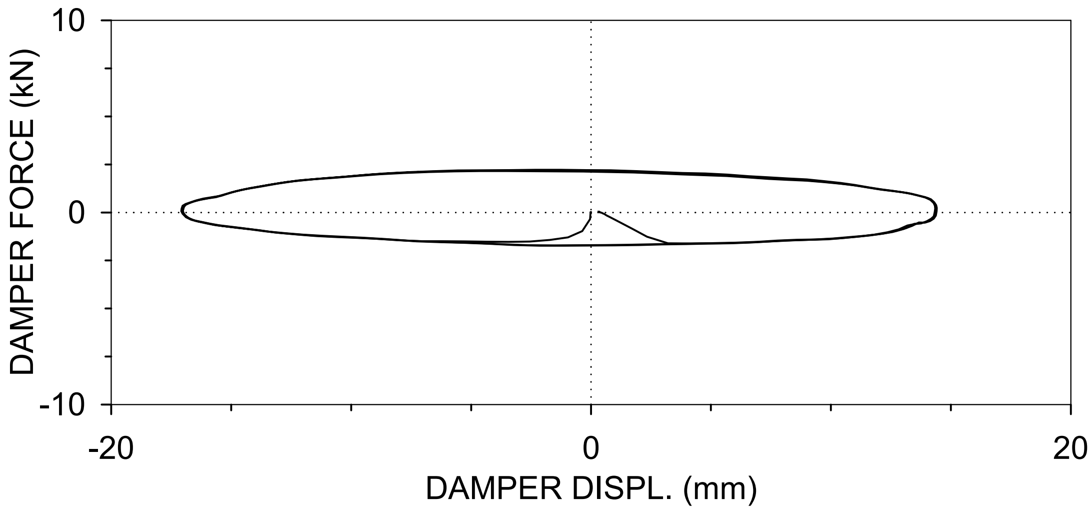

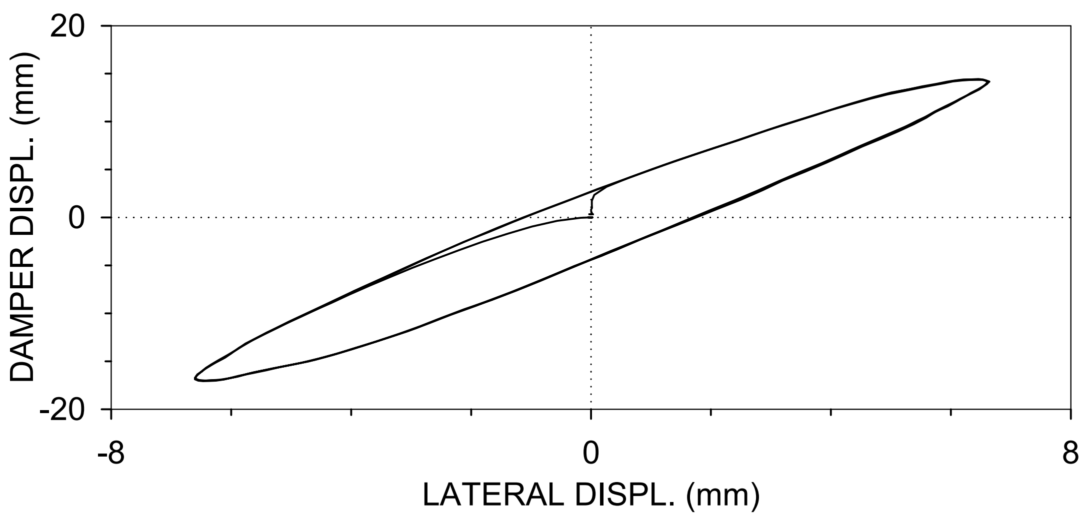

F2RS04 : BRACE 2, RIGID-SIMPLE CONNECTIONS
U_O=6.35 mm, f=1 Hz (03/19/99, 14:02:34)

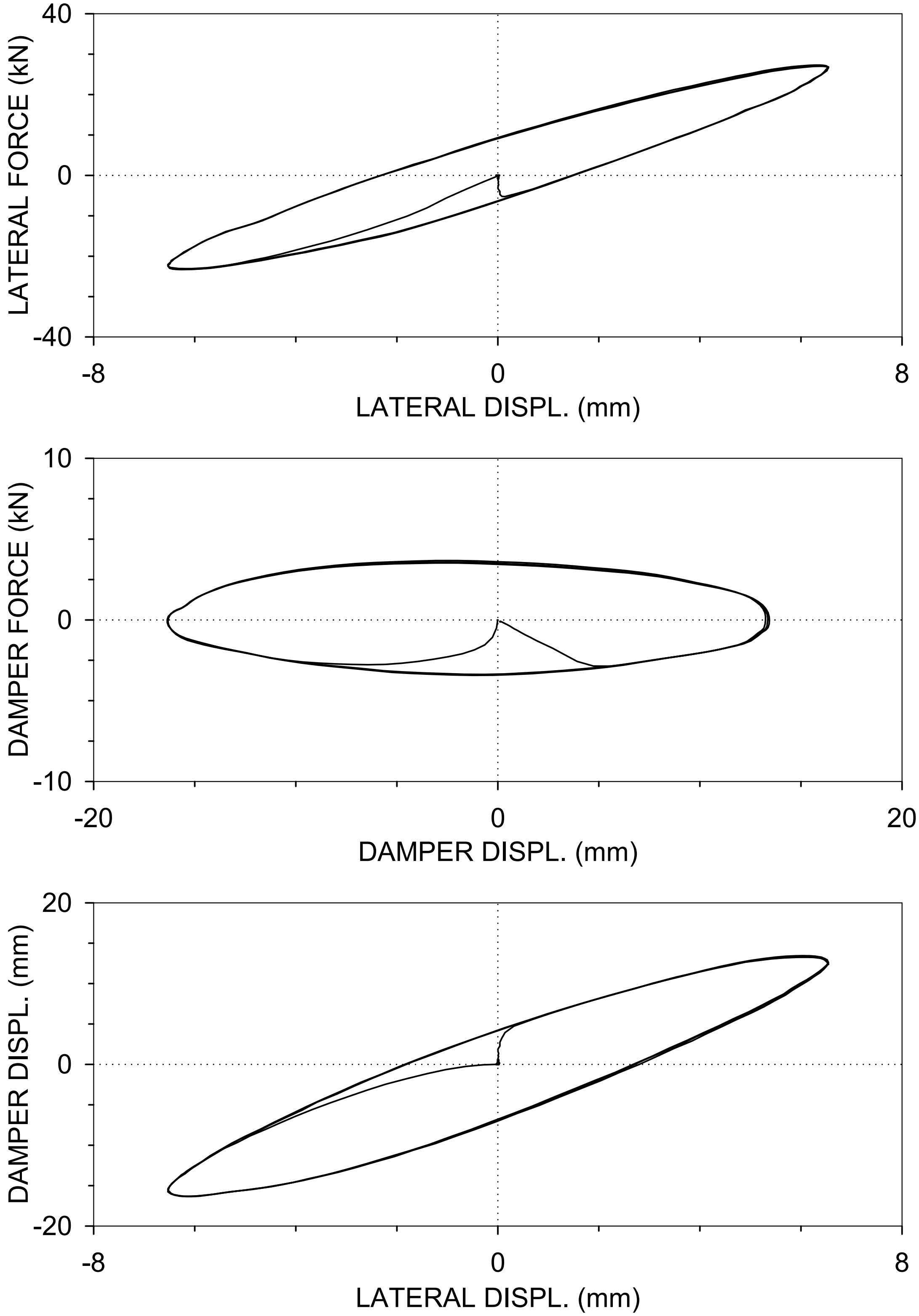

F2RS05 : BRACE 2, RIGID-SIMPLE CONNECTIONS
U_O=6.35 mm, f=2 Hz (03/19/99, 14:04:20)

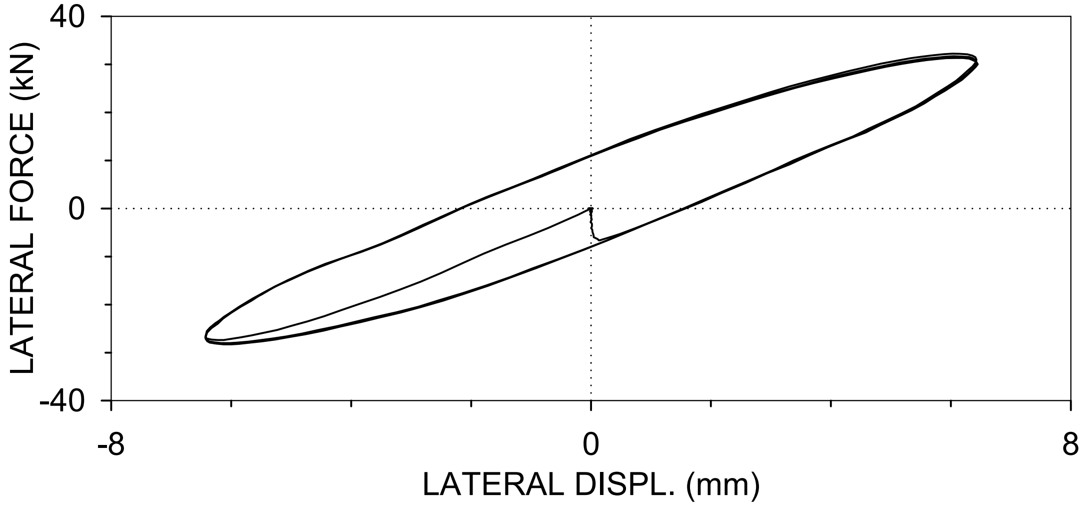

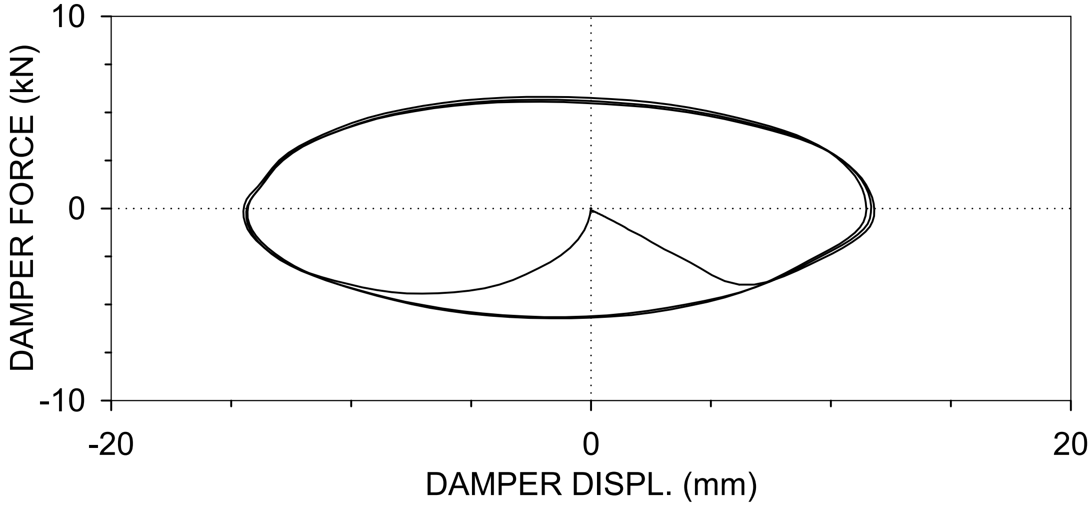

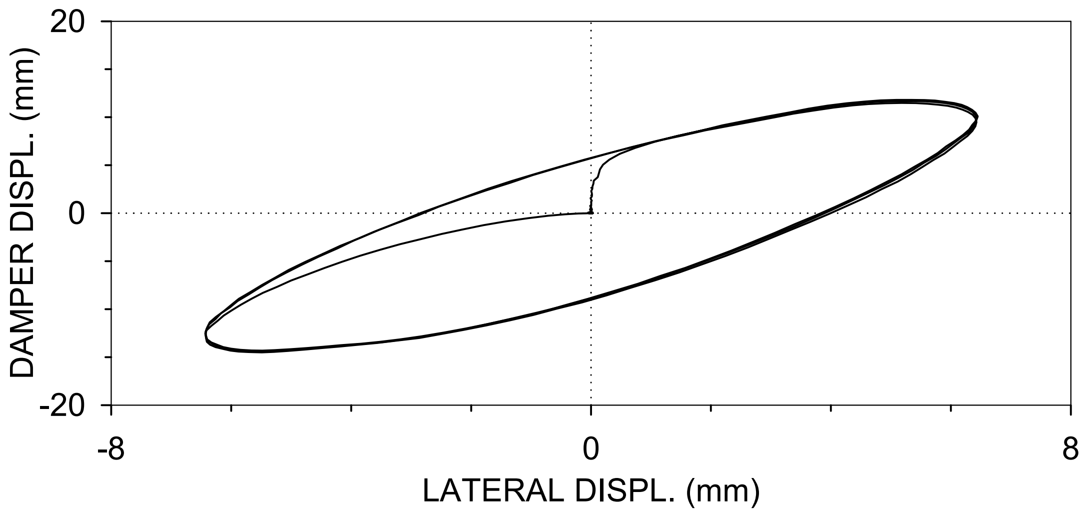

F2RS06 : BRACE 2, RIGID-SIMPLE CONNECTIONS
U_O=6.35 mm, f=3 Hz (03/19/99, 14:05:53)

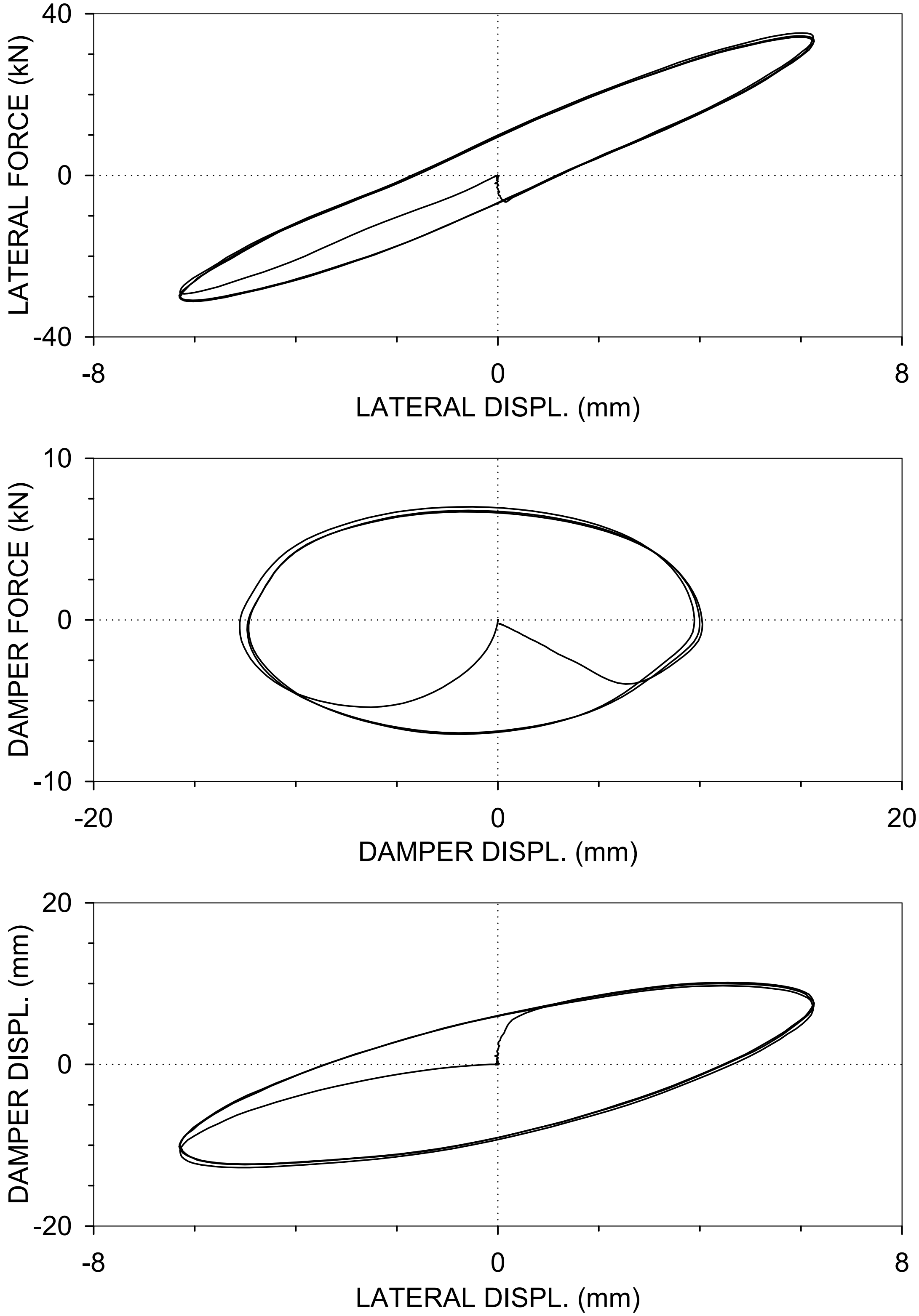

F2RS07 : BRACE 2, RIGID-SIMPLE CONNECTIONS
U_O=6.35 mm, f=4 Hz (03/19/99, 14:07:51)

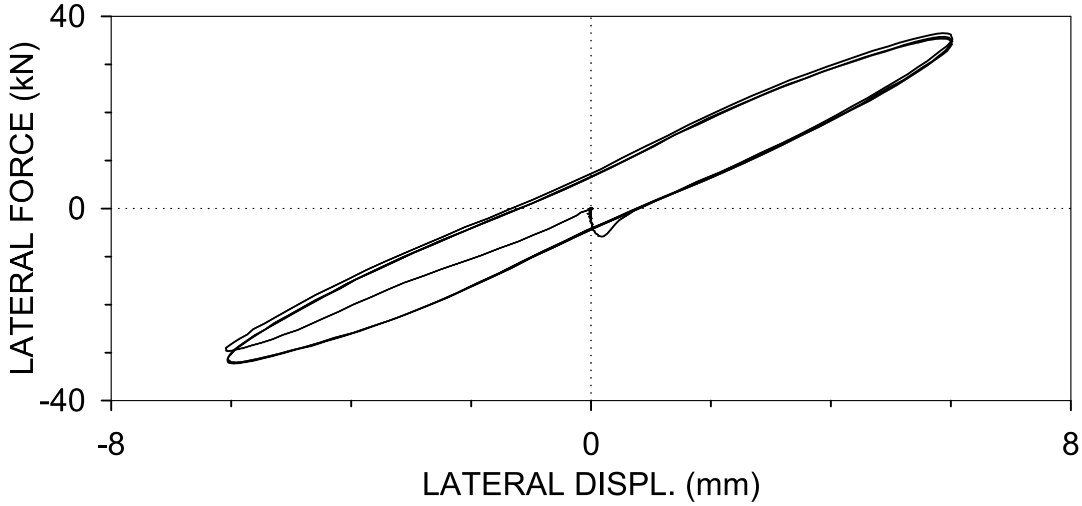

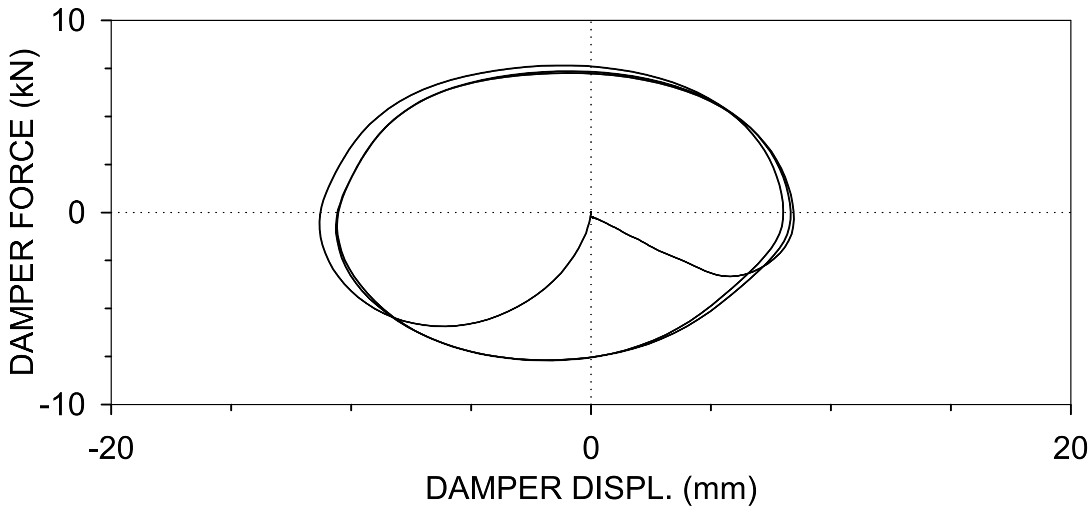

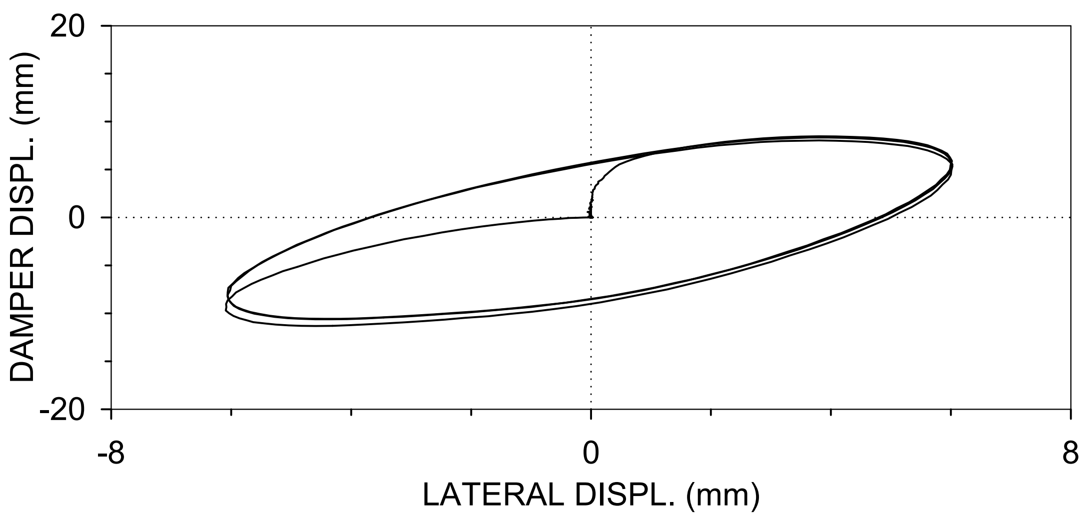

F2RS08 : BRACE 2, RIGID-SIMPLE CONNECTIONS
U_O=8.45 mm, f=0.01 Hz (03/19/99, 14:10:06)

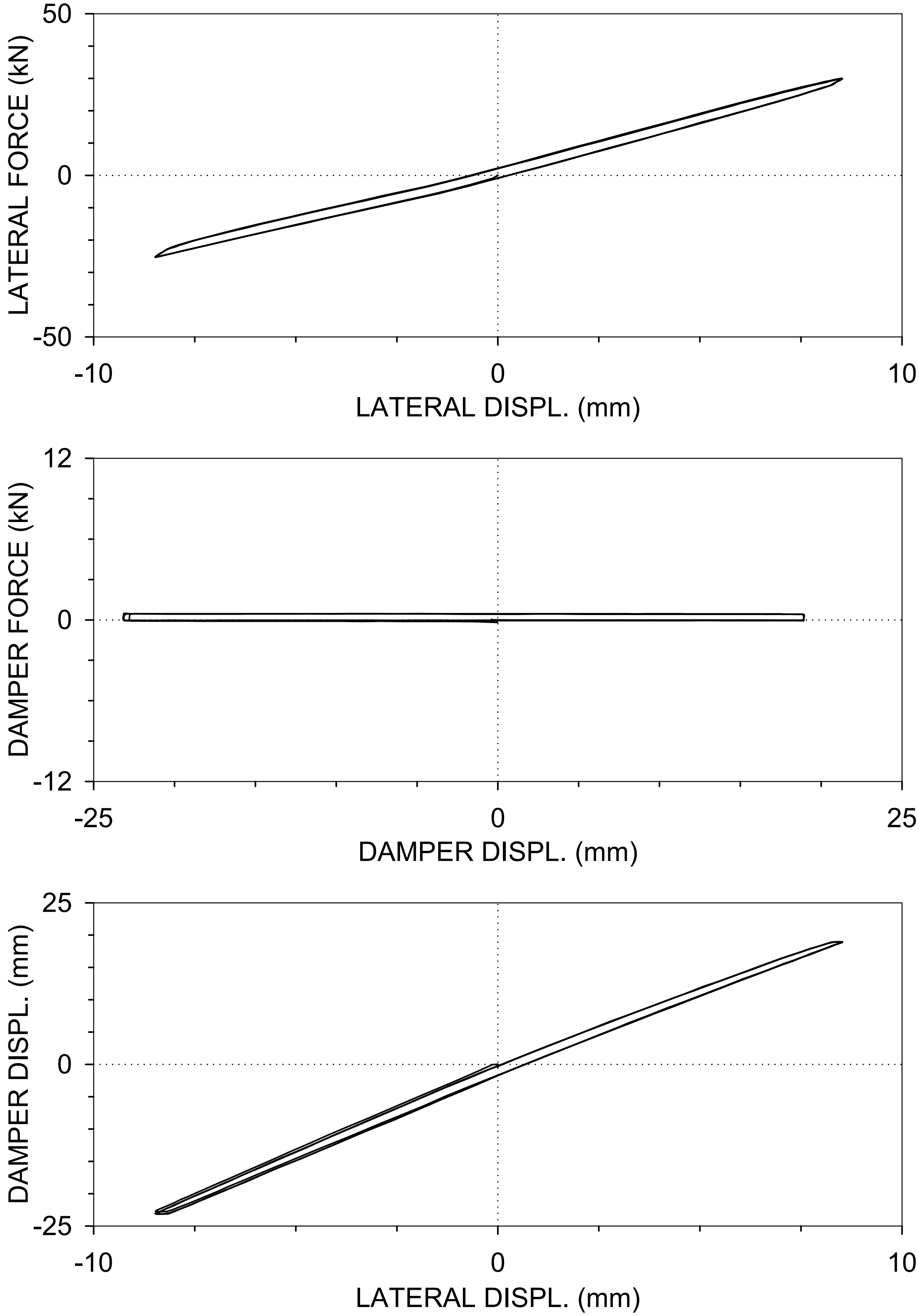

F2RS09 : BRACE 2, RIGID-SIMPLE CONNECTIONS
U_O=8.45 mm, f=0.05 Hz (03/19/99, 14:16:38)

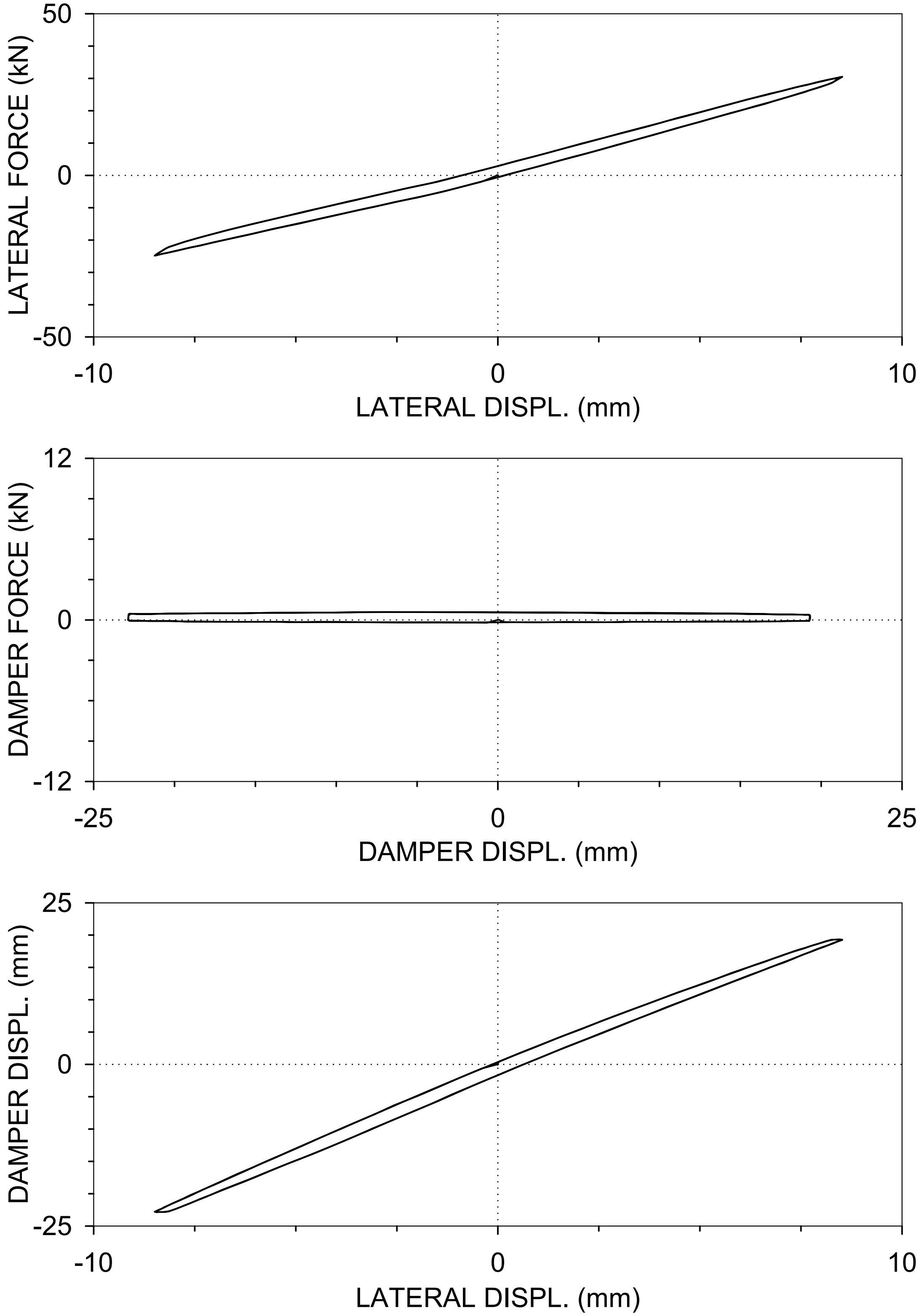

F2RS10 : BRACE 2, RIGID-SIMPLE CONNECTIONS
U_O=8.45 mm, f=0.5 Hz (03/19/99, 14:18:52)

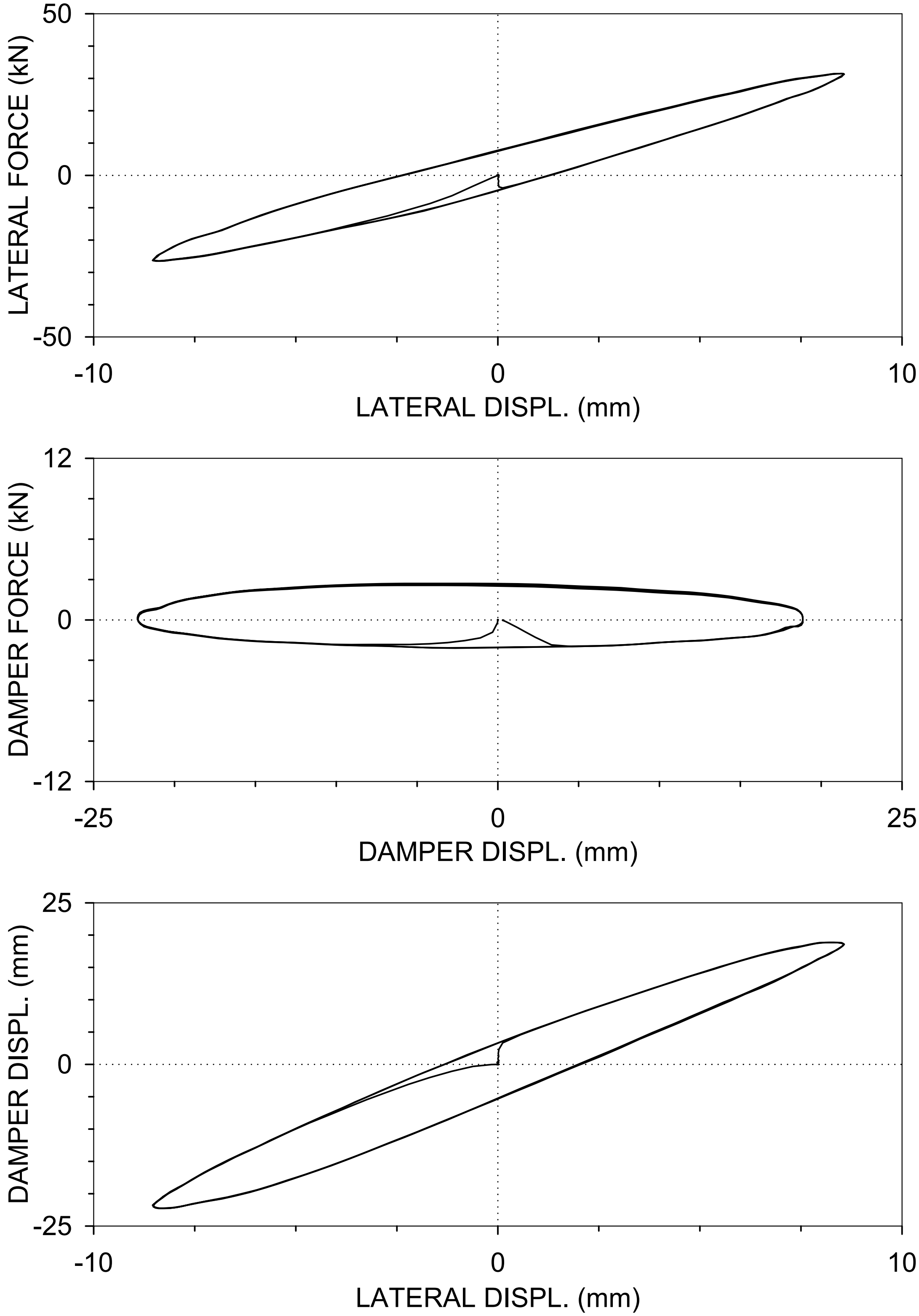

F2RS11 : BRACE 2, RIGID-SIMPLE CONNECTIONS
U_O=8.45 mm, f=1 Hz (03/19/99, 14:20:34)

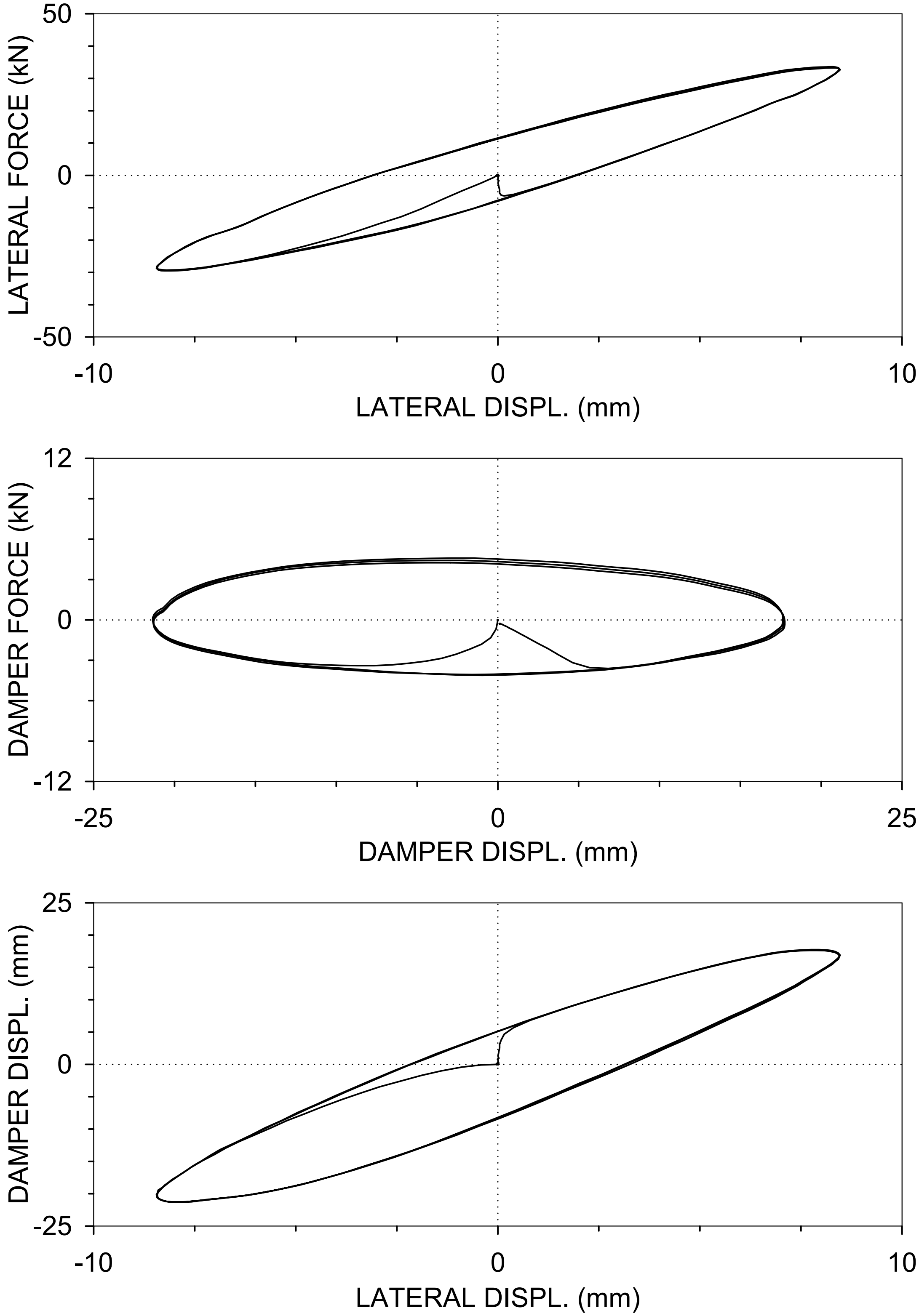

F2RS12 : BRACE 2, RIGID-SIMPLE CONNECTIONS
U_O=8.45 mm, f=2 Hz (03/19/99, 14:21:53)

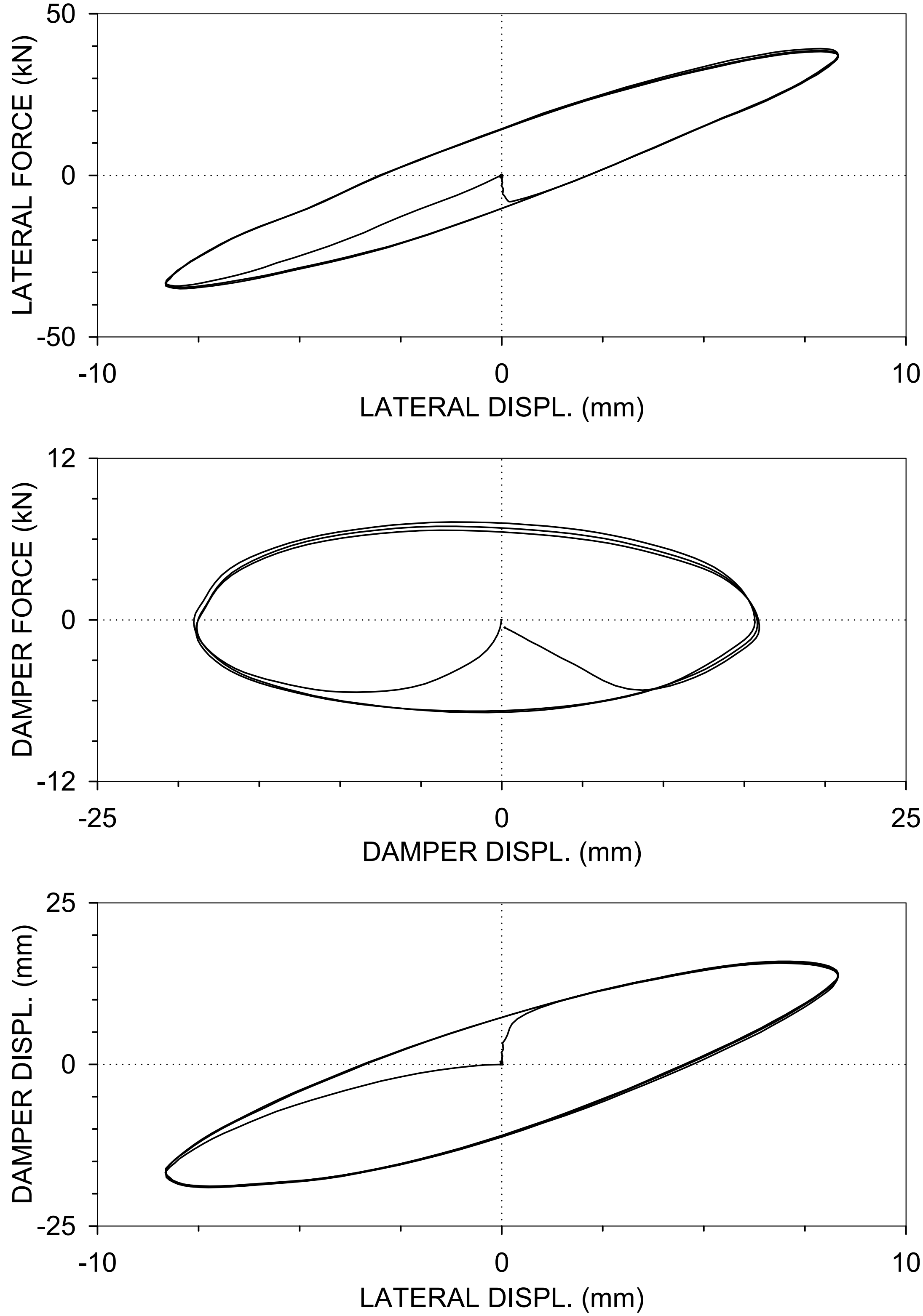

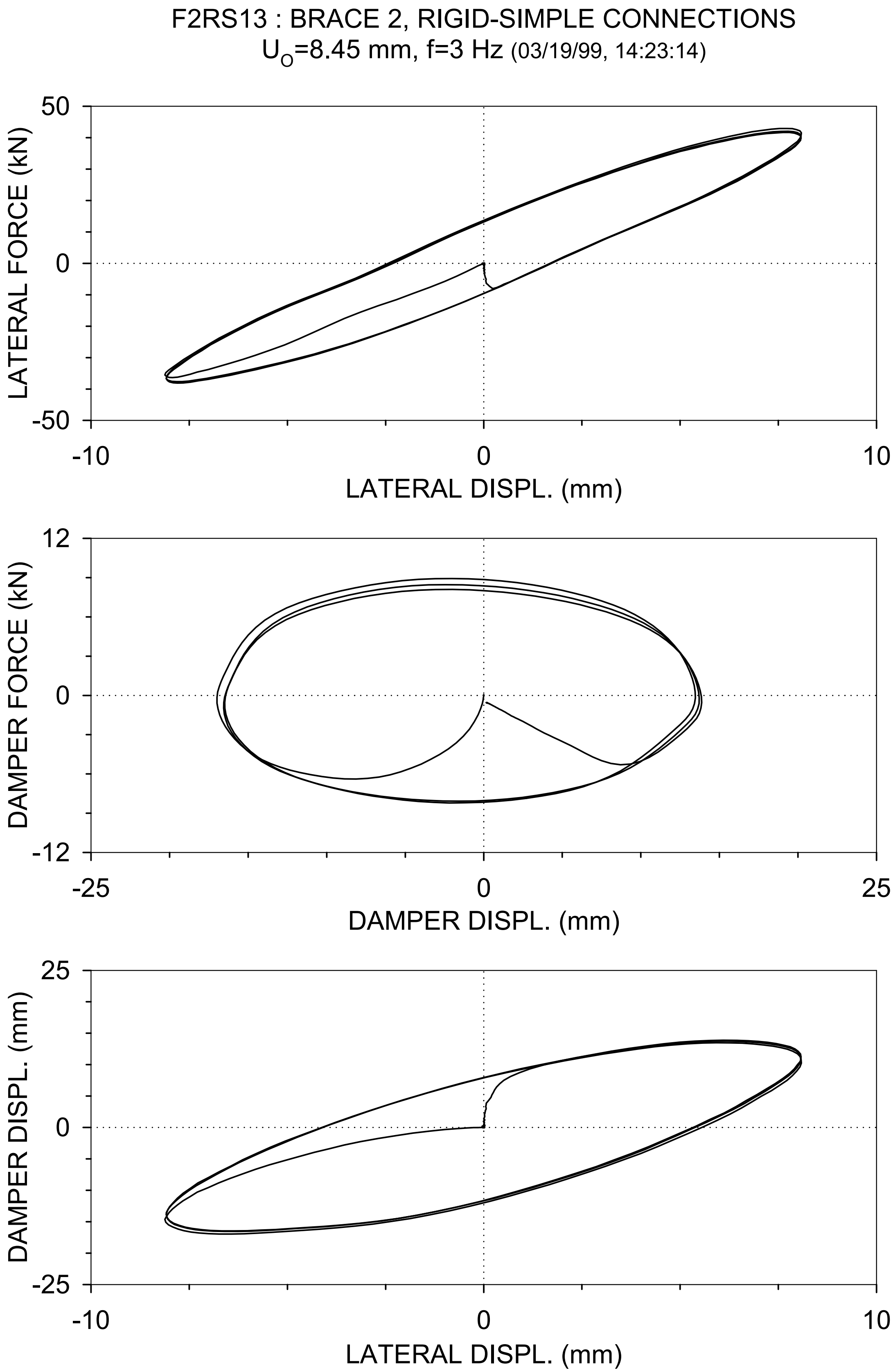
F2RS13 : BRACE 2, RIGID-SIMPLE CONNECTIONS
U_O=8.45 mm, f=3 Hz (03/19/99, 14:23:14)
LATERAL FORCE (kN)
50
0
-50
-10
0
10
LATERAL DISPL. (mm)
DAMPER FORCE (kN)
12
0
-12
-25
0
25
DAMPER DISPL. (mm)
DAMPER DISPL. (mm)
25
0
-25
-10
0
10
LATERAL DISPL. (mm)

F2RS14 : BRACE 2, RIGID-SIMPLE CONNECTIONS
U_O=8.45 mm, f=4 Hz (03/19/99, 14:24:43)

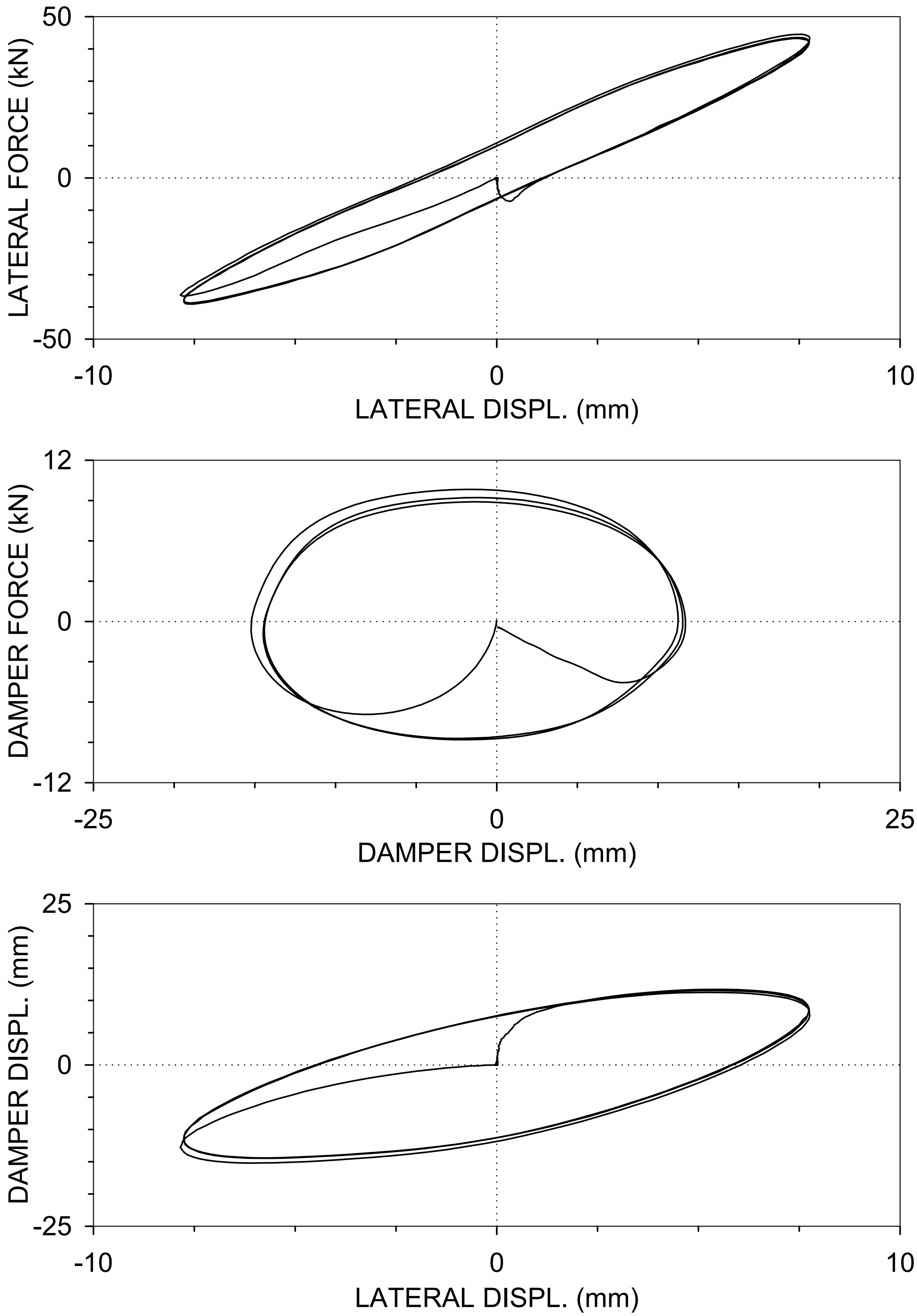

F2RR08 : BRACE 2, RIGID-RIGID CONNECTIONS

U_O=8.45 mm, f=0.01 Hz (03/26/99, 14:34:34)

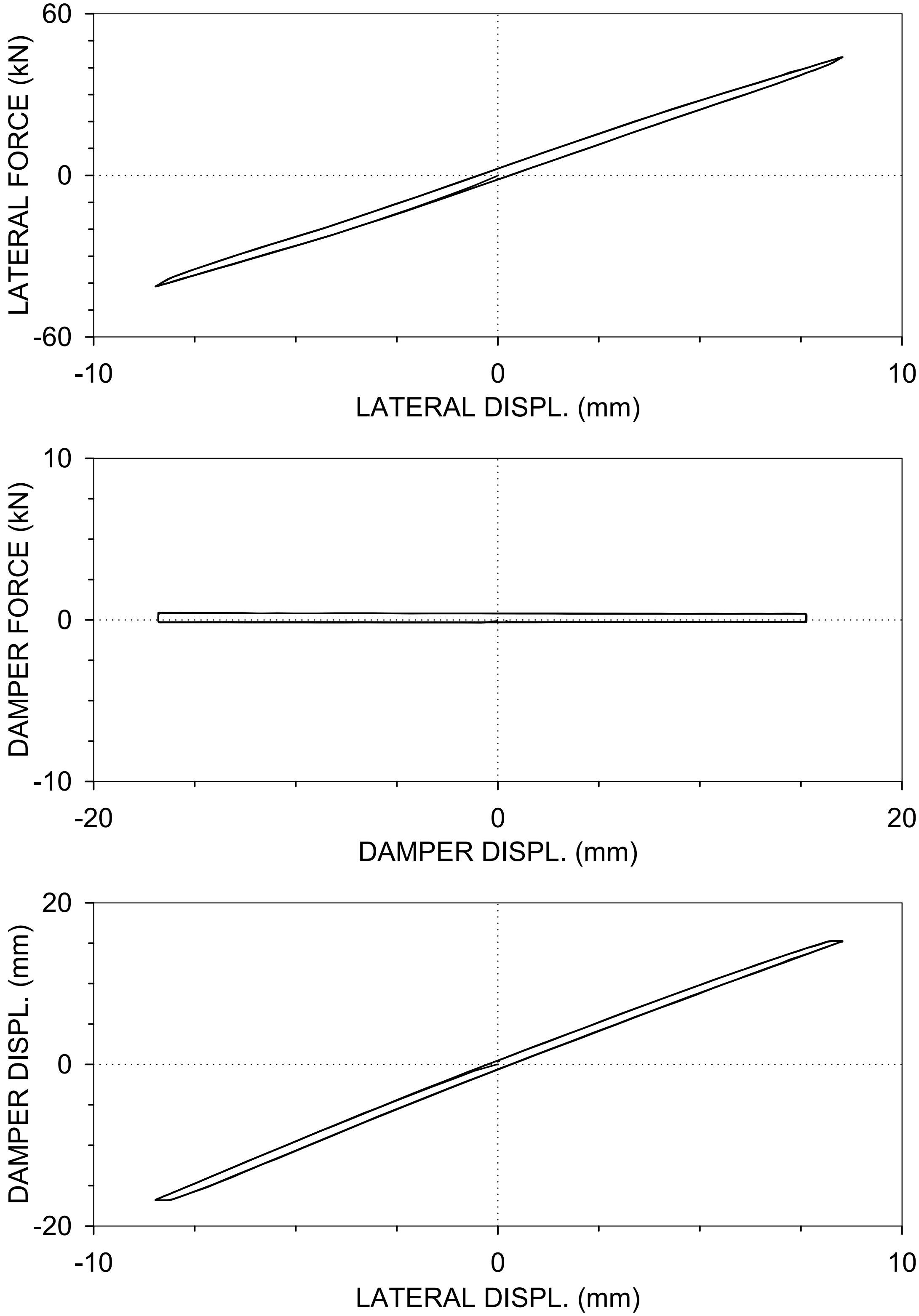

F2RR11 : BRACE 2, RIGID-RIGID CONNECTIONS
U_O=8.45 mm, f=1 Hz (03/26/99, 14:43:03)

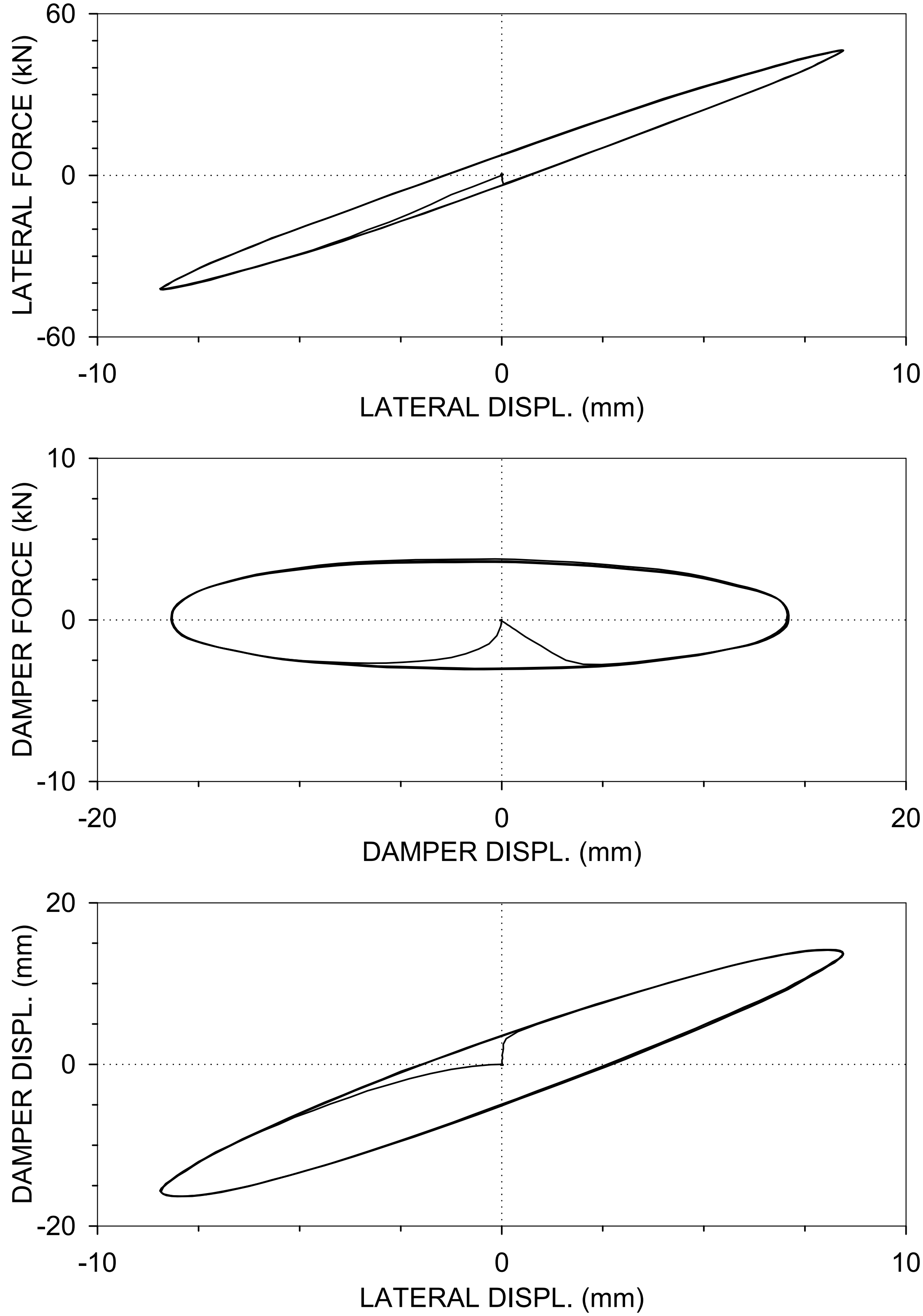

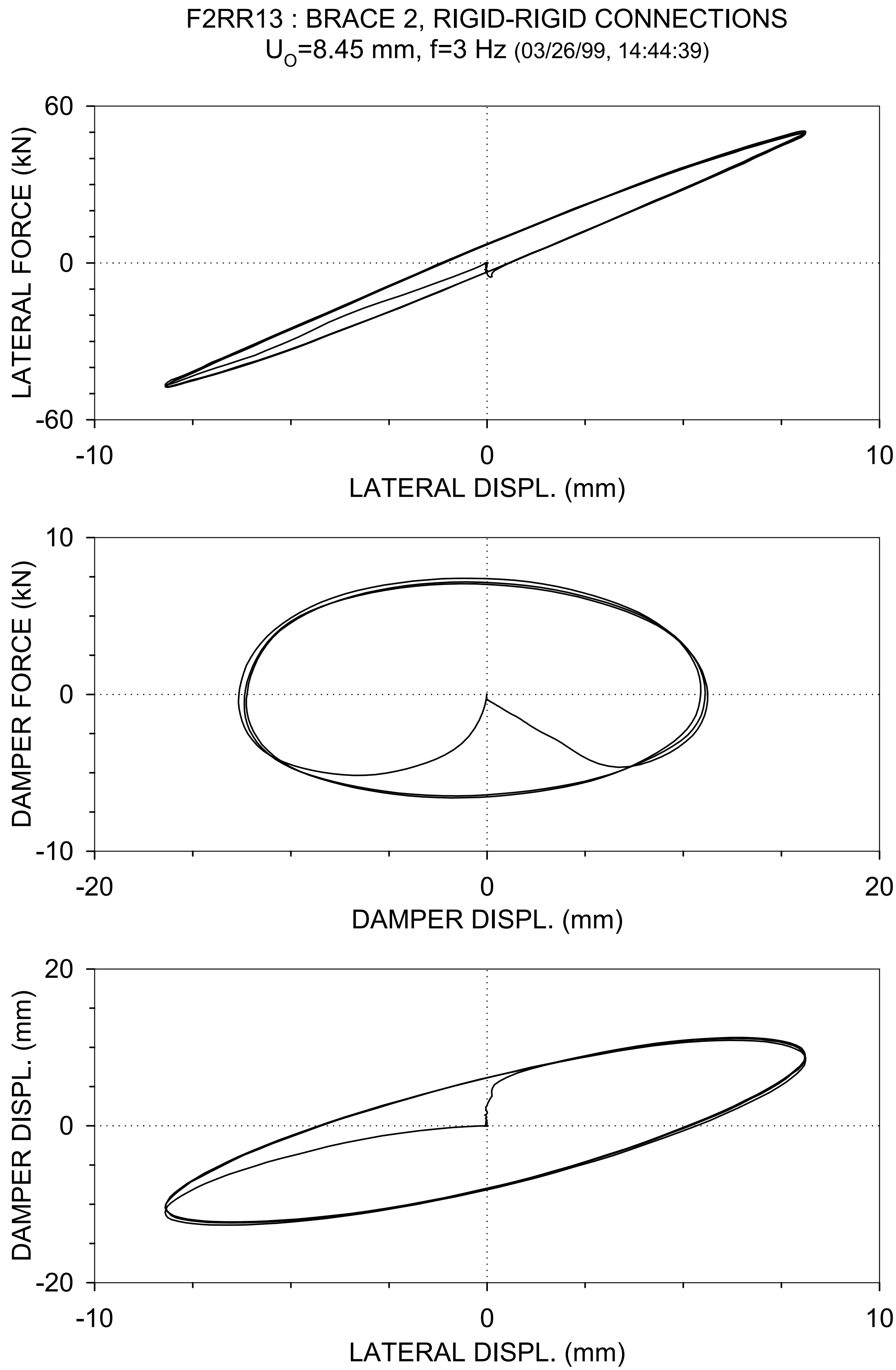
F2RR13 : BRACE 2, RIGID-RIGID CONNECTIONS
U$_O$=8.45 mm, f=3 Hz (03/26/99, 14:44:39)
60
0
-60
LATERAL FORCE (kN)
-10
0
10
LATERAL DISPL. (mm)
10
0
-10
DAMPER FORCE (kN)
-20
0
20
DAMPER DISPL. (mm)
20
0
-20
DAMPER DISPL. (mm)
-10
0
10
LATERAL DISPL. (mm)

F2RR14 : BRACE 2, RIGID-RIGID CONNECTIONS
U_O=8.45 mm, f=4 Hz (03/26/99, 14:46:47)

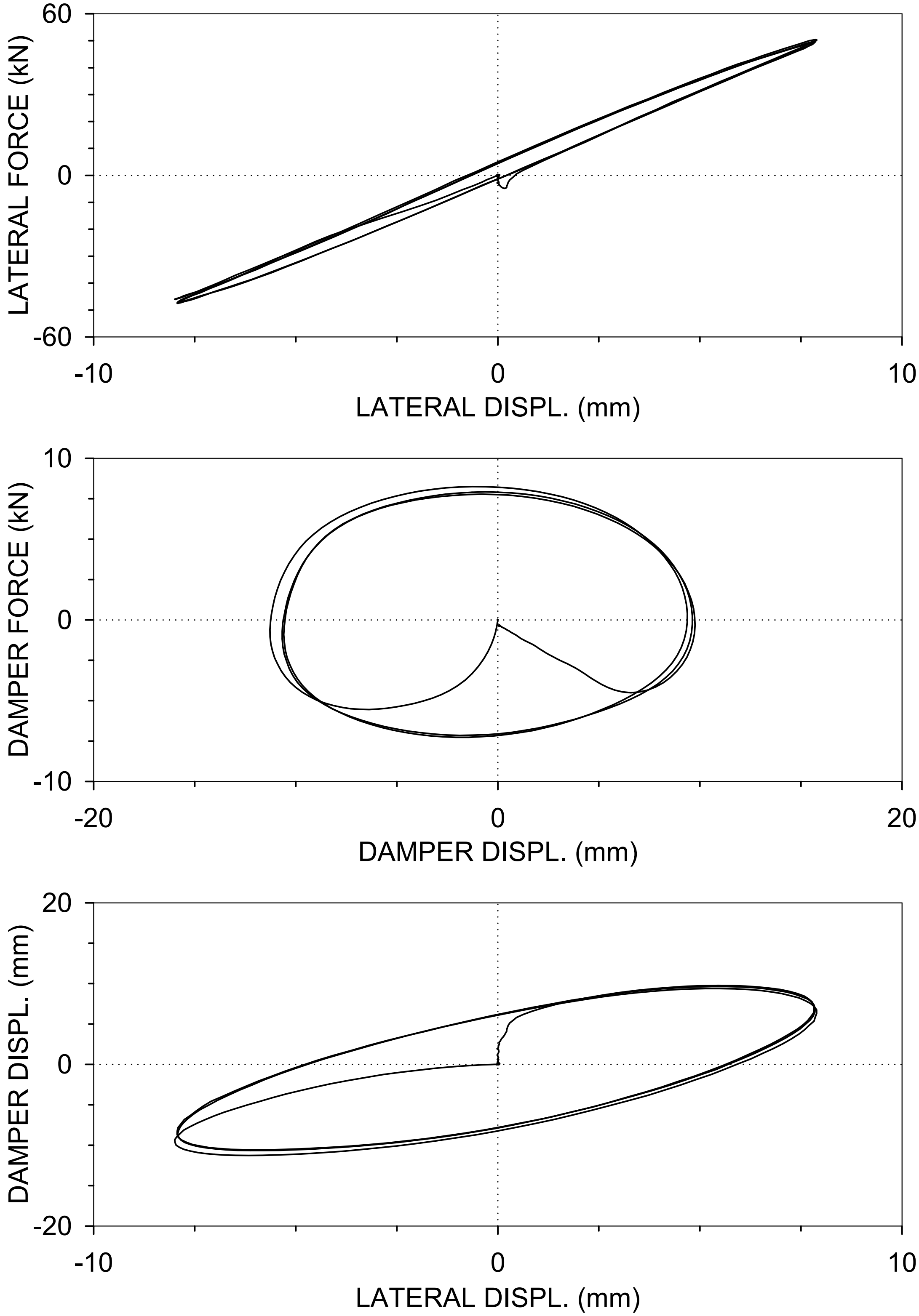

F1RS01 : BRACE 1, RIGID-SIMPLE CONNECTIONS

U_O=6.35 mm, f=0.01 Hz (04/05/99, 13:48:00)

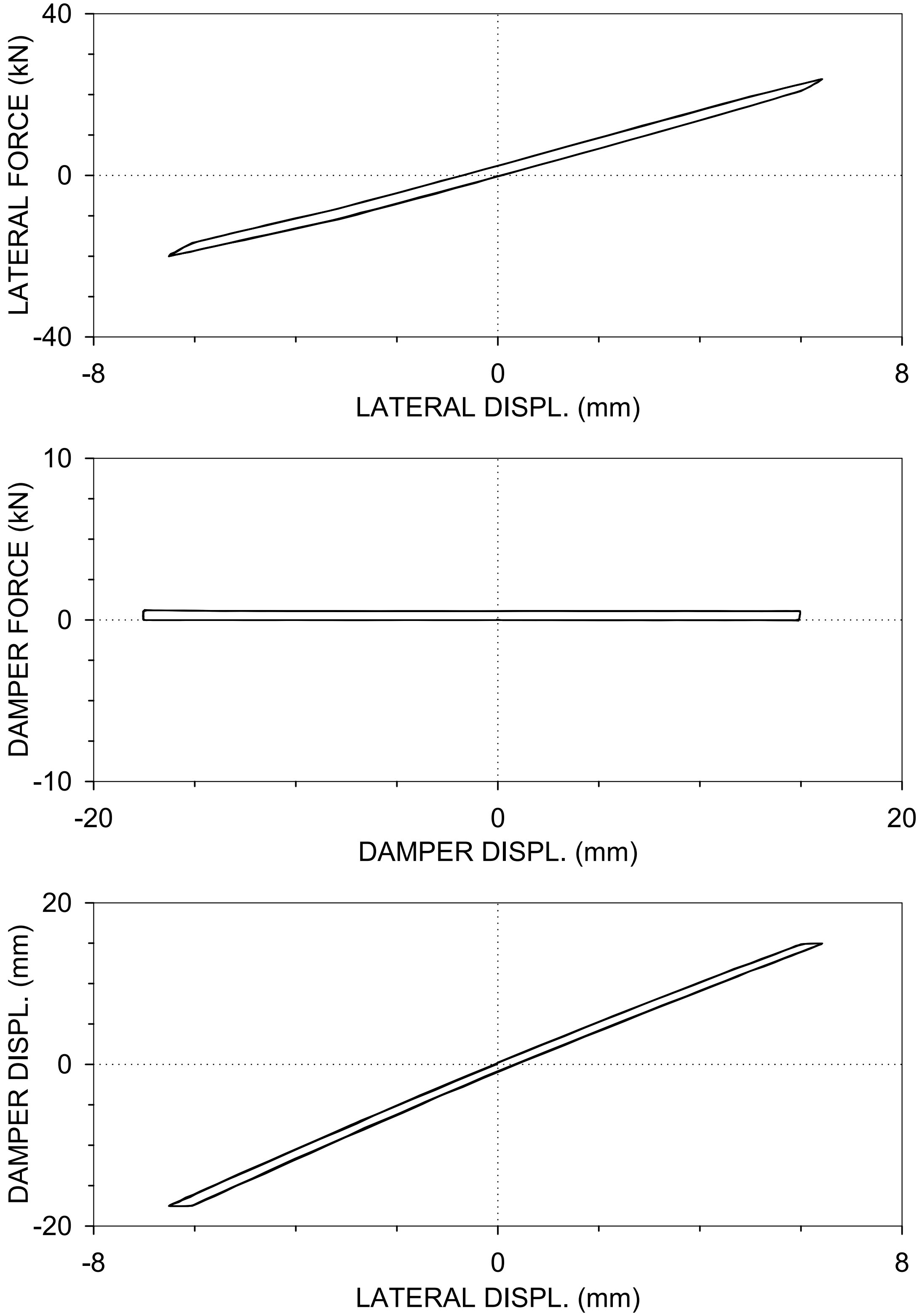

F1RS04 : BRACE 1, RIGID-SIMPLE CONNECTIONS
U_O=6.35 mm, f=1 Hz (04/05/99, 13:56:13)

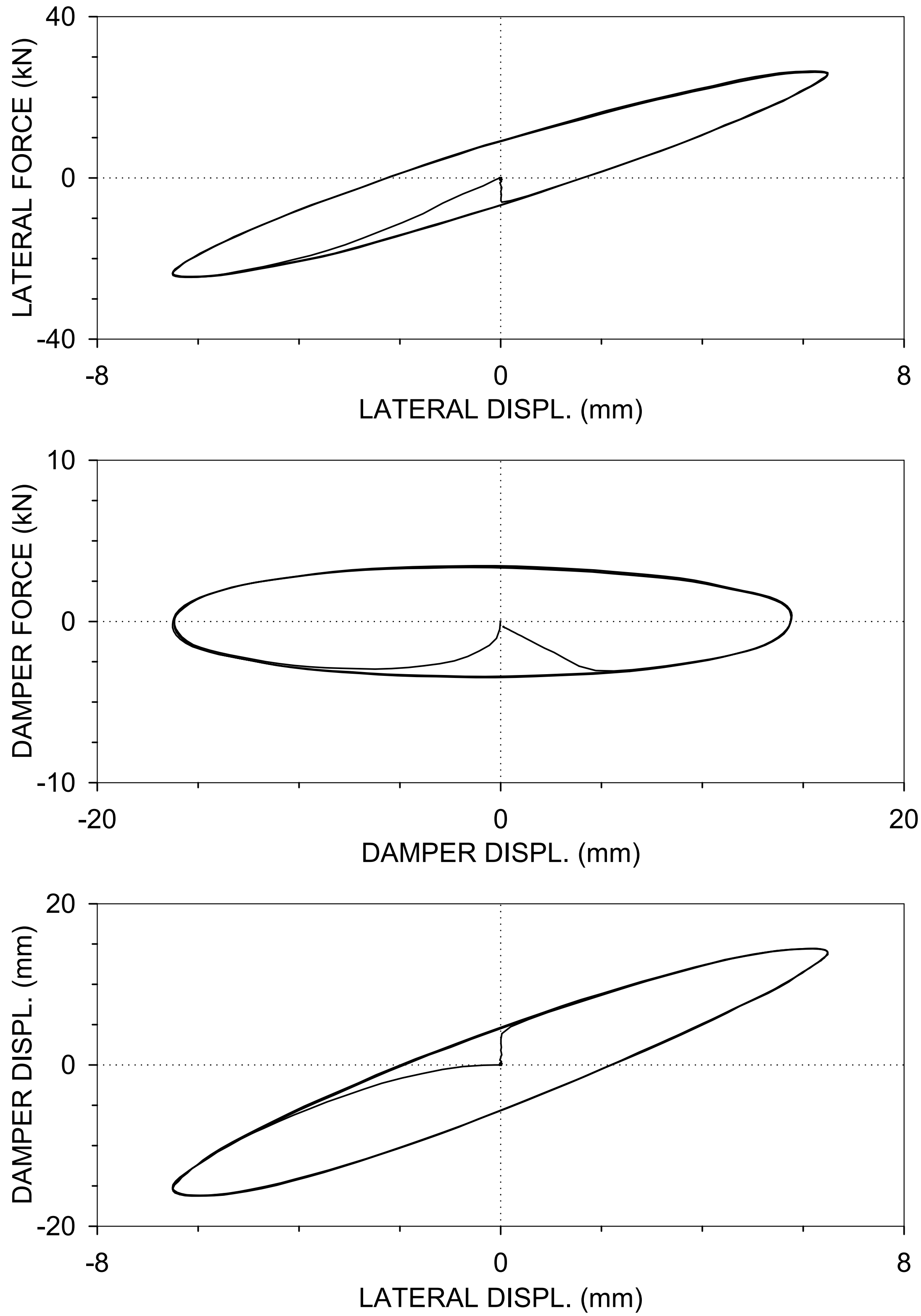

F1RS06 : BRACE 1, RIGID-SIMPLE CONNECTIONS
U_O=6.35 mm, f=3 Hz (04/05/99, 14:01:38)

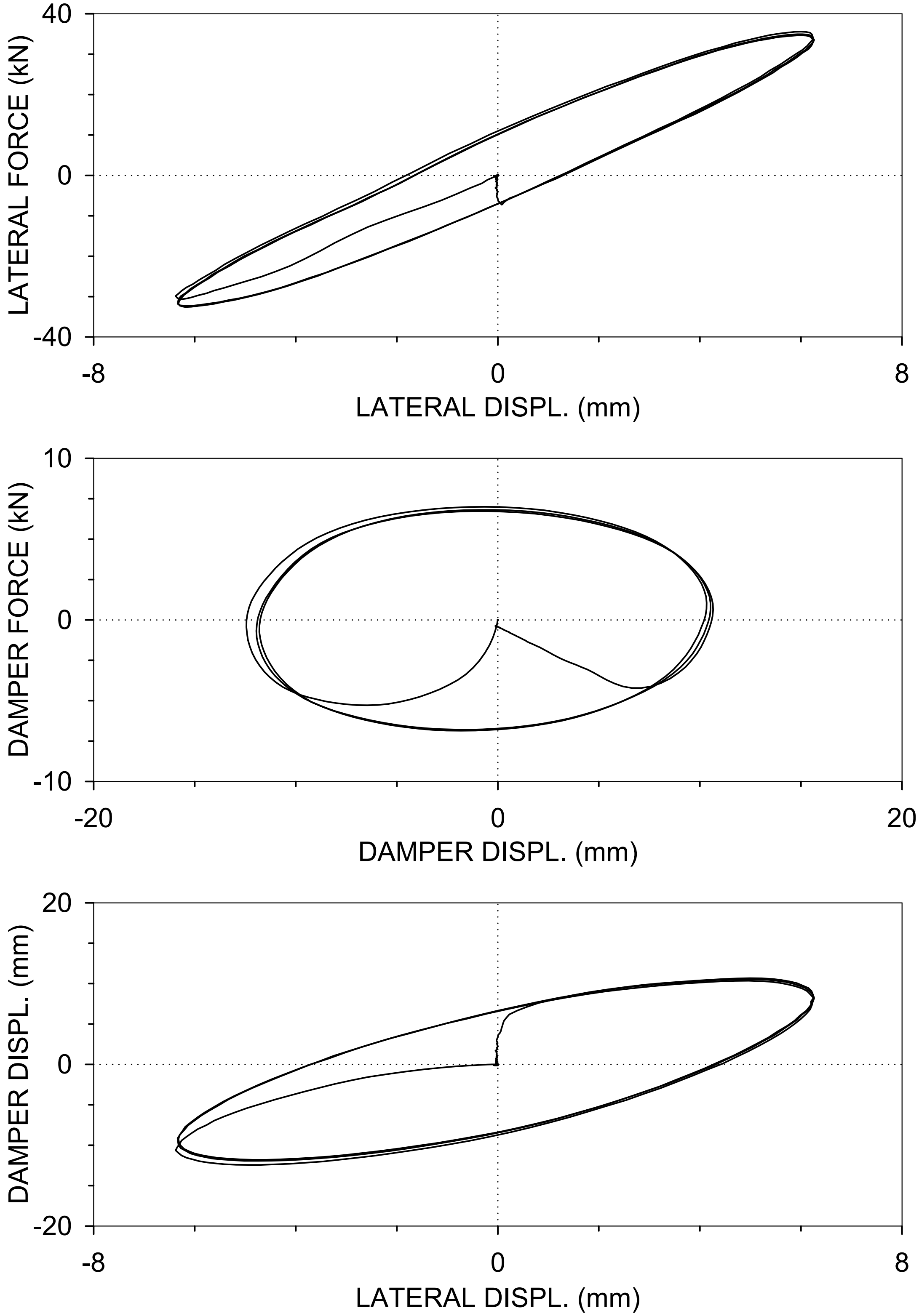

F1RS07 : BRACE 1, RIGID-SIMPLE CONNECTIONS

U_O=6.35 mm, f=4 Hz (04/05/99, 14:04:30)

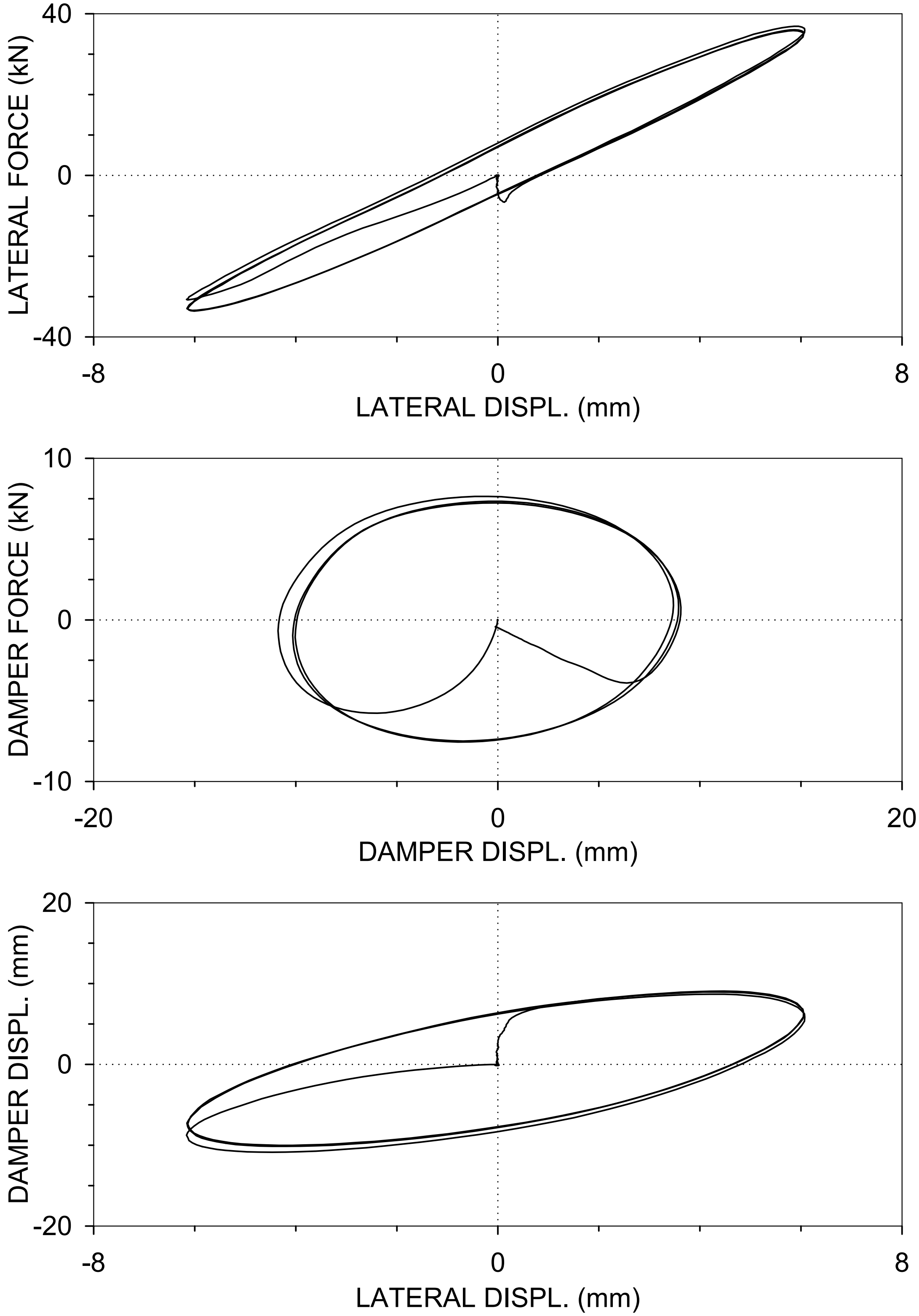

F1RSMAX : BRACE 1, RIGID-SIMPLE CONNECTIONS
U_O=9.7 mm, manual movement (04/05/99, 14:10:39)

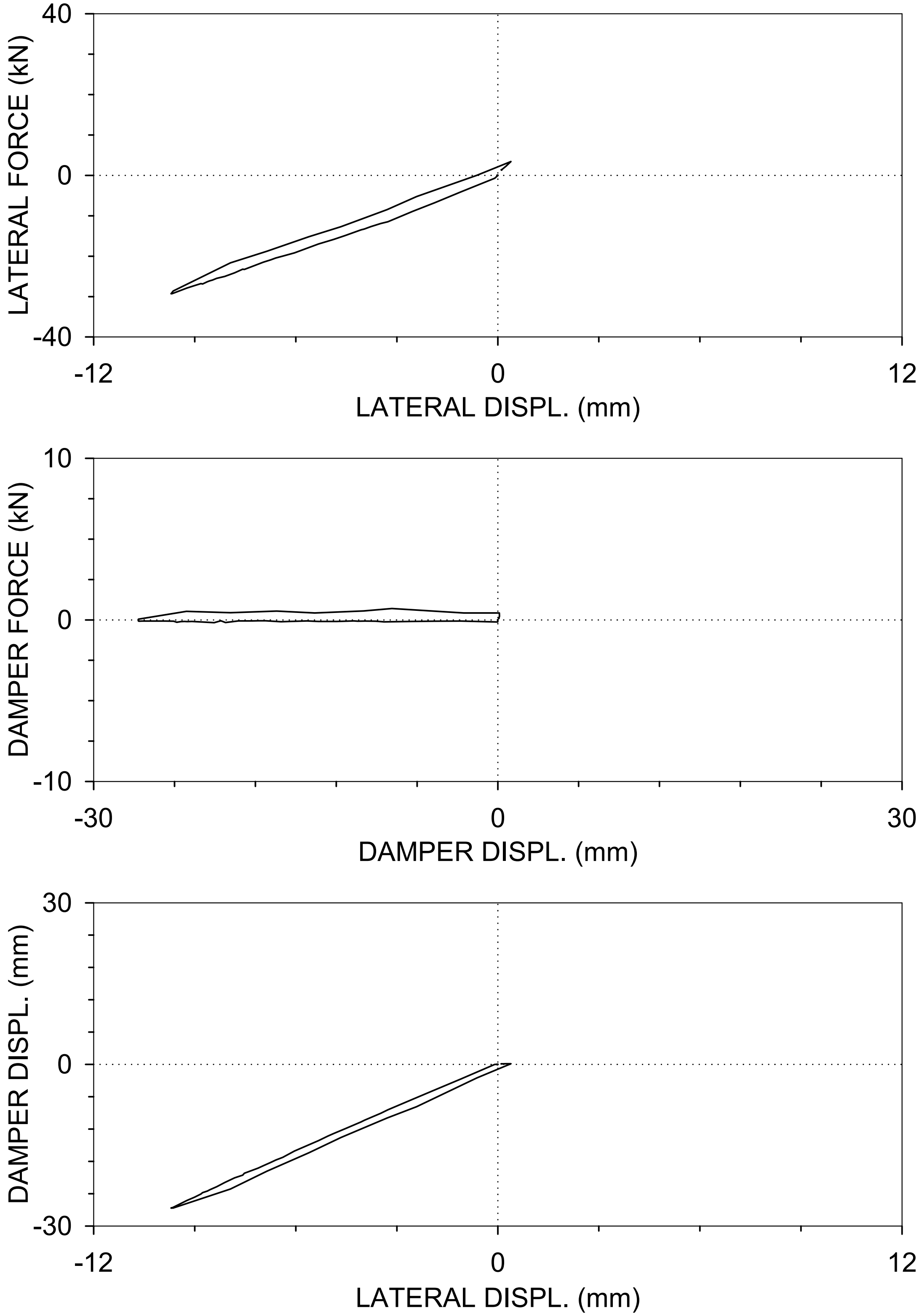

F2RSMAX : BRACE 2, RIGID-SIMPLE CONNECTIONS
U_O=10.1 mm, manual movement (04/06/99, 14:05:57)

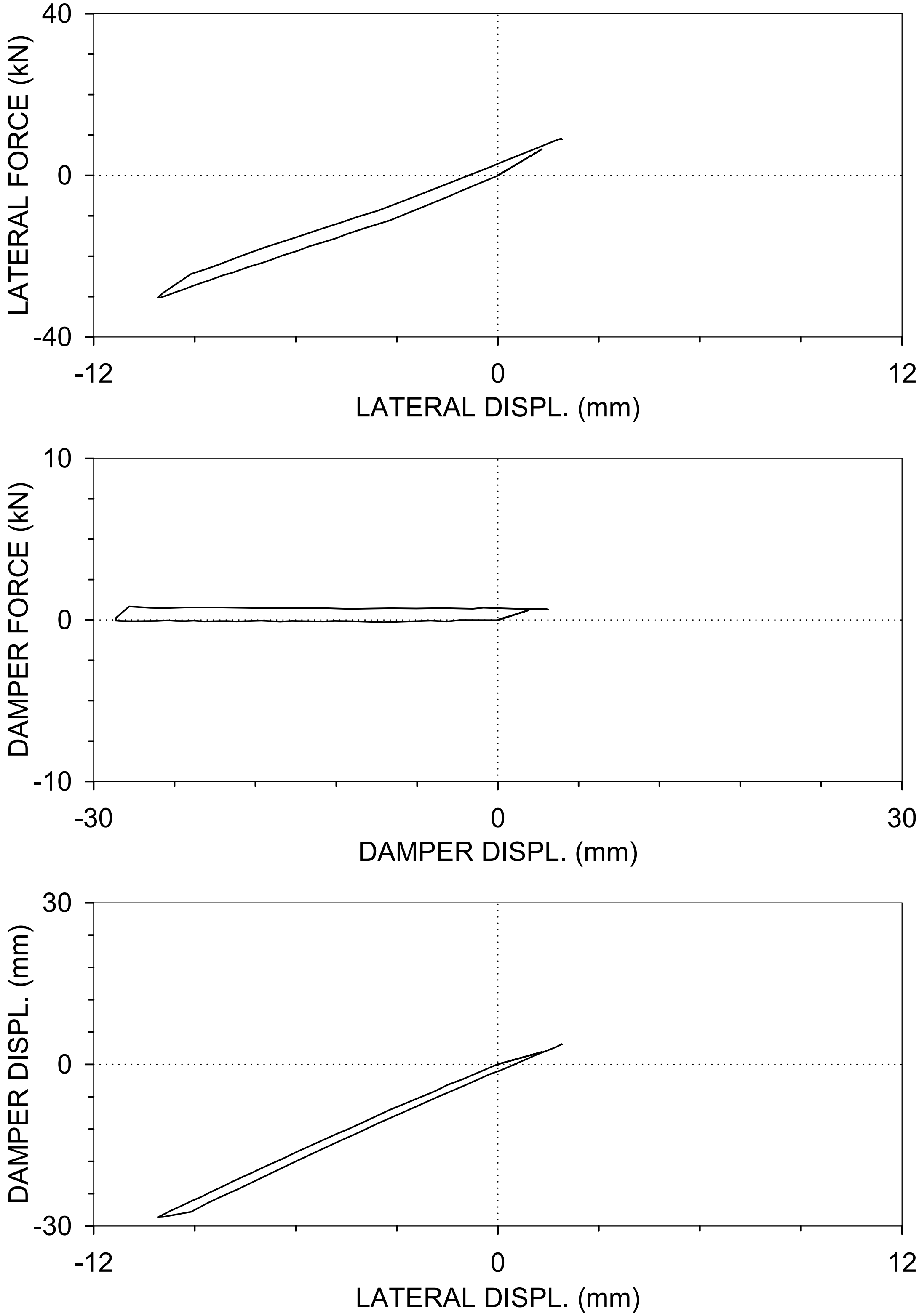

APPENDIX C

RESULTS OF EARTHQUAKE-SIMULATOR TESTING

(ALL TESTS PERFORMED WITH RIGID-SIMPLE BEAM-TO-COLUMN CONNECTIONS)

ELRSBD025 : EL CENTRO S00E 25% (05/06/99)

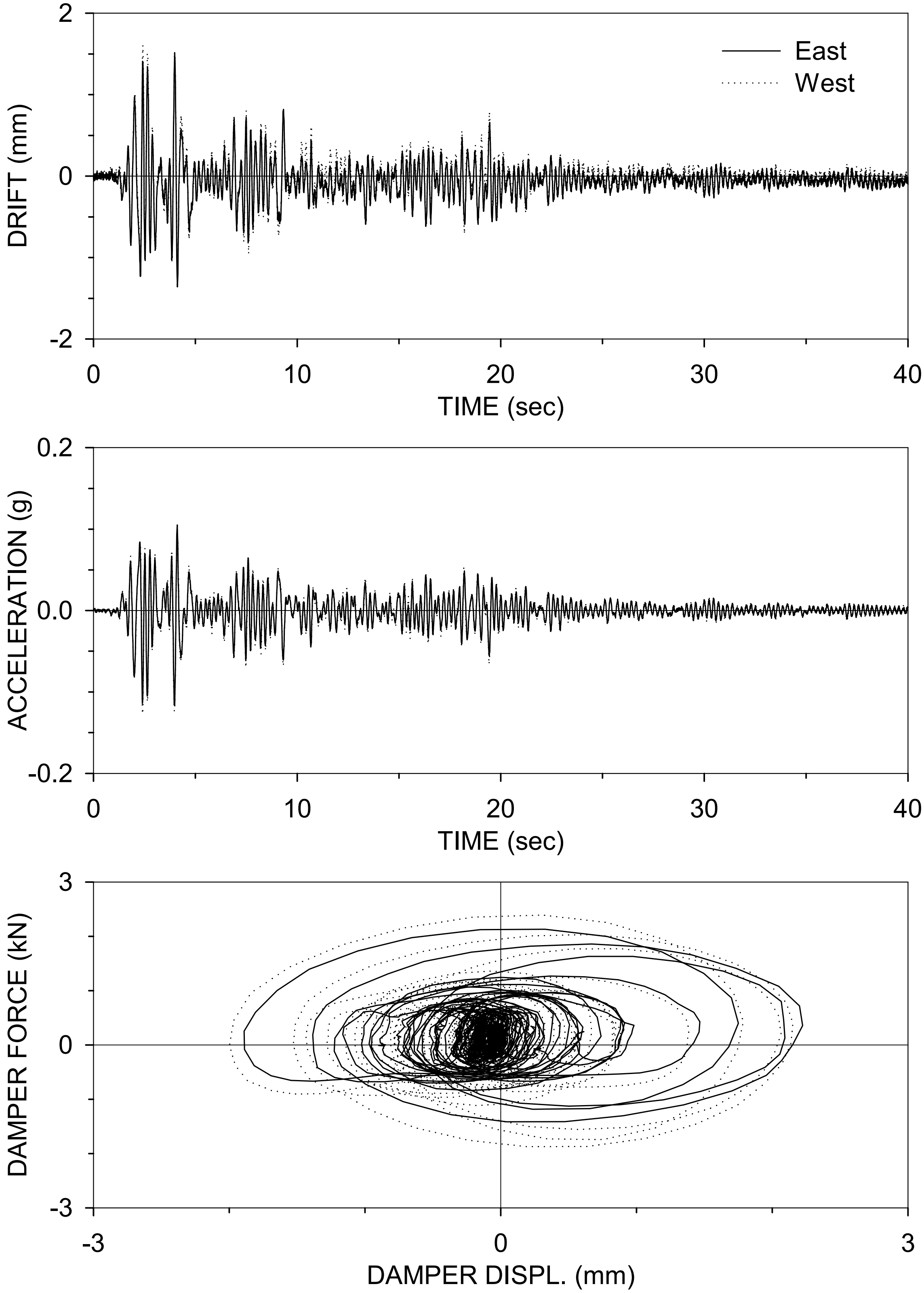

ELRSBD050 : EL CENTRO S00E 50% (05/06/99)

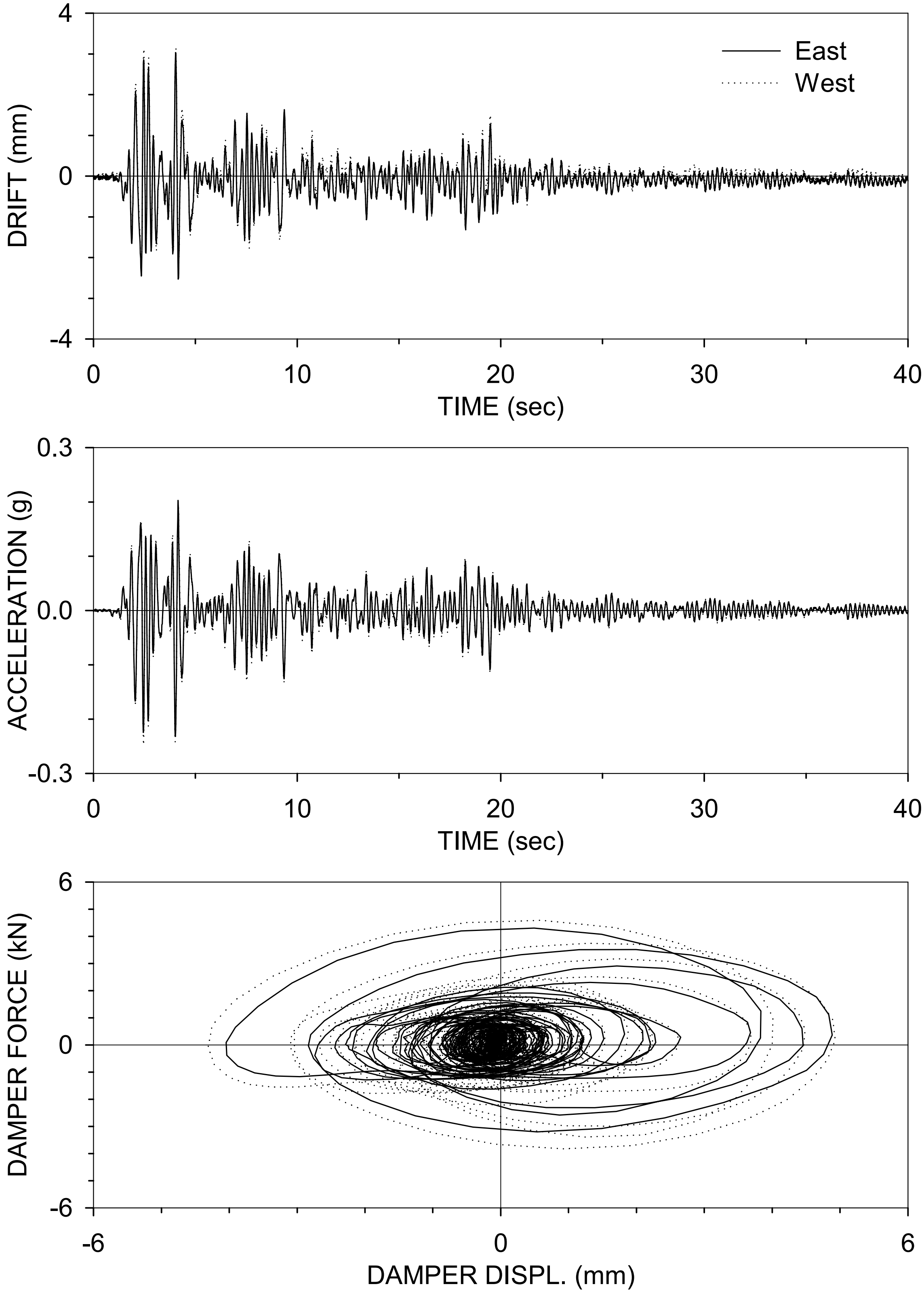

ELRSBD100 : EL CENTRO S00E 100% (05/06/99)

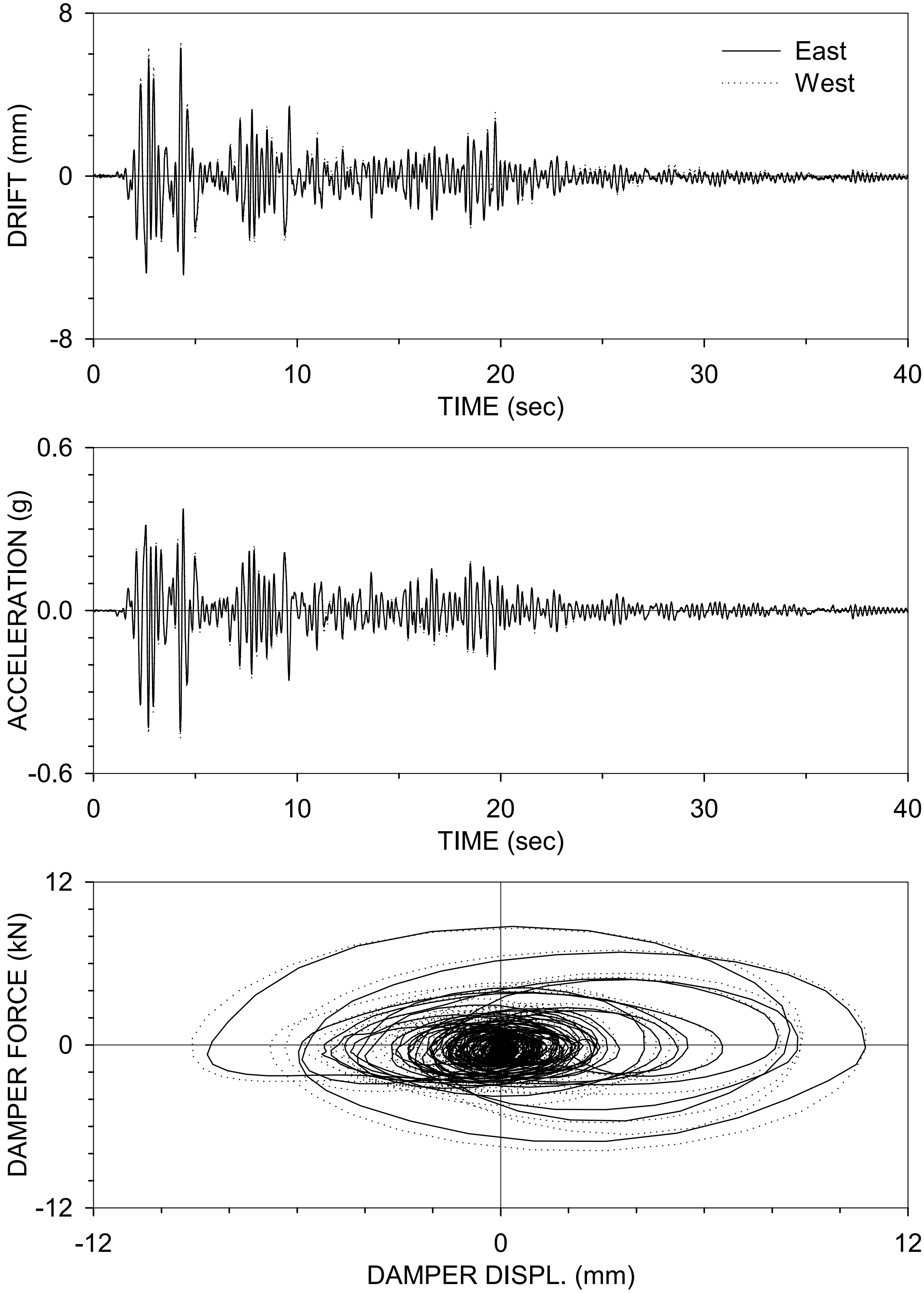

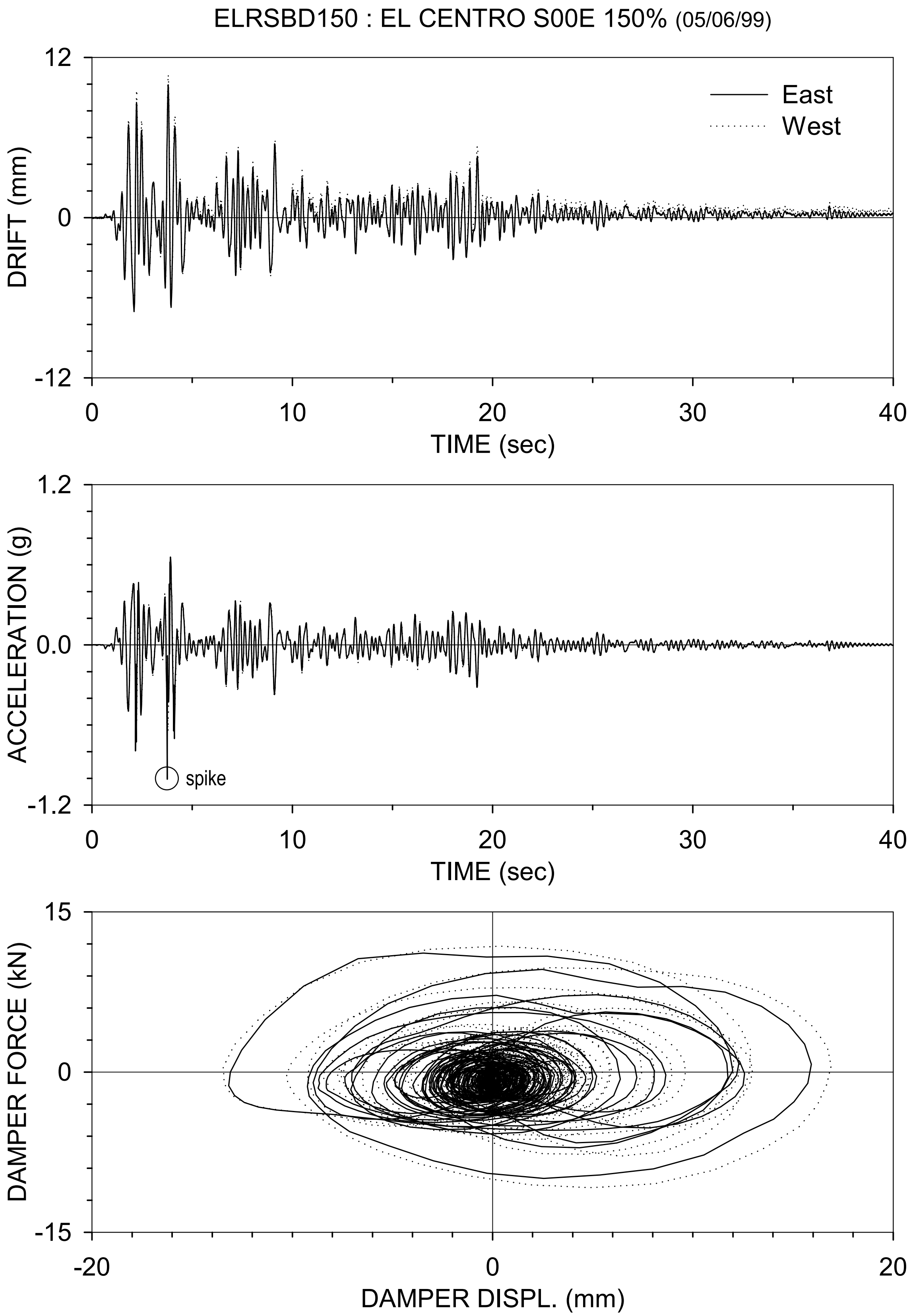
ELRSBD150 : EL CENTRO S00E 150% (05/06/99)
East
West
DRIFT (mm)
12
0
-12
TIME (sec)
0
10
20
30
40
ACCELERATION (g)
1.2
0.0
-1.2
spike
TIME (sec)
DAMPER FORCE (kN)
15
0
-15
DAMPER DISPL. (mm)
-20
0
20

ELRSBD150.2 : EL CENTRO S00E 150% (05/06/99)

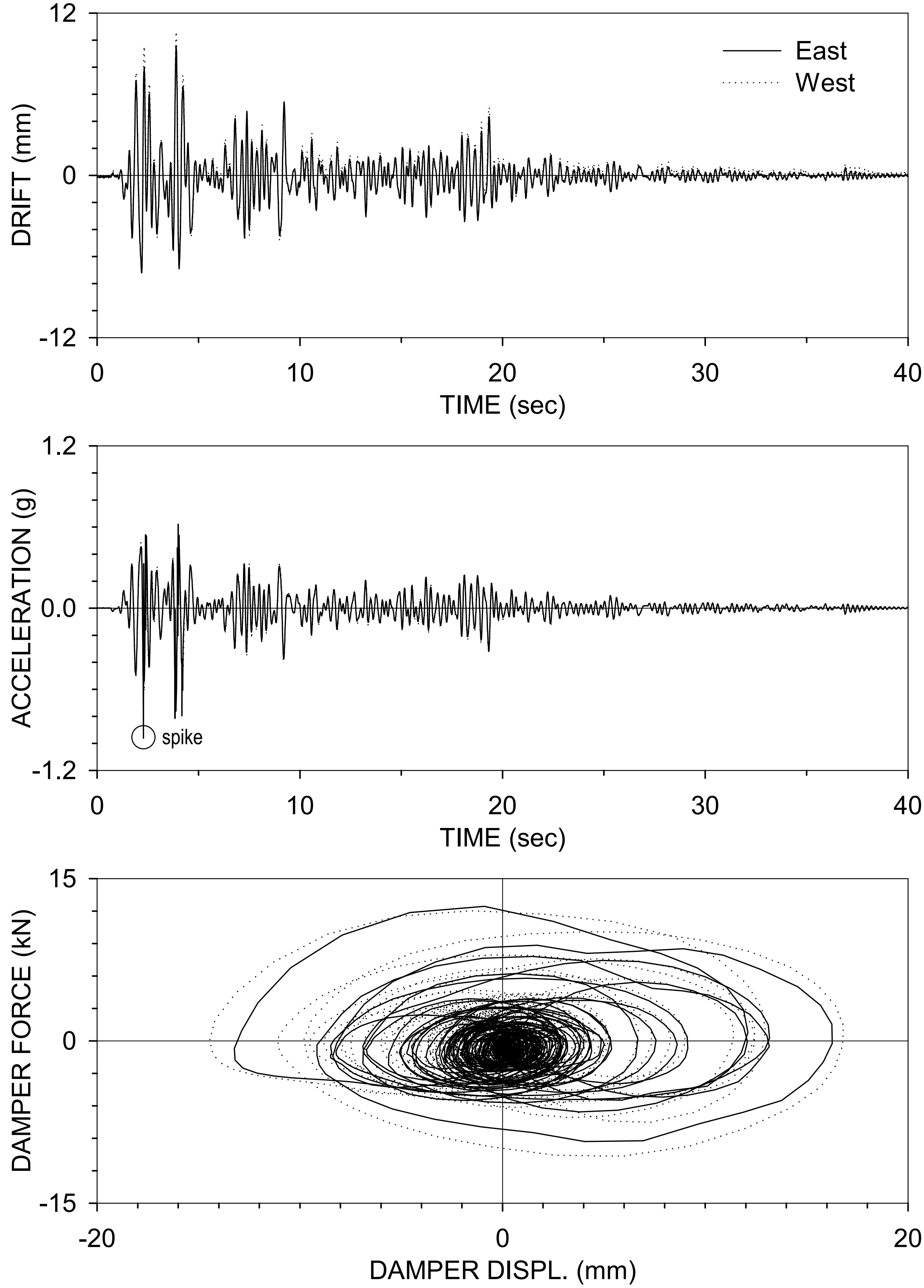

ELRSBD150.3 : EL CENTRO S00E 150% (05/07/99)

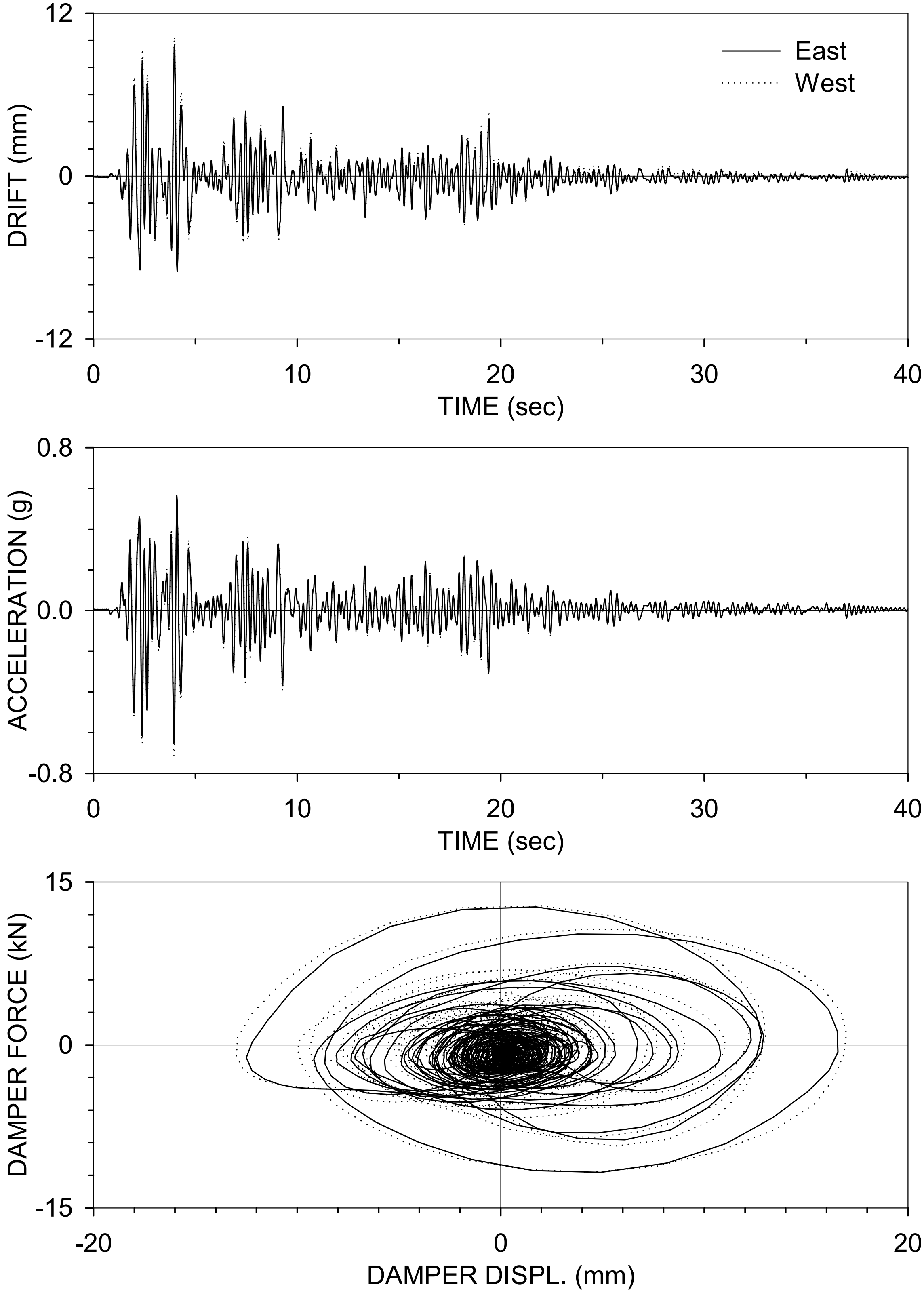

EVRSBD050 : EL CENTRO S00E H&V 50% (05/07/99)

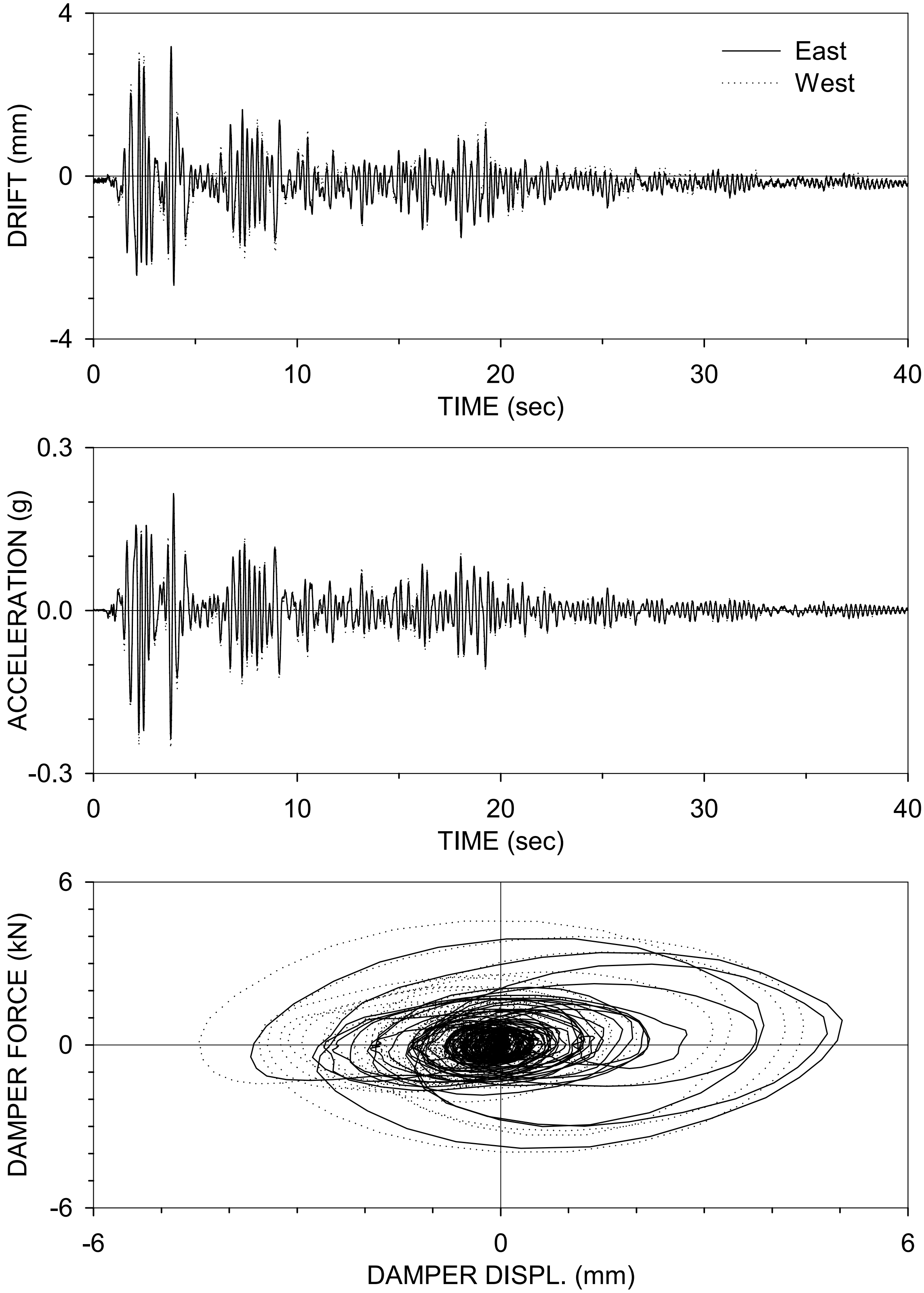

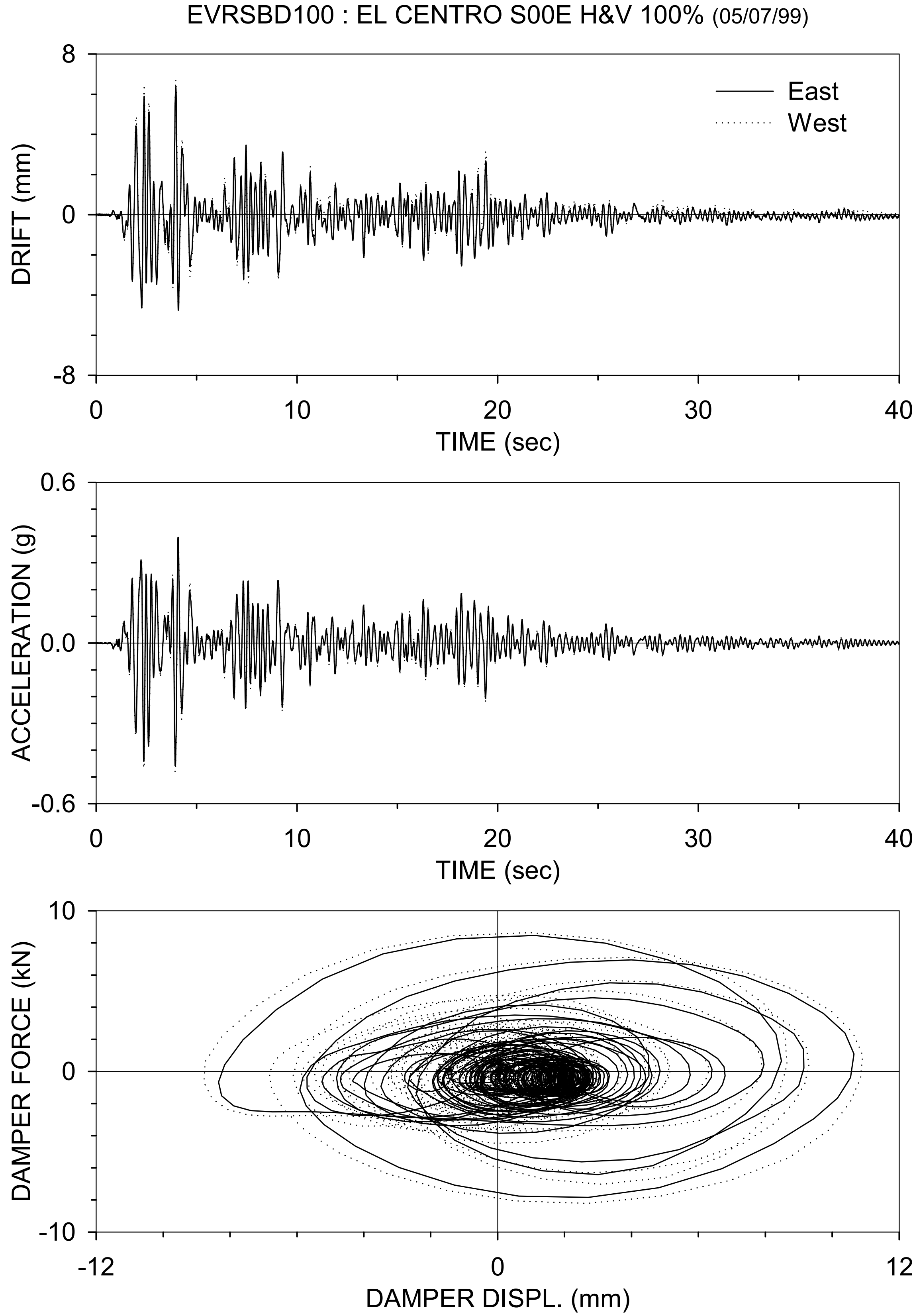
EVRSBD100 : EL CENTRO S00E H&V 100% (05/07/99)
East
West
DRIFT (mm)
8
0
-8
0
10
20
30
40
TIME (sec)
ACCELERATION (g)
0.6
0.0
-0.6
0
10
20
30
40
TIME (sec)
DAMPER FORCE (kN)
10
0
-10
-12
0
12
DAMPER DISPL. (mm)

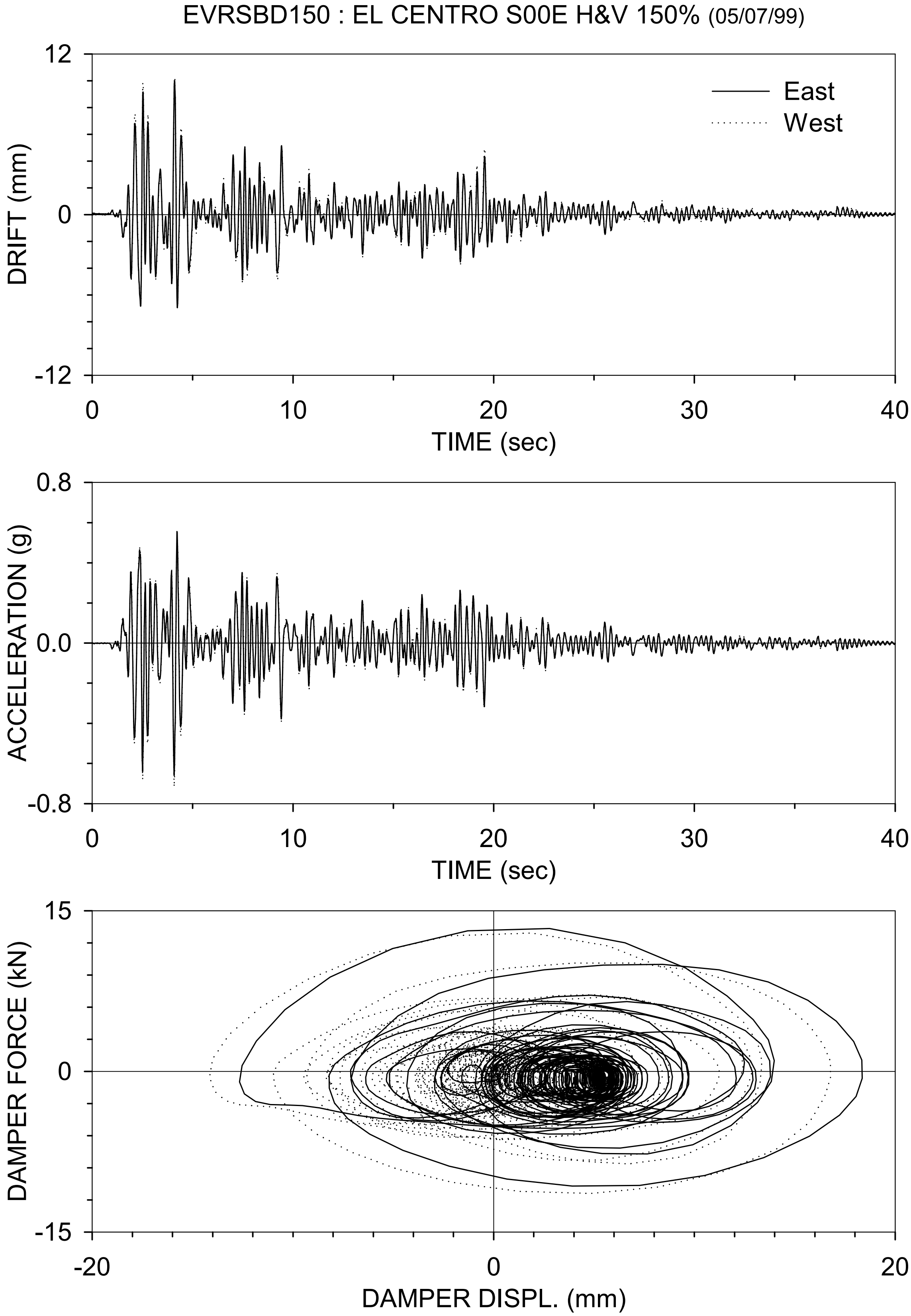
EVRSBD150 : EL CENTRO S00E H&V 150% (05/07/99)
East
West
DRIFT (mm)
12
0
-12
TIME (sec)
0
10
20
30
40
ACCELERATION (g)
0.8
0.0
-0.8
TIME (sec)
DAMPER FORCE (kN)
15
0
-15
-20
0
20
DAMPER DISPL. (mm)

TARSBD075 : TAFT N21E 75% (05/10/99)

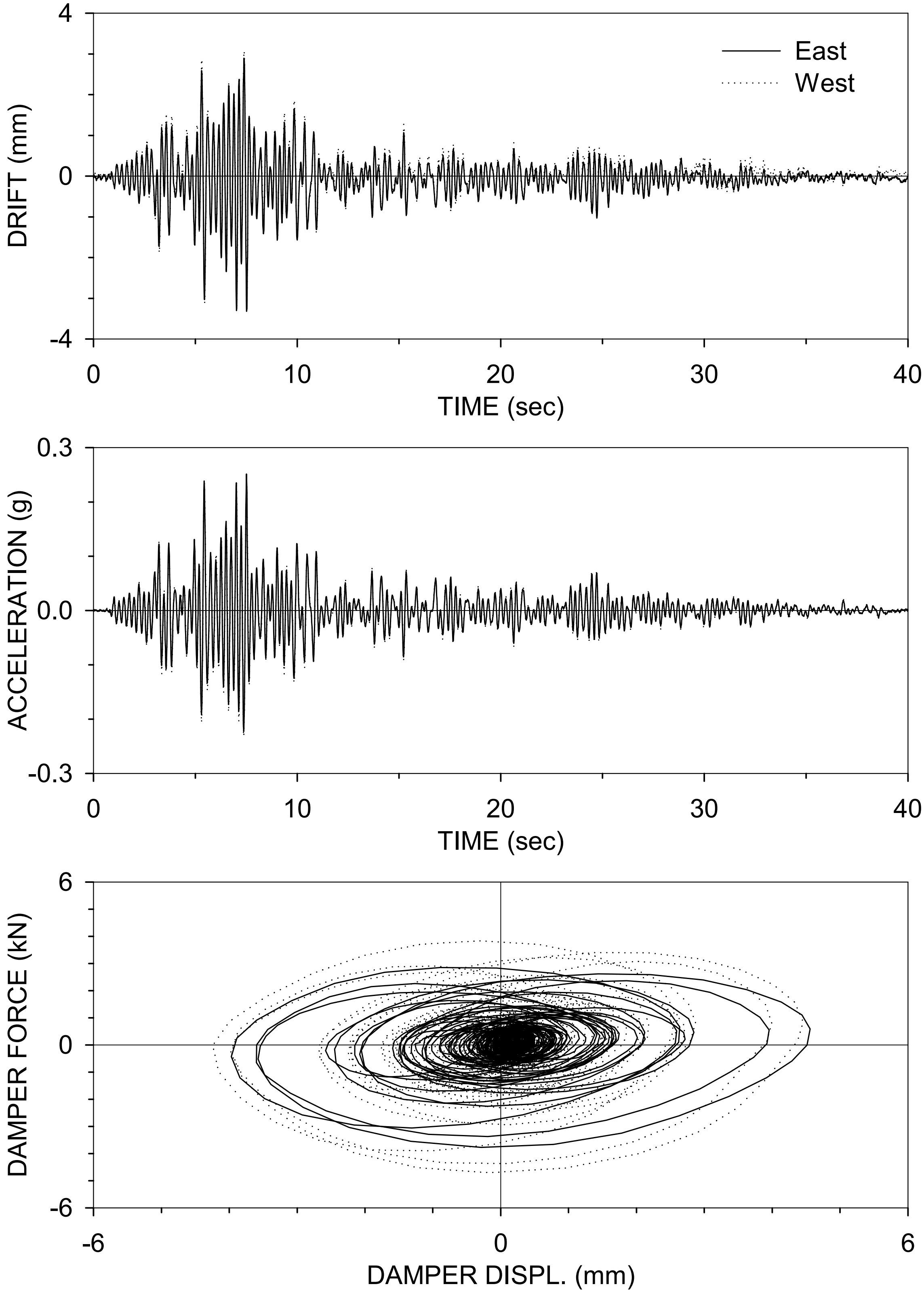

TARSBD100 : TAFT N21E 100% (05/10/99)

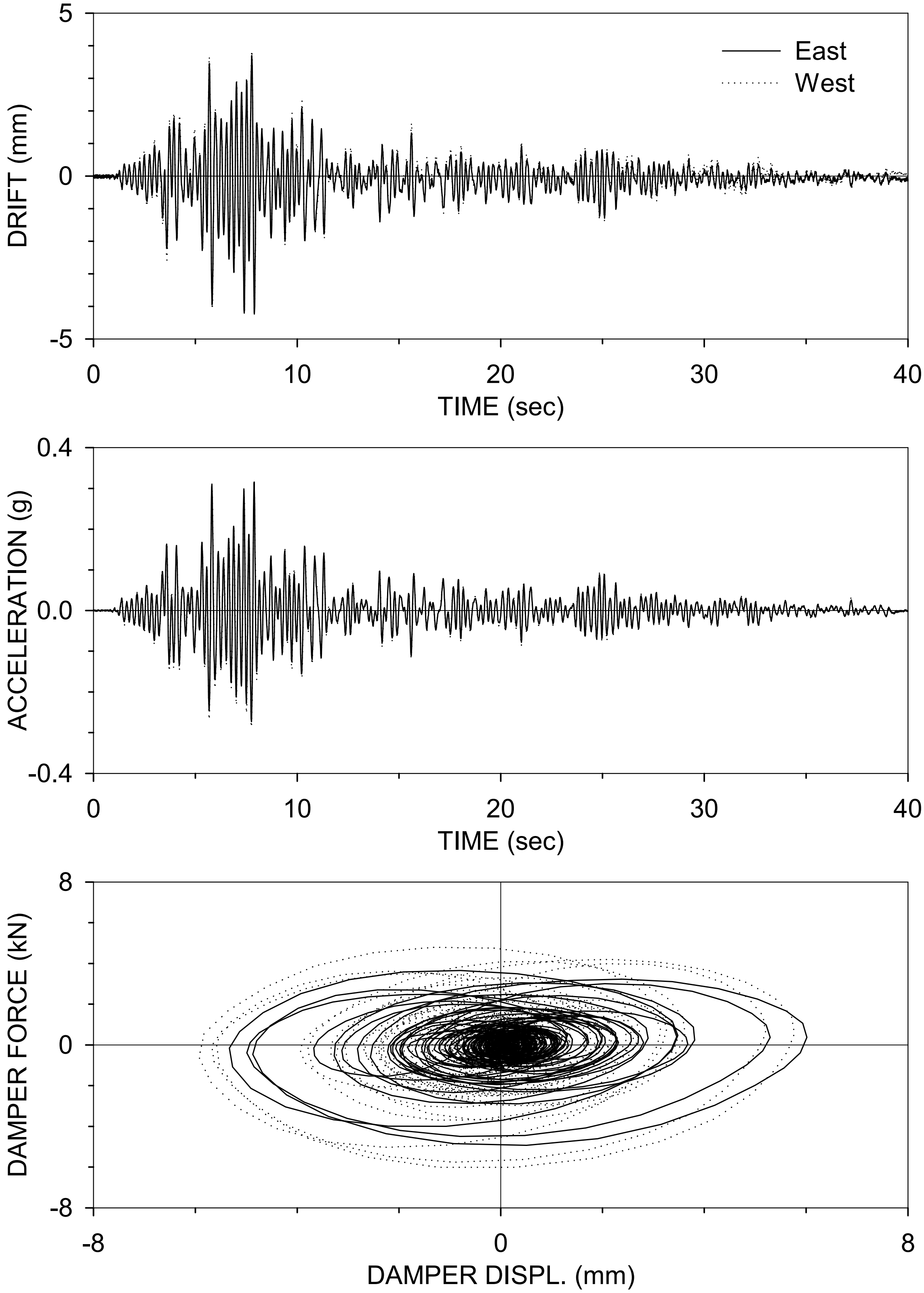

TARSBD200 : TAFT N21E 200% (05/10/99)

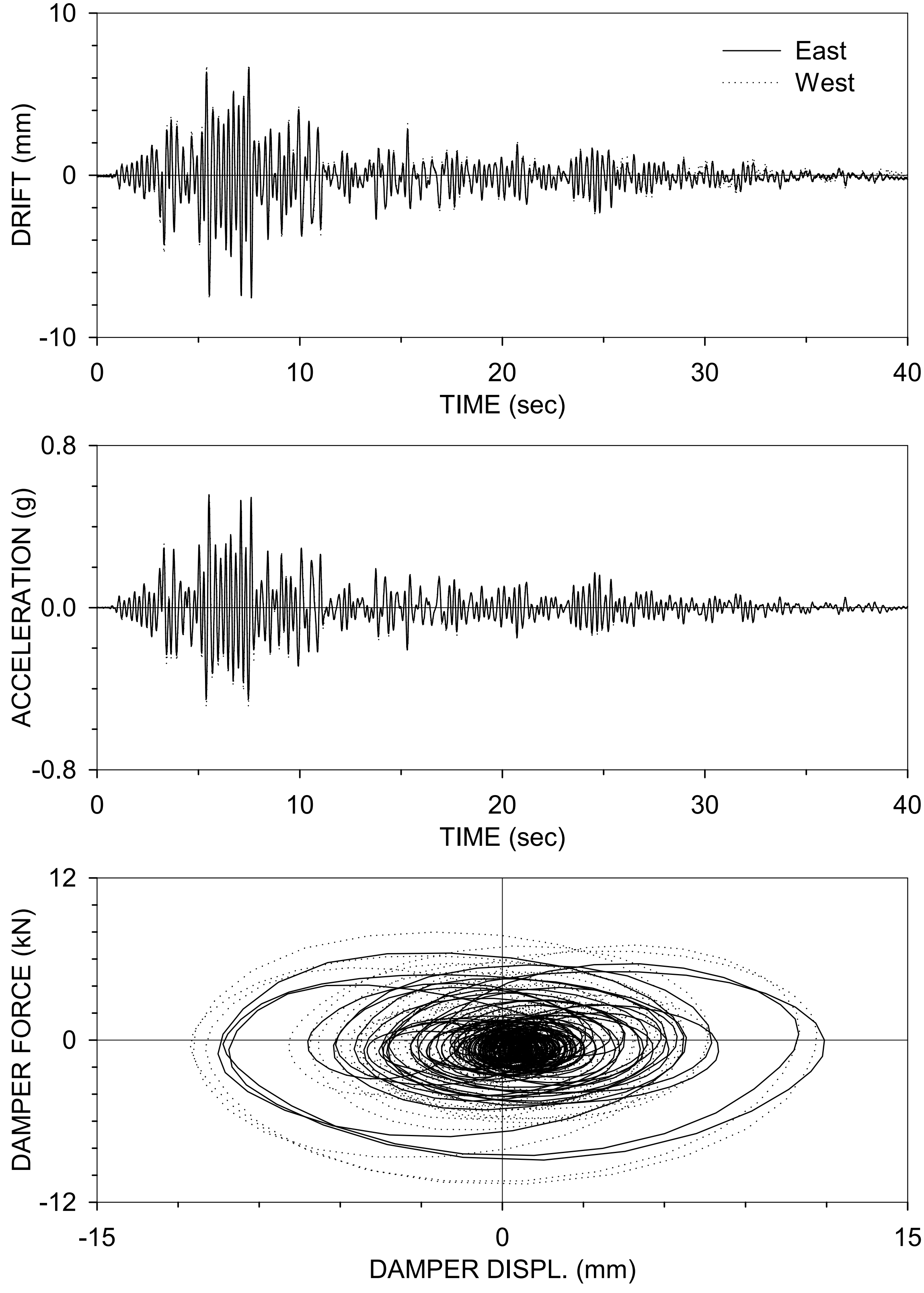

TARSBD300 : TAFT N21E 300% (05/10/99)

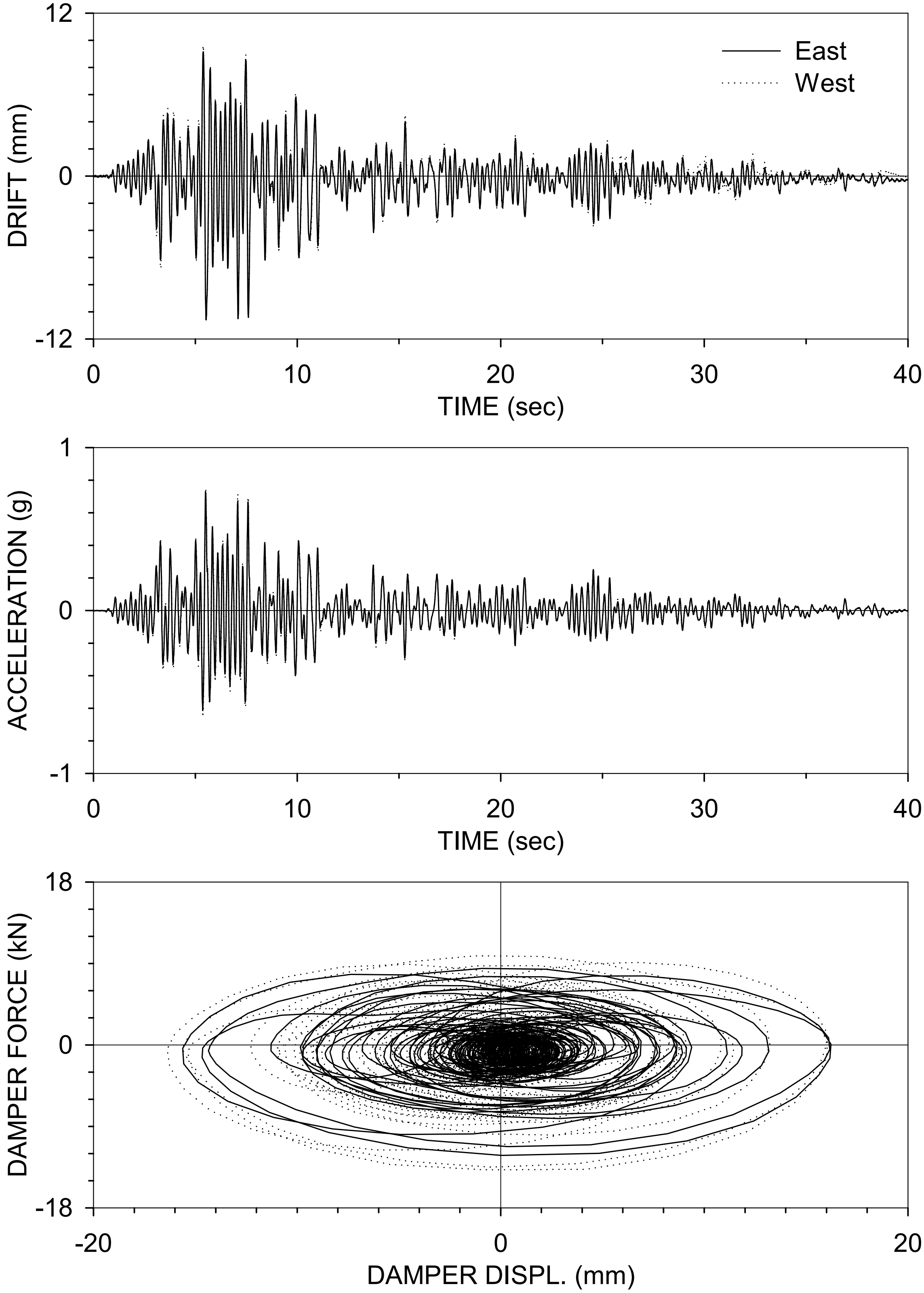

TARSBD300.2 : TAFT N21E 300% (05/10/99)

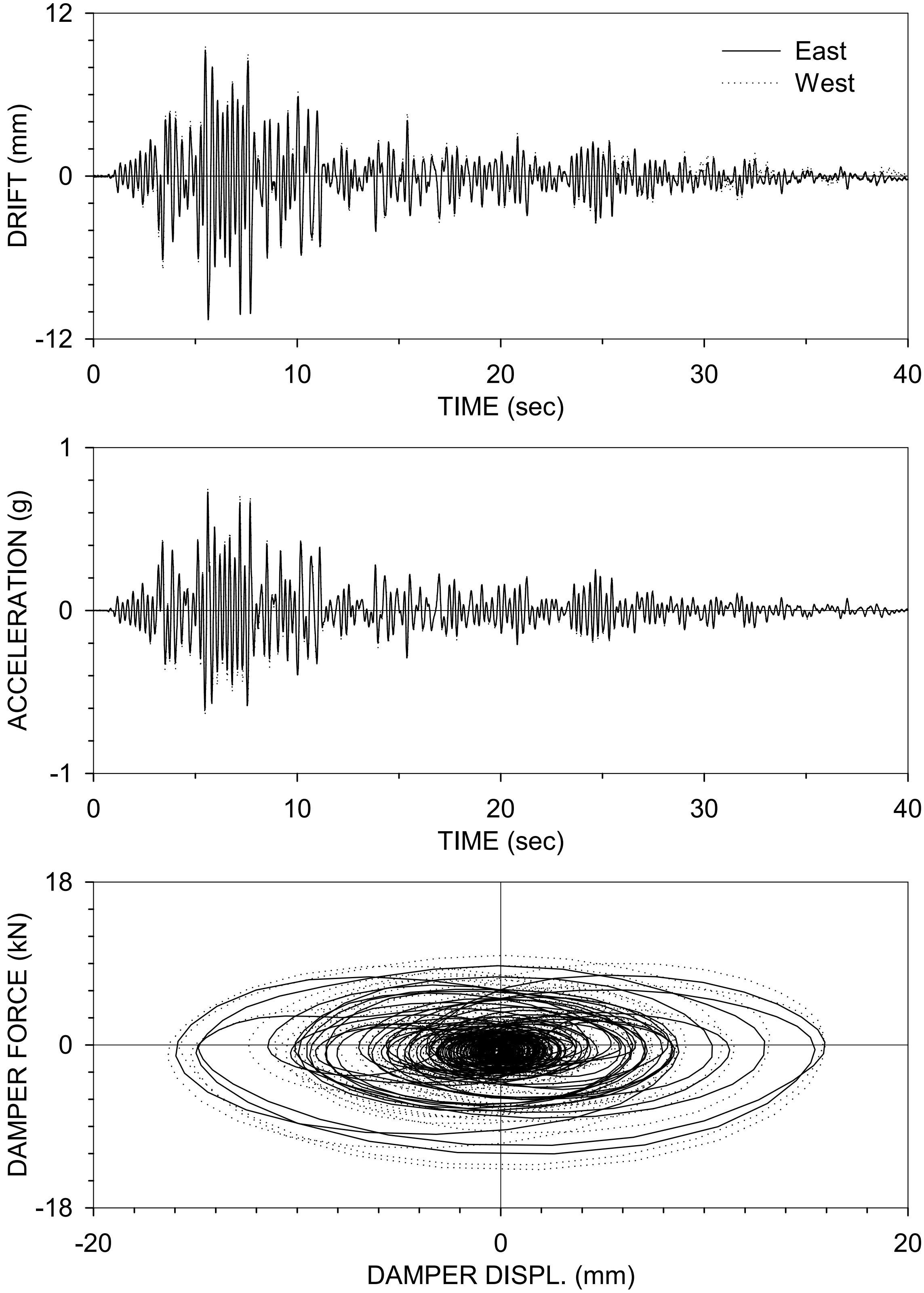

TARSBD300.3 : TAFT N21E 300% (05/13/99)

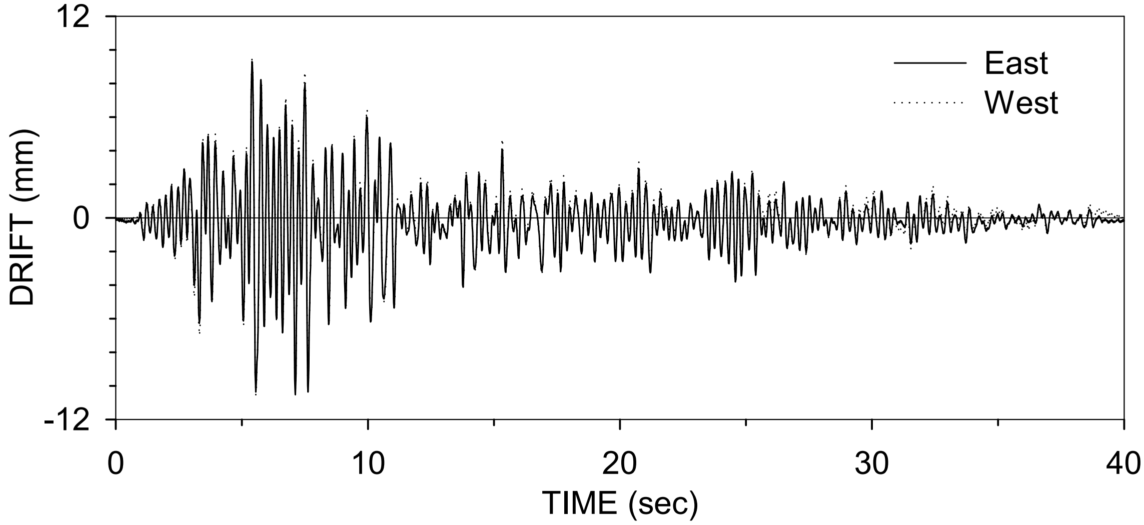

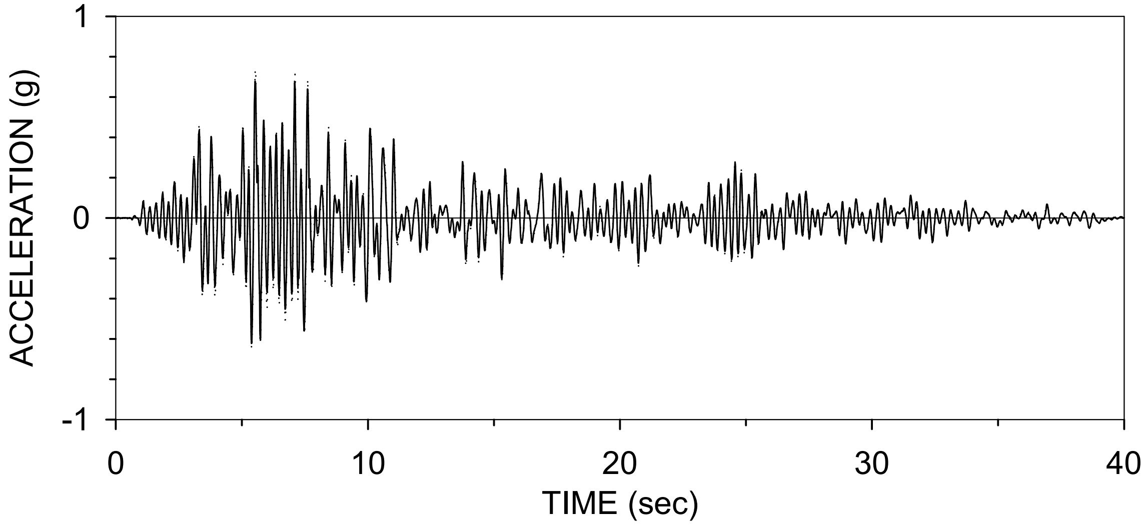

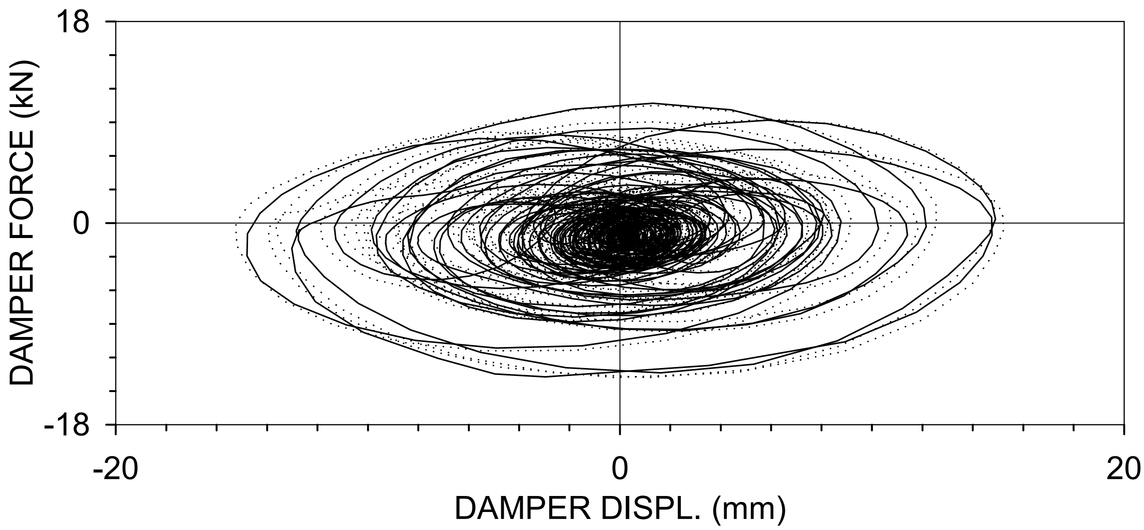

TVRSBD200 : TAFT N21E H&V 200% (05/13/99)

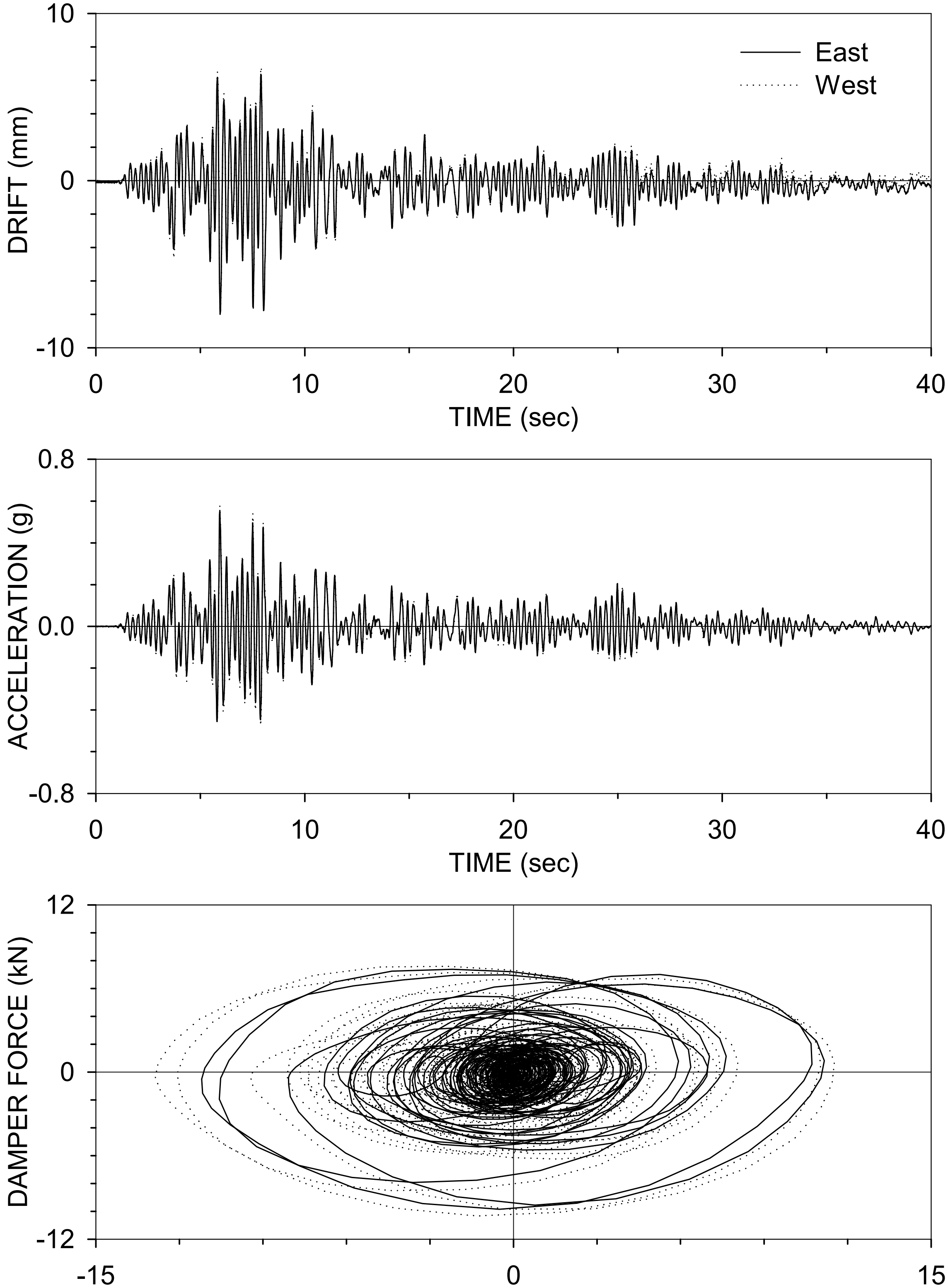

HARSBD050 : HACHINOHE NS 50% (05/13/99)

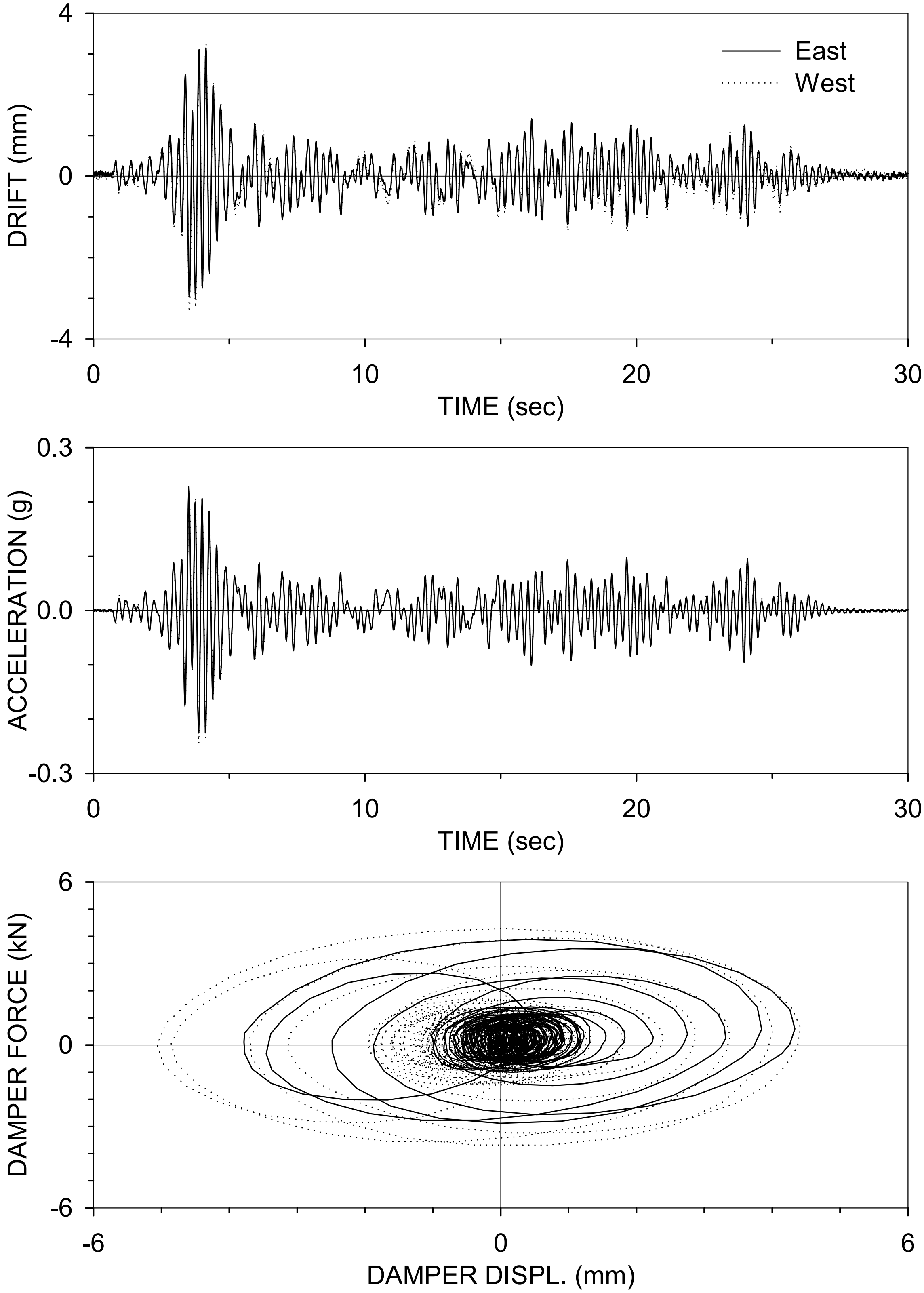

HARSBD100 : HACHINOHE NS 100% (05/13/99)

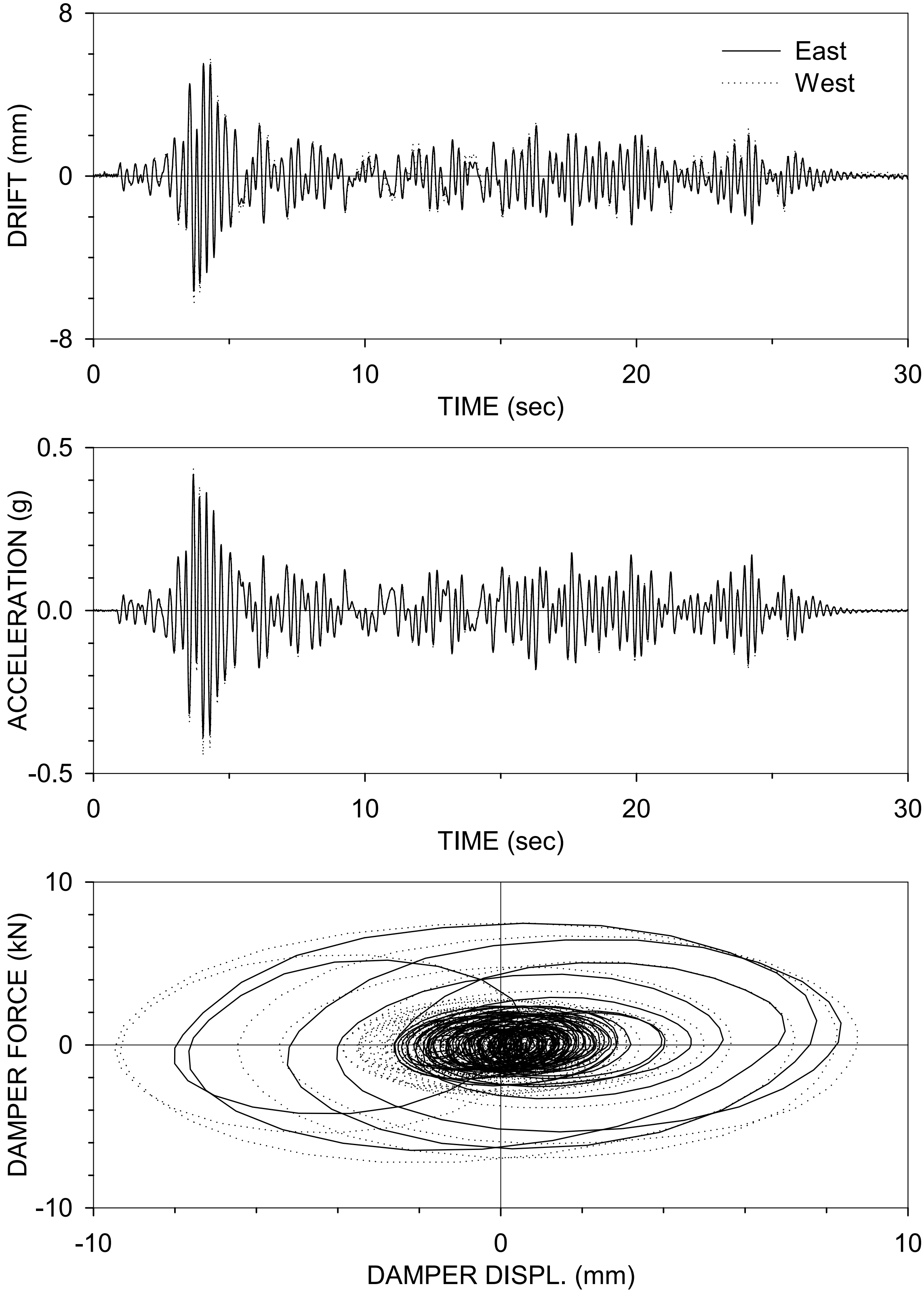

HARSBD150 : HACHINOHE NS 150% (05/13/99)

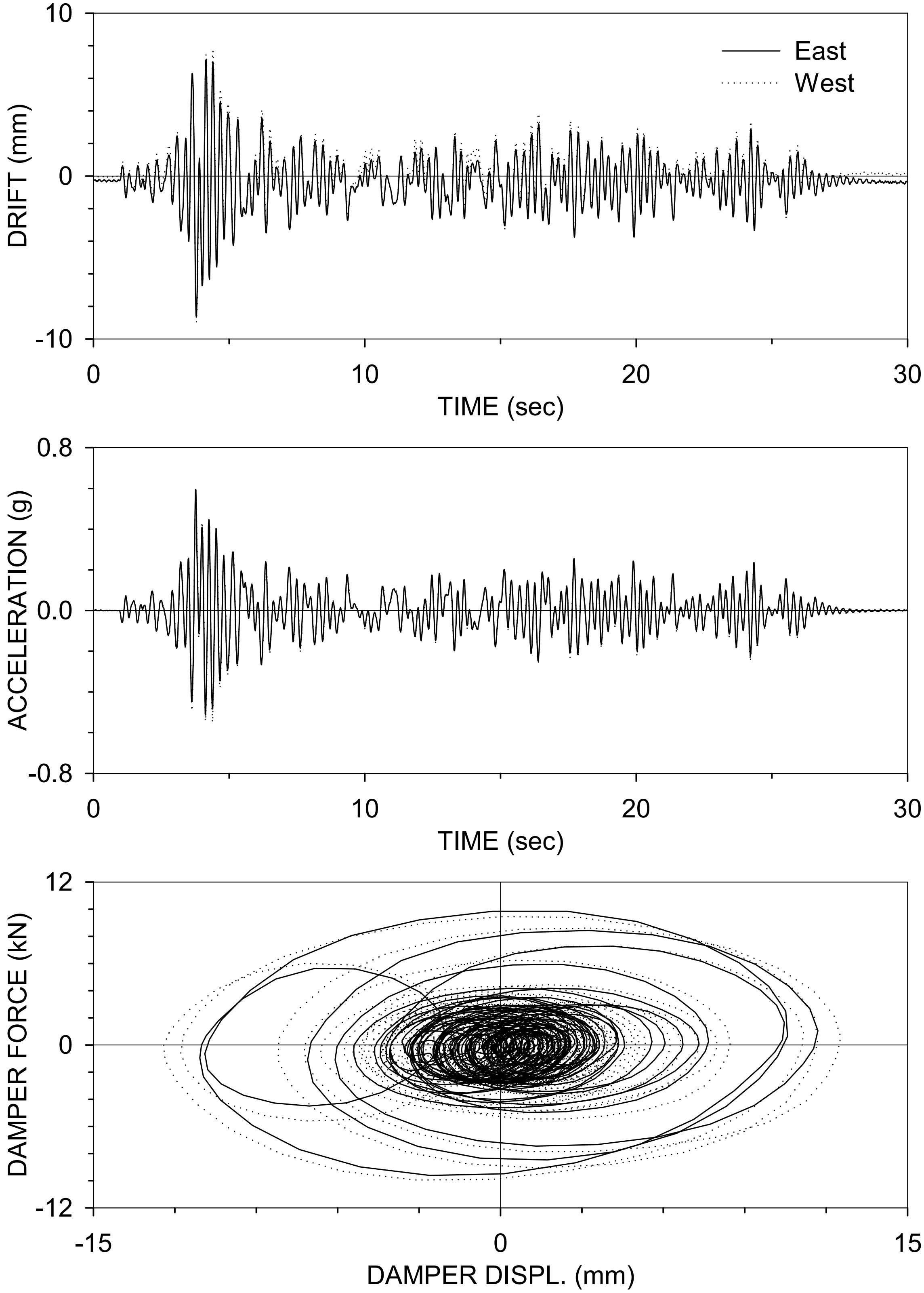

MIRSBD100 : MIYAGIKEN-OKI 100% (05/13/99)

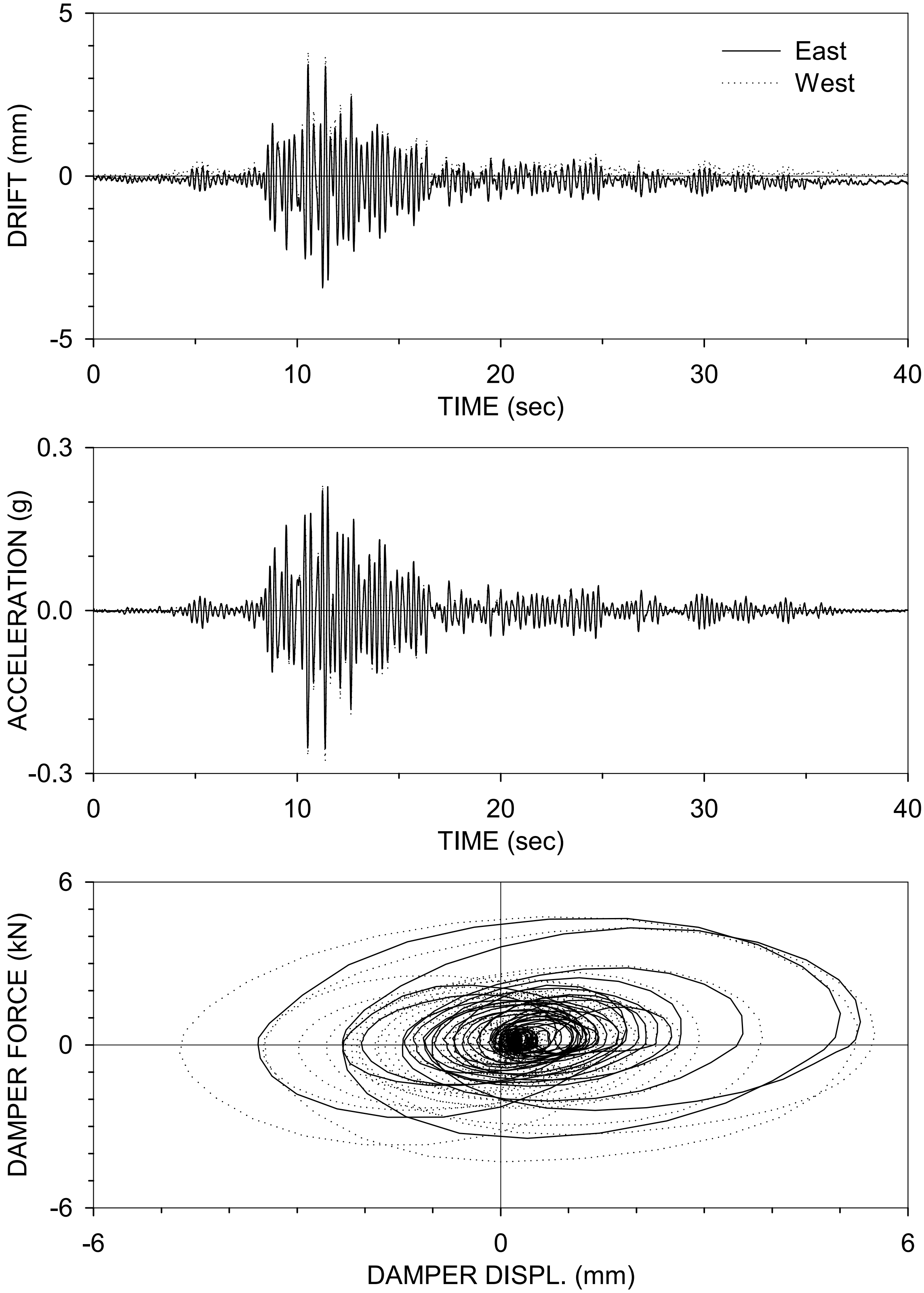

MIRSBD200 : MIYAGIKEN-OKI 200% (05/13/99)

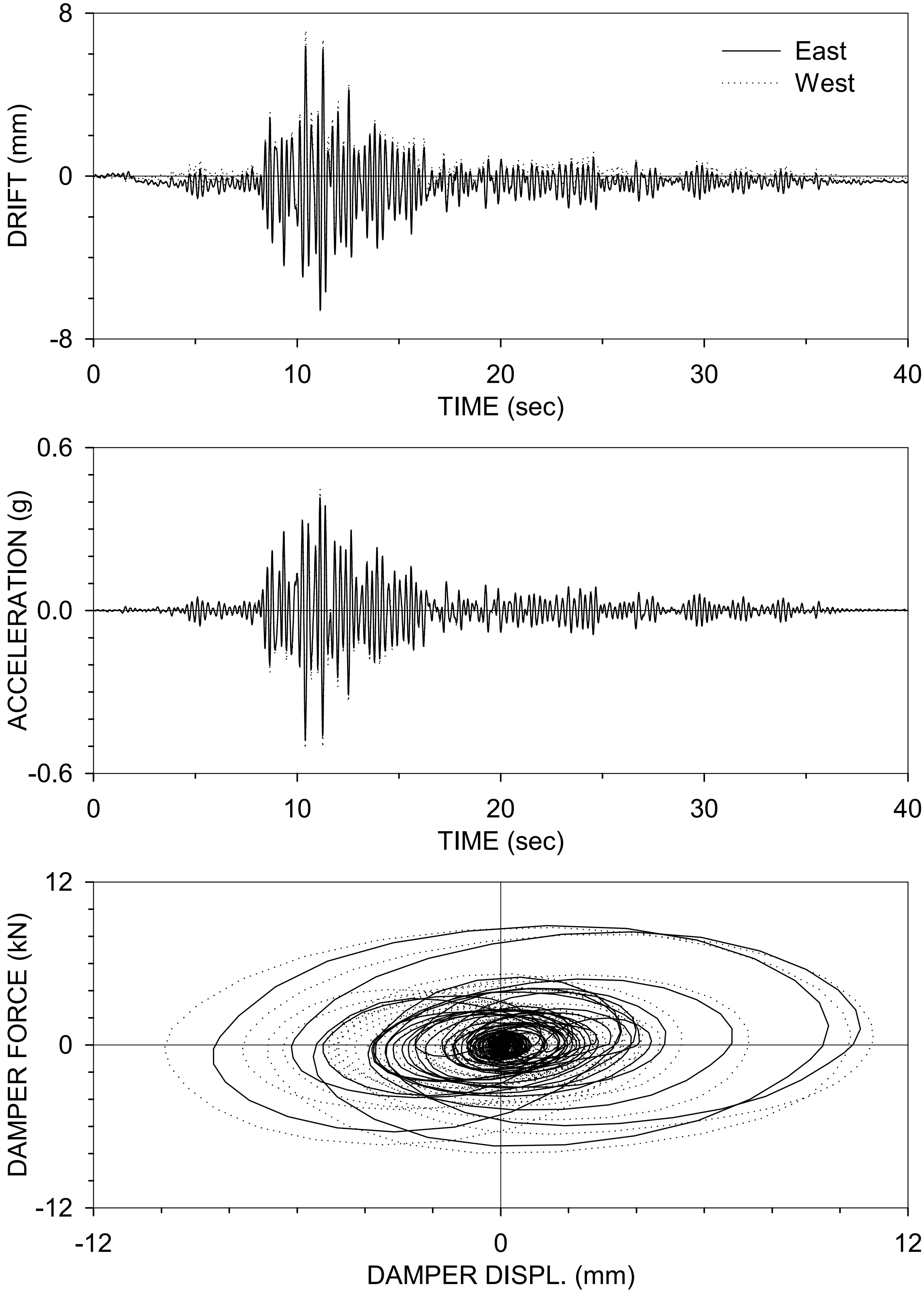

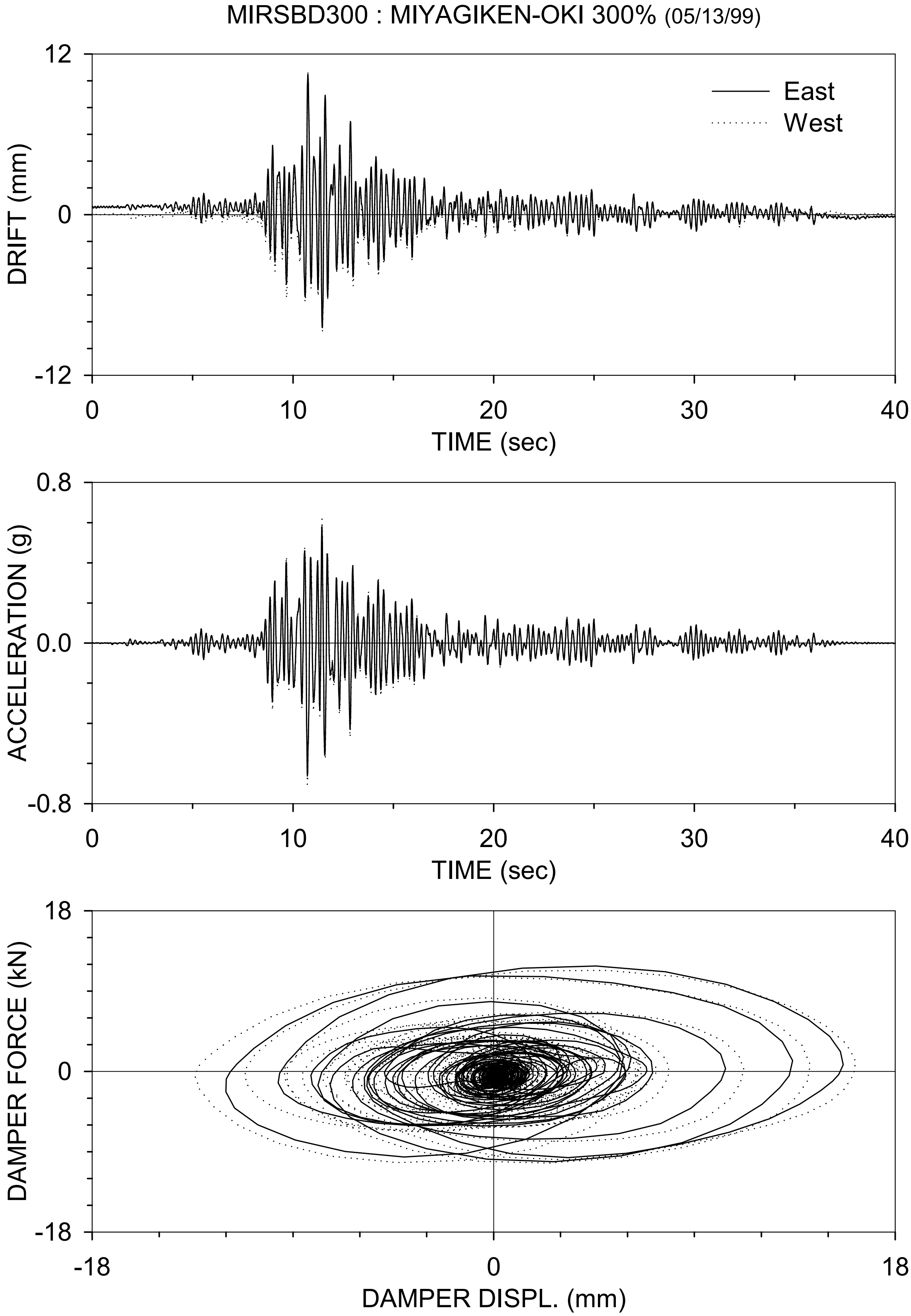
MIRSBD300 : MIYAGIKEN-OKI 300% (05/13/99)
DRIFT (mm)
12
0
-12
East
West
0
10
20
30
40
TIME (sec)
ACCELERATION (g)
0.8
0.0
-0.8
0
10
20
30
40
TIME (sec)
DAMPER FORCE (kN)
18
0
-18
-18
0
18
DAMPER DISPL. (mm)

MXRSBD100 : MEXICO CITY N90W 100% (05/13/99)

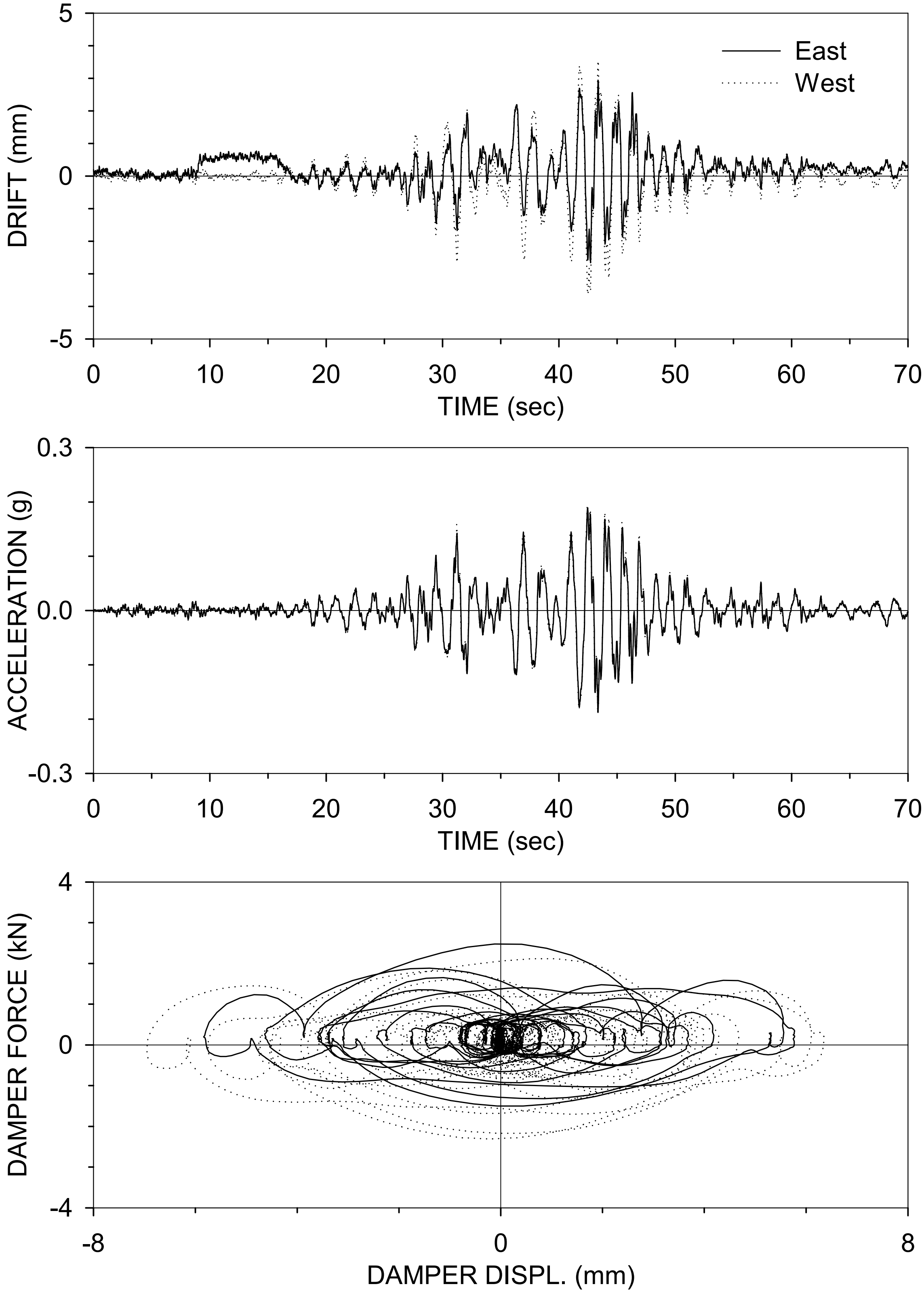

PWRSBD025 : PACOIMA S74W 25% (05/14/99)

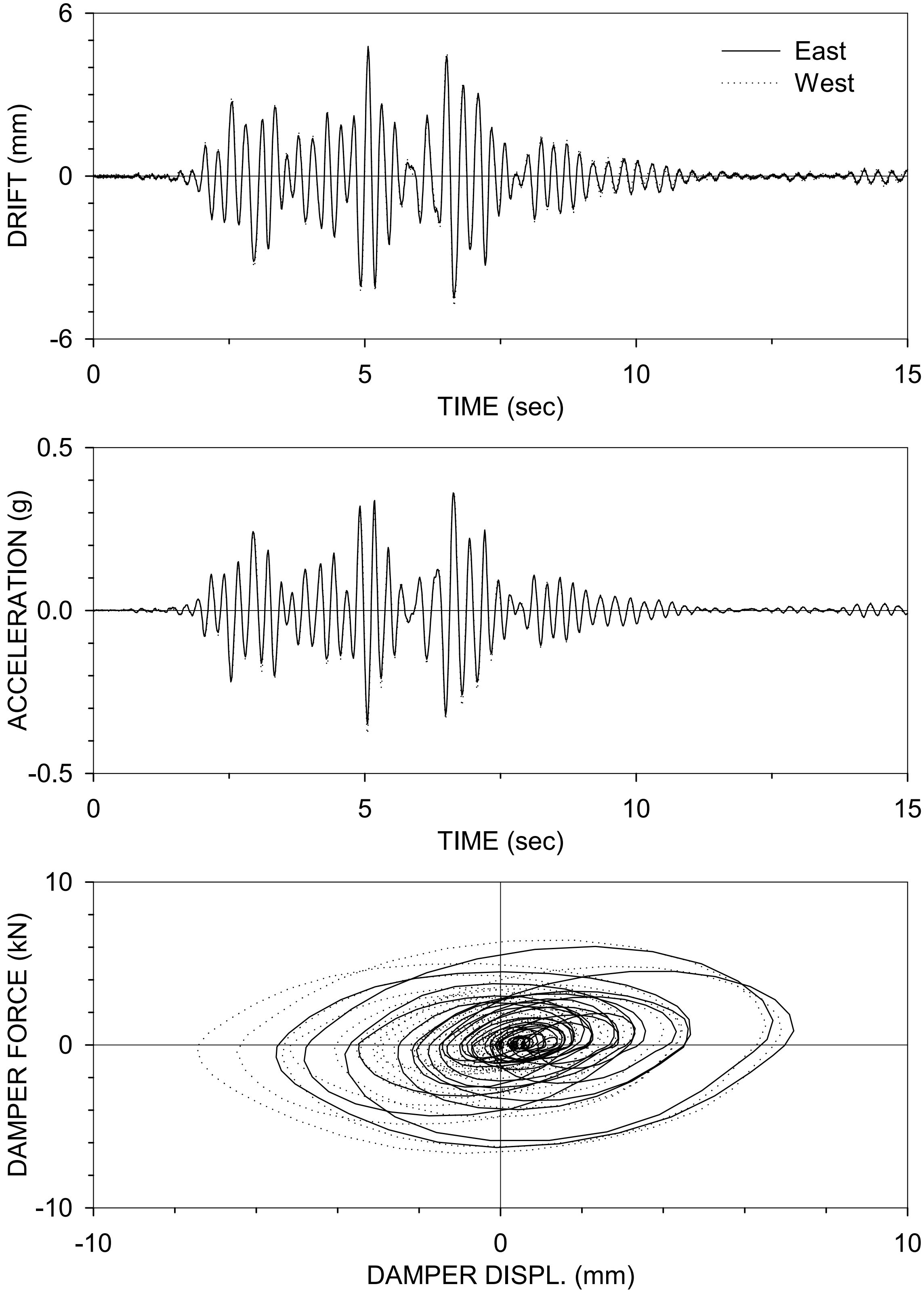

PWRSBD050 : PACOIMA S74W 50% (05/14/99)

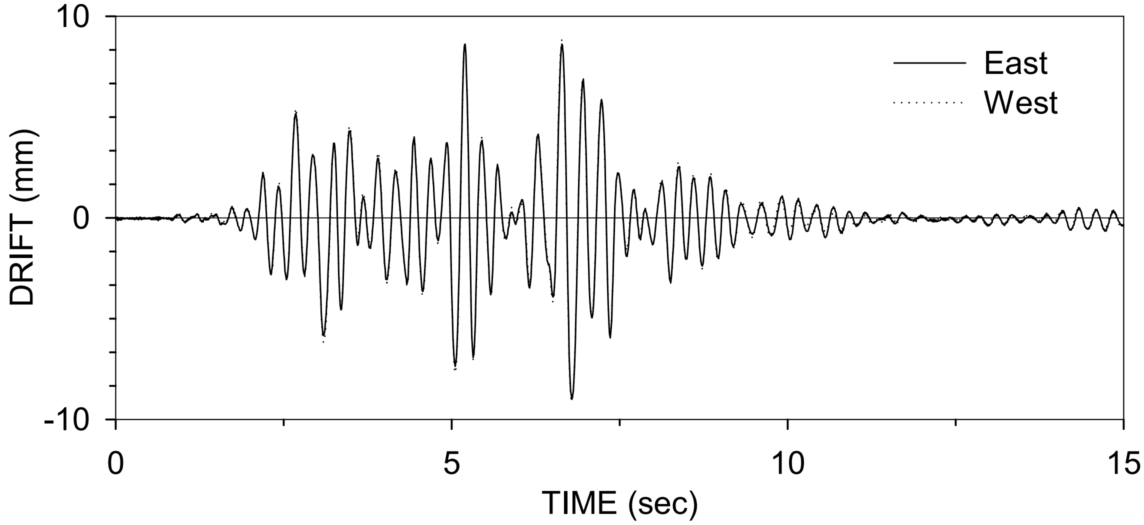

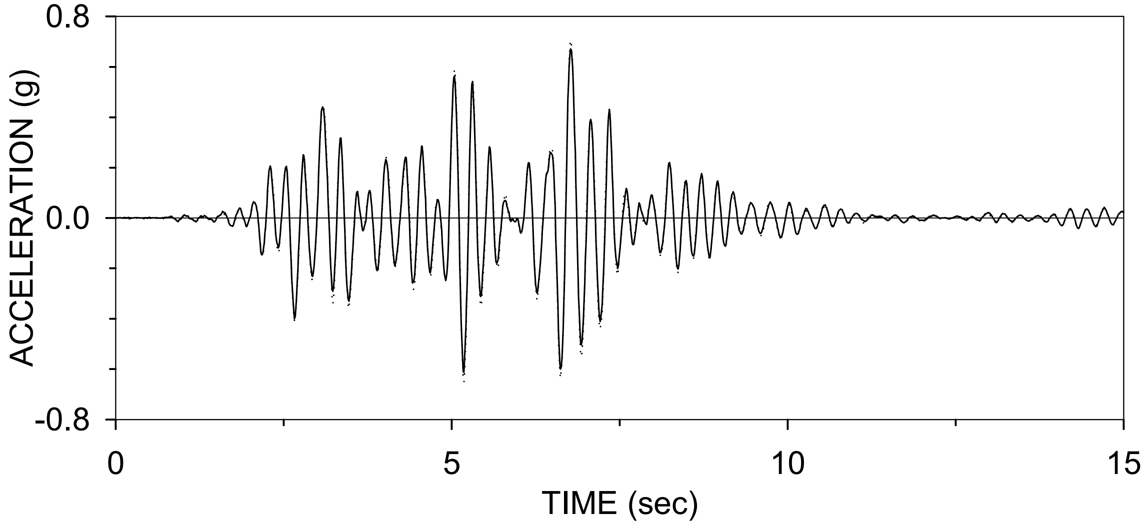

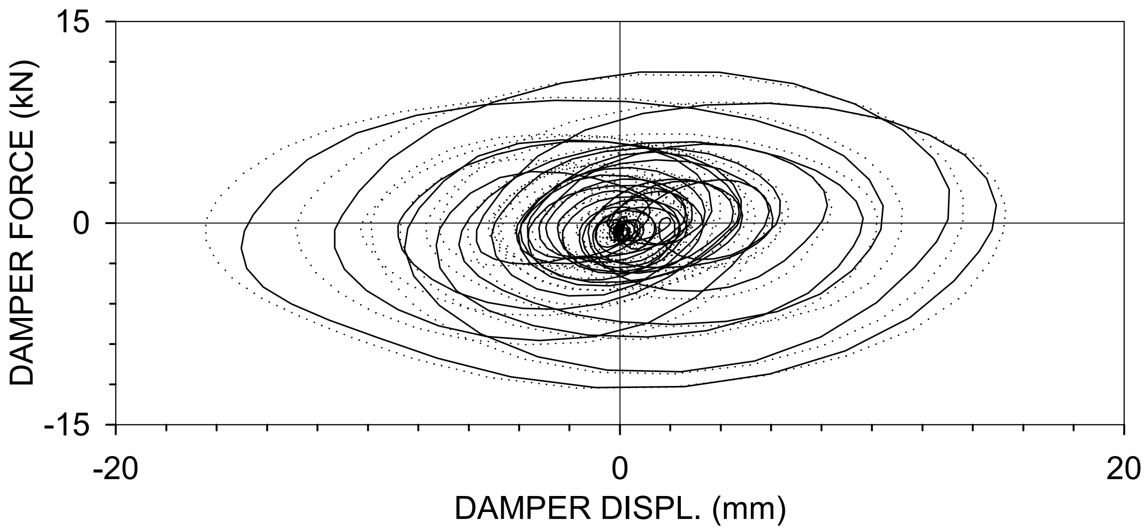

PERSBD010 : PACOIMA S16E 10% (05/14/99)

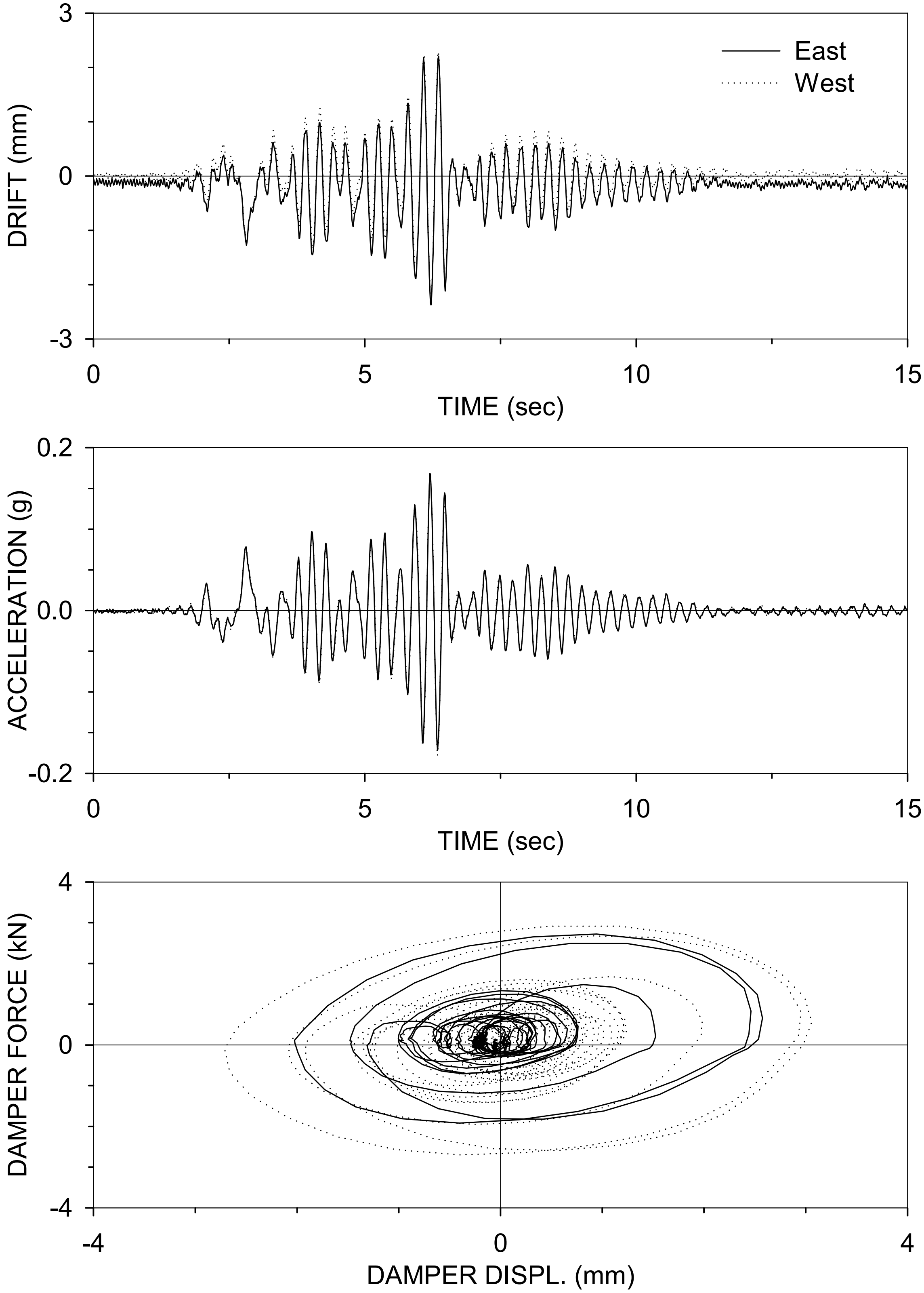

PERSBD025 : PACOIMA S16E 25% (05/14/99)

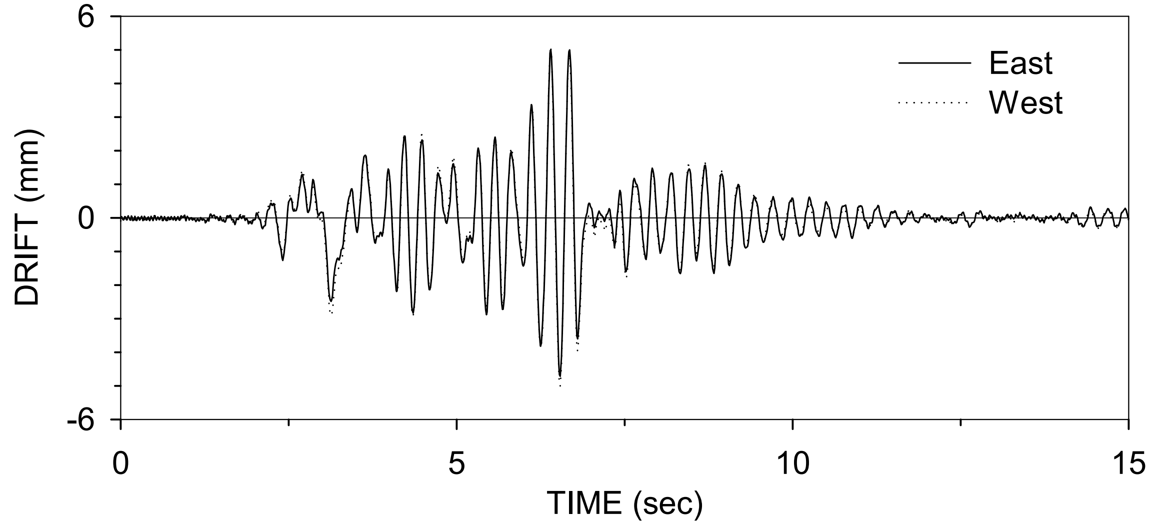

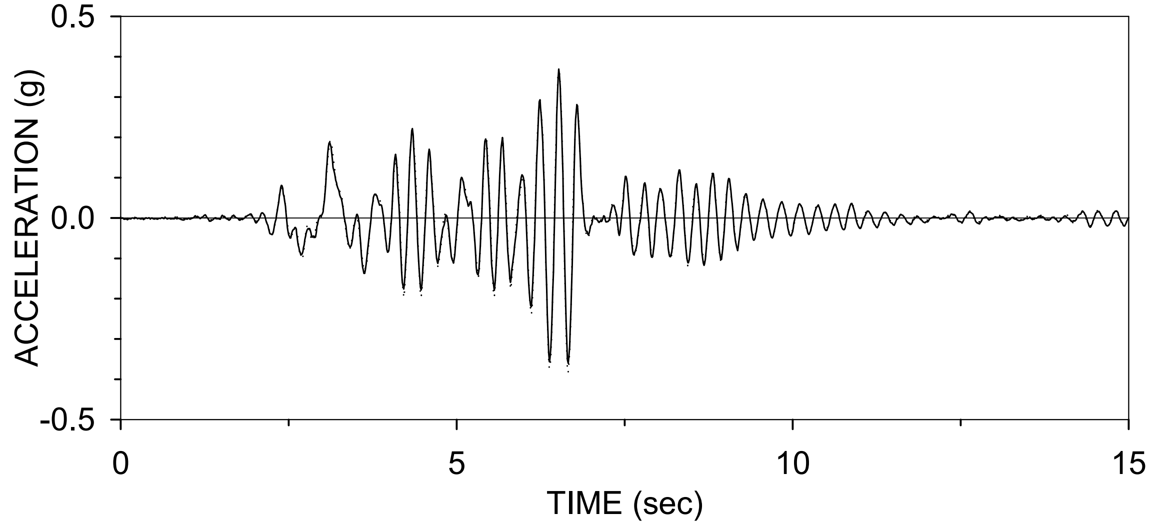

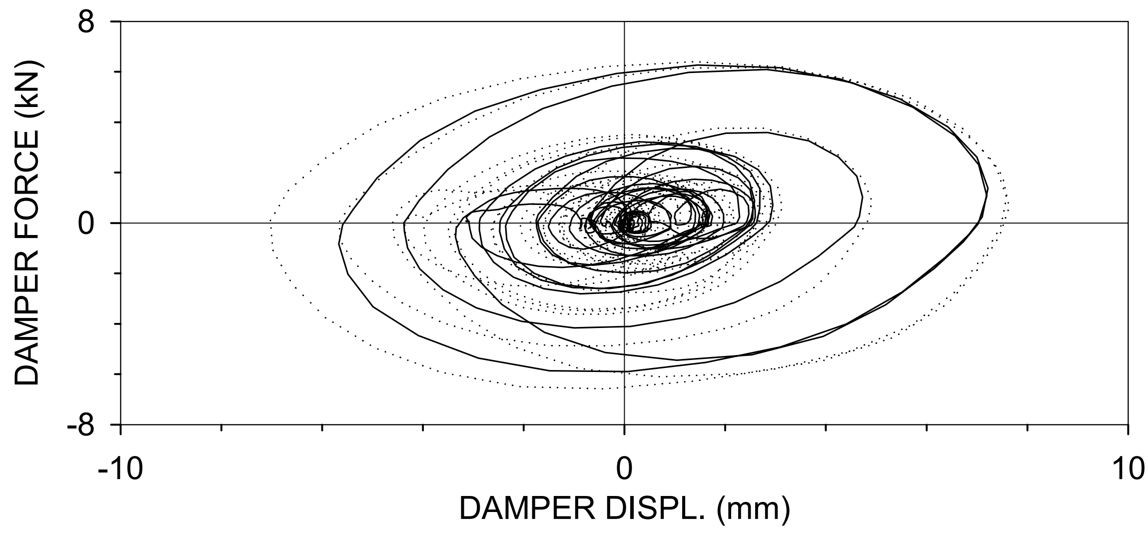

PERSBD050 : PACOIMA S16E 50% (05/14/99)

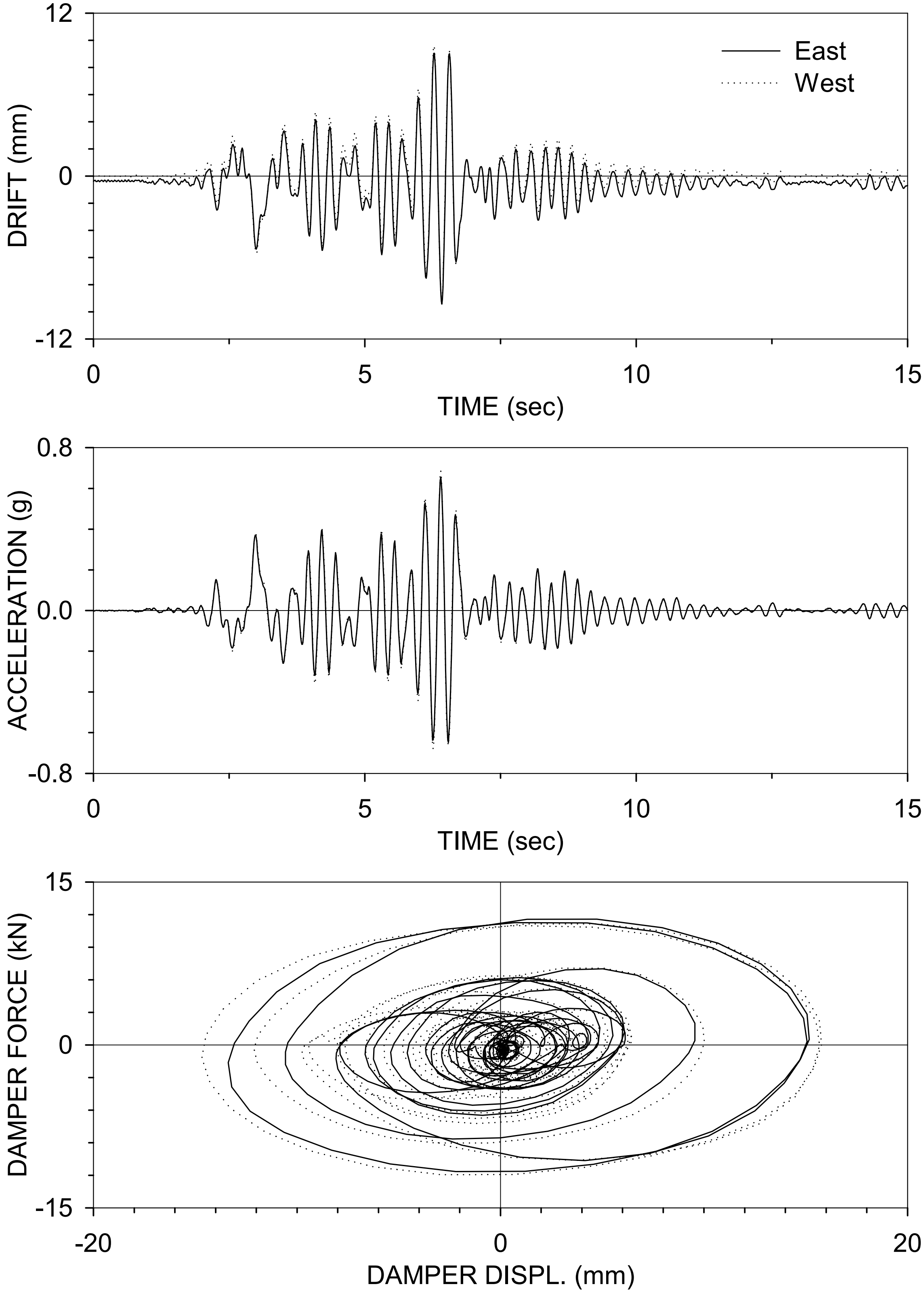

SYRSBD025 : SYLMAR 90 25% (05/14/99)

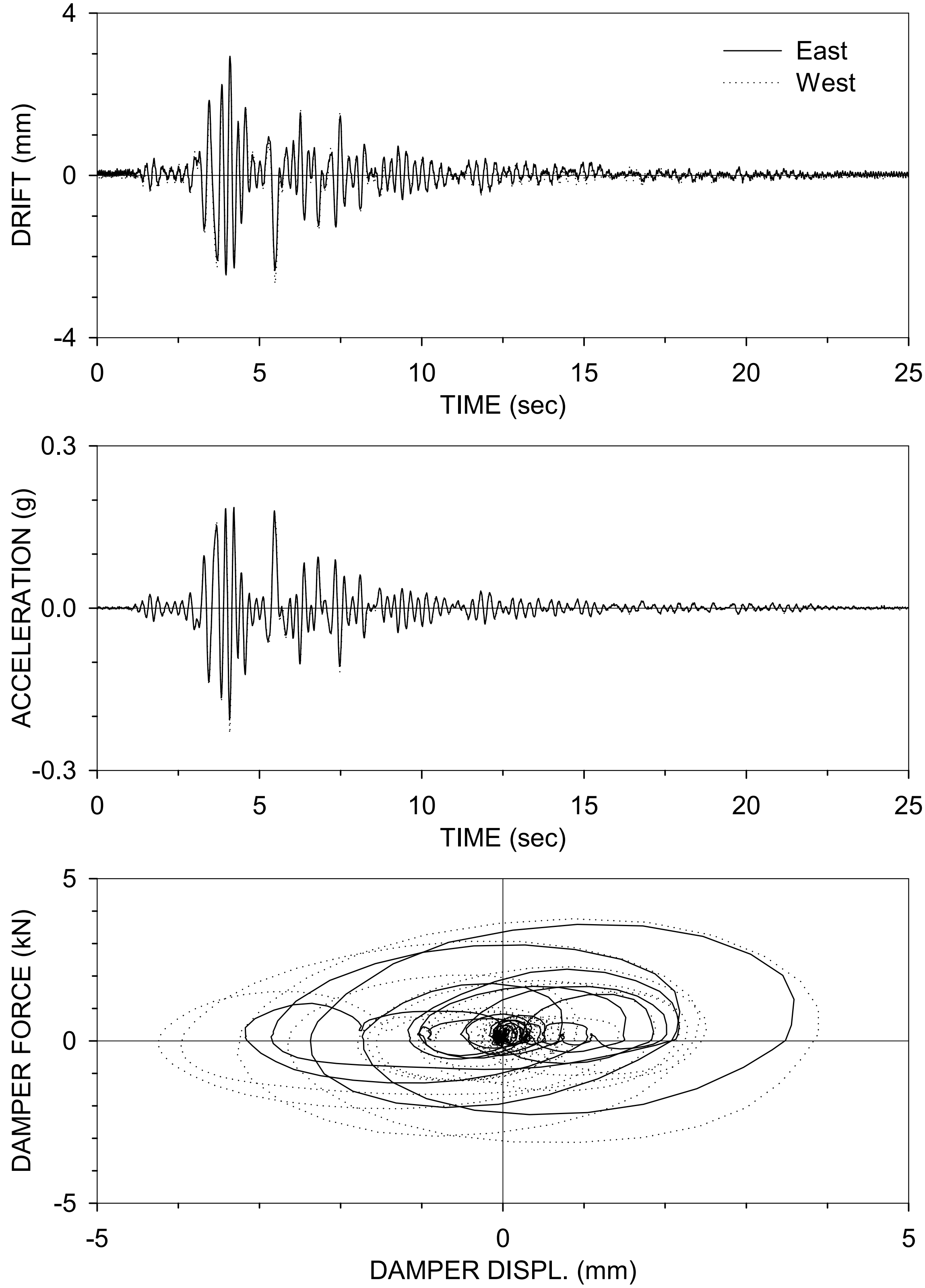

SYRSBD040 : SYLMAR 90 40% (05/14/99)

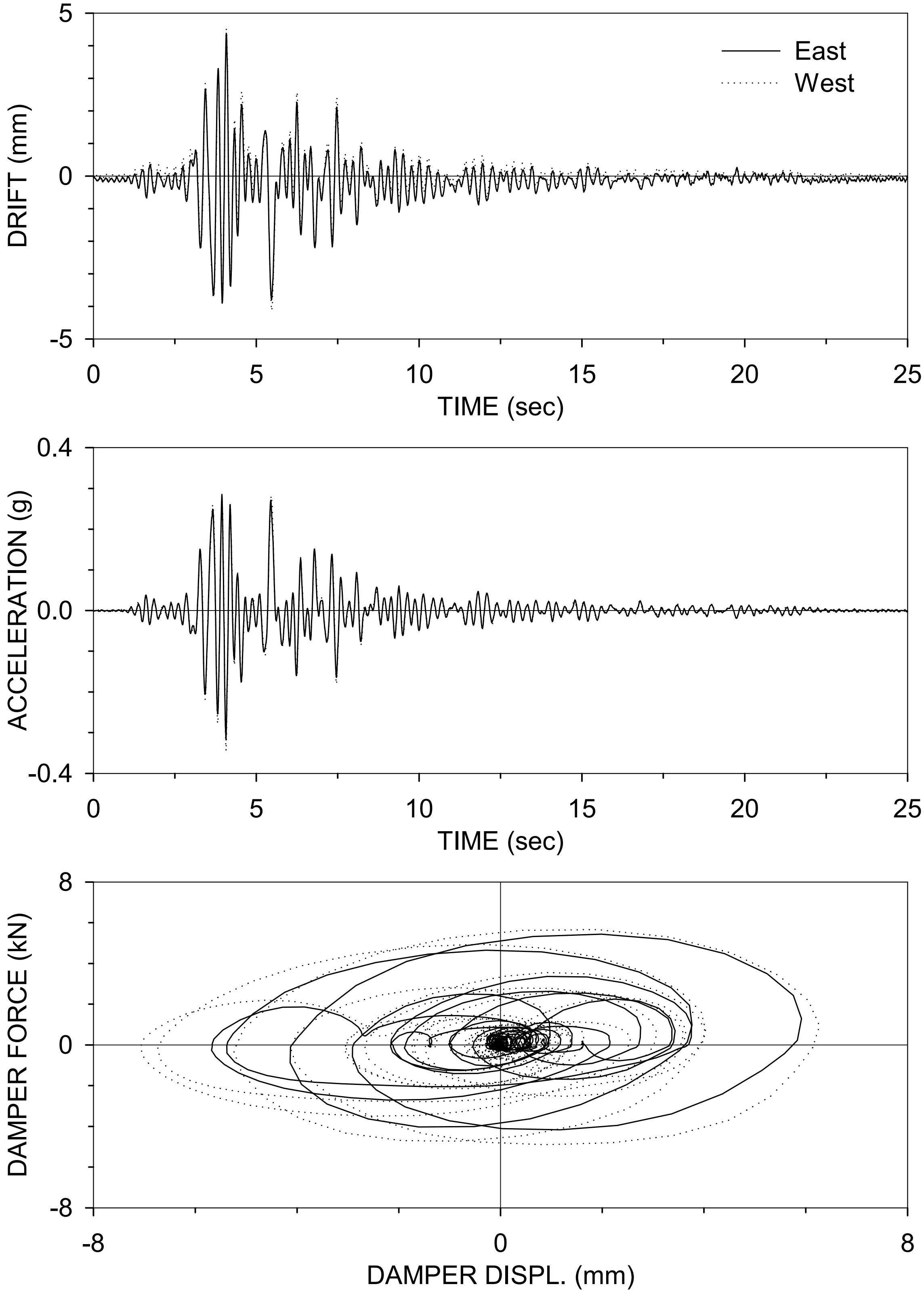

SYRSBD050 : SYLMAR 90 50% (05/14/99)

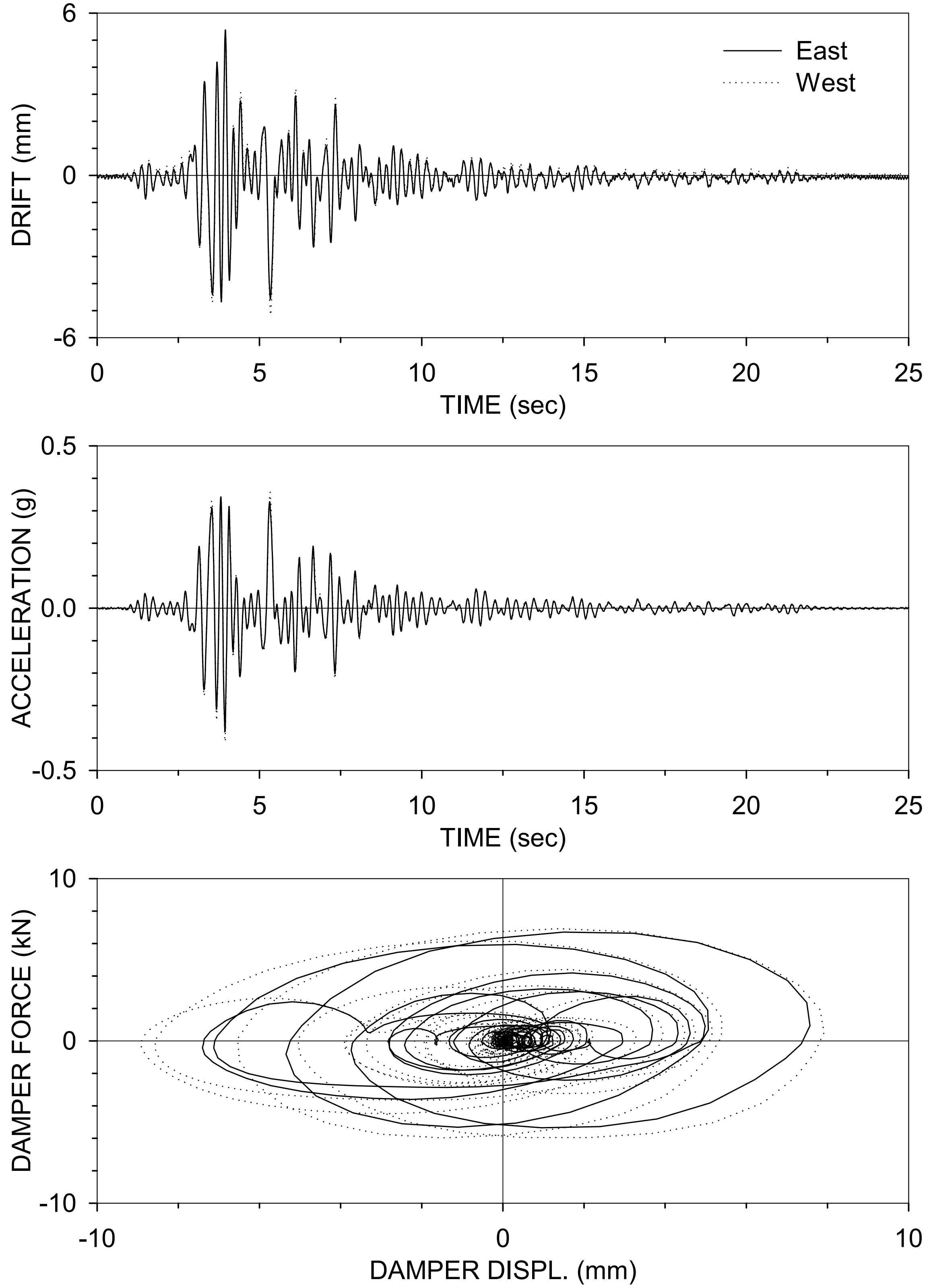

SYRSBD010 : SYLMAR 90 10% (05/14/99)

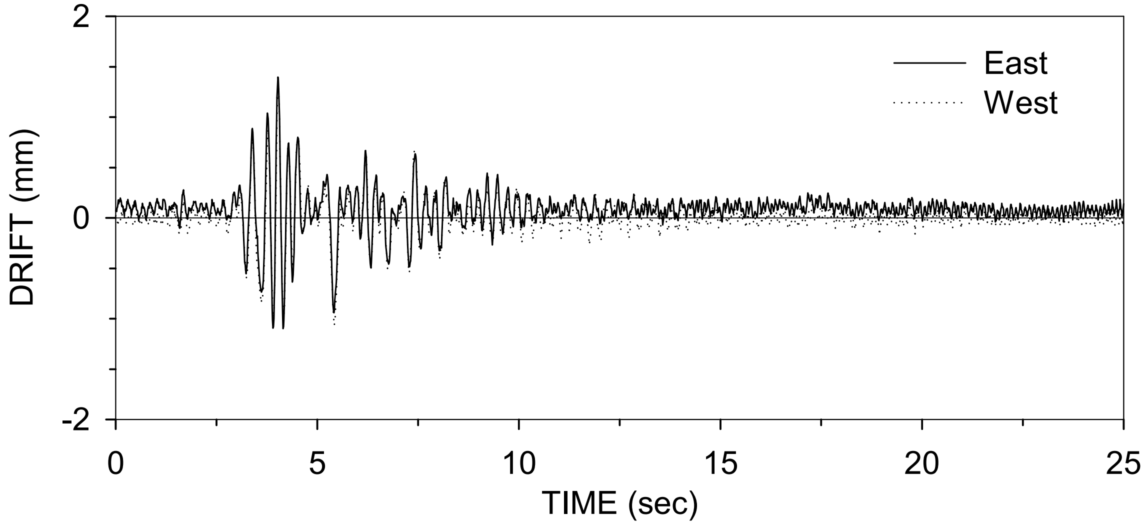

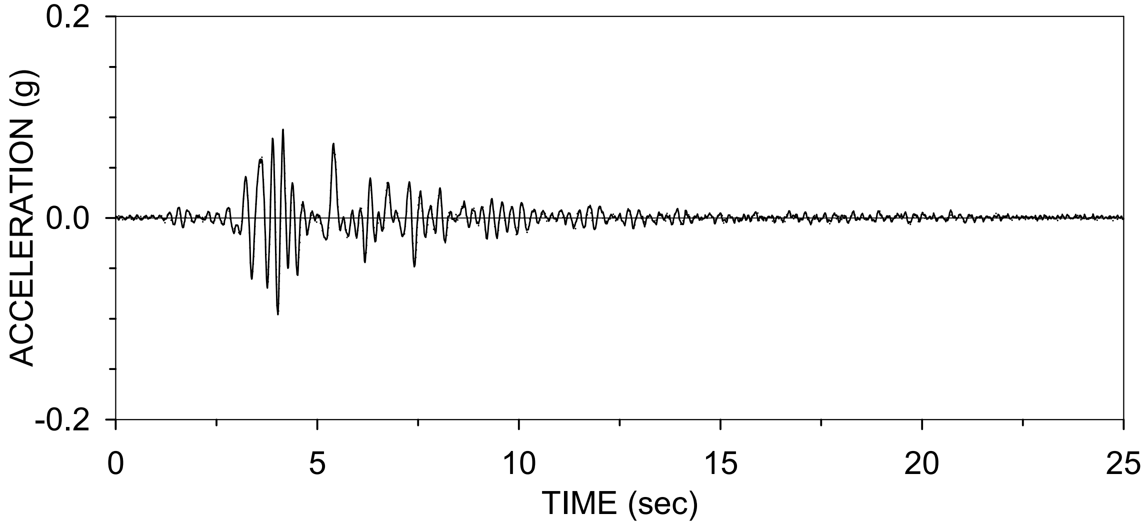

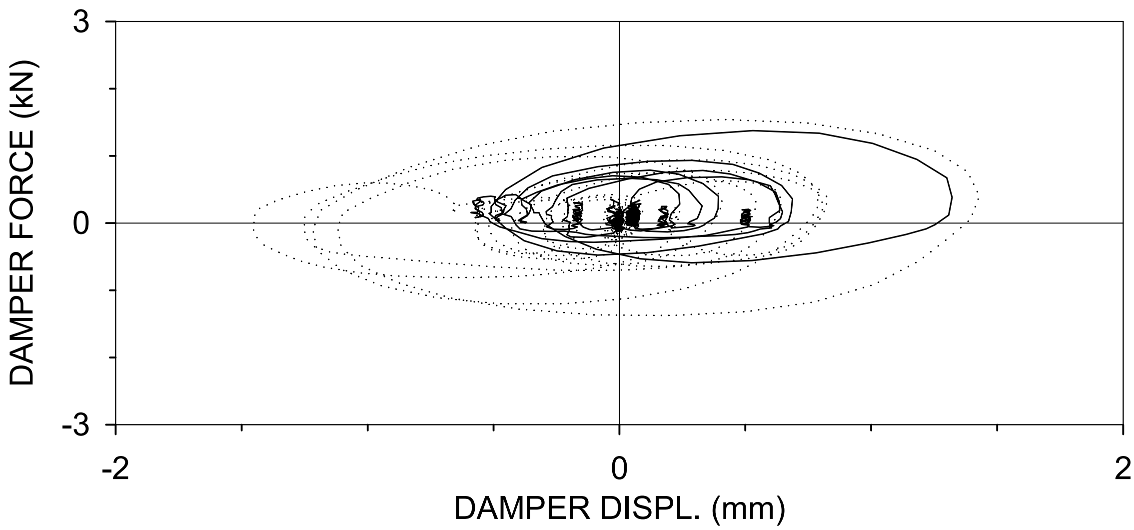

SYRSBD075 : SYLMAR 90 75% (05/14/99)

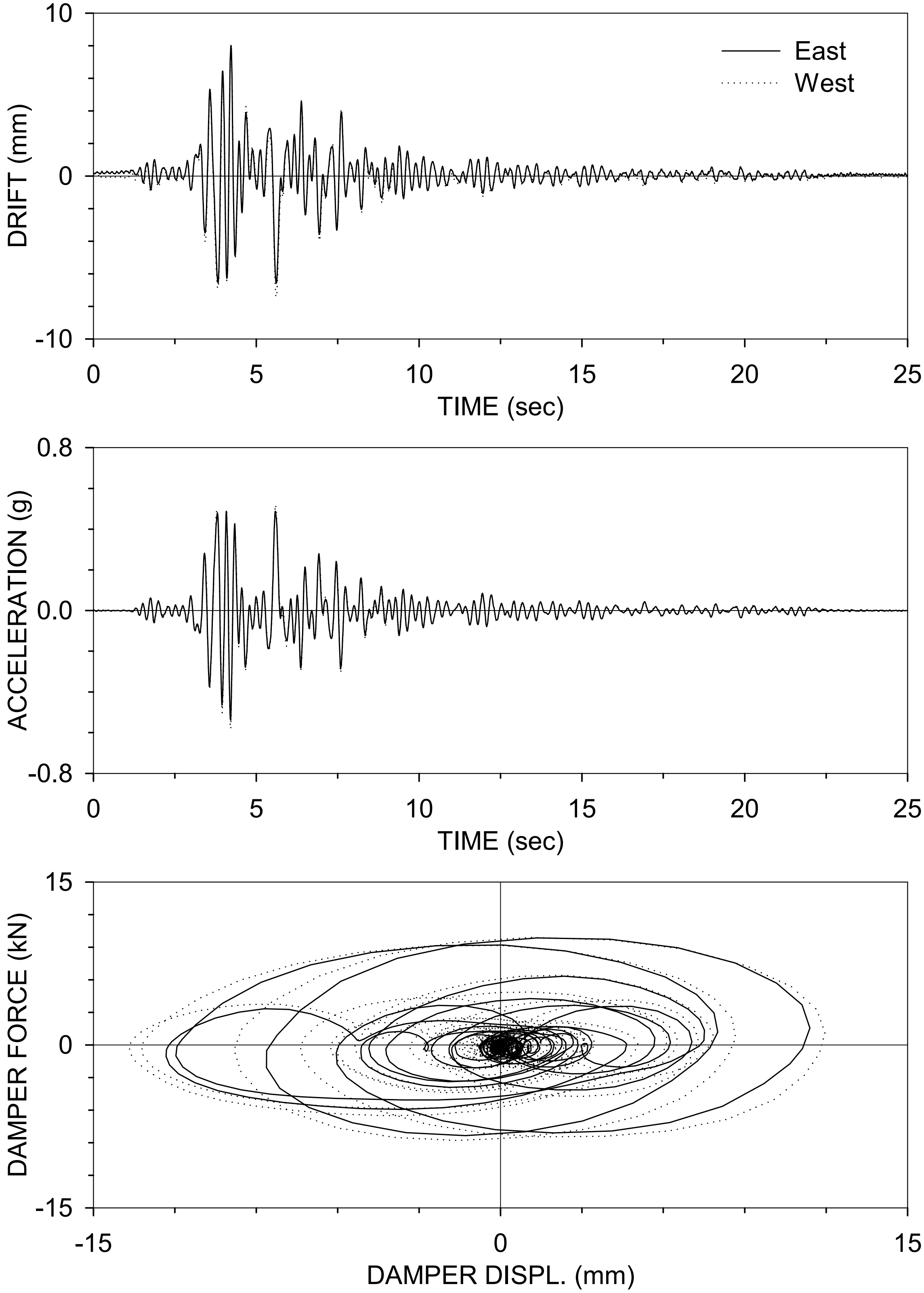

SYRSBD100 : SYLMAR 90 100% (05/17/99)

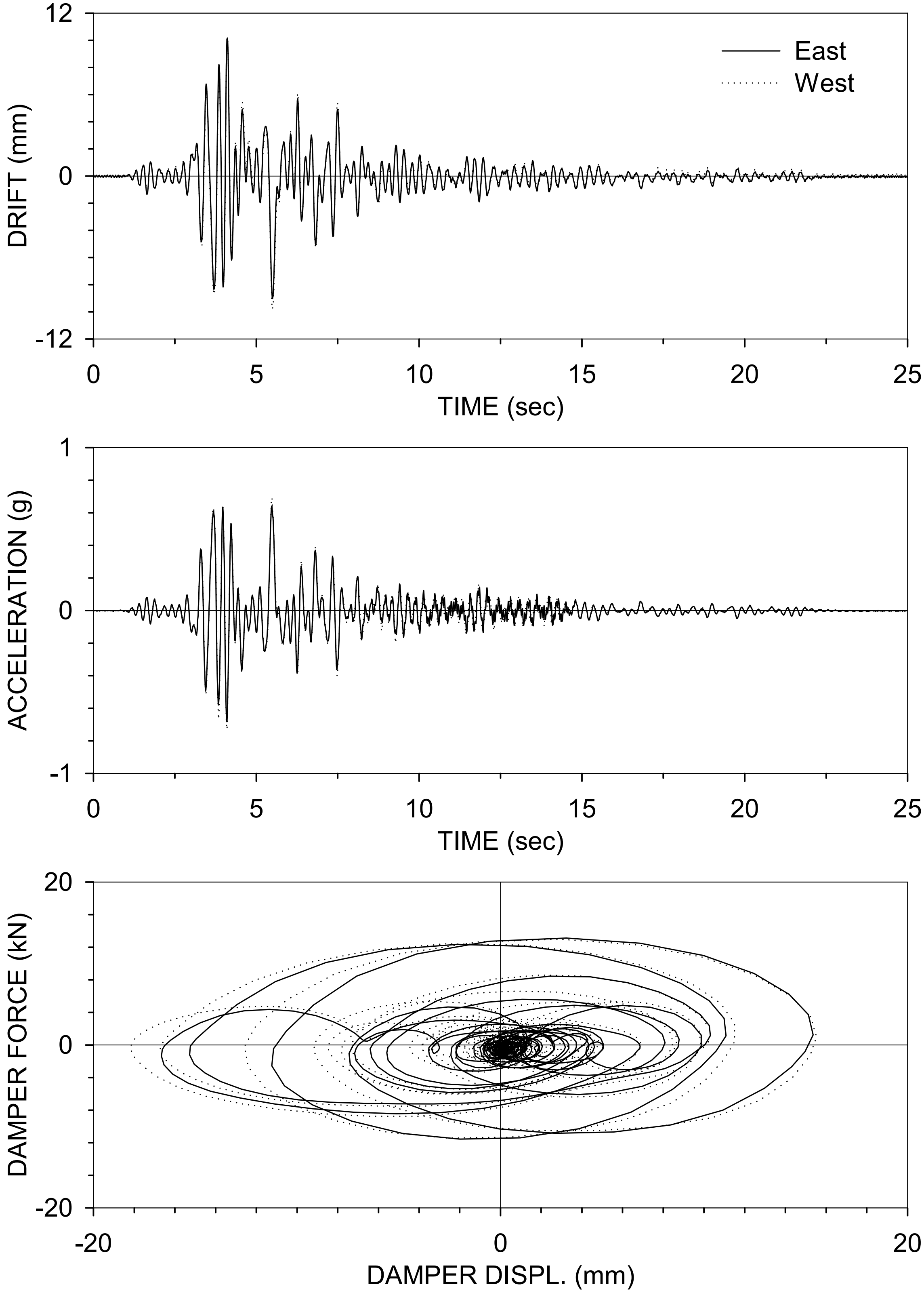

SYRSBD100.2 : SYLMAR 90 100% (05/17/99)

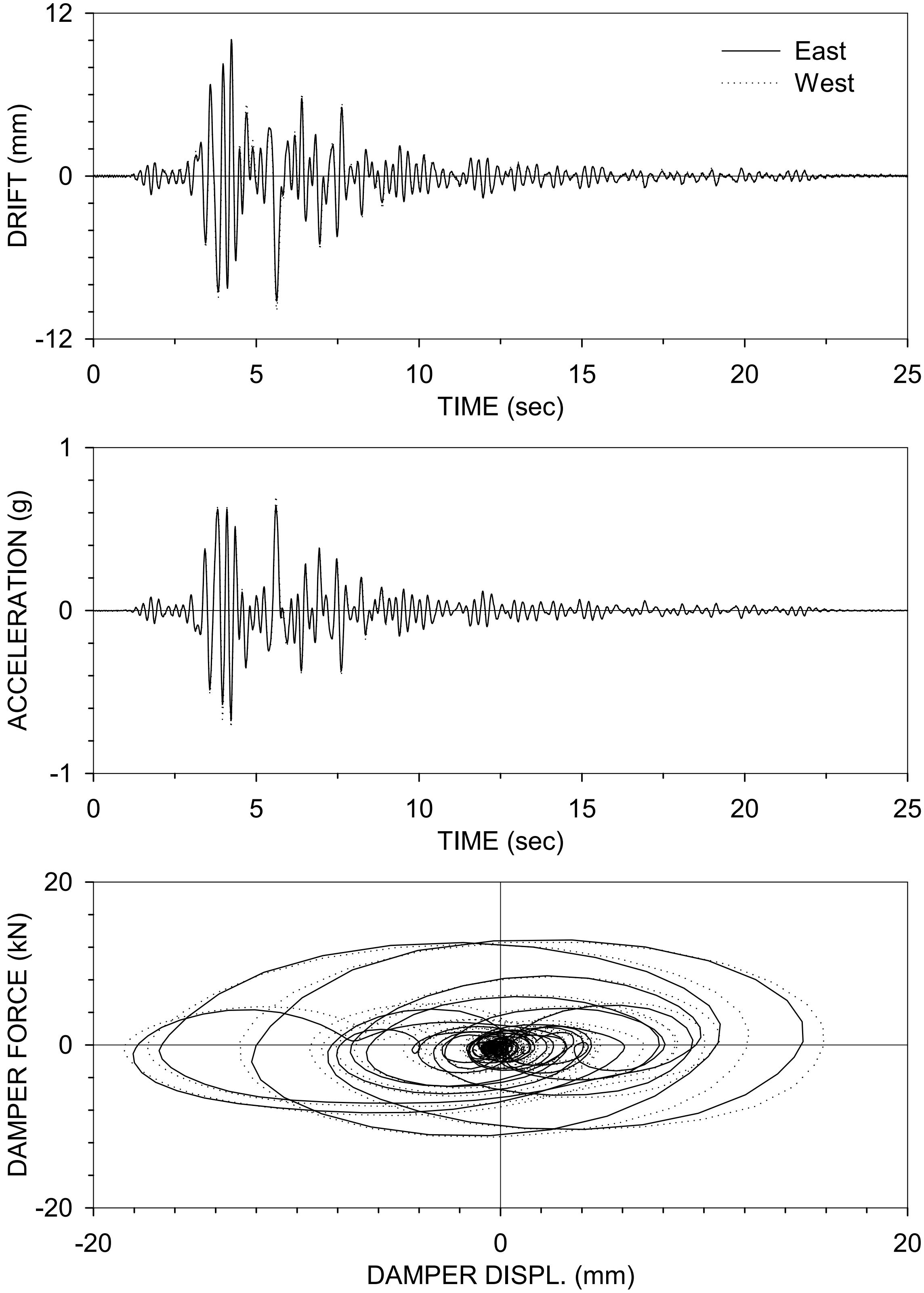

N3RSBD025 : NEWHALL 360 25% (05/17/99)

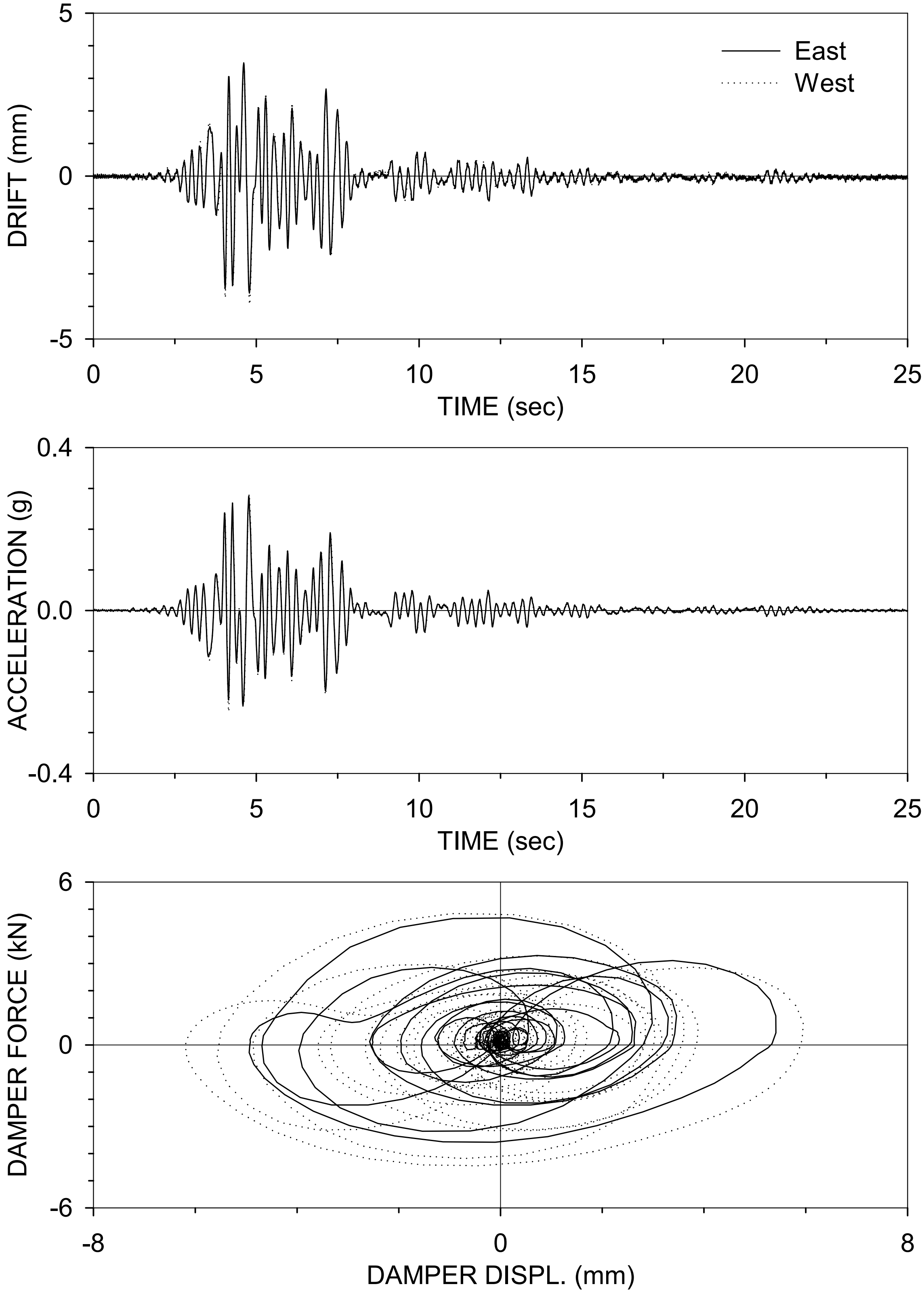

N3RSBD040 : NEWHALL 360 40% (05/17/99)

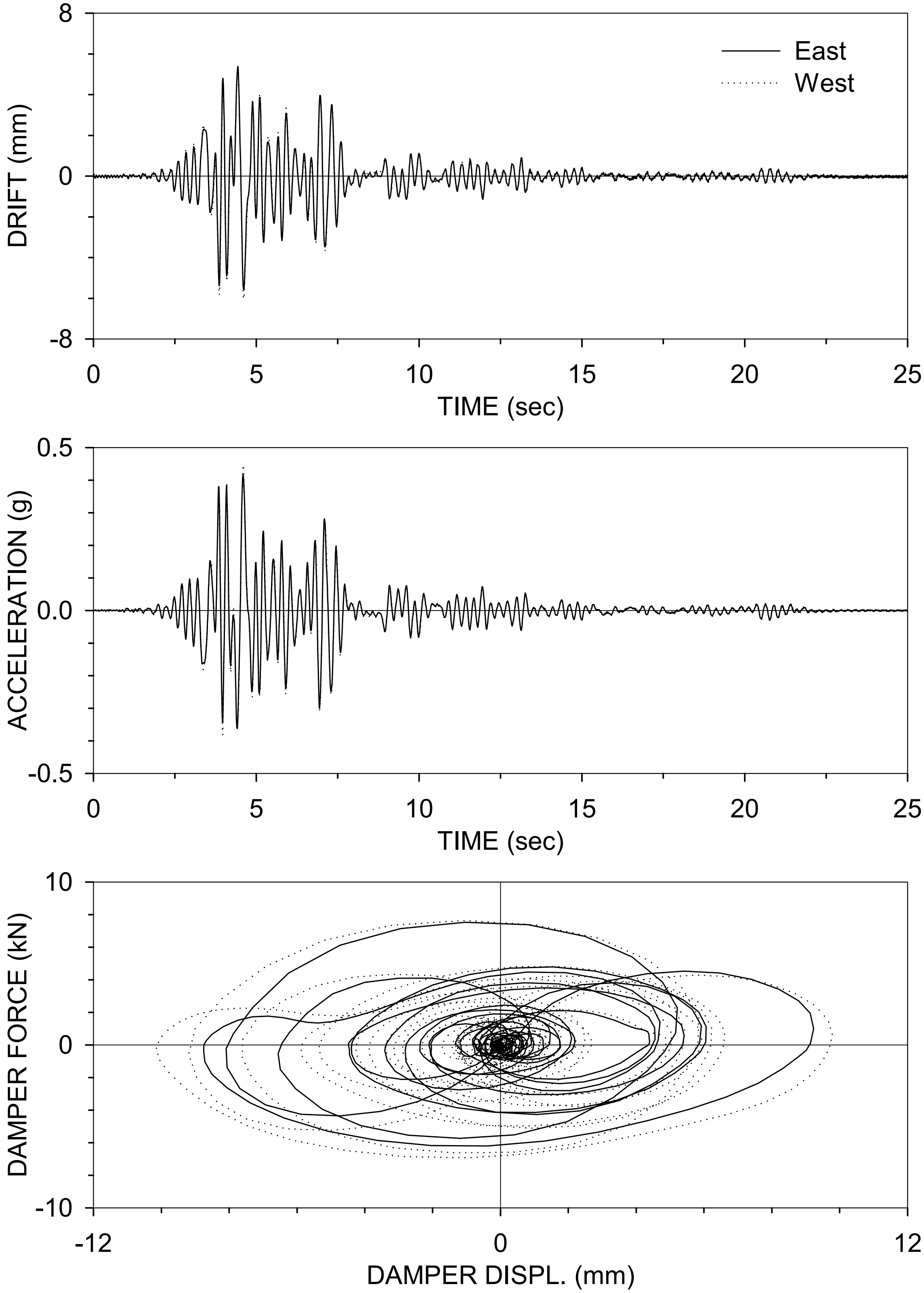

N3RSBD050 : NEWHALL 360 50% (05/17/99)

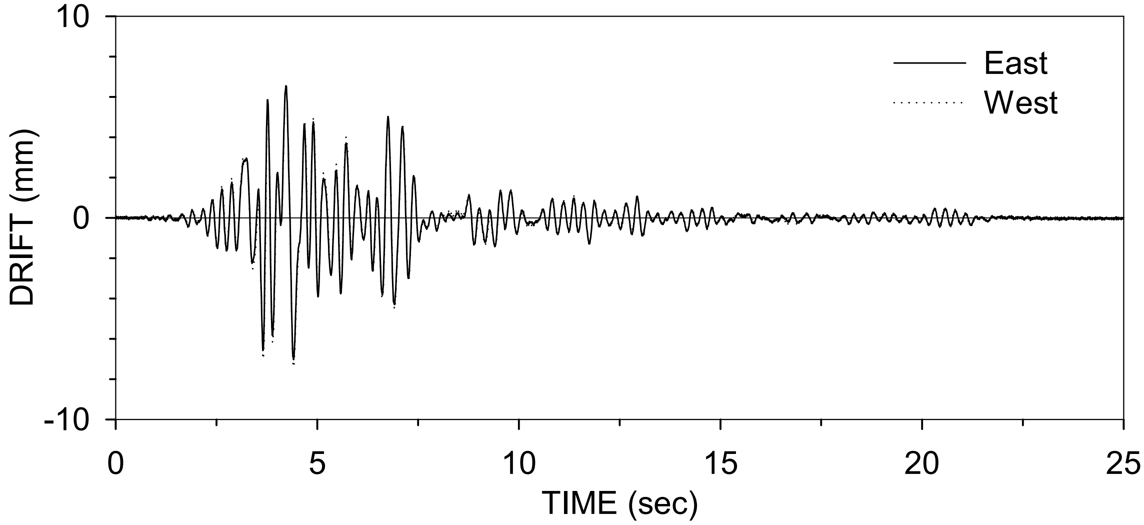

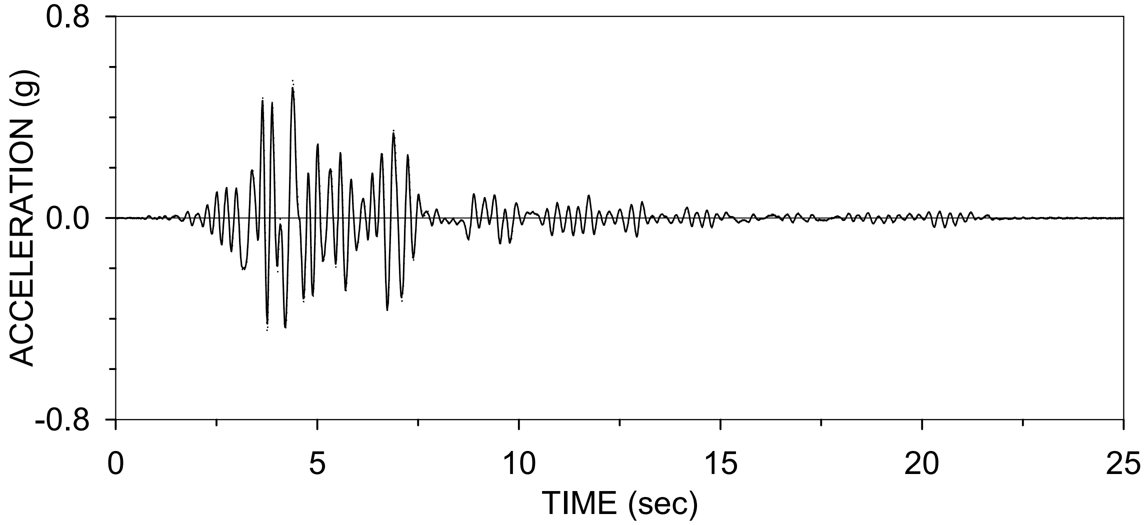

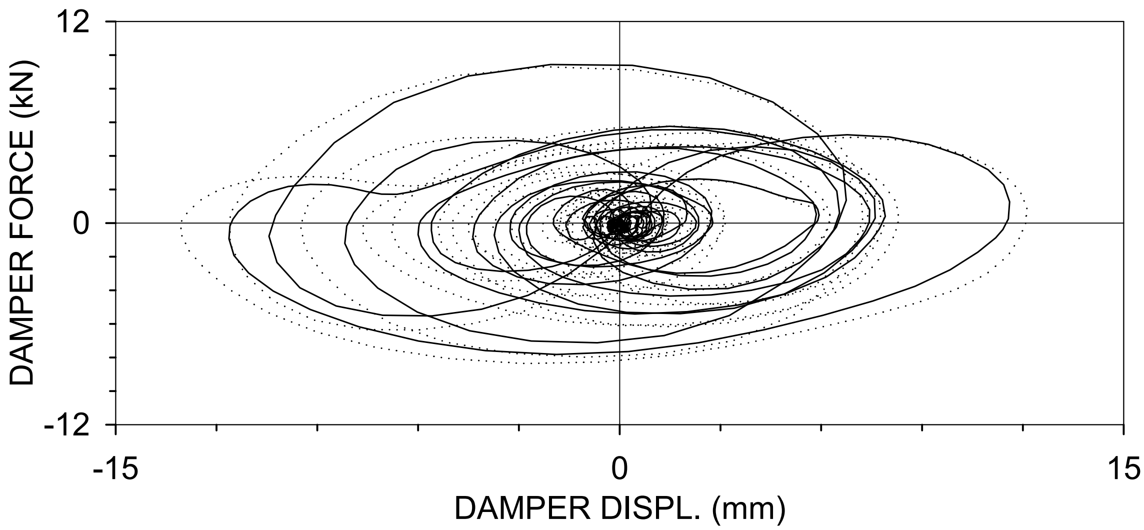

N3RSBD075 : NEWHALL 360 75% (05/17/99)

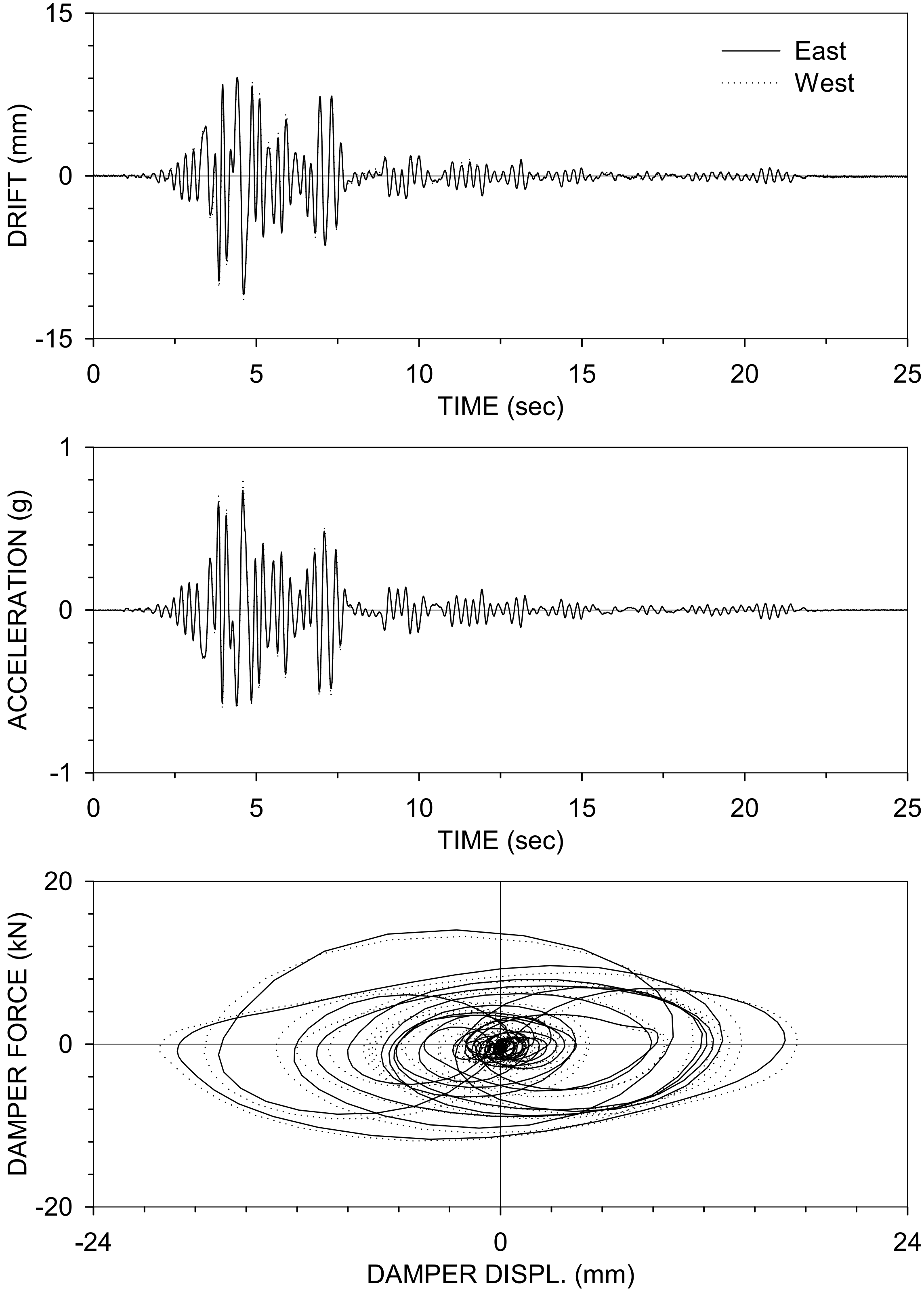

N9RSBD025 : NEWHALL 90 25% (05/17/99)

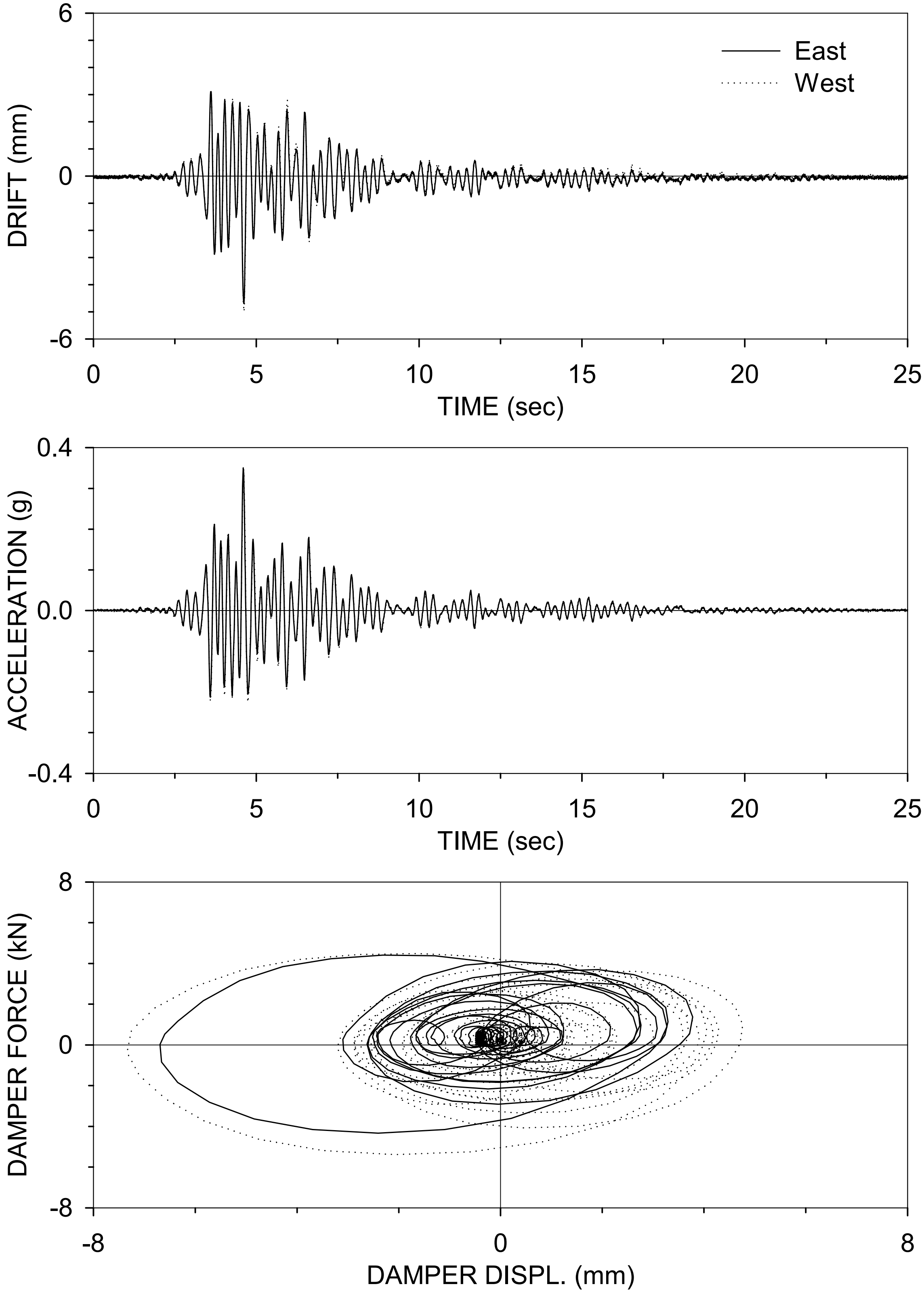

N9RSBD040 : NEWHALL 90 40% (05/17/99)

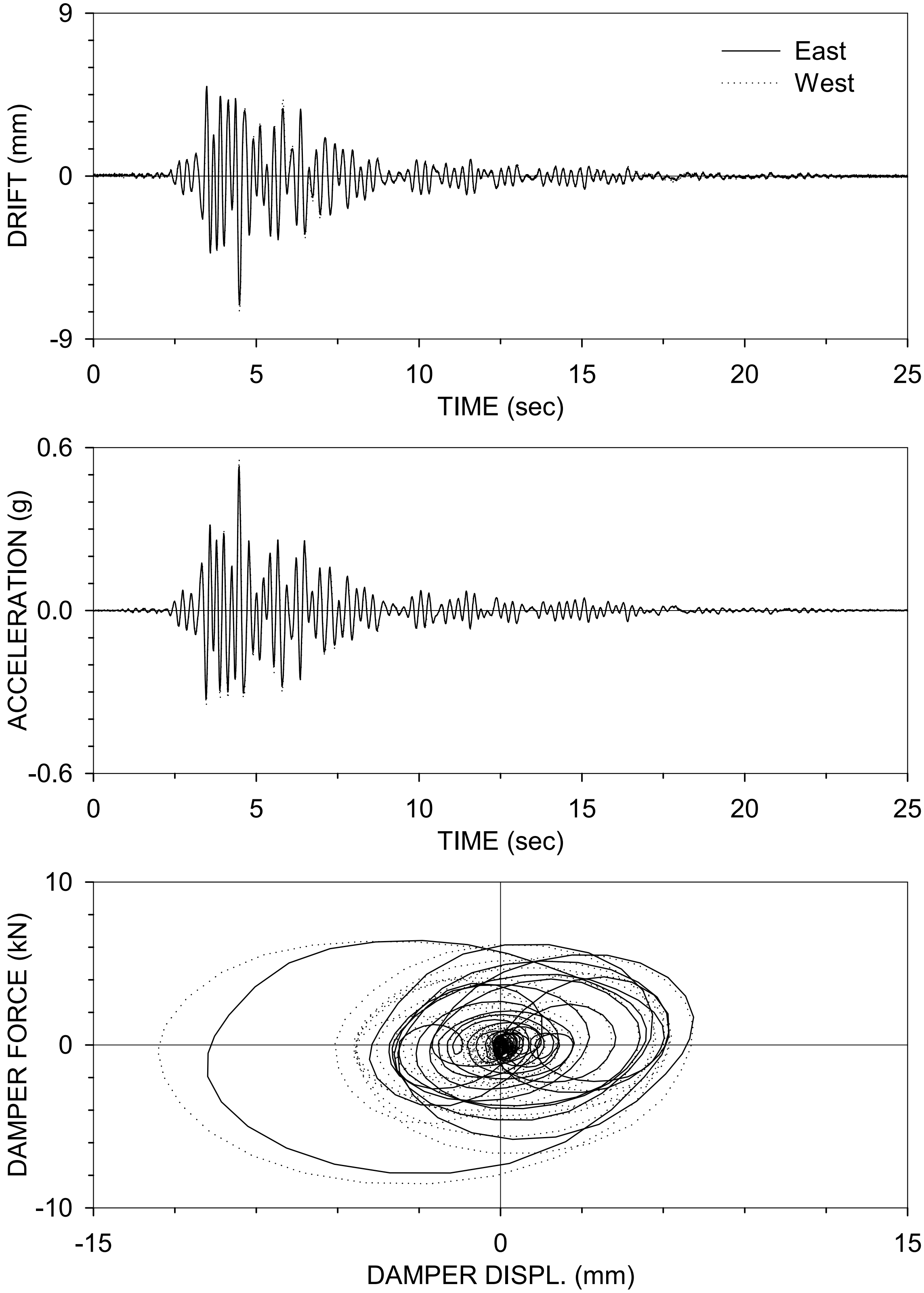

N9RSBD050 : NEWHALL 90 50% (05/17/99)

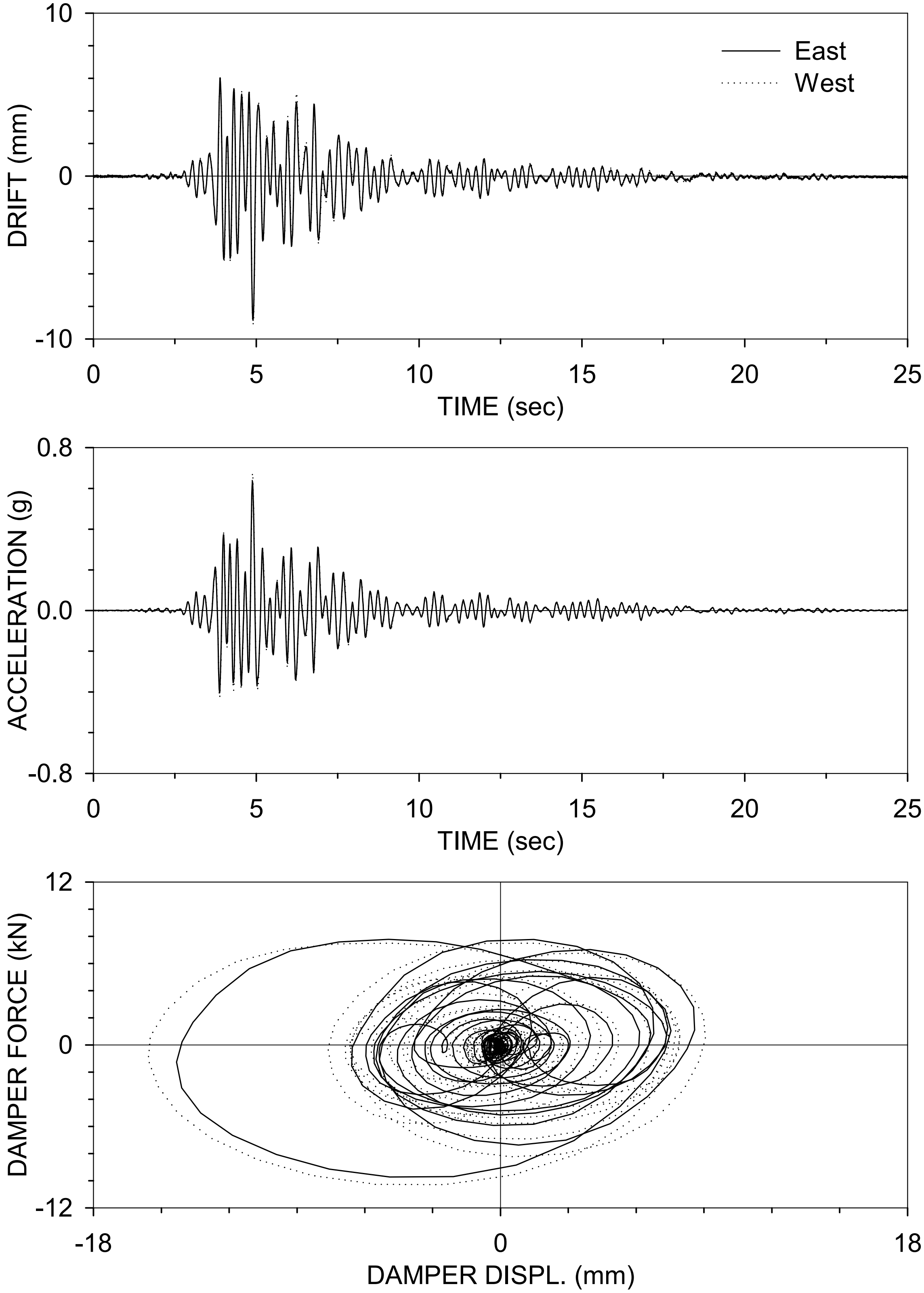

KORSBD025 : KOBE EW 25% (05/17/99)

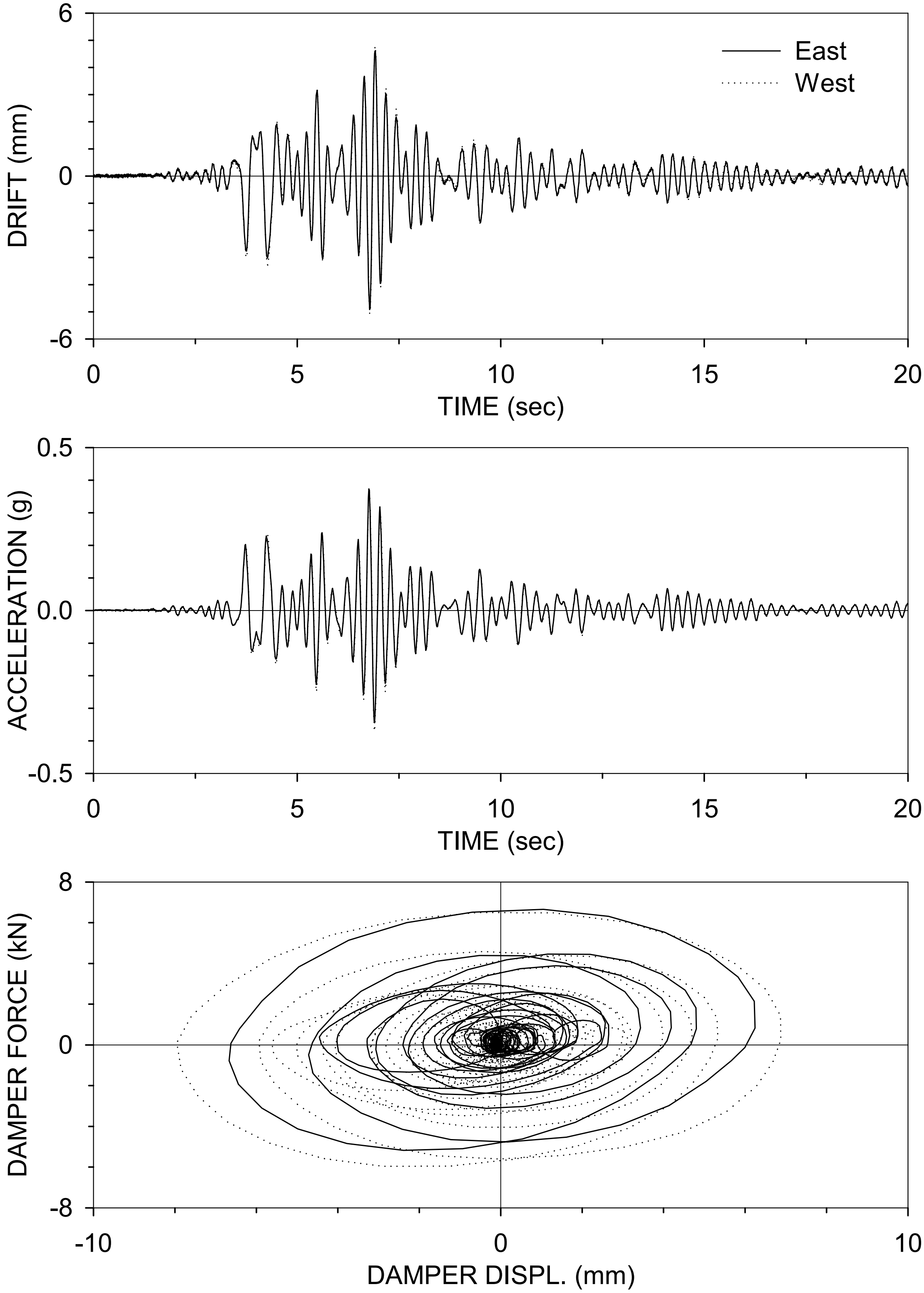

KORSBD040 : KOBE EW 40% (05/17/99)

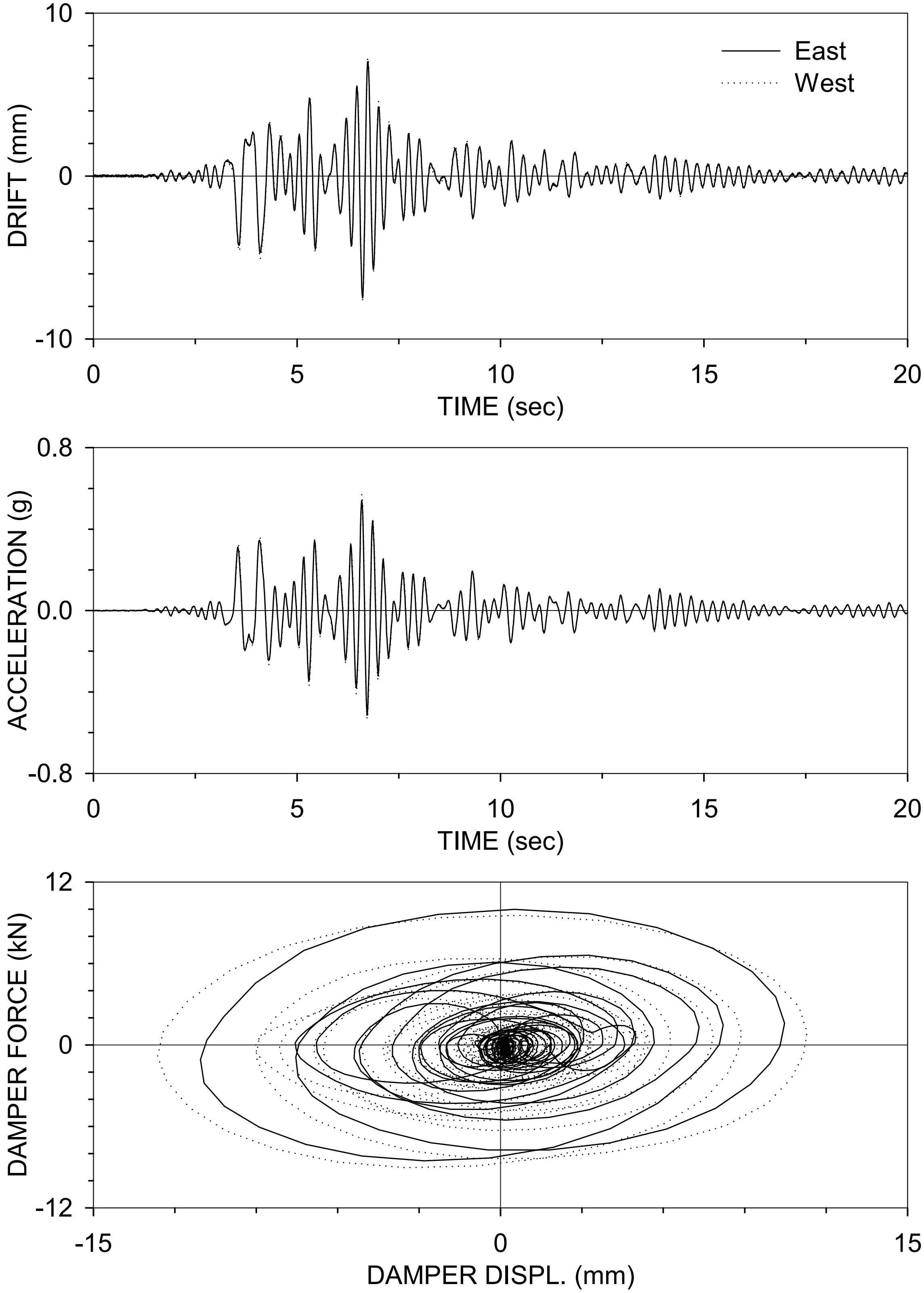

KORSBD050 : KOBE EW 50% (05/17/99)

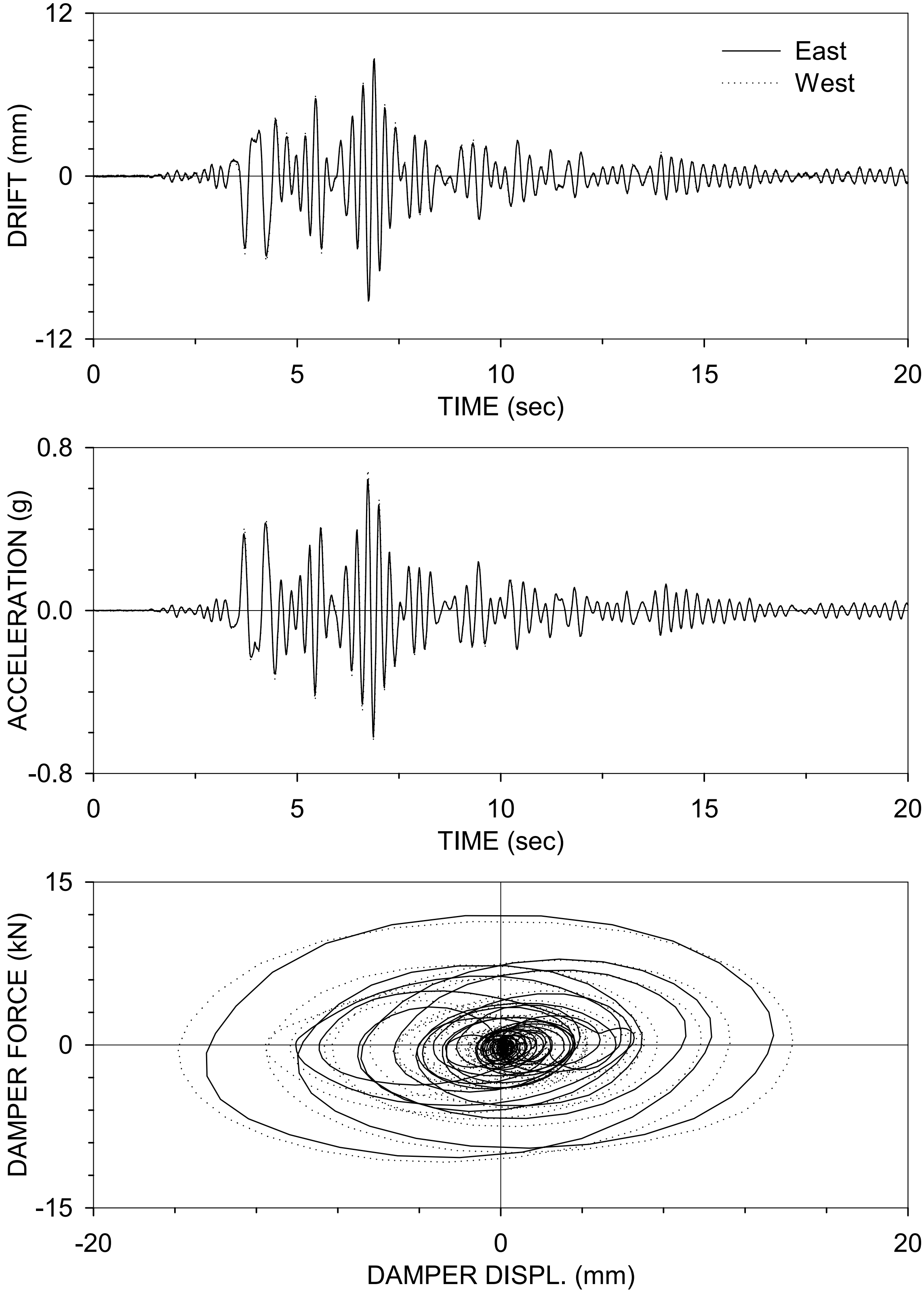

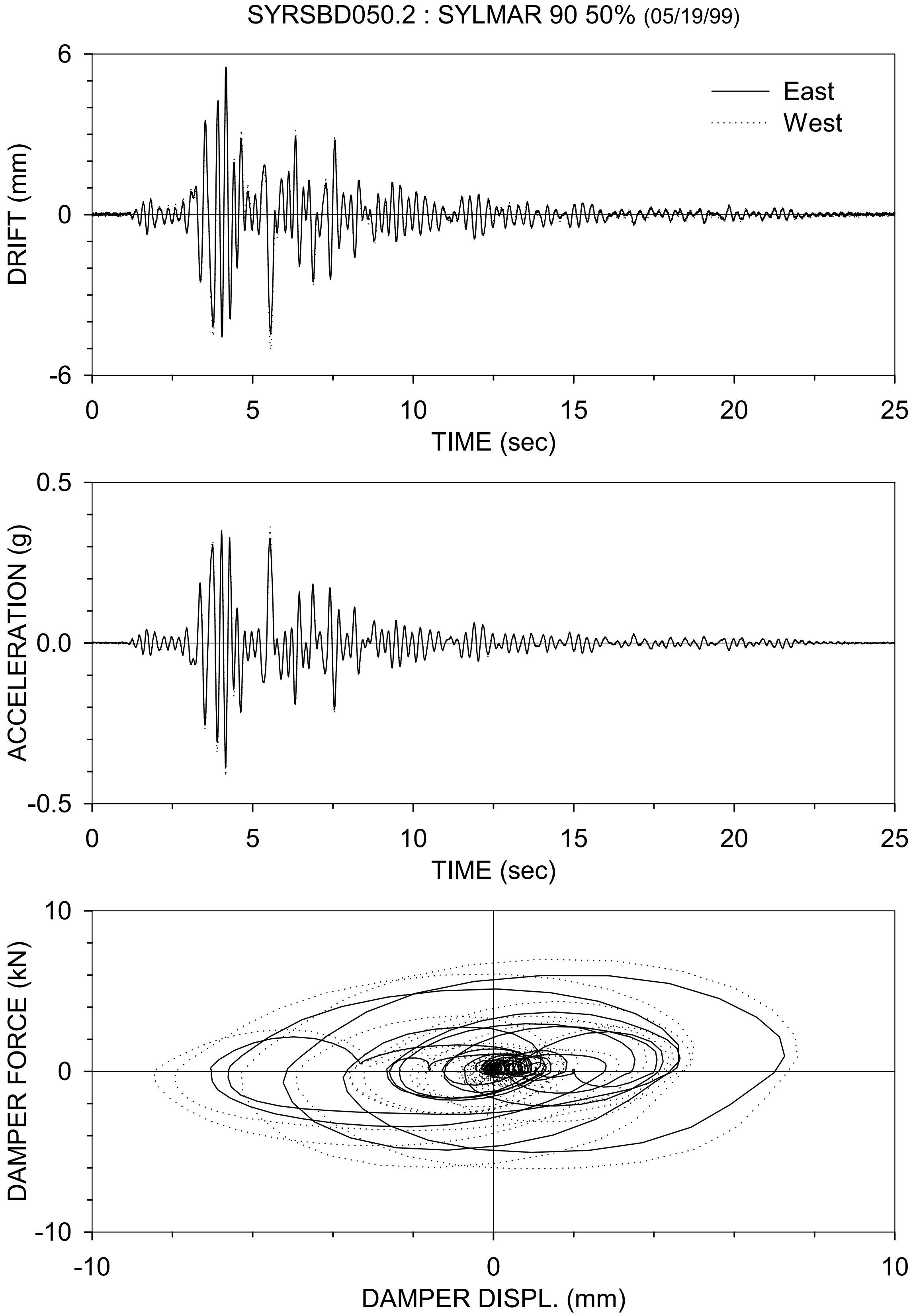
SYRSBD050.2 : SYLMAR 90 50% (05/19/99)
East
West
DRIFT (mm)
TIME (sec)
ACCELERATION (g)
TIME (sec)
DAMPER FORCE (kN)
DAMPER DISPL. (mm)

SYRSBD075.2 : SYLMAR 90 75% (05/19/99)

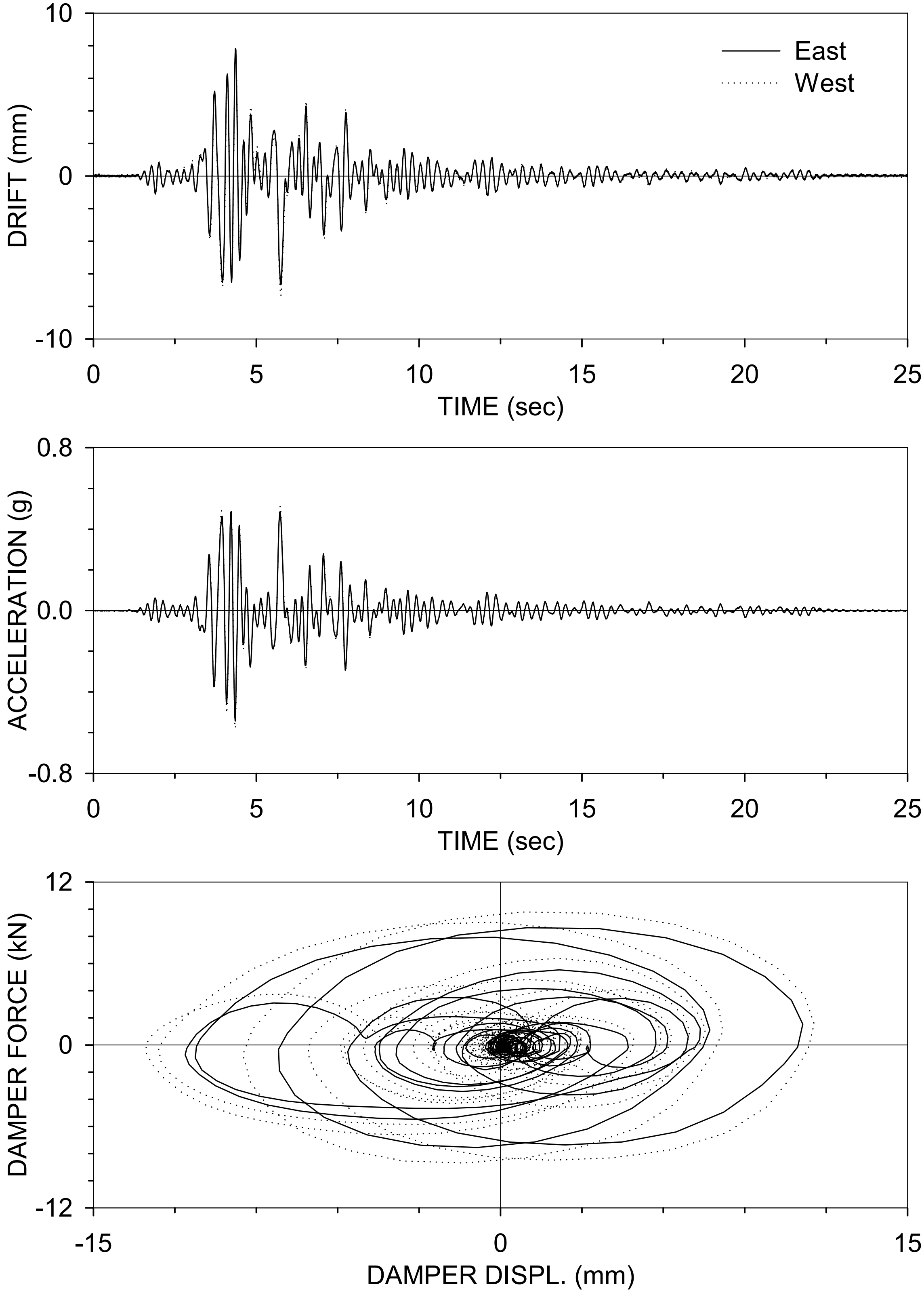

TARSBD200.2 : TAFT N21E 200% (05/19/99)

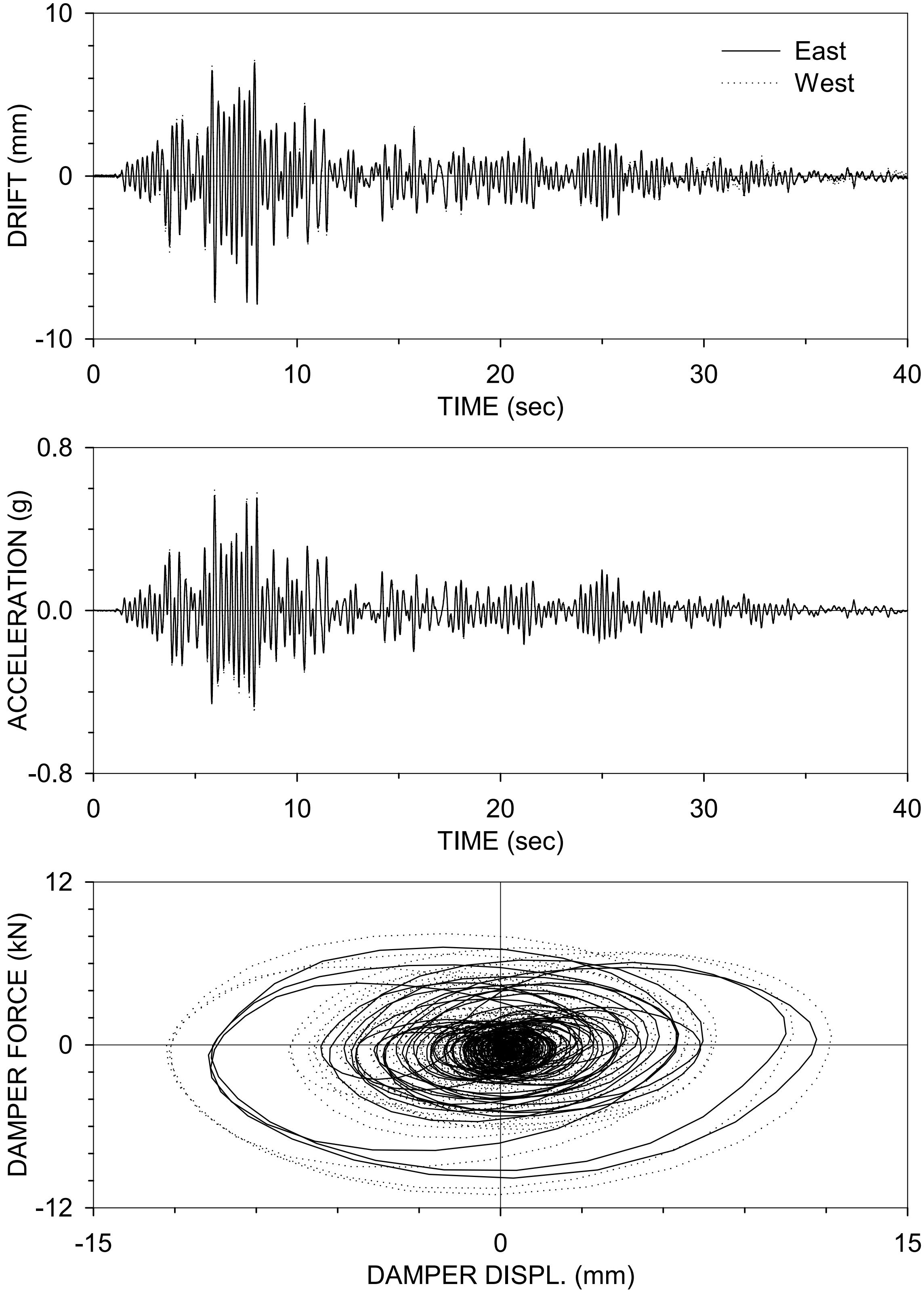

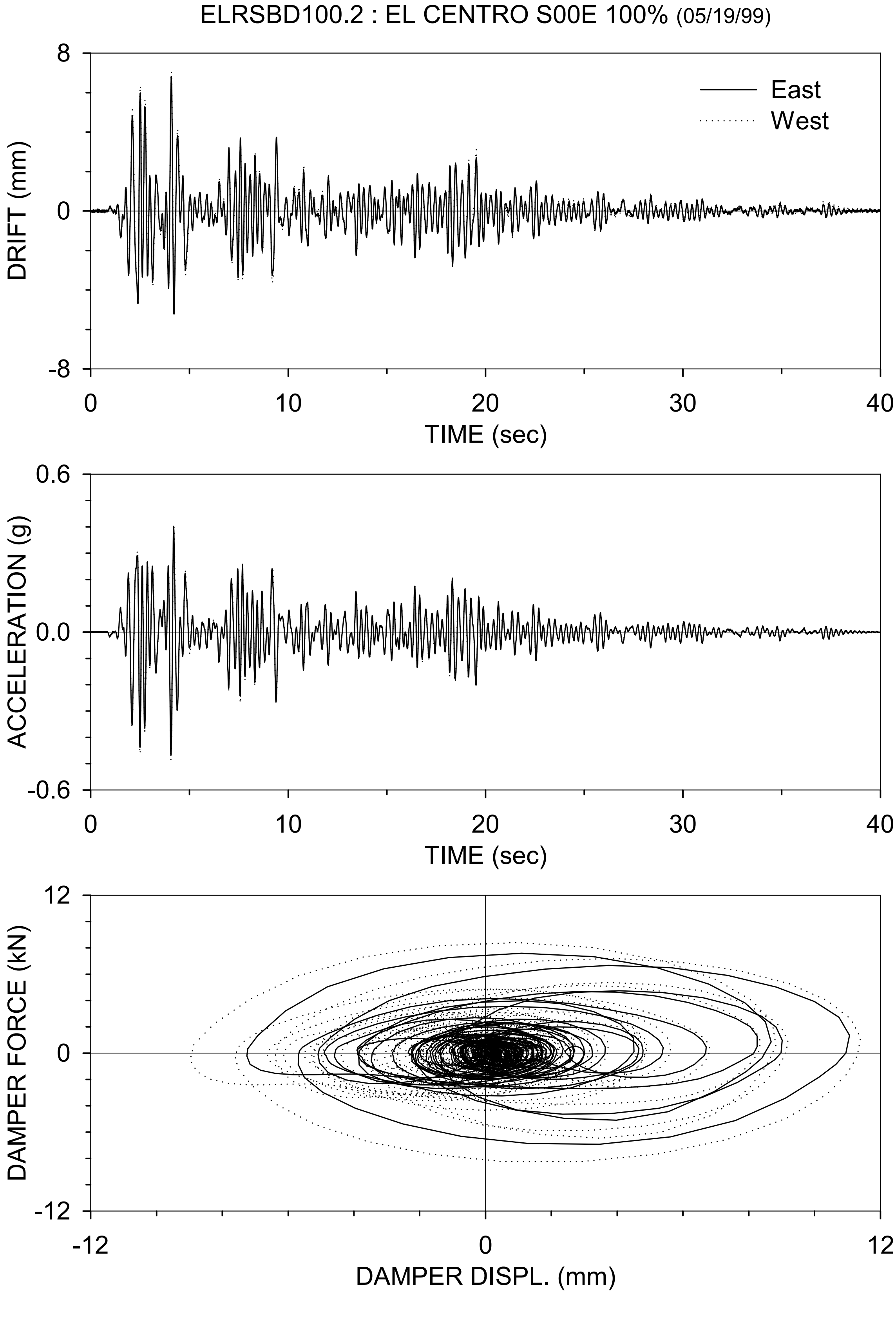
ELRSBD100.2 : EL CENTRO S00E 100% (05/19/99)
East
West
DRIFT (mm)
8
0
-8
0
10
20
30
40
TIME (sec)
ACCELERATION (g)
0.6
0.0
-0.6
0
10
20
30
40
TIME (sec)
DAMPER FORCE (kN)
12
0
-12
-12
0
12
DAMPER DISPL. (mm)

ELRSNN025 : EL CENTRO S00E 25%, BARE FRAME (05/21/99)

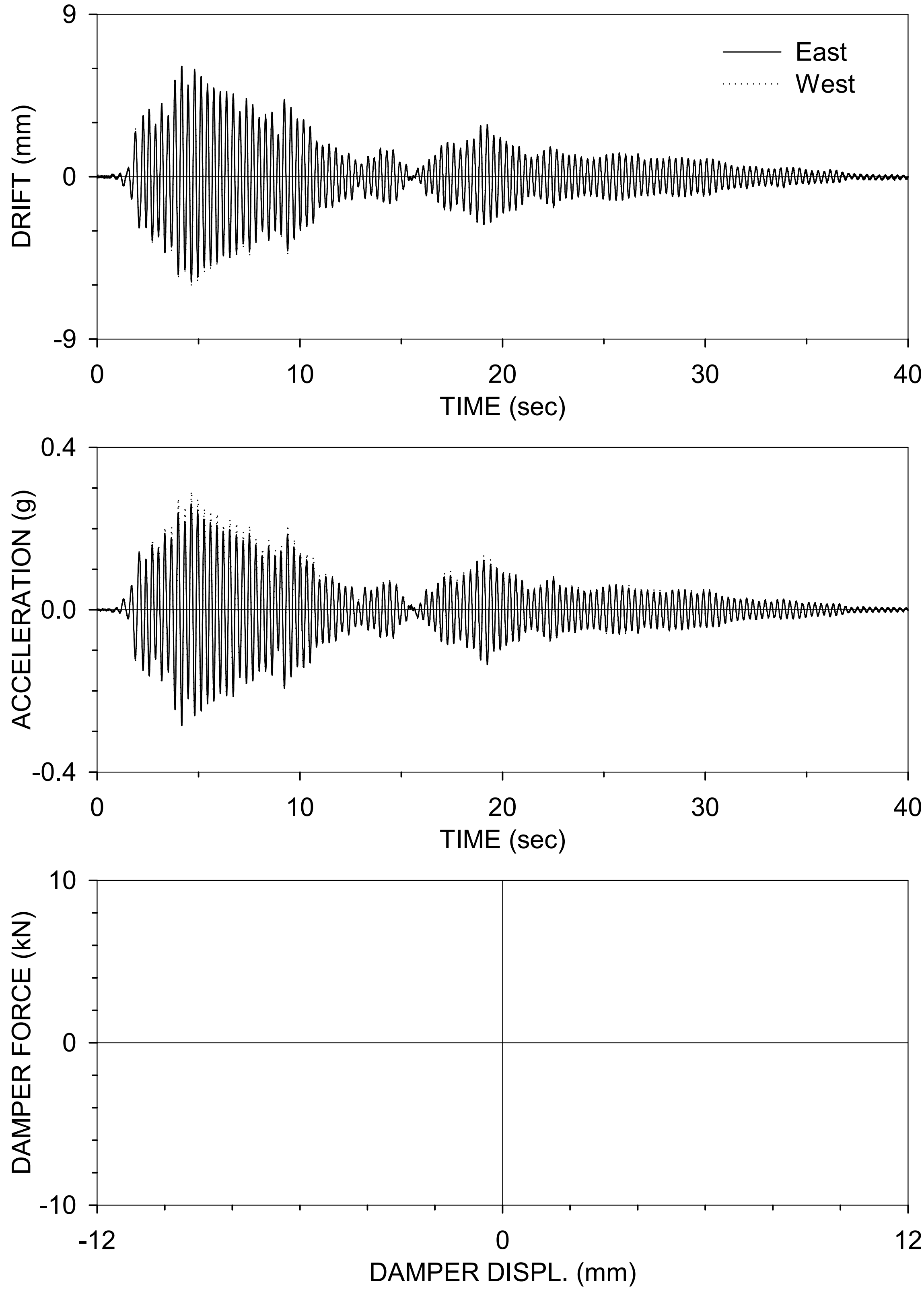

ELRSNN050 : EL CENTRO S00E 50%, BARE FRAME (05/21/99)

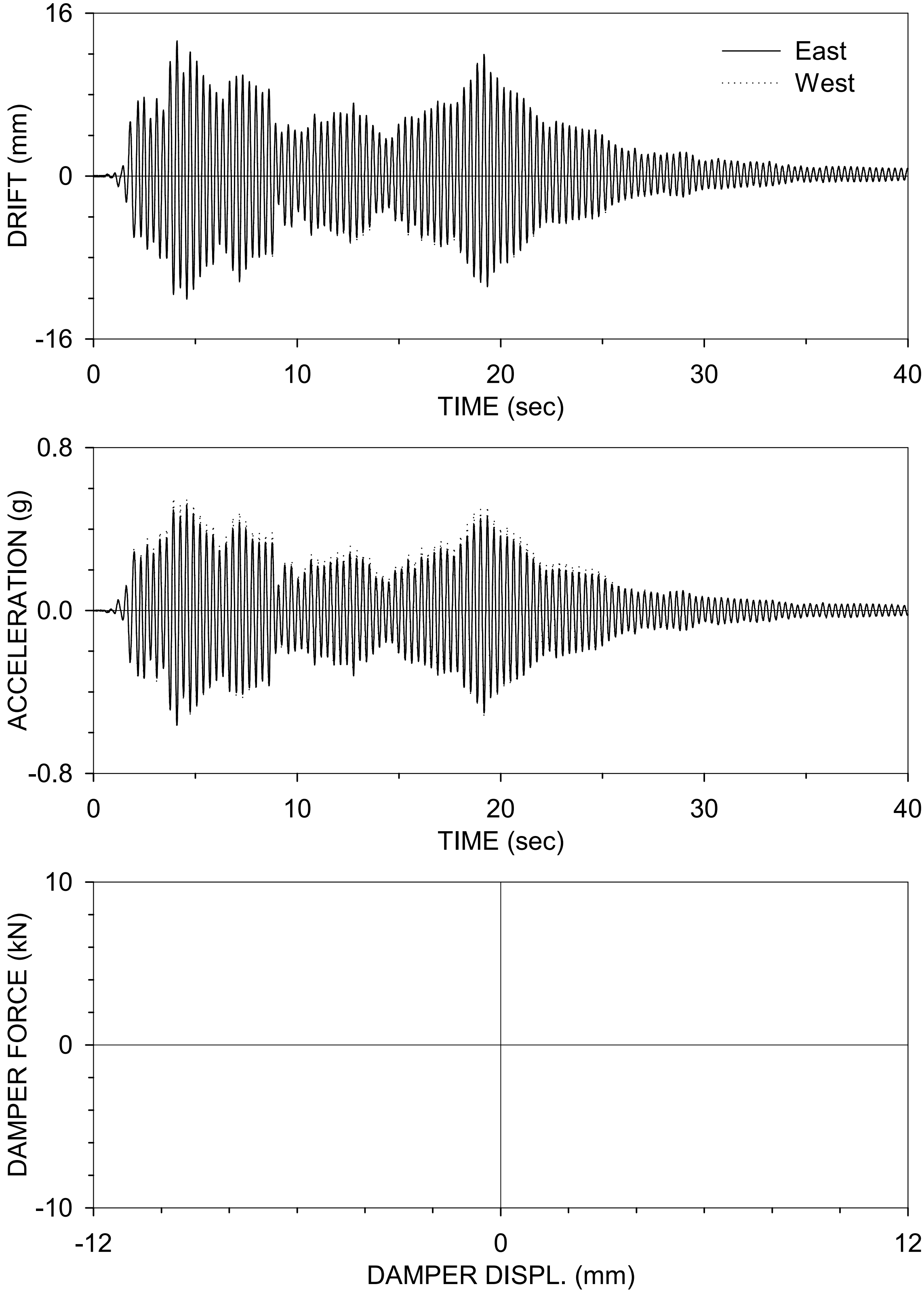

TARSNN100 : EL CENTRO S00E 100%, BARE FRAME (05/21/99)

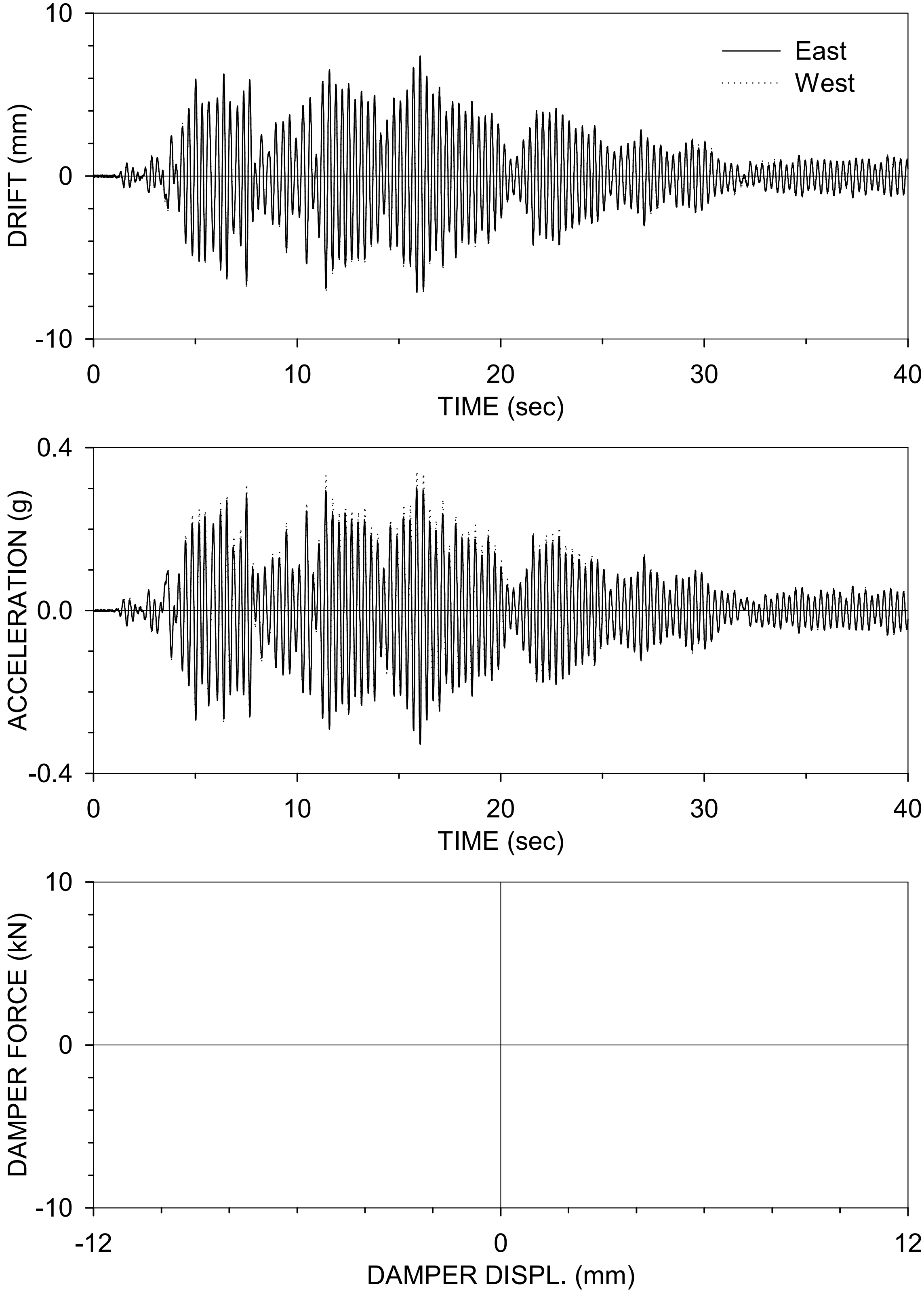

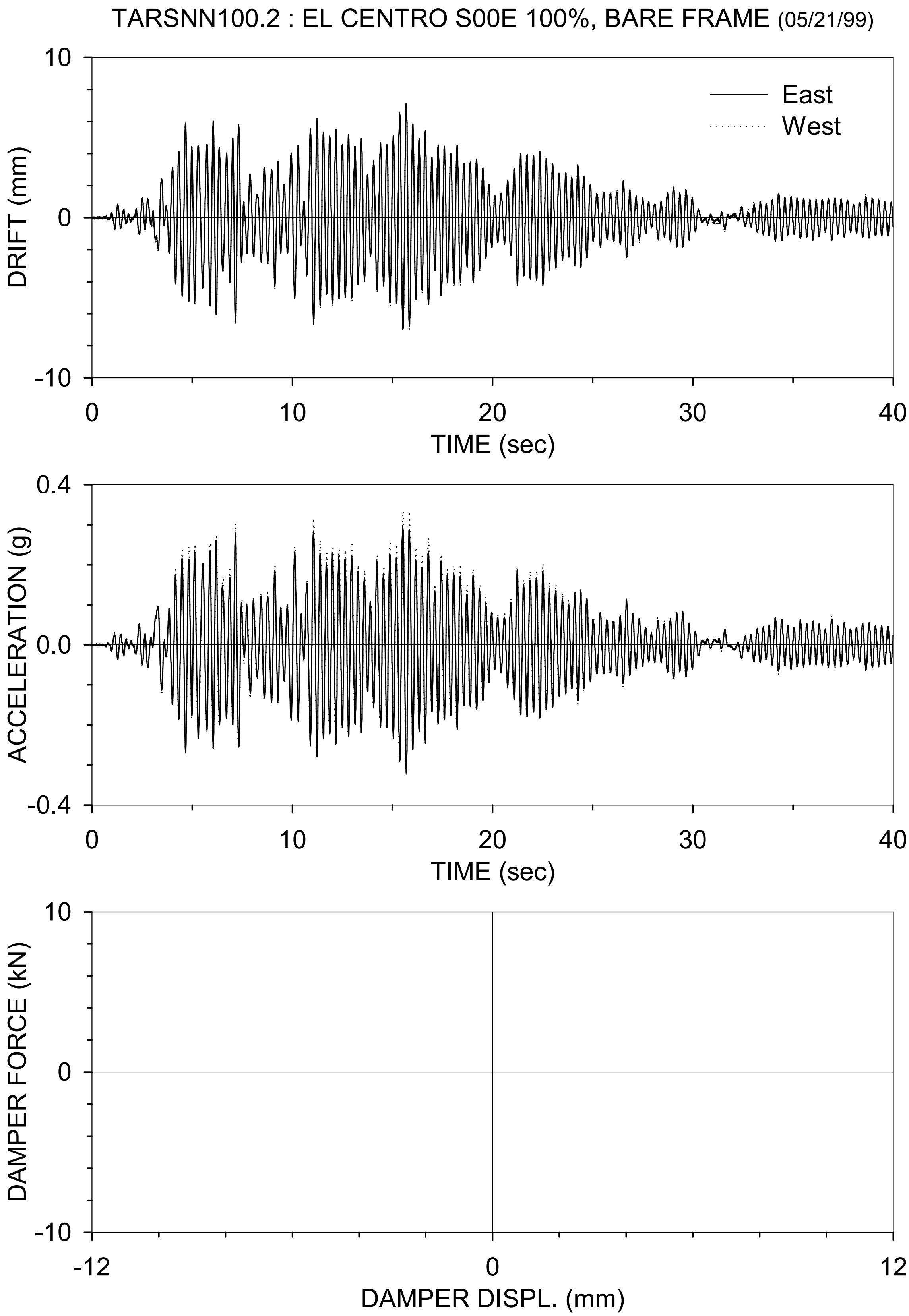

TARSNN100.2 : EL CENTRO S00E 100%, BARE FRAME (05/21/99)
East
West
DRIFT (mm)
10
0
-10
0
10
20
30
40
TIME (sec)
ACCELERATION (g)
0.4
0.0
-0.4
0
10
20
30
40
TIME (sec)
DAMPER FORCE (kN)
10
0
-10
-12
0
12
DAMPER DISPL. (mm)

ELRSNN050.2 : EL CENTRO S00E 50%, BARE FRAME (05/21/99)

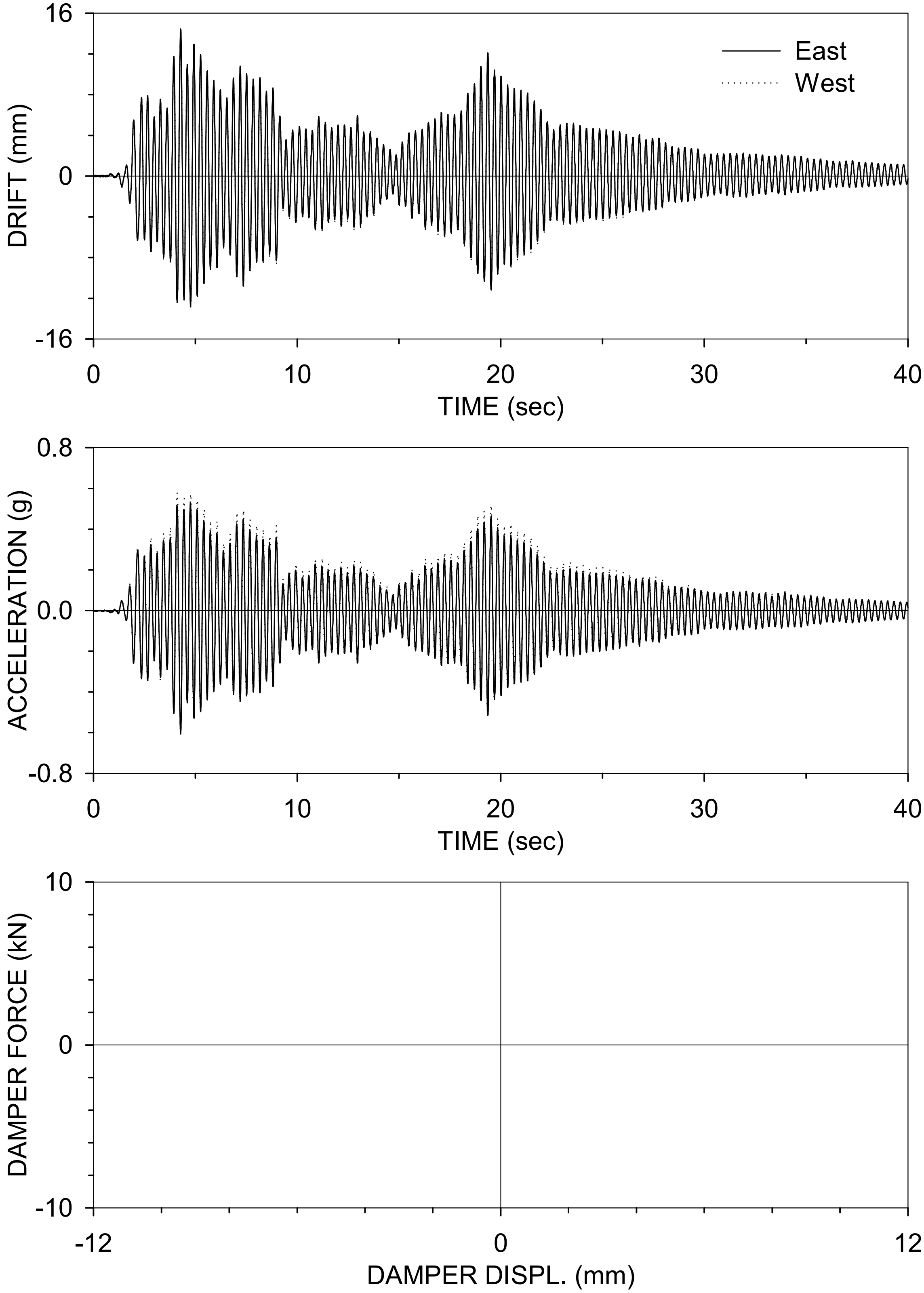

ELRSNN025.2 : EL CENTRO S00E 25%, BARE FRAME (05/21/99)

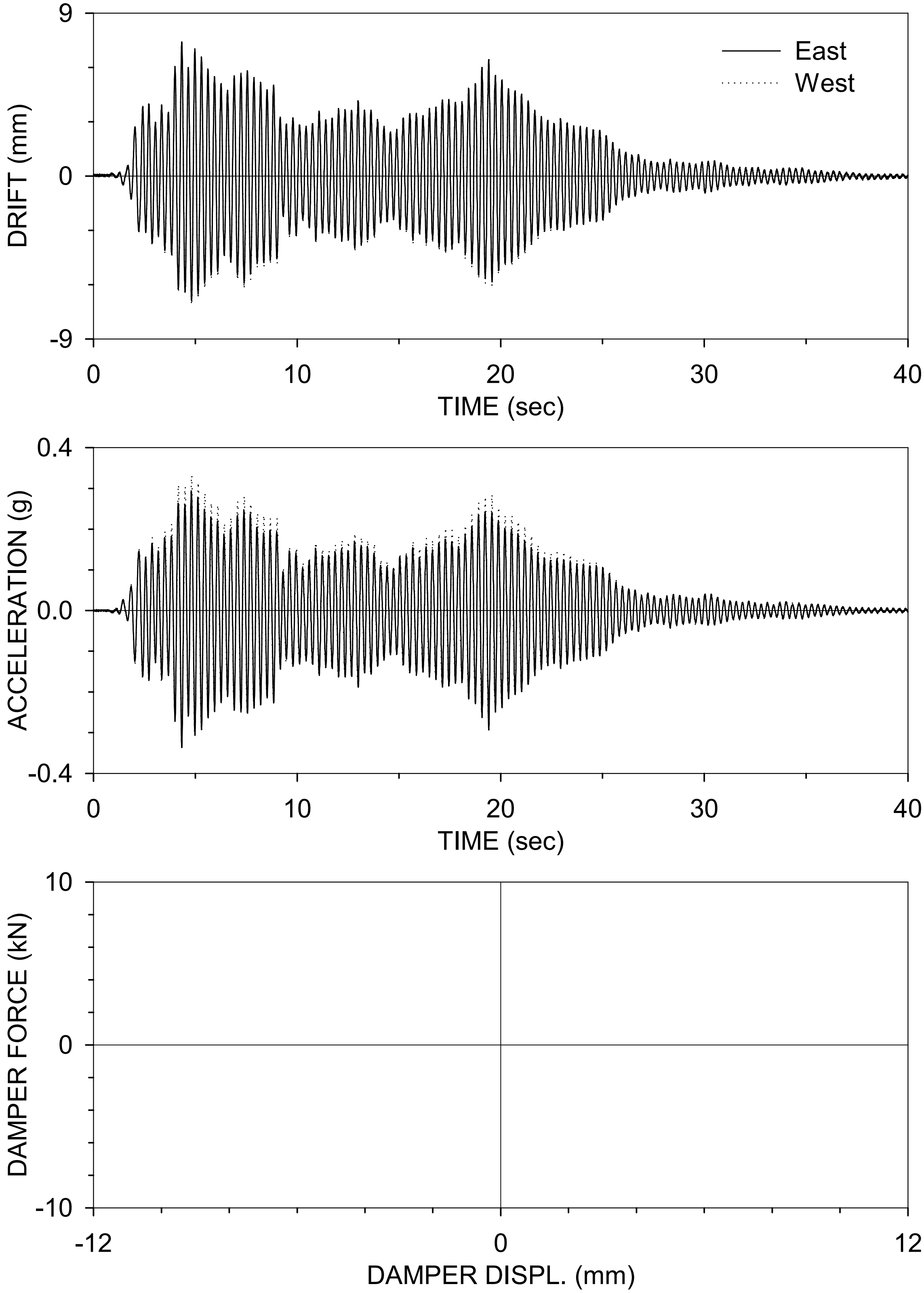

MIRSNN100 : MIYAGIKEN-OKI 100%, BARE FRAME (05/21/99)

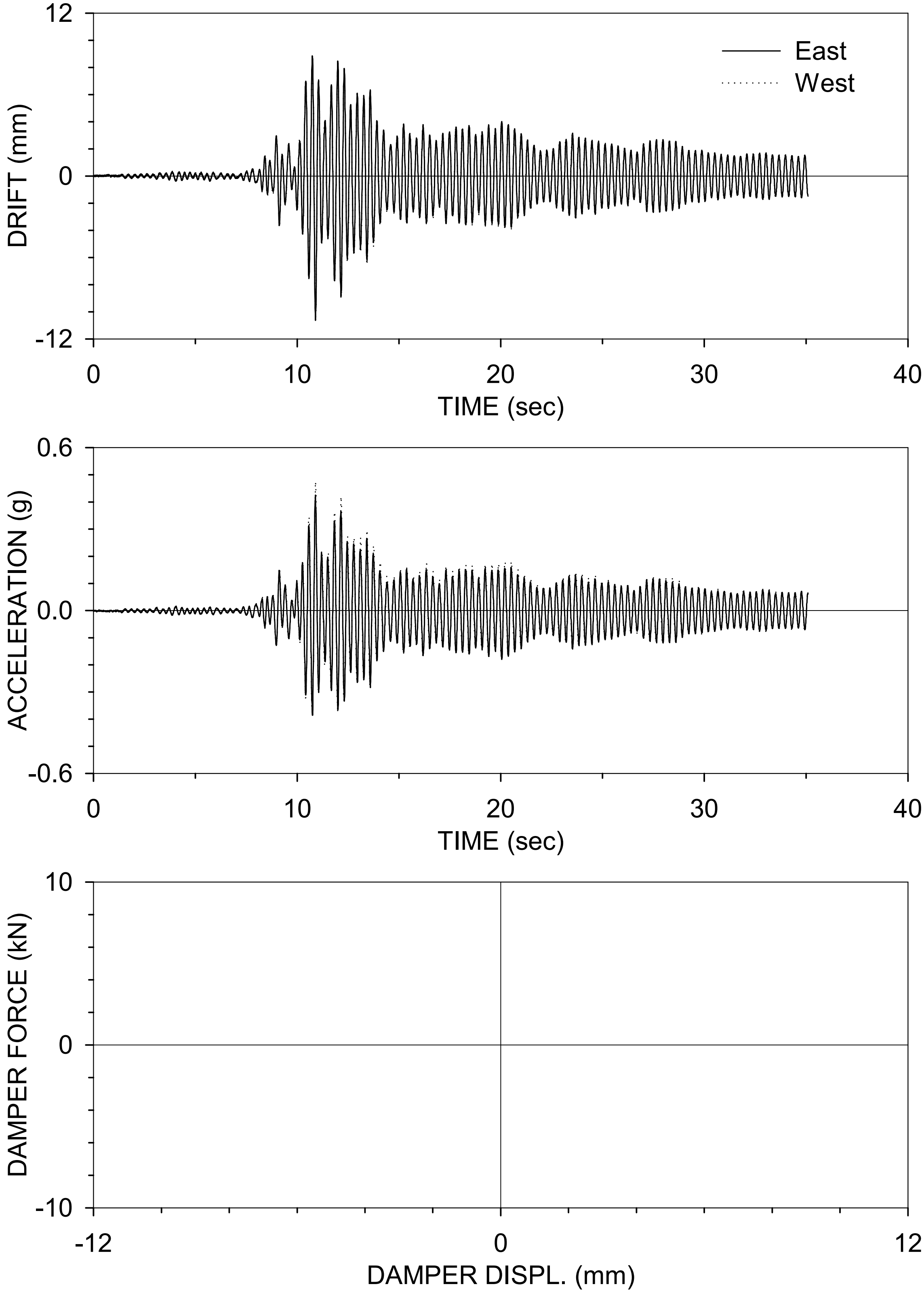

MXRSNN100 : MEXICO CITY 100%, BARE FRAME (05/21/99)

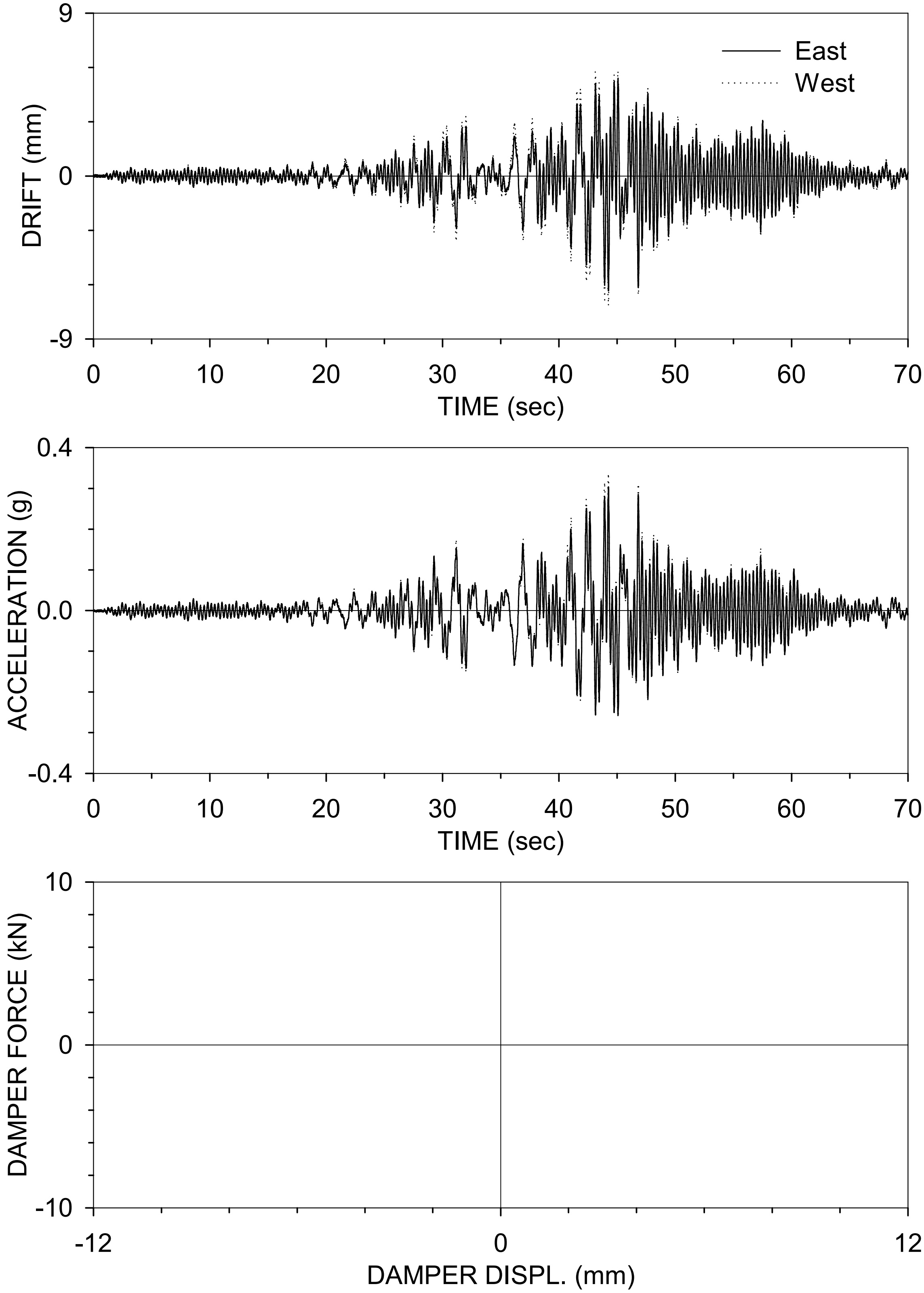

SYRSNN025 : SYLMAR 90 25%, BARE FRAME (05/21/99)

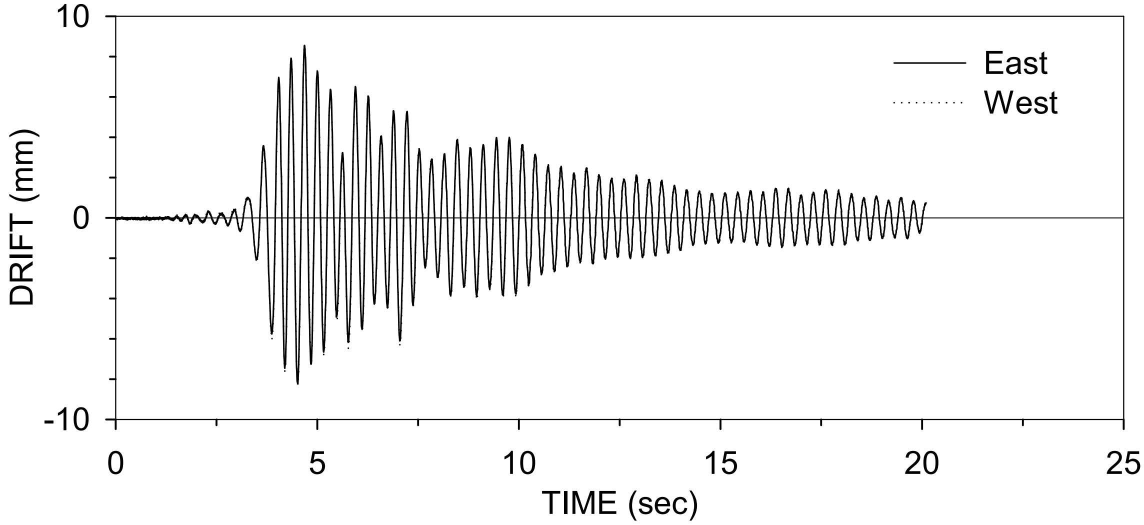

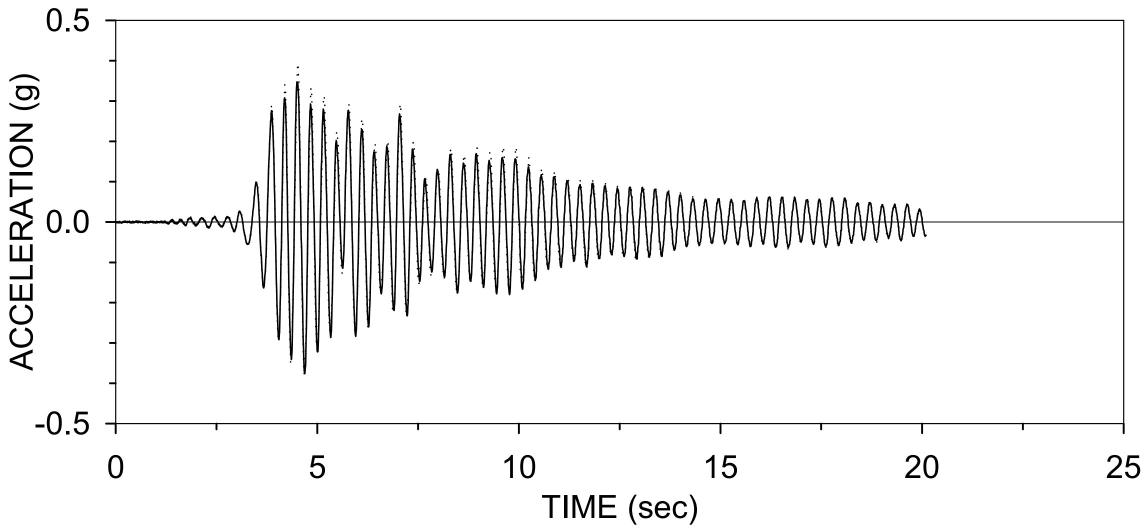

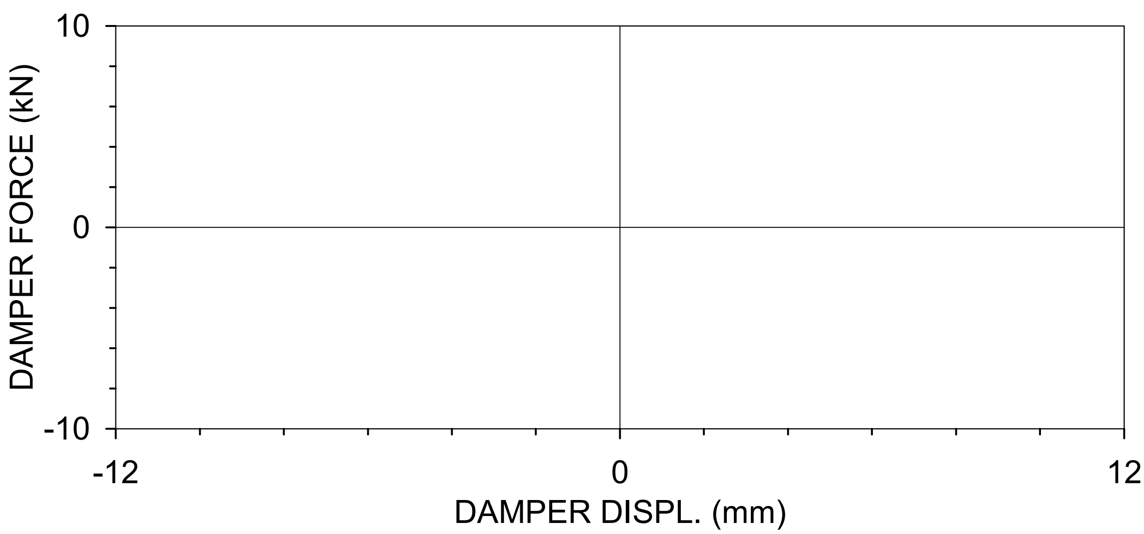

HARSNN050 : HACHINOHE NS 50%, BARE FRAME (05/21/99)

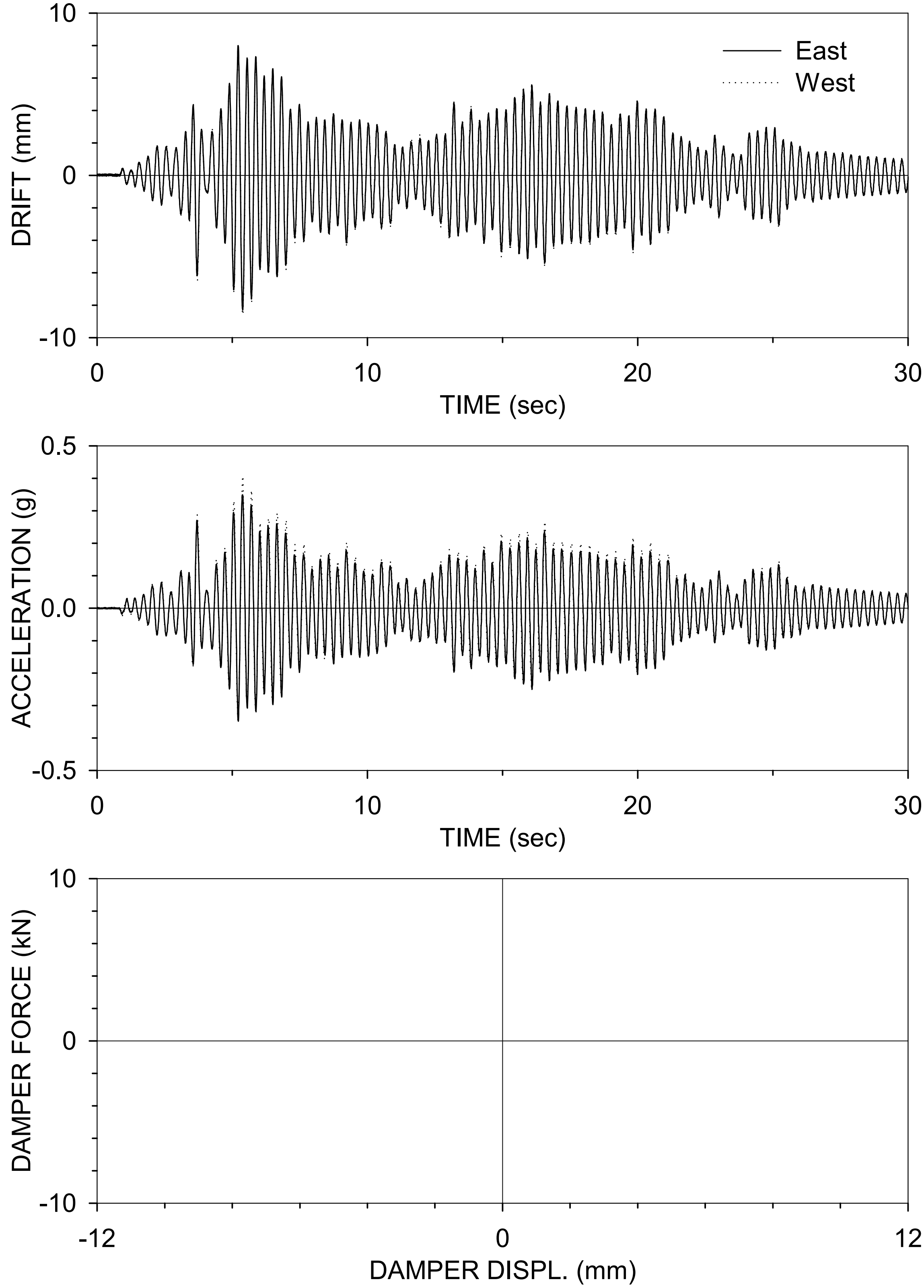

N9RSNN025 : NEWHALL 90 25%, BARE FRAME (05/21/99)

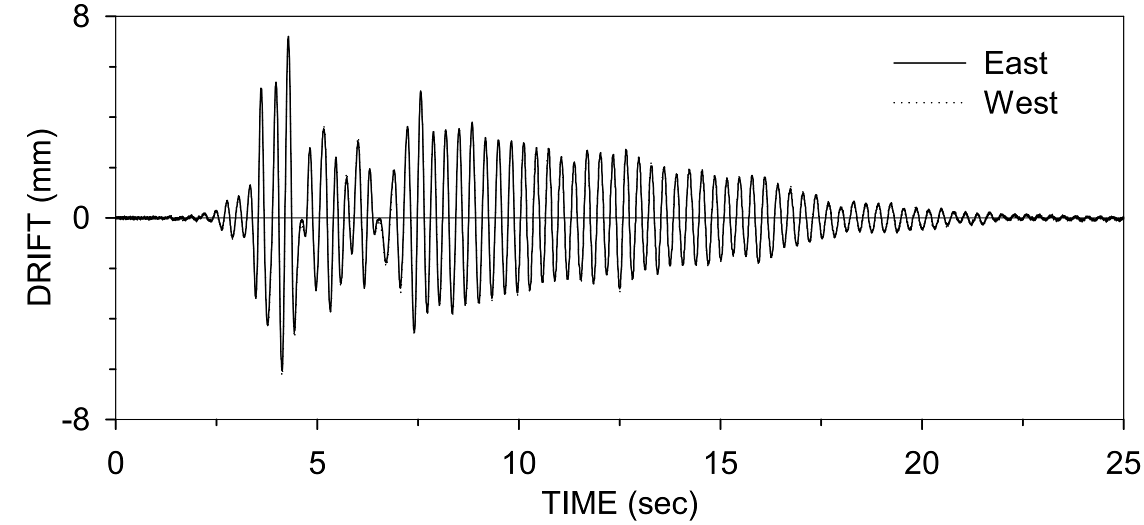

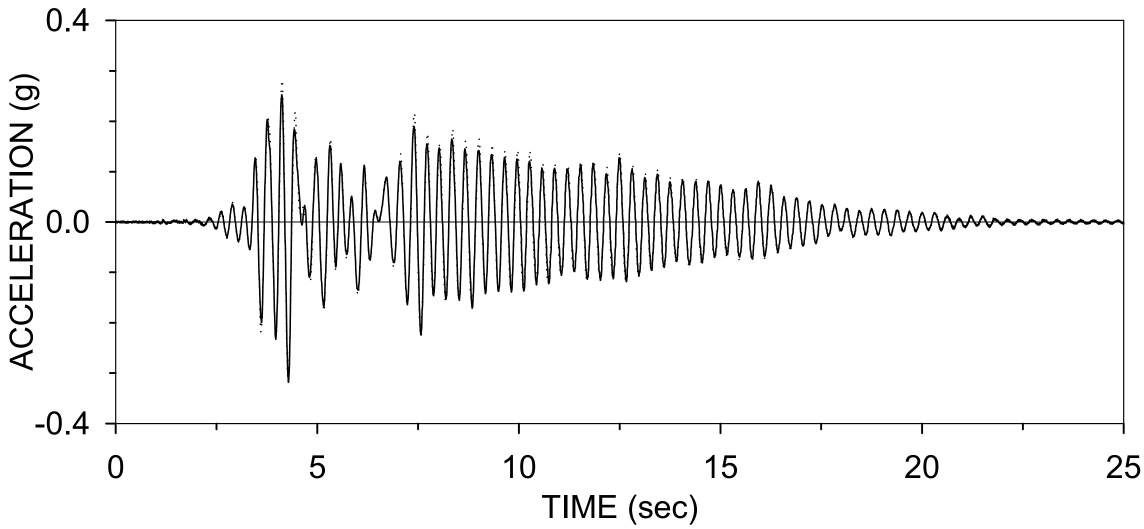

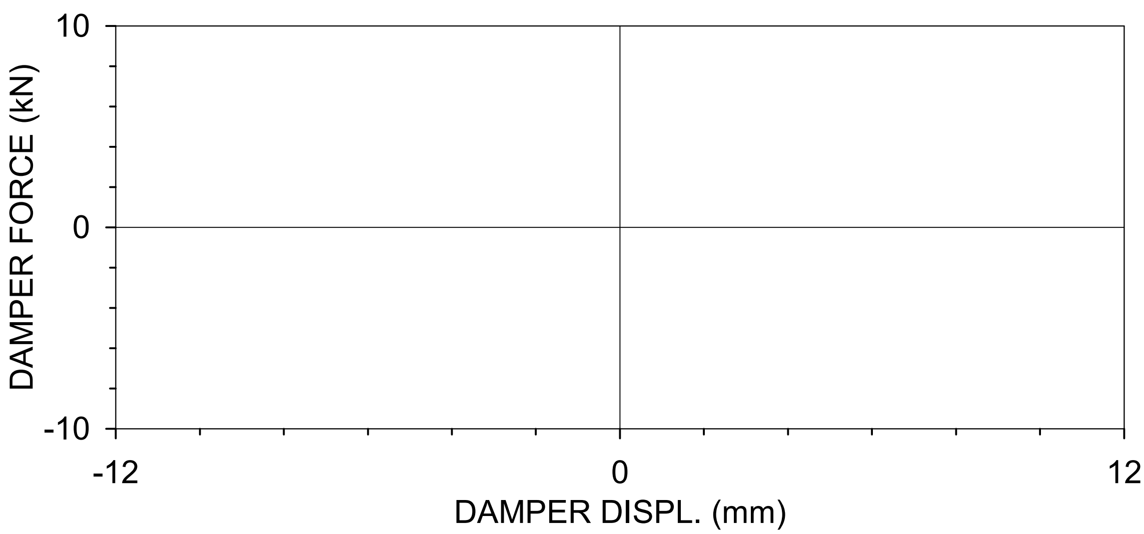

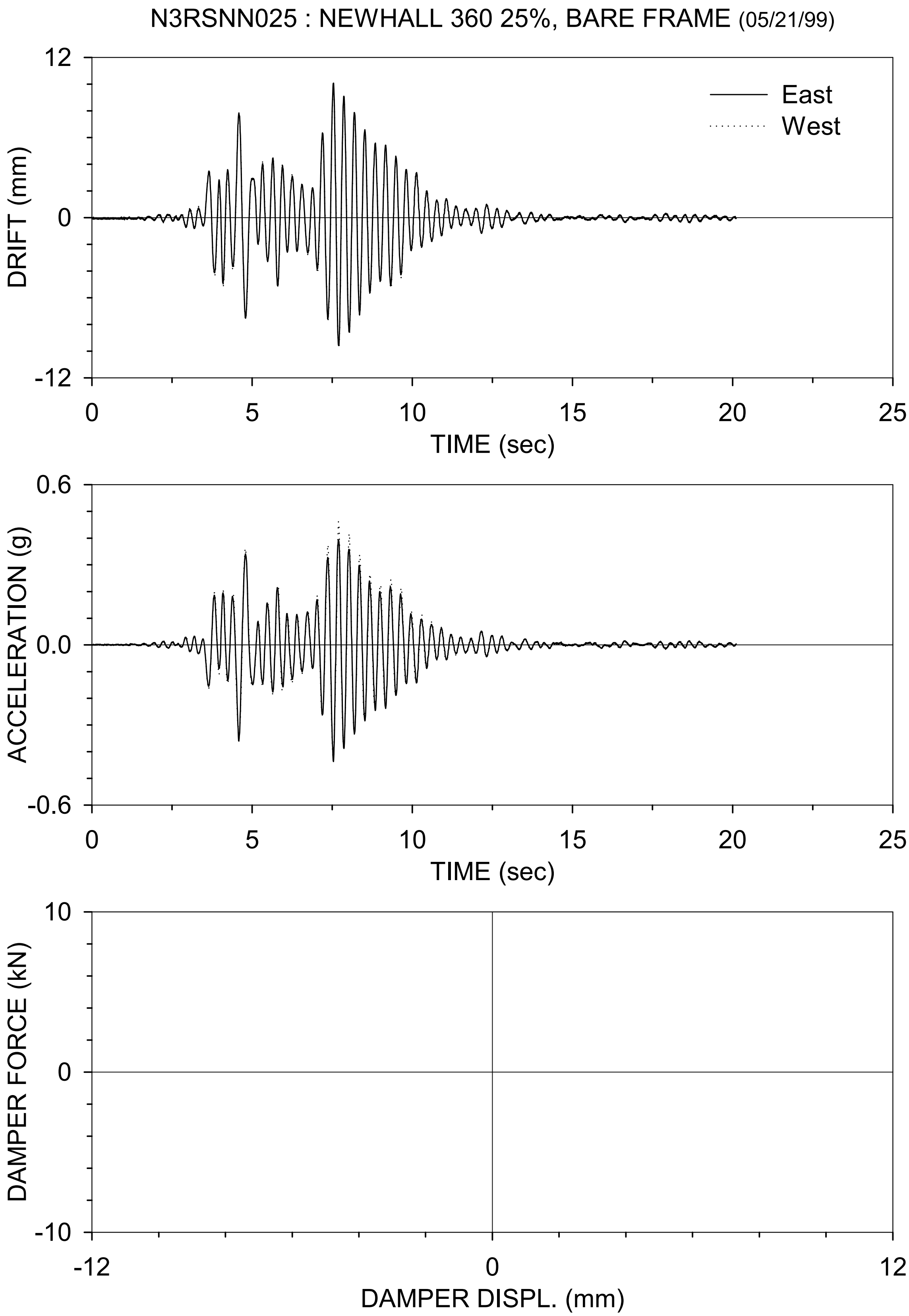
N3RSNN025 : NEWHALL 360 25%, BARE FRAME (05/21/99)
12
0
-12
DRIFT (mm)
East
West
0
5
10
15
20
25
TIME (sec)
0.6
0.0
-0.6
ACCELERATION (g)
0
5
10
15
20
25
TIME (sec)
10
0
-10
DAMPER FORCE (kN)
-12
0
12
DAMPER DISPL. (mm)

APPENDIX D

INPUT FILE FOR RESPONSE-HISTORY ANALYSIS OF FRAME WITH SAP2000 (USING FNA METHOD)

```
; scissor_elcen.s2k
; SAP2000 input file for earthquake-simulator testing using fast nonlinear analysis (FNA)
method.
;This file can be imported to SAP2000 version 7, or translated to run in version 8.
;
; E L  C E N T R O 100%
;
SYSTEM
  DOF=UX,UZ,RY  LENGTH=IN  FORCE=Kip  PAGE=SECTIONS

JOINT
  1  X=0  Y=0  Z=0
  2  X=0  Y=0  Z=75.875
  3  X=0  Y=0  Z=91.9375
  4  X=70.98813  Y=0  Z=75.875
  5  X=96.035  Y=0  Z=75.875
  6  X=96.035  Y=0  Z=75.875
  7  X=100  Y=0  Z=91.9375
  8  X=100  Y=0  Z=75.875
  9  X=100  Y=0  Z=9.5625
  10  X=100  Y=0  Z=0
  11  X=70.98813  Y=0  Z=73.14069
  12  X=73.17303  Y=0  Z=61.90036
  13  X=76.53955  Y=0  Z=63.12567
  14  X=77.52354  Y=0  Z=39.51905
  15  X=87.59333  Y=0  Z=43.18417
  16  X=89.02393  Y=0  Z=18.77181
  17  X=92.11961  Y=0  Z=19.89855
  18  X=94.12875  Y=0  Z=9.5625
  19  X=0  Y=0  Z=117.7375
  20  X=50  Y=0  Z=117.7375
  21  X=100  Y=0  Z=117.7375
  22  X=77.52354  Y=0  Z=39.51905
  23  X=87.59333  Y=0  Z=43.18417

RESTRAINT
  ADD=1  DOF=U1,U3
  ADD=10  DOF=U1,U3

CONSTRAINT
  NAME=EQUAL1  TYPE=EQUAL  DOF=UX,UZ,RY  CSYS=0
    ADD=9
    ADD=18
  NAME=EQUAL2  TYPE=EQUAL  DOF=UX,UZ,RY  CSYS=0
    ADD=4
    ADD=11
  NAME=EQUAL3  TYPE=EQUAL  DOF=UX,UZ  CSYS=0
    ADD=14
    ADD=22
  NAME=EQUAL4  TYPE=EQUAL  DOF=UX,UZ  CSYS=0
    ADD=15
```

```
  ADD=23
 NAME=TRANS1  TYPE=EQUAL  DOF=UX,UZ  CSYS=0
  ADD=5
  ADD=6

PATTERN
 NAME=DEFAULT

SPRING
 ADD=1  R2=45000
 ADD=10  R2=45000

MASS
 ADD=2  U1=4.605691E-04  U3=4.605691E-04
 ADD=3  U1=1.336188E-03  U3=1.336188E-03
 ADD=4  U1=2.291214E-04  U3=2.291214E-04
 ADD=7  U1=1.336188E-03  U3=1.336188E-03
 ADD=8  U1=3.050554E-04  U3=3.050554E-04
 ADD=11  U1=3.970103E-05  U3=3.970103E-05
 ADD=14  U1=7.940207E-05  U3=7.940207E-05
 ADD=15  U1=7.940207E-05  U3=7.940207E-05
 ADD=18  U1=3.970103E-05  U3=3.970103E-05
 ADD=19  U1=9.709492E-03  U3=9.709492E-03
 ADD=20  U1=1.941898E-02  U3=1.941898E-02
 ADD=21  U1=9.709492E-03  U3=9.709492E-03

MATERIAL
 NAME=STEEL  IDES=N
  T=0  E=29000  U=.3  A=0

FRAME SECTION
 NAME=W8X21 MAT=STEEL A=6.16 J=.28 I=75.3,9.77 AS=2.07,3.5133
S=18.18841,3.70778 Z=20.4,5.69 R=3.496288,1.25938 T=8.28,5.27,.4,.25,5.27,.4 SHN=W8X21
DSG=W
 NAME=W8X24 MAT=STEEL A=7.08 J=.35 I=82.8,18.3 AS=1.9429,4.33
S=20.88272,5.635104 Z=23.2,8.57 R=3.419783,1.607714 T=7.93,6.495,.4,.245,6.495,.4
SHN=W8X24 DSG=W
 NAME=PLATE MAT=STEEL SH=R T=.25,4 A=1 J=2.001302E-02 I=5.208333E-03,1.333333
AS=.8333333,.8333333
 NAME=TUBE MAT=STEEL A=1.59 J=1.36 I=.766,.766 AS=1,1 S=.766,.766 Z=1,1
R=.69409,.69409 T=2,2,.25,.25,0,0 SHN=TS2X2X1/4 DSG=B
 NAME=RIGID MAT=STEEL A=100 J=0 I=1000,0 AS=0,0 T=1,1

NLPROP
 NAME=DAMPER    TYPE=Damper
  DOF=U1  KE=0  CE=0  K=1000  C=.36  CEXP=.76
 NAME=SPRING1    TYPE=Damper
  DOF=R3  KE=1660  CE=0
 NAME=SPRING3    TYPE=Damper
  DOF=R3  KE=1000  CE=0
 NAME=SPRING2    TYPE=Damper
```

```
   DOF=R3  KE=45000  CE=0

FRAME
 1  J=1,2  SEC=W8X24  NSEG=2  ANG=0  JOFF=12.14  RIGID=.3
 2  J=2,3  SEC=W8X24  NSEG=2  ANG=0  IOFF=12.14  RIGID=.3
 3  J=2,4  SEC=W8X21  NSEG=2  ANG=0  IOFF=11.965  RIGID=.3
 4  J=4,5  SEC=W8X21  NSEG=2  ANG=0
 5  J=6,8  SEC=W8X24  NSEG=2  ANG=0  JOFF=3.92535  RIGID=1
 6  J=7,8  SEC=W8X24  NSEG=2  ANG=0  JOFF=12.14  RIGID=.3
 7  J=8,9  SEC=W8X24  NSEG=2  ANG=0  IOFF=12.14  RIGID=.3
 8  J=9,10  SEC=W8X24  NSEG=2  ANG=0
 9  J=11,12  SEC=PLATE  NSEG=2  ANG=0
 10  J=11,13  SEC=PLATE  NSEG=2  ANG=0
 11  J=12,14  SEC=TUBE  NSEG=2  ANG=0
 12  J=13,15  SEC=TUBE  NSEG=2  ANG=0
 13  J=22,16  SEC=TUBE  NSEG=2  ANG=0
 14  J=23,17  SEC=TUBE  NSEG=2  ANG=0
 15  J=16,18  SEC=PLATE  NSEG=2  ANG=0
 16  J=17,18  SEC=PLATE  NSEG=2  ANG=0
 17  J=3,19  SEC=RIGID  NSEG=2  ANG=0  IREL=R3
 18  J=19,20  SEC=RIGID  NSEG=2  ANG=0
 19  J=20,21  SEC=RIGID  NSEG=2  ANG=0
 20  J=21,7  SEC=RIGID  NSEG=2  ANG=0  JREL=R3

NLLINK
 1  J=14,15  NLP=DAMPER  ANG=0
 2  J=5,6  NLP=SPRING1  ANG=0  AXDIR=+Z
 3  J=14,22  NLP=SPRING3  ANG=0  AXDIR=+Z
 4  J=15,23  NLP=SPRING3  ANG=0  AXDIR=+Z

LOAD
 NAME=LOAD1  CSYS=0

MODE
 TYPE=RITZ  N=10
   ACC=UX
   ACC=UZ
   NLLINK=*

FUNCTION
 NAME=ELCEN106   DT=0.01  NPL=1 PRINT=N FILE=ELRSD106.txt  ; ground motion input
in a separate file.

HISTORY
 NAME=ELRSD106 TYPE=NON NSTEP=4009 DT=.01 DAMP=.02
   ACC=U1  ANG=0 FUNC=ELCEN106 SF=386.22 AT=0

OUTPUT

END
```

Multidisciplinary Center for Earthquake Engineering Research
List of Technical Reports

The Multidisciplinary Center for Earthquake Engineering Research (MCEER) publishes technical reports on a variety of subjects related to earthquake engineering written by authors funded through MCEER. These reports are available from both MCEER Publications and the National Technical Information Service (NTIS). Requests for reports should be directed to MCEER Publications, Multidisciplinary Center for Earthquake Engineering Research, State University of New York at Buffalo, Red Jacket Quadrangle, Buffalo, New York 14261. Reports can also be requested through NTIS, 5285 Port Royal Road, Springfield, Virginia 22161. NTIS accession numbers are shown in parenthesis, if available.

NCEER-87-0001 "First-Year Program in Research, Education and Technology Transfer," 3/5/87, (PB88-134275, A04, MF-A01).

NCEER-87-0002 "Experimental Evaluation of Instantaneous Optimal Algorithms for Structural Control," by R.C. Lin, T.T. Soong and A.M. Reinhorn, 4/20/87, (PB88-134341, A04, MF-A01).

NCEER-87-0003 "Experimentation Using the Earthquake Simulation Facilities at University at Buffalo," by A.M. Reinhorn and R.L. Ketter, to be published.

NCEER-87-0004 "The System Characteristics and Performance of a Shaking Table," by J.S. Hwang, K.C. Chang and G.C. Lee, 6/1/87, (PB88-134259, A03, MF-A01). This report is available only through NTIS (see address given above).

NCEER-87-0005 "A Finite Element Formulation for Nonlinear Viscoplastic Material Using a Q Model," by O. Gyebi and G. Dasgupta, 11/2/87, (PB88-213764, A08, MF-A01).

NCEER-87-0006 "Symbolic Manipulation Program (SMP) - Algebraic Codes for Two and Three Dimensional Finite Element Formulations," by X. Lee and G. Dasgupta, 11/9/87, (PB88-218522, A05, MF-A01).

NCEER-87-0007 "Instantaneous Optimal Control Laws for Tall Buildings Under Seismic Excitations," by J.N. Yang, A. Akbarpour and P. Ghaemmaghami, 6/10/87, (PB88-134333, A06, MF-A01). This report is only available through NTIS (see address given above).

NCEER-87-0008 "IDARC: Inelastic Damage Analysis of Reinforced Concrete Frame - Shear-Wall Structures," by Y.J. Park, A.M. Reinhorn and S.K. Kunnath, 7/20/87, (PB88-134325, A09, MF-A01). This report is only available through NTIS (see address given above).

NCEER-87-0009 "Liquefaction Potential for New York State: A Preliminary Report on Sites in Manhattan and Buffalo," by M. Budhu, V. Vijayakumar, R.F. Giese and L. Baumgras, 8/31/87, (PB88-163704, A03, MF-A01). This report is available only through NTIS (see address given above).

NCEER-87-0010 "Vertical and Torsional Vibration of Foundations in Inhomogeneous Media," by A.S. Veletsos and K.W. Dotson, 6/1/87, (PB88-134291, A03, MF-A01). This report is only available through NTIS (see address given above).

NCEER-87-0011 "Seismic Probabilistic Risk Assessment and Seismic Margins Studies for Nuclear Power Plants," by Howard H.M. Hwang, 6/15/87, (PB88-134267, A03, MF-A01). This report is only available through NTIS (see address given above).

NCEER-87-0012 "Parametric Studies of Frequency Response of Secondary Systems Under Ground-Acceleration Excitations," by Y. Yong and Y.K. Lin, 6/10/87, (PB88-134309, A03, MF-A01). This report is only available through NTIS (see address given above).

NCEER-87-0013 "Frequency Response of Secondary Systems Under Seismic Excitation," by J.A. HoLung, J. Cai and Y.K. Lin, 7/31/87, (PB88-134317, A05, MF-A01). This report is only available through NTIS (see address given above).

NCEER-87-0014 "Modelling Earthquake Ground Motions in Seismically Active Regions Using Parametric Time Series Methods," by G.W. Ellis and A.S. Cakmak, 8/25/87, (PB88-134283, A08, MF-A01). This report is only available through NTIS (see address given above).

NCEER-87-0015 "Detection and Assessment of Seismic Structural Damage," by E. DiPasquale and A.S. Cakmak, 8/25/87, (PB88-163712, A05, MF-A01). This report is only available through NTIS (see address given above).

NCEER-87-0016 "Pipeline Experiment at Parkfield, California," by J. Isenberg and E. Richardson, 9/15/87, (PB88-163720, A03, MF-A01). This report is available only through NTIS (see address given above).

NCEER-87-0017 "Digital Simulation of Seismic Ground Motion," by M. Shinozuka, G. Deodatis and T. Harada, 8/31/87, (PB88-155197, A04, MF-A01). This report is available only through NTIS (see address given above).

NCEER-87-0018 "Practical Considerations for Structural Control: System Uncertainty, System Time Delay and Truncation of Small Control Forces," J.N. Yang and A. Akbarpour, 8/10/87, (PB88-163738, A08, MF-A01). This report is only available through NTIS (see address given above).

NCEER-87-0019 "Modal Analysis of Nonclassically Damped Structural Systems Using Canonical Transformation," by J.N. Yang, S. Sarkani and F.X. Long, 9/27/87, (PB88-187851, A04, MF-A01).

NCEER-87-0020 "A Nonstationary Solution in Random Vibration Theory," by J.R. Red-Horse and P.D. Spanos, 11/3/87, (PB88-163746, A03, MF-A01).

NCEER-87-0021 "Horizontal Impedances for Radially Inhomogeneous Viscoelastic Soil Layers," by A.S. Veletsos and K.W. Dotson, 10/15/87, (PB88-150859, A04, MF-A01).

NCEER-87-0022 "Seismic Damage Assessment of Reinforced Concrete Members," by Y.S. Chung, C. Meyer and M. Shinozuka, 10/9/87, (PB88-150867, A05, MF-A01). This report is available only through NTIS (see address given above).

NCEER-87-0023 "Active Structural Control in Civil Engineering," by T.T. Soong, 11/11/87, (PB88-187778, A03, MF-A01).

NCEER-87-0024 "Vertical and Torsional Impedances for Radially Inhomogeneous Viscoelastic Soil Layers," by K.W. Dotson and A.S. Veletsos, 12/87, (PB88-187786, A03, MF-A01).

NCEER-87-0025 "Proceedings from the Symposium on Seismic Hazards, Ground Motions, Soil-Liquefaction and Engineering Practice in Eastern North America," October 20-22, 1987, edited by K.H. Jacob, 12/87, (PB88-188115, A23, MF-A01). This report is available only through NTIS (see address given above).

NCEER-87-0026 "Report on the Whittier-Narrows, California, Earthquake of October 1, 1987," by J. Pantelic and A. Reinhorn, 11/87, (PB88-187752, A03, MF-A01). This report is available only through NTIS (see address given above).

NCEER-87-0027 "Design of a Modular Program for Transient Nonlinear Analysis of Large 3-D Building Structures," by S. Srivastav and J.F. Abel, 12/30/87, (PB88-187950, A05, MF-A01). This report is only available through NTIS (see address given above).

NCEER-87-0028 "Second-Year Program in Research, Education and Technology Transfer," 3/8/88, (PB88-219480, A04, MF-A01).

NCEER-88-0001 "Workshop on Seismic Computer Analysis and Design of Buildings With Interactive Graphics," by W. McGuire, J.F. Abel and C.H. Conley, 1/18/88, (PB88-187760, A03, MF-A01). This report is only available through NTIS (see address given above).

NCEER-88-0002 "Optimal Control of Nonlinear Flexible Structures," by J.N. Yang, F.X. Long and D. Wong, 1/22/88, (PB88-213772, A06, MF-A01).

NCEER-88-0003 "Substructuring Techniques in the Time Domain for Primary-Secondary Structural Systems," by G.D. Manolis and G. Juhn, 2/10/88, (PB88-213780, A04, MF-A01).

NCEER-88-0004 "Iterative Seismic Analysis of Primary-Secondary Systems," by A. Singhal, L.D. Lutes and P.D. Spanos, 2/23/88, (PB88-213798, A04, MF-A01).

NCEER-88-0005 "Stochastic Finite Element Expansion for Random Media," by P.D. Spanos and R. Ghanem, 3/14/88, (PB88-213806, A03, MF-A01).

NCEER-88-0006 "Combining Structural Optimization and Structural Control," by F.Y. Cheng and C.P. Pantelides, 1/10/88, (PB88-213814, A05, MF-A01).

NCEER-88-0007 "Seismic Performance Assessment of Code-Designed Structures," by H.H-M. Hwang, J-W. Jaw and H-J. Shau, 3/20/88, (PB88-219423, A04, MF-A01). This report is only available through NTIS (see address given above).

NCEER-88-0008 "Reliability Analysis of Code-Designed Structures Under Natural Hazards," by H.H-M. Hwang, H. Ushiba and M. Shinozuka, 2/29/88, (PB88-229471, A07, MF-A01). This report is only available through NTIS (see address given above).

NCEER-88-0009 "Seismic Fragility Analysis of Shear Wall Structures," by J-W Jaw and H.H-M. Hwang, 4/30/88, (PB89-102867, A04, MF-A01).

NCEER-88-0010 "Base Isolation of a Multi-Story Building Under a Harmonic Ground Motion - A Comparison of Performances of Various Systems," by F-G Fan, G. Ahmadi and I.G. Tadjbakhsh, 5/18/88, (PB89-122238, A06, MF-A01). This report is only available through NTIS (see address given above).

NCEER-88-0011 "Seismic Floor Response Spectra for a Combined System by Green's Functions," by F.M. Lavelle, L.A. Bergman and P.D. Spanos, 5/1/88, (PB89-102875, A03, MF-A01).

NCEER-88-0012 "A New Solution Technique for Randomly Excited Hysteretic Structures," by G.Q. Cai and Y.K. Lin, 5/16/88, (PB89-102883, A03, MF-A01).

NCEER-88-0013 "A Study of Radiation Damping and Soil-Structure Interaction Effects in the Centrifuge," by K. Weissman, supervised by J.H. Prevost, 5/24/88, (PB89-144703, A06, MF-A01).

NCEER-88-0014 "Parameter Identification and Implementation of a Kinematic Plasticity Model for Frictional Soils," by J.H. Prevost and D.V. Griffiths, to be published.

NCEER-88-0015 "Two- and Three- Dimensional Dynamic Finite Element Analyses of the Long Valley Dam," by D.V. Griffiths and J.H. Prevost, 6/17/88, (PB89-144711, A04, MF-A01).

NCEER-88-0016 "Damage Assessment of Reinforced Concrete Structures in Eastern United States," by A.M. Reinhorn, M.J. Seidel, S.K. Kunnath and Y.J. Park, 6/15/88, (PB89-122220, A04, MF-A01). This report is only available through NTIS (see address given above).

NCEER-88-0017 "Dynamic Compliance of Vertically Loaded Strip Foundations in Multilayered Viscoelastic Soils," by S. Ahmad and A.S.M. Israil, 6/17/88, (PB89-102891, A04, MF-A01).

NCEER-88-0018 "An Experimental Study of Seismic Structural Response With Added Viscoelastic Dampers," by R.C. Lin, Z. Liang, T.T. Soong and R.H. Zhang, 6/30/88, (PB89-122212, A05, MF-A01). This report is available only through NTIS (see address given above).

NCEER-88-0019 "Experimental Investigation of Primary - Secondary System Interaction," by G.D. Manolis, G. Juhn and A.M. Reinhorn, 5/27/88, (PB89-122204, A04, MF-A01).

NCEER-88-0020 "A Response Spectrum Approach For Analysis of Nonclassically Damped Structures," by J.N. Yang, S. Sarkani and F.X. Long, 4/22/88, (PB89-102909, A04, MF-A01).

NCEER-88-0021 "Seismic Interaction of Structures and Soils: Stochastic Approach," by A.S. Veletsos and A.M. Prasad, 7/21/88, (PB89-122196, A04, MF-A01). This report is only available through NTIS (see address given above).

NCEER-88-0022 "Identification of the Serviceability Limit State and Detection of Seismic Structural Damage," by E. DiPasquale and A.S. Cakmak, 6/15/88, (PB89-122188, A05, MF-A01). This report is available only through NTIS (see address given above).

NCEER-88-0023 "Multi-Hazard Risk Analysis: Case of a Simple Offshore Structure," by B.K. Bhartia and E.H. Vanmarcke, 7/21/88, (PB89-145213, A05, MF-A01).

NCEER-88-0024 "Automated Seismic Design of Reinforced Concrete Buildings," by Y.S. Chung, C. Meyer and M. Shinozuka, 7/5/88, (PB89-122170, A06, MF-A01). This report is available only through NTIS (see address given above).

NCEER-88-0025 "Experimental Study of Active Control of MDOF Structures Under Seismic Excitations," by L.L. Chung, R.C. Lin, T.T. Soong and A.M. Reinhorn, 7/10/88, (PB89-122600, A04, MF-A01).

NCEER-88-0026 "Earthquake Simulation Tests of a Low-Rise Metal Structure," by J.S. Hwang, K.C. Chang, G.C. Lee and R.L. Ketter, 8/1/88, (PB89-102917, A04, MF-A01).

NCEER-88-0027 "Systems Study of Urban Response and Reconstruction Due to Catastrophic Earthquakes," by F. Kozin and H.K. Zhou, 9/22/88, (PB90-162348, A04, MF-A01).

NCEER-88-0028 "Seismic Fragility Analysis of Plane Frame Structures," by H.H-M. Hwang and Y.K. Low, 7/31/88, (PB89-131445, A06, MF-A01).

NCEER-88-0029 "Response Analysis of Stochastic Structures," by A. Kardara, C. Bucher and M. Shinozuka, 9/22/88, (PB89-174429, A04, MF-A01).

NCEER-88-0030 "Nonnormal Accelerations Due to Yielding in a Primary Structure," by D.C.K. Chen and L.D. Lutes, 9/19/88, (PB89-131437, A04, MF-A01).

NCEER-88-0031 "Design Approaches for Soil-Structure Interaction," by A.S. Veletsos, A.M. Prasad and Y. Tang, 12/30/88, (PB89-174437, A03, MF-A01). This report is available only through NTIS (see address given above).

NCEER-88-0032 "A Re-evaluation of Design Spectra for Seismic Damage Control," by C.J. Turkstra and A.G. Tallin, 11/7/88, (PB89-145221, A05, MF-A01).

NCEER-88-0033 "The Behavior and Design of Noncontact Lap Splices Subjected to Repeated Inelastic Tensile Loading," by V.E. Sagan, P. Gergely and R.N. White, 12/8/88, (PB89-163737, A08, MF-A01).

NCEER-88-0034 "Seismic Response of Pile Foundations," by S.M. Mamoon, P.K. Banerjee and S. Ahmad, 11/1/88, (PB89-145239, A04, MF-A01).

NCEER-88-0035 "Modeling of R/C Building Structures With Flexible Floor Diaphragms (IDARC2)," by A.M. Reinhorn, S.K. Kunnath and N. Panahshahi, 9/7/88, (PB89-207153, A07, MF-A01).

NCEER-88-0036 "Solution of the Dam-Reservoir Interaction Problem Using a Combination of FEM, BEM with Particular Integrals, Modal Analysis, and Substructuring," by C-S. Tsai, G.C. Lee and R.L. Ketter, 12/31/88, (PB89-207146, A04, MF-A01).

NCEER-88-0037 "Optimal Placement of Actuators for Structural Control," by F.Y. Cheng and C.P. Pantelides, 8/15/88, (PB89-162846, A05, MF-A01).

NCEER-88-0038 "Teflon Bearings in Aseismic Base Isolation: Experimental Studies and Mathematical Modeling," by A. Mokha, M.C. Constantinou and A.M. Reinhorn, 12/5/88, (PB89-218457, A10, MF-A01). This report is available only through NTIS (see address given above).

NCEER-88-0039 "Seismic Behavior of Flat Slab High-Rise Buildings in the New York City Area," by P. Weidlinger and M. Ettouney, 10/15/88, (PB90-145681, A04, MF-A01).

NCEER-88-0040 "Evaluation of the Earthquake Resistance of Existing Buildings in New York City," by P. Weidlinger and M. Ettouney, 10/15/88, to be published.

NCEER-88-0041 "Small-Scale Modeling Techniques for Reinforced Concrete Structures Subjected to Seismic Loads," by W. Kim, A. El-Attar and R.N. White, 11/22/88, (PB89-189625, A05, MF-A01).

NCEER-88-0042 "Modeling Strong Ground Motion from Multiple Event Earthquakes," by G.W. Ellis and A.S. Cakmak, 10/15/88, (PB89-174445, A03, MF-A01).

NCEER-88-0043 "Nonstationary Models of Seismic Ground Acceleration," by M. Grigoriu, S.E. Ruiz and E. Rosenblueth, 7/15/88, (PB89-189617, A04, MF-A01).

NCEER-88-0044 "SARCF User's Guide: Seismic Analysis of Reinforced Concrete Frames," by Y.S. Chung, C. Meyer and M. Shinozuka, 11/9/88, (PB89-174452, A08, MF-A01).

NCEER-88-0045 "First Expert Panel Meeting on Disaster Research and Planning," edited by J. Pantelic and J. Stoyle, 9/15/88, (PB89-174460, A05, MF-A01).

NCEER-88-0046 "Preliminary Studies of the Effect of Degrading Infill Walls on the Nonlinear Seismic Response of Steel Frames," by C.Z. Chrysostomou, P. Gergely and J.F. Abel, 12/19/88, (PB89-208383, A05, MF-A01).

NCEER-88-0047 "Reinforced Concrete Frame Component Testing Facility - Design, Construction, Instrumentation and Operation," by S.P. Pessiki, C. Conley, T. Bond, P. Gergely and R.N. White, 12/16/88, (PB89-174478, A04, MF-A01).

NCEER-89-0001 "Effects of Protective Cushion and Soil Compliancy on the Response of Equipment Within a Seismically Excited Building," by J.A. HoLung, 2/16/89, (PB89-207179, A04, MF-A01).

NCEER-89-0002 "Statistical Evaluation of Response Modification Factors for Reinforced Concrete Structures," by H.H-M. Hwang and J-W. Jaw, 2/17/89, (PB89-207187, A05, MF-A01).

NCEER-89-0003 "Hysteretic Columns Under Random Excitation," by G-Q. Cai and Y.K. Lin, 1/9/89, (PB89-196513, A03, MF-A01).

NCEER-89-0004 "Experimental Study of `Elephant Foot Bulge' Instability of Thin-Walled Metal Tanks," by Z-H. Jia and R.L. Ketter, 2/22/89, (PB89-207195, A03, MF-A01).

NCEER-89-0005 "Experiment on Performance of Buried Pipelines Across San Andreas Fault," by J. Isenberg, E. Richardson and T.D. O'Rourke, 3/10/89, (PB89-218440, A04, MF-A01). This report is available only through NTIS (see address given above).

NCEER-89-0006 "A Knowledge-Based Approach to Structural Design of Earthquake-Resistant Buildings," by M. Subramani, P. Gergely, C.H. Conley, J.F. Abel and A.H. Zaghw, 1/15/89, (PB89-218465, A06, MF-A01).

NCEER-89-0007 "Liquefaction Hazards and Their Effects on Buried Pipelines," by T.D. O'Rourke and P.A. Lane, 2/1/89, (PB89-218481, A09, MF-A01).

NCEER-89-0008 "Fundamentals of System Identification in Structural Dynamics," by H. Imai, C-B. Yun, O. Maruyama and M. Shinozuka, 1/26/89, (PB89-207211, A04, MF-A01).

NCEER-89-0009 "Effects of the 1985 Michoacan Earthquake on Water Systems and Other Buried Lifelines in Mexico," by A.G. Ayala and M.J. O'Rourke, 3/8/89, (PB89-207229, A06, MF-A01).

NCEER-89-R010 "NCEER Bibliography of Earthquake Education Materials," by K.E.K. Ross, Second Revision, 9/1/89, (PB90-125352, A05, MF-A01). This report is replaced by NCEER-92-0018.

NCEER-89-0011 "Inelastic Three-Dimensional Response Analysis of Reinforced Concrete Building Structures (IDARC-3D), Part I - Modeling," by S.K. Kunnath and A.M. Reinhorn, 4/17/89, (PB90-114612, A07, MF-A01). This report is available only through NTIS (see address given above).

NCEER-89-0012 "Recommended Modifications to ATC-14," by C.D. Poland and J.O. Malley, 4/12/89, (PB90-108648, A15, MF-A01).

NCEER-89-0013 "Repair and Strengthening of Beam-to-Column Connections Subjected to Earthquake Loading," by M. Corazao and A.J. Durrani, 2/28/89, (PB90-109885, A06, MF-A01).

NCEER-89-0014 "Program EXKAL2 for Identification of Structural Dynamic Systems," by O. Maruyama, C-B. Yun, M. Hoshiya and M. Shinozuka, 5/19/89, (PB90-109877, A09, MF-A01).

NCEER-89-0015 "Response of Frames With Bolted Semi-Rigid Connections, Part I - Experimental Study and Analytical Predictions," by P.J. DiCorso, A.M. Reinhorn, J.R. Dickerson, J.B. Radziminski and W.L. Harper, 6/1/89, to be published.

NCEER-89-0016 "ARMA Monte Carlo Simulation in Probabilistic Structural Analysis," by P.D. Spanos and M.P. Mignolet, 7/10/89, (PB90-109893, A03, MF-A01).

NCEER-89-P017 "Preliminary Proceedings from the Conference on Disaster Preparedness - The Place of Earthquake Education in Our Schools," Edited by K.E.K. Ross, 6/23/89, (PB90-108606, A03, MF-A01).

NCEER-89-0017 "Proceedings from the Conference on Disaster Preparedness - The Place of Earthquake Education in Our Schools," Edited by K.E.K. Ross, 12/31/89, (PB90-207895, A012, MF-A02). This report is available only through NTIS (see address given above).

NCEER-89-0018 "Multidimensional Models of Hysteretic Material Behavior for Vibration Analysis of Shape Memory Energy Absorbing Devices, by E.J. Graesser and F.A. Cozzarelli, 6/7/89, (PB90-164146, A04, MF-A01).

NCEER-89-0019 "Nonlinear Dynamic Analysis of Three-Dimensional Base Isolated Structures (3D-BASIS)," by S. Nagarajaiah, A.M. Reinhorn and M.C. Constantinou, 8/3/89, (PB90-161936, A06, MF-A01). This report has been replaced by NCEER-93-0011.

NCEER-89-0020 "Structural Control Considering Time-Rate of Control Forces and Control Rate Constraints," by F.Y. Cheng and C.P. Pantelides, 8/3/89, (PB90-120445, A04, MF-A01).

NCEER-89-0021 "Subsurface Conditions of Memphis and Shelby County," by K.W. Ng, T-S. Chang and H-H.M. Hwang, 7/26/89, (PB90-120437, A03, MF-A01).

NCEER-89-0022 "Seismic Wave Propagation Effects on Straight Jointed Buried Pipelines," by K. Elhmadi and M.J. O'Rourke, 8/24/89, (PB90-162322, A10, MF-A02).

NCEER-89-0023 "Workshop on Serviceability Analysis of Water Delivery Systems," edited by M. Grigoriu, 3/6/89, (PB90-127424, A03, MF-A01).

NCEER-89-0024 "Shaking Table Study of a 1/5 Scale Steel Frame Composed of Tapered Members," by K.C. Chang, J.S. Hwang and G.C. Lee, 9/18/89, (PB90-160169, A04, MF-A01).

NCEER-89-0025 "DYNA1D: A Computer Program for Nonlinear Seismic Site Response Analysis - Technical Documentation," by Jean H. Prevost, 9/14/89, (PB90-161944, A07, MF-A01). This report is available only through NTIS (see address given above).

NCEER-89-0026 "1:4 Scale Model Studies of Active Tendon Systems and Active Mass Dampers for Aseismic Protection," by A.M. Reinhorn, T.T. Soong, R.C. Lin, Y.P. Yang, Y. Fukao, H. Abe and M. Nakai, 9/15/89, (PB90-173246, A10, MF-A02). This report is available only through NTIS (see address given above).

NCEER-89-0027 "Scattering of Waves by Inclusions in a Nonhomogeneous Elastic Half Space Solved by Boundary Element Methods," by P.K. Hadley, A. Askar and A.S. Cakmak, 6/15/89, (PB90-145699, A07, MF-A01).

NCEER-89-0028 "Statistical Evaluation of Deflection Amplification Factors for Reinforced Concrete Structures," by H.H.M. Hwang, J-W. Jaw and A.L. Ch'ng, 8/31/89, (PB90-164633, A05, MF-A01).

NCEER-89-0029 "Bedrock Accelerations in Memphis Area Due to Large New Madrid Earthquakes," by H.H.M. Hwang, C.H.S. Chen and G. Yu, 11/7/89, (PB90-162330, A04, MF-A01).

NCEER-89-0030 "Seismic Behavior and Response Sensitivity of Secondary Structural Systems," by Y.Q. Chen and T.T. Soong, 10/23/89, (PB90-164658, A08, MF-A01).

NCEER-89-0031 "Random Vibration and Reliability Analysis of Primary-Secondary Structural Systems," by Y. Ibrahim, M. Grigoriu and T.T. Soong, 11/10/89, (PB90-161951, A04, MF-A01).

NCEER-89-0032 "Proceedings from the Second U.S. - Japan Workshop on Liquefaction, Large Ground Deformation and Their Effects on Lifelines, September 26-29, 1989," Edited by T.D. O'Rourke and M. Hamada, 12/1/89, (PB90-209388, A22, MF-A03).

NCEER-89-0033 "Deterministic Model for Seismic Damage Evaluation of Reinforced Concrete Structures," by J.M. Bracci, A.M. Reinhorn, J.B. Mander and S.K. Kunnath, 9/27/89, (PB91-108803, A06, MF-A01).

NCEER-89-0034 "On the Relation Between Local and Global Damage Indices," by E. DiPasquale and A.S. Cakmak, 8/15/89, (PB90-173865, A05, MF-A01).

NCEER-89-0035 "Cyclic Undrained Behavior of Nonplastic and Low Plasticity Silts," by A.J. Walker and H.E. Stewart, 7/26/89, (PB90-183518, A10, MF-A01).

NCEER-89-0036 "Liquefaction Potential of Surficial Deposits in the City of Buffalo, New York," by M. Budhu, R. Giese and L. Baumgrass, 1/17/89, (PB90-208455, A04, MF-A01).

NCEER-89-0037 "A Deterministic Assessment of Effects of Ground Motion Incoherence," by A.S. Veletsos and Y. Tang, 7/15/89, (PB90-164294, A03, MF-A01).

NCEER-89-0038 "Workshop on Ground Motion Parameters for Seismic Hazard Mapping," July 17-18, 1989, edited by R.V. Whitman, 12/1/89, (PB90-173923, A04, MF-A01).

NCEER-89-0039 "Seismic Effects on Elevated Transit Lines of the New York City Transit Authority," by C.J. Costantino, C.A. Miller and E. Heymsfield, 12/26/89, (PB90-207887, A06, MF-A01).

NCEER-89-0040 "Centrifugal Modeling of Dynamic Soil-Structure Interaction," by K. Weissman, Supervised by J.H. Prevost, 5/10/89, (PB90-207879, A07, MF-A01).

NCEER-89-0041 "Linearized Identification of Buildings With Cores for Seismic Vulnerability Assessment," by I-K. Ho and A.E. Aktan, 11/1/89, (PB90-251943, A07, MF-A01).

NCEER-90-0001 "Geotechnical and Lifeline Aspects of the October 17, 1989 Loma Prieta Earthquake in San Francisco," by T.D. O'Rourke, H.E. Stewart, F.T. Blackburn and T.S. Dickerman, 1/90, (PB90-208596, A05, MF-A01).

NCEER-90-0002 "Nonnormal Secondary Response Due to Yielding in a Primary Structure," by D.C.K. Chen and L.D. Lutes, 2/28/90, (PB90-251976, A07, MF-A01).

NCEER-90-0003 "Earthquake Education Materials for Grades K-12," by K.E.K. Ross, 4/16/90, (PB91-251984, A05, MF-A05). This report has been replaced by NCEER-92-0018.

NCEER-90-0004 "Catalog of Strong Motion Stations in Eastern North America," by R.W. Busby, 4/3/90, (PB90-251984, A05, MF-A01).

NCEER-90-0005 "NCEER Strong-Motion Data Base: A User Manual for the GeoBase Release (Version 1.0 for the Sun3)," by P. Friberg and K. Jacob, 3/31/90 (PB90-258062, A04, MF-A01).

NCEER-90-0006 "Seismic Hazard Along a Crude Oil Pipeline in the Event of an 1811-1812 Type New Madrid Earthquake," by H.H.M. Hwang and C-H.S. Chen, 4/16/90, (PB90-258054, A04, MF-A01).

NCEER-90-0007 "Site-Specific Response Spectra for Memphis Sheahan Pumping Station," by H.H.M. Hwang and C.S. Lee, 5/15/90, (PB91-108811, A05, MF-A01).

NCEER-90-0008 "Pilot Study on Seismic Vulnerability of Crude Oil Transmission Systems," by T. Ariman, R. Dobry, M. Grigoriu, F. Kozin, M. O'Rourke, T. O'Rourke and M. Shinozuka, 5/25/90, (PB91-108837, A06, MF-A01).

NCEER-90-0009 "A Program to Generate Site Dependent Time Histories: EQGEN," by G.W. Ellis, M. Srinivasan and A.S. Cakmak, 1/30/90, (PB91-108829, A04, MF-A01).

NCEER-90-0010 "Active Isolation for Seismic Protection of Operating Rooms," by M.E. Talbott, Supervised by M. Shinozuka, 6/8/9, (PB91-110205, A05, MF-A01).

NCEER-90-0011 "Program LINEARID for Identification of Linear Structural Dynamic Systems," by C-B. Yun and M. Shinozuka, 6/25/90, (PB91-110312, A08, MF-A01).

NCEER-90-0012 "Two-Dimensional Two-Phase Elasto-Plastic Seismic Response of Earth Dams," by A.N. Yiagos, Supervised by J.H. Prevost, 6/20/90, (PB91-110197, A13, MF-A02).

NCEER-90-0013 "Secondary Systems in Base-Isolated Structures: Experimental Investigation, Stochastic Response and Stochastic Sensitivity," by G.D. Manolis, G. Juhn, M.C. Constantinou and A.M. Reinhorn, 7/1/90, (PB91-110320, A08, MF-A01).

NCEER-90-0014 "Seismic Behavior of Lightly-Reinforced Concrete Column and Beam-Column Joint Details," by S.P. Pessiki, C.H. Conley, P. Gergely and R.N. White, 8/22/90, (PB91-108795, A11, MF-A02).

NCEER-90-0015 "Two Hybrid Control Systems for Building Structures Under Strong Earthquakes," by J.N. Yang and A. Danielians, 6/29/90, (PB91-125393, A04, MF-A01).

NCEER-90-0016 "Instantaneous Optimal Control with Acceleration and Velocity Feedback," by J.N. Yang and Z. Li, 6/29/90, (PB91-125401, A03, MF-A01).

NCEER-90-0017 "Reconnaissance Report on the Northern Iran Earthquake of June 21, 1990," by M. Mehrain, 10/4/90, (PB91-125377, A03, MF-A01).

NCEER-90-0018 "Evaluation of Liquefaction Potential in Memphis and Shelby County," by T.S. Chang, P.S. Tang, C.S. Lee and H. Hwang, 8/10/90, (PB91-125427, A09, MF-A01).

NCEER-90-0019 "Experimental and Analytical Study of a Combined Sliding Disc Bearing and Helical Steel Spring Isolation System," by M.C. Constantinou, A.S. Mokha and A.M. Reinhorn, 10/4/90, (PB91-125385, A06, MF-A01). This report is available only through NTIS (see address given above).

NCEER-90-0020 "Experimental Study and Analytical Prediction of Earthquake Response of a Sliding Isolation System with a Spherical Surface," by A.S. Mokha, M.C. Constantinou and A.M. Reinhorn, 10/11/90, (PB91-125419, A05, MF-A01).

NCEER-90-0021 "Dynamic Interaction Factors for Floating Pile Groups," by G. Gazetas, K. Fan, A. Kaynia and E. Kausel, 9/10/90, (PB91-170381, A05, MF-A01).

NCEER-90-0022 "Evaluation of Seismic Damage Indices for Reinforced Concrete Structures," by S. Rodriguez-Gomez and A.S. Cakmak, 9/30/90, PB91-171322, A06, MF-A01).

NCEER-90-0023 "Study of Site Response at a Selected Memphis Site," by H. Desai, S. Ahmad, E.S. Gazetas and M.R. Oh, 10/11/90, (PB91-196857, A03, MF-A01).

NCEER-90-0024 "A User's Guide to Strongmo: Version 1.0 of NCEER's Strong-Motion Data Access Tool for PCs and Terminals," by P.A. Friberg and C.A.T. Susch, 11/15/90, (PB91-171272, A03, MF-A01).

NCEER-90-0025 "A Three-Dimensional Analytical Study of Spatial Variability of Seismic Ground Motions," by L-L. Hong and A.H.-S. Ang, 10/30/90, (PB91-170399, A09, MF-A01).

NCEER-90-0026 "MUMOID User's Guide - A Program for the Identification of Modal Parameters," by S. Rodriguez-Gomez and E. DiPasquale, 9/30/90, (PB91-171298, A04, MF-A01).

NCEER-90-0027 "SARCF-II User's Guide - Seismic Analysis of Reinforced Concrete Frames," by S. Rodriguez-Gomez, Y.S. Chung and C. Meyer, 9/30/90, (PB91-171280, A05, MF-A01).

NCEER-90-0028 "Viscous Dampers: Testing, Modeling and Application in Vibration and Seismic Isolation," by N. Makris and M.C. Constantinou, 12/20/90 (PB91-190561, A06, MF-A01).

NCEER-90-0029 "Soil Effects on Earthquake Ground Motions in the Memphis Area," by H. Hwang, C.S. Lee, K.W. Ng and T.S. Chang, 8/2/90, (PB91-190751, A05, MF-A01).

NCEER-91-0001 "Proceedings from the Third Japan-U.S. Workshop on Earthquake Resistant Design of Lifeline Facilities and Countermeasures for Soil Liquefaction, December 17-19, 1990," edited by T.D. O'Rourke and M. Hamada, 2/1/91, (PB91-179259, A99, MF-A04).

NCEER-91-0002 "Physical Space Solutions of Non-Proportionally Damped Systems," by M. Tong, Z. Liang and G.C. Lee, 1/15/91, (PB91-179242, A04, MF-A01).

NCEER-91-0003 "Seismic Response of Single Piles and Pile Groups," by K. Fan and G. Gazetas, 1/10/91, (PB92-174994, A04, MF-A01).

NCEER-91-0004 "Damping of Structures: Part 1 - Theory of Complex Damping," by Z. Liang and G. Lee, 10/10/91, (PB92-197235, A12, MF-A03).

NCEER-91-0005 "3D-BASIS - Nonlinear Dynamic Analysis of Three Dimensional Base Isolated Structures: Part II," by S. Nagarajaiah, A.M. Reinhorn and M.C. Constantinou, 2/28/91, (PB91-190553, A07, MF-A01). This report has been replaced by NCEER-93-0011.

NCEER-91-0006 "A Multidimensional Hysteretic Model for Plasticity Deforming Metals in Energy Absorbing Devices," by E.J. Graesser and F.A. Cozzarelli, 4/9/91, (PB92-108364, A04, MF-A01).

NCEER-91-0007 "A Framework for Customizable Knowledge-Based Expert Systems with an Application to a KBES for Evaluating the Seismic Resistance of Existing Buildings," by E.G. Ibarra-Anaya and S.J. Fenves, 4/9/91, (PB91-210930, A08, MF-A01).

NCEER-91-0008 "Nonlinear Analysis of Steel Frames with Semi-Rigid Connections Using the Capacity Spectrum Method," by G.G. Deierlein, S-H. Hsieh, Y-J. Shen and J.F. Abel, 7/2/91, (PB92-113828, A05, MF-A01).

NCEER-91-0009 "Earthquake Education Materials for Grades K-12," by K.E.K. Ross, 4/30/91, (PB91-212142, A06, MF-A01). This report has been replaced by NCEER-92-0018.

NCEER-91-0010 "Phase Wave Velocities and Displacement Phase Differences in a Harmonically Oscillating Pile," by N. Makris and G. Gazetas, 7/8/91, (PB92-108356, A04, MF-A01).

NCEER-91-0011 "Dynamic Characteristics of a Full-Size Five-Story Steel Structure and a 2/5 Scale Model," by K.C. Chang, G.C. Yao, G.C. Lee, D.S. Hao and Y.C. Yeh," 7/2/91, (PB93-116648, A06, MF-A02).

NCEER-91-0012 "Seismic Response of a 2/5 Scale Steel Structure with Added Viscoelastic Dampers," by K.C. Chang, T.T. Soong, S-T. Oh and M.L. Lai, 5/17/91, (PB92-110816, A05, MF-A01).

NCEER-91-0013 "Earthquake Response of Retaining Walls; Full-Scale Testing and Computational Modeling," by S. Alampalli and A-W.M. Elgamal, 6/20/91, to be published.

NCEER-91-0014 "3D-BASIS-M: Nonlinear Dynamic Analysis of Multiple Building Base Isolated Structures," by P.C. Tsopelas, S. Nagarajaiah, M.C. Constantinou and A.M. Reinhorn, 5/28/91, (PB92-113885, A09, MF-A02).

NCEER-91-0015 "Evaluation of SEAOC Design Requirements for Sliding Isolated Structures," by D. Theodossiou and M.C. Constantinou, 6/10/91, (PB92-114602, A11, MF-A03).

NCEER-91-0016 "Closed-Loop Modal Testing of a 27-Story Reinforced Concrete Flat Plate-Core Building," by H.R. Somaprasad, T. Toksoy, H. Yoshiyuki and A.E. Aktan, 7/15/91, (PB92-129980, A07, MF-A02).

NCEER-91-0017 "Shake Table Test of a 1/6 Scale Two-Story Lightly Reinforced Concrete Building," by A.G. El-Attar, R.N. White and P. Gergely, 2/28/91, (PB92-222447, A06, MF-A02).

NCEER-91-0018 "Shake Table Test of a 1/8 Scale Three-Story Lightly Reinforced Concrete Building," by A.G. El-Attar, R.N. White and P. Gergely, 2/28/91, (PB93-116630, A08, MF-A02).

NCEER-91-0019 "Transfer Functions for Rigid Rectangular Foundations," by A.S. Veletsos, A.M. Prasad and W.H. Wu, 7/31/91, to be published.

NCEER-91-0020 "Hybrid Control of Seismic-Excited Nonlinear and Inelastic Structural Systems," by J.N. Yang, Z. Li and A. Danielians, 8/1/91, (PB92-143171, A06, MF-A02).

NCEER-91-0021 "The NCEER-91 Earthquake Catalog: Improved Intensity-Based Magnitudes and Recurrence Relations for U.S. Earthquakes East of New Madrid," by L. Seeber and J.G. Armbruster, 8/28/91, (PB92-176742, A06, MF-A02).

NCEER-91-0022 "Proceedings from the Implementation of Earthquake Planning and Education in Schools: The Need for Change - The Roles of the Changemakers," by K.E.K. Ross and F. Winslow, 7/23/91, (PB92-129998, A12, MF-A03).

NCEER-91-0023 "A Study of Reliability-Based Criteria for Seismic Design of Reinforced Concrete Frame Buildings," by H.H.M. Hwang and H-M. Hsu, 8/10/91, (PB92-140235, A09, MF-A02).

NCEER-91-0024 "Experimental Verification of a Number of Structural System Identification Algorithms," by R.G. Ghanem, H. Gavin and M. Shinozuka, 9/18/91, (PB92-176577, A18, MF-A04).

NCEER-91-0025 "Probabilistic Evaluation of Liquefaction Potential," by H.H.M. Hwang and C.S. Lee," 11/25/91, (PB92-143429, A05, MF-A01).

NCEER-91-0026 "Instantaneous Optimal Control for Linear, Nonlinear and Hysteretic Structures - Stable Controllers," by J.N. Yang and Z. Li, 11/15/91, (PB92-163807, A04, MF-A01).

NCEER-91-0027 "Experimental and Theoretical Study of a Sliding Isolation System for Bridges," by M.C. Constantinou, A. Kartoum, A.M. Reinhorn and P. Bradford, 11/15/91, (PB92-176973, A10, MF-A03).

NCEER-92-0001 "Case Studies of Liquefaction and Lifeline Performance During Past Earthquakes, Volume 1: Japanese Case Studies," Edited by M. Hamada and T. O'Rourke, 2/17/92, (PB92-197243, A18, MF-A04).

NCEER-92-0002 "Case Studies of Liquefaction and Lifeline Performance During Past Earthquakes, Volume 2: United States Case Studies," Edited by T. O'Rourke and M. Hamada, 2/17/92, (PB92-197250, A20, MF-A04).

NCEER-92-0003 "Issues in Earthquake Education," Edited by K. Ross, 2/3/92, (PB92-222389, A07, MF-A02).

NCEER-92-0004 "Proceedings from the First U.S. - Japan Workshop on Earthquake Protective Systems for Bridges," Edited by I.G. Buckle, 2/4/92, (PB94-142239, A99, MF-A06).

NCEER-92-0005 "Seismic Ground Motion from a Haskell-Type Source in a Multiple-Layered Half-Space," A.P. Theoharis, G. Deodatis and M. Shinozuka, 1/2/92, to be published.

NCEER-92-0006 "Proceedings from the Site Effects Workshop," Edited by R. Whitman, 2/29/92, (PB92-197201, A04, MF-A01).

NCEER-92-0007 "Engineering Evaluation of Permanent Ground Deformations Due to Seismically-Induced Liquefaction," by M.H. Baziar, R. Dobry and A-W.M. Elgamal, 3/24/92, (PB92-222421, A13, MF-A03).

NCEER-92-0008 "A Procedure for the Seismic Evaluation of Buildings in the Central and Eastern United States," by C.D. Poland and J.O. Malley, 4/2/92, (PB92-222439, A20, MF-A04).

NCEER-92-0009 "Experimental and Analytical Study of a Hybrid Isolation System Using Friction Controllable Sliding Bearings," by M.Q. Feng, S. Fujii and M. Shinozuka, 5/15/92, (PB93-150282, A06, MF-A02).

NCEER-92-0010 "Seismic Resistance of Slab-Column Connections in Existing Non-Ductile Flat-Plate Buildings," by A.J. Durrani and Y. Du, 5/18/92, (PB93-116812, A06, MF-A02).

NCEER-92-0011 "The Hysteretic and Dynamic Behavior of Brick Masonry Walls Upgraded by Ferrocement Coatings Under Cyclic Loading and Strong Simulated Ground Motion," by H. Lee and S.P. Prawel, 5/11/92, to be published.

NCEER-92-0012 "Study of Wire Rope Systems for Seismic Protection of Equipment in Buildings," by G.F. Demetriades, M.C. Constantinou and A.M. Reinhorn, 5/20/92, (PB93-116655, A08, MF-A02).

NCEER-92-0013 "Shape Memory Structural Dampers: Material Properties, Design and Seismic Testing," by P.R. Witting and F.A. Cozzarelli, 5/26/92, (PB93-116663, A05, MF-A01).

NCEER-92-0014 "Longitudinal Permanent Ground Deformation Effects on Buried Continuous Pipelines," by M.J. O'Rourke, and C. Nordberg, 6/15/92, (PB93-116671, A08, MF-A02).

NCEER-92-0015 "A Simulation Method for Stationary Gaussian Random Functions Based on the Sampling Theorem," by M. Grigoriu and S. Balopoulou, 6/11/92, (PB93-127496, A05, MF-A01).

NCEER-92-0016 "Gravity-Load-Designed Reinforced Concrete Buildings: Seismic Evaluation of Existing Construction and Detailing Strategies for Improved Seismic Resistance," by G.W. Hoffmann, S.K. Kunnath, A.M. Reinhorn and J.B. Mander, 7/15/92, (PB94-142007, A08, MF-A02).

NCEER-92-0017 "Observations on Water System and Pipeline Performance in the Limón Area of Costa Rica Due to the April 22, 1991 Earthquake," by M. O'Rourke and D. Ballantyne, 6/30/92, (PB93-126811, A06, MF-A02).

NCEER-92-0018 "Fourth Edition of Earthquake Education Materials for Grades K-12," Edited by K.E.K. Ross, 8/10/92, (PB93-114023, A07, MF-A02).

NCEER-92-0019 "Proceedings from the Fourth Japan-U.S. Workshop on Earthquake Resistant Design of Lifeline Facilities and Countermeasures for Soil Liquefaction," Edited by M. Hamada and T.D. O'Rourke, 8/12/92, (PB93-163939, A99, MF-E11).

NCEER-92-0020 "Active Bracing System: A Full Scale Implementation of Active Control," by A.M. Reinhorn, T.T. Soong, R.C. Lin, M.A. Riley, Y.P. Wang, S. Aizawa and M. Higashino, 8/14/92, (PB93-127512, A06, MF-A02).

NCEER-92-0021 "Empirical Analysis of Horizontal Ground Displacement Generated by Liquefaction-Induced Lateral Spreads," by S.F. Bartlett and T.L. Youd, 8/17/92, (PB93-188241, A06, MF-A02).

NCEER-92-0022 "IDARC Version 3.0: Inelastic Damage Analysis of Reinforced Concrete Structures," by S.K. Kunnath, A.M. Reinhorn and R.F. Lobo, 8/31/92, (PB93-227502, A07, MF-A02).

NCEER-92-0023 "A Semi-Empirical Analysis of Strong-Motion Peaks in Terms of Seismic Source, Propagation Path and Local Site Conditions, by M. Kamiyama, M.J. O'Rourke and R. Flores-Berrones, 9/9/92, (PB93-150266, A08, MF-A02).

NCEER-92-0024 "Seismic Behavior of Reinforced Concrete Frame Structures with Nonductile Details, Part I: Summary of Experimental Findings of Full Scale Beam-Column Joint Tests," by A. Beres, R.N. White and P. Gergely, 9/30/92, (PB93-227783, A05, MF-A01).

NCEER-92-0025 "Experimental Results of Repaired and Retrofitted Beam-Column Joint Tests in Lightly Reinforced Concrete Frame Buildings," by A. Beres, S. El-Borgi, R.N. White and P. Gergely, 10/29/92, (PB93-227791, A05, MF-A01).

NCEER-92-0026 "A Generalization of Optimal Control Theory: Linear and Nonlinear Structures," by J.N. Yang, Z. Li and S. Vongchavalitkul, 11/2/92, (PB93-188621, A05, MF-A01).

NCEER-92-0027 "Seismic Resistance of Reinforced Concrete Frame Structures Designed Only for Gravity Loads: Part I - Design and Properties of a One-Third Scale Model Structure," by J.M. Bracci, A.M. Reinhorn and J.B. Mander, 12/1/92, (PB94-104502, A08, MF-A02).

NCEER-92-0028 "Seismic Resistance of Reinforced Concrete Frame Structures Designed Only for Gravity Loads: Part II - Experimental Performance of Subassemblages," by L.E. Aycardi, J.B. Mander and A.M. Reinhorn, 12/1/92, (PB94-104510, A08, MF-A02).

NCEER-92-0029 "Seismic Resistance of Reinforced Concrete Frame Structures Designed Only for Gravity Loads: Part III - Experimental Performance and Analytical Study of a Structural Model," by J.M. Bracci, A.M. Reinhorn and J.B. Mander, 12/1/92, (PB93-227528, A09, MF-A01).

NCEER-92-0030 "Evaluation of Seismic Retrofit of Reinforced Concrete Frame Structures: Part I - Experimental Performance of Retrofitted Subassemblages," by D. Choudhuri, J.B. Mander and A.M. Reinhorn, 12/8/92, (PB93-198307, A07, MF-A02).

NCEER-92-0031 "Evaluation of Seismic Retrofit of Reinforced Concrete Frame Structures: Part II - Experimental Performance and Analytical Study of a Retrofitted Structural Model," by J.M. Bracci, A.M. Reinhorn and J.B. Mander, 12/8/92, (PB93-198315, A09, MF-A03).

NCEER-92-0032 "Experimental and Analytical Investigation of Seismic Response of Structures with Supplemental Fluid Viscous Dampers," by M.C. Constantinou and M.D. Symans, 12/21/92, (PB93-191435, A10, MF-A03). This report is available only through NTIS (see address given above).

NCEER-92-0033 "Reconnaissance Report on the Cairo, Egypt Earthquake of October 12, 1992," by M. Khater, 12/23/92, (PB93-188621, A03, MF-A01).

NCEER-92-0034 "Low-Level Dynamic Characteristics of Four Tall Flat-Plate Buildings in New York City," by H. Gavin, S. Yuan, J. Grossman, E. Pekelis and K. Jacob, 12/28/92, (PB93-188217, A07, MF-A02).

NCEER-93-0001 "An Experimental Study on the Seismic Performance of Brick-Infilled Steel Frames With and Without Retrofit," by J.B. Mander, B. Nair, K. Wojtkowski and J. Ma, 1/29/93, (PB93-227510, A07, MF-A02).

NCEER-93-0002 "Social Accounting for Disaster Preparedness and Recovery Planning," by S. Cole, E. Pantoja and V. Razak, 2/22/93, (PB94-142114, A12, MF-A03).

NCEER-93-0003 "Assessment of 1991 NEHRP Provisions for Nonstructural Components and Recommended Revisions," by T.T. Soong, G. Chen, Z. Wu, R-H. Zhang and M. Grigoriu, 3/1/93, (PB93-188639, A06, MF-A02).

NCEER-93-0004 "Evaluation of Static and Response Spectrum Analysis Procedures of SEAOC/UBC for Seismic Isolated Structures," by C.W. Winters and M.C. Constantinou, 3/23/93, (PB93-198299, A10, MF-A03).

NCEER-93-0005 "Earthquakes in the Northeast - Are We Ignoring the Hazard? A Workshop on Earthquake Science and Safety for Educators," edited by K.E.K. Ross, 4/2/93, (PB94-103066, A09, MF-A02).

NCEER-93-0006 "Inelastic Response of Reinforced Concrete Structures with Viscoelastic Braces," by R.F. Lobo, J.M. Bracci, K.L. Shen, A.M. Reinhorn and T.T. Soong, 4/5/93, (PB93-227486, A05, MF-A02).

NCEER-93-0007 "Seismic Testing of Installation Methods for Computers and Data Processing Equipment," by K. Kosar, T.T. Soong, K.L. Shen, J.A. HoLung and Y.K. Lin, 4/12/93, (PB93-198299, A07, MF-A02).

NCEER-93-0008 "Retrofit of Reinforced Concrete Frames Using Added Dampers," by A. Reinhorn, M. Constantinou and C. Li, to be published.

NCEER-93-0009 "Seismic Behavior and Design Guidelines for Steel Frame Structures with Added Viscoelastic Dampers," by K.C. Chang, M.L. Lai, T.T. Soong, D.S. Hao and Y.C. Yeh, 5/1/93, (PB94-141959, A07, MF-A02).

NCEER-93-0010 "Seismic Performance of Shear-Critical Reinforced Concrete Bridge Piers," by J.B. Mander, S.M. Waheed, M.T.A. Chaudhary and S.S. Chen, 5/12/93, (PB93-227494, A08, MF-A02).

NCEER-93-0011 "3D-BASIS-TABS: Computer Program for Nonlinear Dynamic Analysis of Three Dimensional Base Isolated Structures," by S. Nagarajaiah, C. Li, A.M. Reinhorn and M.C. Constantinou, 8/2/93, (PB94-141819, A09, MF-A02).

NCEER-93-0012 "Effects of Hydrocarbon Spills from an Oil Pipeline Break on Ground Water," by O.J. Helweg and H.H.M. Hwang, 8/3/93, (PB94-141942, A06, MF-A02).

NCEER-93-0013 "Simplified Procedures for Seismic Design of Nonstructural Components and Assessment of Current Code Provisions," by M.P. Singh, L.E. Suarez, E.E. Matheu and G.O. Maldonado, 8/4/93, (PB94-141827, A09, MF-A02).

NCEER-93-0014 "An Energy Approach to Seismic Analysis and Design of Secondary Systems," by G. Chen and T.T. Soong, 8/6/93, (PB94-142767, A11, MF-A03).

NCEER-93-0015 "Proceedings from School Sites: Becoming Prepared for Earthquakes - Commemorating the Third Anniversary of the Loma Prieta Earthquake," Edited by F.E. Winslow and K.E.K. Ross, 8/16/93, (PB94-154275, A16, MF-A02).

NCEER-93-0016 "Reconnaissance Report of Damage to Historic Monuments in Cairo, Egypt Following the October 12, 1992 Dahshur Earthquake," by D. Sykora, D. Look, G. Croci, E. Karaesmen and E. Karaesmen, 8/19/93, (PB94-142221, A08, MF-A02).

NCEER-93-0017 "The Island of Guam Earthquake of August 8, 1993," by S.W. Swan and S.K. Harris, 9/30/93, (PB94-141843, A04, MF-A01).

NCEER-93-0018 "Engineering Aspects of the October 12, 1992 Egyptian Earthquake," by A.W. Elgamal, M. Amer, K. Adalier and A. Abul-Fadl, 10/7/93, (PB94-141983, A05, MF-A01).

NCEER-93-0019 "Development of an Earthquake Motion Simulator and its Application in Dynamic Centrifuge Testing," by I. Krstelj, Supervised by J.H. Prevost, 10/23/93, (PB94-181773, A-10, MF-A03).

NCEER-93-0020 "NCEER-Taisei Corporation Research Program on Sliding Seismic Isolation Systems for Bridges: Experimental and Analytical Study of a Friction Pendulum System (FPS)," by M.C. Constantinou, P. Tsopelas, Y-S. Kim and S. Okamoto, 11/1/93, (PB94-142775, A08, MF-A02).

NCEER-93-0021 "Finite Element Modeling of Elastomeric Seismic Isolation Bearings," by L.J. Billings, Supervised by R. Shepherd, 11/8/93, to be published.

NCEER-93-0022 "Seismic Vulnerability of Equipment in Critical Facilities: Life-Safety and Operational Consequences," by K. Porter, G.S. Johnson, M.M. Zadeh, C. Scawthorn and S. Eder, 11/24/93, (PB94-181765, A16, MF-A03).

NCEER-93-0023 "Hokkaido Nansei-oki, Japan Earthquake of July 12, 1993, by P.I. Yanev and C.R. Scawthorn, 12/23/93, (PB94-181500, A07, MF-A01).

NCEER-94-0001 "An Evaluation of Seismic Serviceability of Water Supply Networks with Application to the San Francisco Auxiliary Water Supply System," by I. Markov, Supervised by M. Grigoriu and T. O'Rourke, 1/21/94, (PB94-204013, A07, MF-A02).

NCEER-94-0002 "NCEER-Taisei Corporation Research Program on Sliding Seismic Isolation Systems for Bridges: Experimental and Analytical Study of Systems Consisting of Sliding Bearings, Rubber Restoring Force Devices and Fluid Dampers," Volumes I and II, by P. Tsopelas, S. Okamoto, M.C. Constantinou, D. Ozaki and S. Fujii, 2/4/94, (PB94-181740, A09, MF-A02 and PB94-181757, A12, MF-A03).

NCEER-94-0003 "A Markov Model for Local and Global Damage Indices in Seismic Analysis," by S. Rahman and M. Grigoriu, 2/18/94, (PB94-206000, A12, MF-A03).

NCEER-94-0004 "Proceedings from the NCEER Workshop on Seismic Response of Masonry Infills," edited by D.P. Abrams, 3/1/94, (PB94-180783, A07, MF-A02).

NCEER-94-0005 "The Northridge, California Earthquake of January 17, 1994: General Reconnaissance Report," edited by J.D. Goltz, 3/11/94, (PB94-193943, A10, MF-A03).

NCEER-94-0006 "Seismic Energy Based Fatigue Damage Analysis of Bridge Columns: Part I - Evaluation of Seismic Capacity," by G.A. Chang and J.B. Mander, 3/14/94, (PB94-219185, A11, MF-A03).

NCEER-94-0007 "Seismic Isolation of Multi-Story Frame Structures Using Spherical Sliding Isolation Systems," by T.M. Al-Hussaini, V.A. Zayas and M.C. Constantinou, 3/17/94, (PB94-193745, A09, MF-A02).

NCEER-94-0008 "The Northridge, California Earthquake of January 17, 1994: Performance of Highway Bridges," edited by I.G. Buckle, 3/24/94, (PB94-193851, A06, MF-A02).

NCEER-94-0009 "Proceedings of the Third U.S.-Japan Workshop on Earthquake Protective Systems for Bridges," edited by I.G. Buckle and I. Friedland, 3/31/94, (PB94-195815, A99, MF-A06).

NCEER-94-0010 "3D-BASIS-ME: Computer Program for Nonlinear Dynamic Analysis of Seismically Isolated Single and Multiple Structures and Liquid Storage Tanks," by P.C. Tsopelas, M.C. Constantinou and A.M. Reinhorn, 4/12/94, (PB94-204922, A09, MF-A02).

NCEER-94-0011 "The Northridge, California Earthquake of January 17, 1994: Performance of Gas Transmission Pipelines," by T.D. O'Rourke and M.C. Palmer, 5/16/94, (PB94-204989, A05, MF-A01).

NCEER-94-0012 "Feasibility Study of Replacement Procedures and Earthquake Performance Related to Gas Transmission Pipelines," by T.D. O'Rourke and M.C. Palmer, 5/25/94, (PB94-206638, A09, MF-A02).

NCEER-94-0013 "Seismic Energy Based Fatigue Damage Analysis of Bridge Columns: Part II - Evaluation of Seismic Demand," by G.A. Chang and J.B. Mander, 6/1/94, (PB95-18106, A08, MF-A02).

NCEER-94-0014 "NCEER-Taisei Corporation Research Program on Sliding Seismic Isolation Systems for Bridges: Experimental and Analytical Study of a System Consisting of Sliding Bearings and Fluid Restoring Force/Damping Devices," by P. Tsopelas and M.C. Constantinou, 6/13/94, (PB94-219144, A10, MF-A03).

NCEER-94-0015 "Generation of Hazard-Consistent Fragility Curves for Seismic Loss Estimation Studies," by H. Hwang and J-R. Huo, 6/14/94, (PB95-181996, A09, MF-A02).

NCEER-94-0016 "Seismic Study of Building Frames with Added Energy-Absorbing Devices," by W.S. Pong, C.S. Tsai and G.C. Lee, 6/20/94, (PB94-219136, A10, A03).

NCEER-94-0017 "Sliding Mode Control for Seismic-Excited Linear and Nonlinear Civil Engineering Structures," by J. Yang, J. Wu, A. Agrawal and Z. Li, 6/21/94, (PB95-138483, A06, MF-A02).

NCEER-94-0018 "3D-BASIS-TABS Version 2.0: Computer Program for Nonlinear Dynamic Analysis of Three Dimensional Base Isolated Structures," by A.M. Reinhorn, S. Nagarajaiah, M.C. Constantinou, P. Tsopelas and R. Li, 6/22/94, (PB95-182176, A08, MF-A02).

NCEER-94-0019 "Proceedings of the International Workshop on Civil Infrastructure Systems: Application of Intelligent Systems and Advanced Materials on Bridge Systems," Edited by G.C. Lee and K.C. Chang, 7/18/94, (PB95-252474, A20, MF-A04).

NCEER-94-0020 "Study of Seismic Isolation Systems for Computer Floors," by V. Lambrou and M.C. Constantinou, 7/19/94, (PB95-138533, A10, MF-A03).

NCEER-94-0021 "Proceedings of the U.S.-Italian Workshop on Guidelines for Seismic Evaluation and Rehabilitation of Unreinforced Masonry Buildings," Edited by D.P. Abrams and G.M. Calvi, 7/20/94, (PB95-138749, A13, MF-A03).

NCEER-94-0022 "NCEER-Taisei Corporation Research Program on Sliding Seismic Isolation Systems for Bridges: Experimental and Analytical Study of a System Consisting of Lubricated PTFE Sliding Bearings and Mild Steel Dampers," by P. Tsopelas and M.C. Constantinou, 7/22/94, (PB95-182184, A08, MF-A02).

NCEER-94-0023 “Development of Reliability-Based Design Criteria for Buildings Under Seismic Load,” by Y.K. Wen, H. Hwang and M. Shinozuka, 8/1/94, (PB95-211934, A08, MF-A02).

NCEER-94-0024 “Experimental Verification of Acceleration Feedback Control Strategies for an Active Tendon System,” by S.J. Dyke, B.F. Spencer, Jr., P. Quast, M.K. Sain, D.C. Kaspari, Jr. and T.T. Soong, 8/29/94, (PB95-212320, A05, MF-A01).

NCEER-94-0025 “Seismic Retrofitting Manual for Highway Bridges,” Edited by I.G. Buckle and I.F. Friedland, published by the Federal Highway Administration (PB95-212676, A15, MF-A03).

NCEER-94-0026 “Proceedings from the Fifth U.S.-Japan Workshop on Earthquake Resistant Design of Lifeline Facilities and Countermeasures Against Soil Liquefaction,” Edited by T.D. O’Rourke and M. Hamada, 11/7/94, (PB95-220802, A99, MF-E08).

NCEER-95-0001 "Experimental and Analytical Investigation of Seismic Retrofit of Structures with Supplemental Damping: Part 1 - Fluid Viscous Damping Devices," by A.M. Reinhorn, C. Li and M.C. Constantinou, 1/3/95, (PB95-266599, A09, MF-A02).

NCEER-95-0002 "Experimental and Analytical Study of Low-Cycle Fatigue Behavior of Semi-Rigid Top-And-Seat Angle Connections," by G. Pekcan, J.B. Mander and S.S. Chen, 1/5/95, (PB95-220042, A07, MF-A02).

NCEER-95-0003 "NCEER-ATC Joint Study on Fragility of Buildings," by T. Anagnos, C. Rojahn and A.S. Kiremidjian, 1/20/95, (PB95-220026, A06, MF-A02).

NCEER-95-0004 "Nonlinear Control Algorithms for Peak Response Reduction," by Z. Wu, T.T. Soong, V. Gattulli and R.C. Lin, 2/16/95, (PB95-220349, A05, MF-A01).

NCEER-95-0005 "Pipeline Replacement Feasibility Study: A Methodology for Minimizing Seismic and Corrosion Risks to Underground Natural Gas Pipelines," by R.T. Eguchi, H.A. Seligson and D.G. Honegger, 3/2/95, (PB95-252326, A06, MF-A02).

NCEER-95-0006 "Evaluation of Seismic Performance of an 11-Story Frame Building During the 1994 Northridge Earthquake," by F. Naeim, R. DiSulio, K. Benuska, A. Reinhorn and C. Li, to be published.

NCEER-95-0007 "Prioritization of Bridges for Seismic Retrofitting," by N. Basöz and A.S. Kiremidjian, 4/24/95, (PB95-252300, A08, MF-A02).

NCEER-95-0008 "Method for Developing Motion Damage Relationships for Reinforced Concrete Frames," by A. Singhal and A.S. Kiremidjian, 5/11/95, (PB95-266607, A06, MF-A02).

NCEER-95-0009 "Experimental and Analytical Investigation of Seismic Retrofit of Structures with Supplemental Damping: Part II - Friction Devices," by C. Li and A.M. Reinhorn, 7/6/95, (PB96-128087, A11, MF-A03).

NCEER-95-0010 "Experimental Performance and Analytical Study of a Non-Ductile Reinforced Concrete Frame Structure Retrofitted with Elastomeric Spring Dampers," by G. Pekcan, J.B. Mander and S.S. Chen, 7/14/95, (PB96-137161, A08, MF-A02).

NCEER-95-0011 "Development and Experimental Study of Semi-Active Fluid Damping Devices for Seismic Protection of Structures," by M.D. Symans and M.C. Constantinou, 8/3/95, (PB96-136940, A23, MF-A04).

NCEER-95-0012 "Real-Time Structural Parameter Modification (RSPM): Development of Innervated Structures," by Z. Liang, M. Tong and G.C. Lee, 4/11/95, (PB96-137153, A06, MF-A01).

NCEER-95-0013 "Experimental and Analytical Investigation of Seismic Retrofit of Structures with Supplemental Damping: Part III - Viscous Damping Walls," by A.M. Reinhorn and C. Li, 10/1/95, (PB96-176409, A11, MF-A03).

NCEER-95-0014 "Seismic Fragility Analysis of Equipment and Structures in a Memphis Electric Substation," by J-R. Huo and H.H.M. Hwang, 8/10/95, (PB96-128087, A09, MF-A02).

NCEER-95-0015 "The Hanshin-Awaji Earthquake of January 17, 1995: Performance of Lifelines," Edited by M. Shinozuka, 11/3/95, (PB96-176383, A15, MF-A03).

NCEER-95-0016 "Highway Culvert Performance During Earthquakes," by T.L. Youd and C.J. Beckman, available as NCEER-96-0015.

NCEER-95-0017 "The Hanshin-Awaji Earthquake of January 17, 1995: Performance of Highway Bridges," Edited by I.G. Buckle, 12/1/95, to be published.

NCEER-95-0018 "Modeling of Masonry Infill Panels for Structural Analysis," by A.M. Reinhorn, A. Madan, R.E. Valles, Y. Reichmann and J.B. Mander, 12/8/95, (PB97-110886, MF-A01, A06).

NCEER-95-0019 "Optimal Polynomial Control for Linear and Nonlinear Structures," by A.K. Agrawal and J.N. Yang, 12/11/95, (PB96-168737, A07, MF-A02).

NCEER-95-0020 "Retrofit of Non-Ductile Reinforced Concrete Frames Using Friction Dampers," by R.S. Rao, P. Gergely and R.N. White, 12/22/95, (PB97-133508, A10, MF-A02).

NCEER-95-0021 "Parametric Results for Seismic Response of Pile-Supported Bridge Bents," by G. Mylonakis, A. Nikolaou and G. Gazetas, 12/22/95, (PB97-100242, A12, MF-A03).

NCEER-95-0022 "Kinematic Bending Moments in Seismically Stressed Piles," by A. Nikolaou, G. Mylonakis and G. Gazetas, 12/23/95, (PB97-113914, MF-A03, A13).

NCEER-96-0001 "Dynamic Response of Unreinforced Masonry Buildings with Flexible Diaphragms," by A.C. Costley and D.P. Abrams," 10/10/96, (PB97-133573, MF-A03, A15).

NCEER-96-0002 "State of the Art Review: Foundations and Retaining Structures," by I. Po Lam, to be published.

NCEER-96-0003 "Ductility of Rectangular Reinforced Concrete Bridge Columns with Moderate Confinement," by N. Wehbe, M. Saiidi, D. Sanders and B. Douglas, 11/7/96, (PB97-133557, A06, MF-A02).

NCEER-96-0004 "Proceedings of the Long-Span Bridge Seismic Research Workshop," edited by I.G. Buckle and I.M. Friedland, to be published.

NCEER-96-0005 "Establish Representative Pier Types for Comprehensive Study: Eastern United States," by J. Kulicki and Z. Prucz, 5/28/96, (PB98-119217, A07, MF-A02).

NCEER-96-0006 "Establish Representative Pier Types for Comprehensive Study: Western United States," by R. Imbsen, R.A. Schamber and T.A. Osterkamp, 5/28/96, (PB98-118607, A07, MF-A02).

NCEER-96-0007 "Nonlinear Control Techniques for Dynamical Systems with Uncertain Parameters," by R.G. Ghanem and M.I. Bujakov, 5/27/96, (PB97-100259, A17, MF-A03).

NCEER-96-0008 "Seismic Evaluation of a 30-Year Old Non-Ductile Highway Bridge Pier and Its Retrofit," by J.B. Mander, B. Mahmoodzadegan, S. Bhadra and S.S. Chen, 5/31/96, (PB97-110902, MF-A03, A10).

NCEER-96-0009 "Seismic Performance of a Model Reinforced Concrete Bridge Pier Before and After Retrofit," by J.B. Mander, J.H. Kim and C.A. Ligozio, 5/31/96, (PB97-110910, MF-A02, A10).

NCEER-96-0010 "IDARC2D Version 4.0: A Computer Program for the Inelastic Damage Analysis of Buildings," by R.E. Valles, A.M. Reinhorn, S.K. Kunnath, C. Li and A. Madan, 6/3/96, (PB97-100234, A17, MF-A03).

NCEER-96-0011 "Estimation of the Economic Impact of Multiple Lifeline Disruption: Memphis Light, Gas and Water Division Case Study," by S.E. Chang, H.A. Seligson and R.T. Eguchi, 8/16/96, (PB97-133490, A11, MF-A03).

NCEER-96-0012 "Proceedings from the Sixth Japan-U.S. Workshop on Earthquake Resistant Design of Lifeline Facilities and Countermeasures Against Soil Liquefaction, Edited by M. Hamada and T. O'Rourke, 9/11/96, (PB97-133581, A99, MF-A06).

NCEER-96-0013 "Chemical Hazards, Mitigation and Preparedness in Areas of High Seismic Risk: A Methodology for Estimating the Risk of Post-Earthquake Hazardous Materials Release," by H.A. Seligson, R.T. Eguchi, K.J. Tierney and K. Richmond, 11/7/96, (PB97-133565, MF-A02, A08).

NCEER-96-0014 "Response of Steel Bridge Bearings to Reversed Cyclic Loading," by J.B. Mander, D-K. Kim, S.S. Chen and G.J. Premus, 11/13/96, (PB97-140735, A12, MF-A03).

NCEER-96-0015 "Highway Culvert Performance During Past Earthquakes," by T.L. Youd and C.J. Beckman, 11/25/96, (PB97-133532, A06, MF-A01).

NCEER-97-0001 "Evaluation, Prevention and Mitigation of Pounding Effects in Building Structures," by R.E. Valles and A.M. Reinhorn, 2/20/97, (PB97-159552, A14, MF-A03).

NCEER-97-0002 "Seismic Design Criteria for Bridges and Other Highway Structures," by C. Rojahn, R. Mayes, D.G. Anderson, J. Clark, J.H. Hom, R.V. Nutt and M.J. O'Rourke, 4/30/97, (PB97-194658, A06, MF-A03).

NCEER-97-0003 "Proceedings of the U.S.-Italian Workshop on Seismic Evaluation and Retrofit," Edited by D.P. Abrams and G.M. Calvi, 3/19/97, (PB97-194666, A13, MF-A03).

NCEER-97-0004 "Investigation of Seismic Response of Buildings with Linear and Nonlinear Fluid Viscous Dampers," by A.A. Seleemah and M.C. Constantinou, 5/21/97, (PB98-109002, A15, MF-A03).

NCEER-97-0005 "Proceedings of the Workshop on Earthquake Engineering Frontiers in Transportation Facilities," edited by G.C. Lee and I.M. Friedland, 8/29/97, (PB98-128911, A25, MR-A04).

NCEER-97-0006 "Cumulative Seismic Damage of Reinforced Concrete Bridge Piers," by S.K. Kunnath, A. El-Bahy, A. Taylor and W. Stone, 9/2/97, (PB98-108814, A11, MF-A03).

NCEER-97-0007 "Structural Details to Accommodate Seismic Movements of Highway Bridges and Retaining Walls," by R.A. Imbsen, R.A. Schamber, E. Thorkildsen, A. Kartoum, B.T. Martin, T.N. Rosser and J.M. Kulicki, 9/3/97, (PB98-108996, A09, MF-A02).

NCEER-97-0008 "A Method for Earthquake Motion-Damage Relationships with Application to Reinforced Concrete Frames," by A. Singhal and A.S. Kiremidjian, 9/10/97, (PB98-108988, A13, MF-A03).

NCEER-97-0009 "Seismic Analysis and Design of Bridge Abutments Considering Sliding and Rotation," by K. Fishman and R. Richards, Jr., 9/15/97, (PB98-108897, A06, MF-A02).

NCEER-97-0010 "Proceedings of the FHWA/NCEER Workshop on the National Representation of Seismic Ground Motion for New and Existing Highway Facilities," edited by I.M. Friedland, M.S. Power and R.L. Mayes, 9/22/97, (PB98-128903, A21, MF-A04).

NCEER-97-0011 "Seismic Analysis for Design or Retrofit of Gravity Bridge Abutments," by K.L. Fishman, R. Richards, Jr. and R.C. Divito, 10/2/97, (PB98-128937, A08, MF-A02).

NCEER-97-0012 "Evaluation of Simplified Methods of Analysis for Yielding Structures," by P. Tsopelas, M.C. Constantinou, C.A. Kircher and A.S. Whittaker, 10/31/97, (PB98-128929, A10, MF-A03).

NCEER-97-0013 "Seismic Design of Bridge Columns Based on Control and Repairability of Damage," by C-T. Cheng and J.B. Mander, 12/8/97, (PB98-144249, A11, MF-A03).

NCEER-97-0014 "Seismic Resistance of Bridge Piers Based on Damage Avoidance Design," by J.B. Mander and C-T. Cheng, 12/10/97, (PB98-144223, A09, MF-A02).

NCEER-97-0015 "Seismic Response of Nominally Symmetric Systems with Strength Uncertainty," by S. Balopoulou and M. Grigoriu, 12/23/97, (PB98-153422, A11, MF-A03).

NCEER-97-0016 "Evaluation of Seismic Retrofit Methods for Reinforced Concrete Bridge Columns," by T.J. Wipf, F.W. Klaiber and F.M. Russo, 12/28/97, (PB98-144215, A12, MF-A03).

NCEER-97-0017 "Seismic Fragility of Existing Conventional Reinforced Concrete Highway Bridges," by C.L. Mullen and A.S. Cakmak, 12/30/97, (PB98-153406, A08, MF-A02).

NCEER-97-0018 "Loss Asssessment of Memphis Buildings," edited by D.P. Abrams and M. Shinozuka, 12/31/97, (PB98-144231, A13, MF-A03).

NCEER-97-0019 "Seismic Evaluation of Frames with Infill Walls Using Quasi-static Experiments," by K.M. Mosalam, R.N. White and P. Gergely, 12/31/97, (PB98-153455, A07, MF-A02).

NCEER-97-0020 "Seismic Evaluation of Frames with Infill Walls Using Pseudo-dynamic Experiments," by K.M. Mosalam, R.N. White and P. Gergely, 12/31/97, (PB98-153430, A07, MF-A02).

NCEER-97-0021 "Computational Strategies for Frames with Infill Walls: Discrete and Smeared Crack Analyses and Seismic Fragility," by K.M. Mosalam, R.N. White and P. Gergely, 12/31/97, (PB98-153414, A10, MF-A02).

NCEER-97-0022 "Proceedings of the NCEER Workshop on Evaluation of Liquefaction Resistance of Soils," edited by T.L. Youd and I.M. Idriss, 12/31/97, (PB98-155617, A15, MF-A03).

MCEER-98-0001 "Extraction of Nonlinear Hysteretic Properties of Seismically Isolated Bridges from Quick-Release Field Tests," by Q. Chen, B.M. Douglas, E.M. Maragakis and I.G. Buckle, 5/26/98, (PB99-118838, A06, MF-A01).

MCEER-98-0002 "Methodologies for Evaluating the Importance of Highway Bridges," by A. Thomas, S. Eshenaur and J. Kulicki, 5/29/98, (PB99-118846, A10, MF-A02).

MCEER-98-0003 "Capacity Design of Bridge Piers and the Analysis of Overstrength," by J.B. Mander, A. Dutta and P. Goel, 6/1/98, (PB99-118853, A09, MF-A02).

MCEER-98-0004 "Evaluation of Bridge Damage Data from the Loma Prieta and Northridge, California Earthquakes," by N. Basoz and A. Kiremidjian, 6/2/98, (PB99-118861, A15, MF-A03).

MCEER-98-0005 "Screening Guide for Rapid Assessment of Liquefaction Hazard at Highway Bridge Sites," by T. L. Youd, 6/16/98, (PB99-118879, A06, not available on microfiche).

MCEER-98-0006 "Structural Steel and Steel/Concrete Interface Details for Bridges," by P. Ritchie, N. Kauhl and J. Kulicki, 7/13/98, (PB99-118945, A06, MF-A01).

MCEER-98-0007 "Capacity Design and Fatigue Analysis of Confined Concrete Columns," by A. Dutta and J.B. Mander, 7/14/98, (PB99-118960, A14, MF-A03).

MCEER-98-0008 "Proceedings of the Workshop on Performance Criteria for Telecommunication Services Under Earthquake Conditions," edited by A.J. Schiff, 7/15/98, (PB99-118952, A08, MF-A02).

MCEER-98-0009 "Fatigue Analysis of Unconfined Concrete Columns," by J.B. Mander, A. Dutta and J.H. Kim, 9/12/98, (PB99-123655, A10, MF-A02).

MCEER-98-0010 "Centrifuge Modeling of Cyclic Lateral Response of Pile-Cap Systems and Seat-Type Abutments in Dry Sands," by A.D. Gadre and R. Dobry, 10/2/98, (PB99-123606, A13, MF-A03).

MCEER-98-0011 "IDARC-BRIDGE: A Computational Platform for Seismic Damage Assessment of Bridge Structures," by A.M. Reinhorn, V. Simeonov, G. Mylonakis and Y. Reichman, 10/2/98, (PB99-162919, A15, MF-A03).

MCEER-98-0012 "Experimental Investigation of the Dynamic Response of Two Bridges Before and After Retrofitting with Elastomeric Bearings," by D.A. Wendichansky, S.S. Chen and J.B. Mander, 10/2/98, (PB99-162927, A15, MF-A03).

MCEER-98-0013 "Design Procedures for Hinge Restrainers and Hinge Sear Width for Multiple-Frame Bridges," by R. Des Roches and G.L. Fenves, 11/3/98, (PB99-140477, A13, MF-A03).

MCEER-98-0014 "Response Modification Factors for Seismically Isolated Bridges," by M.C. Constantinou and J.K. Quarshie, 11/3/98, (PB99-140485, A14, MF-A03).

MCEER-98-0015 "Proceedings of the U.S.-Italy Workshop on Seismic Protective Systems for Bridges," edited by I.M. Friedland and M.C. Constantinou, 11/3/98, (PB2000-101711, A22, MF-A04).

MCEER-98-0016 "Appropriate Seismic Reliability for Critical Equipment Systems: Recommendations Based on Regional Analysis of Financial and Life Loss," by K. Porter, C. Scawthorn, C. Taylor and N. Blais, 11/10/98, (PB99-157265, A08, MF-A02).

MCEER-98-0017 "Proceedings of the U.S. Japan Joint Seminar on Civil Infrastructure Systems Research," edited by M. Shinozuka and A. Rose, 11/12/98, (PB99-156713, A16, MF-A03).

MCEER-98-0018 "Modeling of Pile Footings and Drilled Shafts for Seismic Design," by I. PoLam, M. Kapuskar and D. Chaudhuri, 12/21/98, (PB99-157257, A09, MF-A02).

MCEER-99-0001 "Seismic Evaluation of a Masonry Infilled Reinforced Concrete Frame by Pseudodynamic Testing," by S.G. Buonopane and R.N. White, 2/16/99, (PB99-162851, A09, MF-A02).

MCEER-99-0002 "Response History Analysis of Structures with Seismic Isolation and Energy Dissipation Systems: Verification Examples for Program SAP2000," by J. Scheller and M.C. Constantinou, 2/22/99, (PB99-162869, A08, MF-A02).

MCEER-99-0003 "Experimental Study on the Seismic Design and Retrofit of Bridge Columns Including Axial Load Effects," by A. Dutta, T. Kokorina and J.B. Mander, 2/22/99, (PB99-162877, A09, MF-A02).

MCEER-99-0004 "Experimental Study of Bridge Elastomeric and Other Isolation and Energy Dissipation Systems with Emphasis on Uplift Prevention and High Velocity Near-source Seismic Excitation," by A. Kasalanati and M. C. Constantinou, 2/26/99, (PB99-162885, A12, MF-A03).

MCEER-99-0005 "Truss Modeling of Reinforced Concrete Shear-flexure Behavior," by J.H. Kim and J.B. Mander, 3/8/99, (PB99-163693, A12, MF-A03).

MCEER-99-0006 "Experimental Investigation and Computational Modeling of Seismic Response of a 1:4 Scale Model Steel Structure with a Load Balancing Supplemental Damping System," by G. Pekcan, J.B. Mander and S.S. Chen, 4/2/99, (PB99-162893, A11, MF-A03).

MCEER-99-0007 "Effect of Vertical Ground Motions on the Structural Response of Highway Bridges," by M.R. Button, C.J. Cronin and R.L. Mayes, 4/10/99, (PB2000-101411, A10, MF-A03).

MCEER-99-0008 "Seismic Reliability Assessment of Critical Facilities: A Handbook, Supporting Documentation, and Model Code Provisions," by G.S. Johnson, R.E. Sheppard, M.D. Quilici, S.J. Eder and C.R. Scawthorn, 4/12/99, (PB2000-101701, A18, MF-A04).

MCEER-99-0009 "Impact Assessment of Selected MCEER Highway Project Research on the Seismic Design of Highway Structures," by C. Rojahn, R. Mayes, D.G. Anderson, J.H. Clark, D'Appolonia Engineering, S. Gloyd and R.V. Nutt, 4/14/99, (PB99-162901, A10, MF-A02).

MCEER-99-0010 "Site Factors and Site Categories in Seismic Codes," by R. Dobry, R. Ramos and M.S. Power, 7/19/99, (PB2000-101705, A08, MF-A02).

MCEER-99-0011 "Restrainer Design Procedures for Multi-Span Simply-Supported Bridges," by M.J. Randall, M. Saiidi, E. Maragakis and T. Isakovic, 7/20/99, (PB2000-101702, A10, MF-A02).

MCEER-99-0012 "Property Modification Factors for Seismic Isolation Bearings," by M.C. Constantinou, P. Tsopelas, A. Kasalanati and E. Wolff, 7/20/99, (PB2000-103387, A11, MF-A03).

MCEER-99-0013 "Critical Seismic Issues for Existing Steel Bridges," by P. Ritchie, N. Kauhl and J. Kulicki, 7/20/99, (PB2000-101697, A09, MF-A02).

MCEER-99-0014 "Nonstructural Damage Database," by A. Kao, T.T. Soong and A. Vender, 7/24/99, (PB2000-101407, A06, MF-A01).

MCEER-99-0015 "Guide to Remedial Measures for Liquefaction Mitigation at Existing Highway Bridge Sites," by H.G. Cooke and J. K. Mitchell, 7/26/99, (PB2000-101703, A11, MF-A03).

MCEER-99-0016 "Proceedings of the MCEER Workshop on Ground Motion Methodologies for the Eastern United States," edited by N. Abrahamson and A. Becker, 8/11/99, (PB2000-103385, A07, MF-A02).

MCEER-99-0017 "Quindío, Colombia Earthquake of January 25, 1999: Reconnaissance Report," by A.P. Asfura and P.J. Flores, 10/4/99, (PB2000-106893, A06, MF-A01).

MCEER-99-0018 "Hysteretic Models for Cyclic Behavior of Deteriorating Inelastic Structures," by M.V. Sivaselvan and A.M. Reinhorn, 11/5/99, (PB2000-103386, A08, MF-A02).

MCEER-99-0019 "Proceedings of the 7^{th} U.S.- Japan Workshop on Earthquake Resistant Design of Lifeline Facilities and Countermeasures Against Soil Liquefaction," edited by T.D. O'Rourke, J.P. Bardet and M. Hamada, 11/19/99, (PB2000-103354, A99, MF-A06).

MCEER-99-0020 "Development of Measurement Capability for Micro-Vibration Evaluations with Application to Chip Fabrication Facilities," by G.C. Lee, Z. Liang, J.W. Song, J.D. Shen and W.C. Liu, 12/1/99, (PB2000-105993, A08, MF-A02).

MCEER-99-0021 "Design and Retrofit Methodology for Building Structures with Supplemental Energy Dissipating Systems," by G. Pekcan, J.B. Mander and S.S. Chen, 12/31/99, (PB2000-105994, A11, MF-A03).

MCEER-00-0001 "The Marmara, Turkey Earthquake of August 17, 1999: Reconnaissance Report," edited by C. Scawthorn; with major contributions by M. Bruneau, R. Eguchi, T. Holzer, G. Johnson, J. Mander, J. Mitchell, W. Mitchell, A. Papageorgiou, C. Scaethorn, and G. Webb, 3/23/00, (PB2000-106200, A11, MF-A03).

MCEER-00-0002 "Proceedings of the MCEER Workshop for Seismic Hazard Mitigation of Health Care Facilities," edited by G.C. Lee, M. Ettouney, M. Grigoriu, J. Hauer and J. Nigg, 3/29/00, (PB2000-106892, A08, MF-A02).

MCEER-00-0003 "The Chi-Chi, Taiwan Earthquake of September 21, 1999: Reconnaissance Report," edited by G.C. Lee and C.H. Loh, with major contributions by G.C. Lee, M. Bruneau, I.G. Buckle, S.E. Chang, P.J. Flores, T.D. O'Rourke, M. Shinozuka, T.T. Soong, C-H. Loh, K-C. Chang, Z-J. Chen, J-S. Hwang, M-L. Lin, G-Y. Liu, K-C. Tsai, G.C. Yao and C-L. Yen, 4/30/00, (PB2001-100980, A10, MF-A02).

MCEER-00-0004 "Seismic Retrofit of End-Sway Frames of Steel Deck-Truss Bridges with a Supplemental Tendon System: Experimental and Analytical Investigation," by G. Pekcan, J.B. Mander and S.S. Chen, 7/1/00, (PB2001-100982, A10, MF-A02).

MCEER-00-0005 "Sliding Fragility of Unrestrained Equipment in Critical Facilities," by W.H. Chong and T.T. Soong, 7/5/00, (PB2001-100983, A08, MF-A02).

MCEER-00-0006 "Seismic Response of Reinforced Concrete Bridge Pier Walls in the Weak Direction," by N. Abo-Shadi, M. Saiidi and D. Sanders, 7/17/00, (PB2001-100981, A17, MF-A03).

MCEER-00-0007 "Low-Cycle Fatigue Behavior of Longitudinal Reinforcement in Reinforced Concrete Bridge Columns," by J. Brown and S.K. Kunnath, 7/23/00, (PB2001-104392, A08, MF-A02).

MCEER-00-0008 "Soil Structure Interaction of Bridges for Seismic Analysis," I. PoLam and H. Law, 9/25/00, (PB2001-105397, A08, MF-A02).

MCEER-00-0009 "Proceedings of the First MCEER Workshop on Mitigation of Earthquake Disaster by Advanced Technologies (MEDAT-1), edited by M. Shinozuka, D.J. Inman and T.D. O'Rourke, 11/10/00, (PB2001-105399, A14, MF-A03).

MCEER-00-0010 "Development and Evaluation of Simplified Procedures for Analysis and Design of Buildings with Passive Energy Dissipation Systems," by O.M. Ramirez, M.C. Constantinou, C.A. Kircher, A.S. Whittaker, M.W. Johnson, J.D. Gomez and C. Chrysostomou, 11/16/01, (PB2001-105523, A23, MF-A04).

MCEER-00-0011 "Dynamic Soil-Foundation-Structure Interaction Analyses of Large Caissons," by C-Y. Chang, C-M. Mok, Z-L. Wang, R. Settgast, F. Waggoner, M.A. Ketchum, H.M. Gonnermann and C-C. Chin, 12/30/00, (PB2001-104373, A07, MF-A02).

MCEER-00-0012 "Experimental Evaluation of Seismic Performance of Bridge Restrainers," by A.G. Vlassis, E.M. Maragakis and M. Saiid Saiidi, 12/30/00, (PB2001-104354, A09, MF-A02).

MCEER-00-0013 "Effect of Spatial Variation of Ground Motion on Highway Structures," by M. Shinozuka, V. Saxena and G. Deodatis, 12/31/00, (PB2001-108755, A13, MF-A03).

MCEER-00-0014 "A Risk-Based Methodology for Assessing the Seismic Performance of Highway Systems," by S.D. Werner, C.E. Taylor, J.E. Moore, II, J.S. Walton and S. Cho, 12/31/00, (PB2001-108756, A14, MF-A03).

MCEER-01-0001 "Experimental Investigation of P-Delta Effects to Collapse During Earthquakes," by D. Vian and M. Bruneau, 6/25/01, (PB2002-100534, A17, MF-A03).

MCEER-01-0002 "Proceedings of the Second MCEER Workshop on Mitigation of Earthquake Disaster by Advanced Technologies (MEDAT-2)," edited by M. Bruneau and D.J. Inman, 7/23/01, (PB2002-100434, A16, MF-A03).

MCEER-01-0003 "Sensitivity Analysis of Dynamic Systems Subjected to Seismic Loads," by C. Roth and M. Grigoriu, 9/18/01, (PB2003-100884, A12, MF-A03).

MCEER-01-0004 "Overcoming Obstacles to Implementing Earthquake Hazard Mitigation Policies: Stage 1 Report," by D.J. Alesch and W.J. Petak, 12/17/01, (PB2002-107949, A07, MF-A02).

MCEER-01-0005 "Updating Real-Time Earthquake Loss Estimates: Methods, Problems and Insights," by C.E. Taylor, S.E. Chang and R.T. Eguchi, 12/17/01, (PB2002-107948, A05, MF-A01).

MCEER-01-0006 "Experimental Investigation and Retrofit of Steel Pile Foundations and Pile Bents Under Cyclic Lateral Loadings," by A. Shama, J. Mander, B. Blabac and S. Chen, 12/31/01, (PB2002-107950, A13, MF-A03).

MCEER-02-0001 "Assessment of Performance of Bolu Viaduct in the 1999 Duzce Earthquake in Turkey" by P.C. Roussis, M.C. Constantinou, M. Erdik, E. Durukal and M. Dicleli, 5/8/02, (PB2003-100883, A08, MF-A02).

MCEER-02-0002 "Seismic Behavior of Rail Counterweight Systems of Elevators in Buildings," by M.P. Singh, Rildova and L.E. Suarez, 5/27/02. (PB2003-100882, A11, MF-A03).

MCEER-02-0003 "Development of Analysis and Design Procedures for Spread Footings," by G. Mylonakis, G. Gazetas, S. Nikolaou and A. Chauncey, 10/02/02, (PB2004-101636, A13, MF-A03, CD-A13).

MCEER-02-0004 "Bare-Earth Algorithms for Use with SAR and LIDAR Digital Elevation Models," by C.K. Huyck, R.T. Eguchi and B. Houshmand, 10/16/02, (PB2004-101637, A07, CD-A07).

MCEER-02-0005 "Review of Energy Dissipation of Compression Members in Concentrically Braced Frames," by K.Lee and M. Bruneau, 10/18/02, (PB2004-101638, A10, CD-A10).

MCEER-03-0001 "Experimental Investigation of Light-Gauge Steel Plate Shear Walls for the Seismic Retrofit of Buildings" by J. Berman and M. Bruneau, 5/2/03, (PB2004-101622, A10, MF-A03, CD-A10).

MCEER-03-0002 "Statistical Analysis of Fragility Curves," by M. Shinozuka, M.Q. Feng, H. Kim, T. Uzawa and T. Ueda, 6/16/03, (PB2004-101849, A09, CD-A09).

MCEER-03-0003 "Proceedings of the Eighth U.S.-Japan Workshop on Earthquake Resistant Design f Lifeline Facilities and Countermeasures Against Liquefaction," edited by M. Hamada, J.P. Bardet and T.D. O'Rourke, 6/30/03, (PB2004-104386, A99, CD-A99).

MCEER-03-0004 "Proceedings of the PRC-US Workshop on Seismic Analysis and Design of Special Bridges," edited by L.C. Fan and G.C. Lee, 7/15/03, (PB2004-104387, A14, CD-A14).

MCEER-03-0005 "Urban Disaster Recovery: A Framework and Simulation Model," by S.B. Miles and S.E. Chang, 7/25/03, (PB2004-104388, A07, CD-A07).

MCEER-03-0006 "Behavior of Underground Piping Joints Due to Static and Dynamic Loading," by R.D. Meis, M. Maragakis and R. Siddharthan, 11/17/03.

MCEER-03-0007 "Seismic Vulnerability of Timber Bridges and Timber Substructures," by A.A. Shama, J.B. Mander, I.M. Friedland and D.R. Allicock, 12/15/03.

MCEER-04-0001 "Experimental Study of Seismic Isolation Systems with Emphasis on Secondary System Response and Verification of Accuracy of Dynamic Response History Analysis Methods," by E. Wolff and M. Constantinou, 1/16/04.

MCEER-04-0002 “Tension, Compression and Cyclic Testing of Engineered Cementitious Composite Materials,” by K. Kesner and S.L. Billington, 3/1/04.

MCEER-04-0003 “Cyclic Testing of Braces Laterally Restrained by Steel Studs to Enhance Performance During Earthquakes,” by O.C. Celik, J.W. Berman and M. Bruneau, 3/16/04.

MCEER-04-0004 “Methodologies for Post Earthquake Building Damage Detection Using SAR and Optical Remote Sensing: Application to the August 17, 1999 Marmara, Turkey Earthquake,” by C.K. Huyck, B.J. Adams, S. Cho, R.T. Eguchi, B. Mansouri and B. Houshmand, 6/15/04.

MCEER-04-0005 “Nonlinear Structural Analysis Towards Collapse Simulation: A Dynamical Systems Approach,” by M.V. Sivaselvan and A.M. Reinhorn, 6/16/04.

MCEER-04-0006 “Proceedings of the Second PRC-US Workshop on Seismic Analysis and Design of Special Bridges,” edited by G.C. Lee and L.C. Fan, 6/25/04.

MCEER-04-0007 “Seismic Vulnerability Evaluation of Axially Loaded Steel Built-up Laced Members,” by K. Lee and M. Bruneau, 6/30/04.

MCEER-04-0008 “Evaluation of Accuracy of Simplified Methods of Analysis and Design of Buildings with Damping Systems for Near-Fault and for Soft-Soil Seismic Motions,” by E.A. Pavlou and M.C. Constantinou, 8/16/04.

MCEER-04-0009 “Assessment of Geotechnical Issues in Acute Care Facilities in California,” by M. Lew, T.D. O’Rourke, R. Dobry and M. Koch, 9/15/04.

MCEER-04-0010 “Scissor-Jack-Damper Energy Dissipation System,” by A.N. Sigaher-Boyle and M.C. Constantinou, 12/1/04.

MCEER
MULTIDISCIPLINARY CENTER FOR EARTHQUAKE ENGINEERING RESEARCH
A National Center of Excellence in Advanced Technology Applications
University at Buffalo, State University of New York
Red Jacket Quadrangle ■ Buffalo, New York 14261
Phone: (716) 645-3391 ■ Fax: (716) 645-3399
E-mail: ***mceer@mceermail.buffalo.edu*** **■ WWW Site** ***http://mceer.buffalo.edu***
University at Buffalo *The State University of New York*

ISSN 1520-295X